2017

Key Virus-Host Interactions Required For Arenavirus Particle Assembly And Release

Christopher Michael Ziegler
University of Vermont

KEY VIRUS-HOST INTERACTIONS REQUIRED FOR ARENAVIRUS PARTICLE ASSEMBLY AND RELEASE

A Dissertation Presented

by

Christopher Michael Ziegler

to

The Faculty of the Graduate College

of

The University of Vermont

In Partial Fulfillment of the Requirements
for the Degree of Doctor of Philosophy
Specializing in Cellular, Molecular and Biomedical Sciences

May, 2017

Defense Date: March 24th, 2017
Dissertation Examination Committee:

Jason W. Botten, Ph.D., Advisor
Bryan A. Ballif, Ph.D., Chairperson
Christopher D. Huston, Ph.D.
Dimitry Krementsov, Ph.D.
Cynthia J. Forehand, Ph.D., Dean of the Graduate College

ABSTRACT

Viruses are infectious agents that must infect the cells of living organisms in order to reproduce. They have relatively simple genomes which encode few proteins but can compensate for their simplicity by hijacking components of their cellular hosts. Arenaviruses, a family of zoonotic viruses carried by rodents, encode only 4 proteins. One of these proteins, Z, is responsible for several functions during the virus life cycle including driving the formation and release of new virus particles at the plasma membrane of infected cells. Relatively little is known about how this viral protein is regulated or the complement of host proteins it engages in order to produce new virus particles or augment Z's other functions. To address this gap in knowledge, mass spectrometry was used to identify phosphorylation sites in the Old World arenavirus, lymphocytic choriomeningitis virus (LCMV) Z protein. Phosphorylation sites were identified at serine 41 (S41) and tyrosine 88 (Y88). Functional studies using recombinant (r)LCMV containing mutations at these phosphorylation sites revealed that both were important for the production of defective interfering (DI) particles. DI particles are replication-incompetent virus particles that interfere with the production of infectious virus and mitigate its cytopathic effect. While a mutation that mimics phosphorylation at S41 reduced LCMV's ability to produce both infectious and DI particles, this mutation had a much stronger impact on DI particles. Production of DI particles in Y88-mutant rLCMV was drastically reduced while the impact on infectious virus was minimal. Y88 lies within a type of viral late domain (PPXY) also found in matrix proteins of several disparate virus families where it has been shown to drive infectious virus release by recruiting the membrane scission machinery of the cellular endosomal sorting complex required for transport (ESCRT). Inhibition of the ESCRT pathway drastically reduced LCMV DI particle but not infectious virus release indicating that Z's PPXY late domain and the cellular ESCRT complex are required specifically for the production of DI particles. Mass spectrometry was also used to identify host protein partners of Z as well as the host proteins recruited into virus particles for the New World arenavirus, Junín (JUNV). ESCRT complex proteins were enriched in JUNV virus-like particles (VLPs) and *bona fide* virions. In contrast to LCMV, inhibition of the ESCRT complex resulted in significantly less infectious JUNV release. This indicates that the ultimate role of ESCRT engagement by the Old World arenavirus, LCMV, differs from that of New World, JUNV. This work represents the first demonstration that a viral protein motif and the host machinery it engages selectively drive DI particle production independently of infectious virus. It also suggests that host cell kinases can dynamically regulate the production of DI particles through phosphorylation of Z. Finally, the late domain-mutant rLCMV generated in these studies represents the first LCMV strain known to produce undetectable levels of DI particles which provides the opportunity to assess the impact that a loss of DI particles has on the ability of LCMV to establish or maintain a persistent infection.

CITATIONS

Material from this dissertation has been published in the following form:

Ziegler, C.M., Eisenhauer, P., Bruce, E.A., Weir, M.E., King, B.R., Klaus, J.P., Krementsov, D.N., Shirley, D.J., Ballif, B.A., Botten, J.. (2016). The Lymphocytic Choriomeningitis Virus Matrix Protein PPXY Late Domain Drives the Production of Defective Interfering Particles. PLoS Pathogens, 12:e1005501.

Ziegler, C.M., Eisenhauer, P., Bruce, E.A., Beganovic, V., King, B.R., Weir, M.E., Ballif, B.A., Botten, J.. (2016). A novel phosphoserine motif in the LCMV matrix protein Z regulates the release of infectious virus and defective interfering particles. Journal of General Virology, doi:doi:10.1099/jgv.0.000550.

ACKNOWLEDGEMENTS

I would like to thank my advisor, Jason Botten, for giving me this opportunity and for being such a positive and professional role model. It has been great to work with a fellow Minnesotan and I have really enjoyed my time in your lab. I would like to thank my colleagues in the Botten lab for all the support and advice over the years and for making the lab such a positive and enjoyable place to work. I would especially like to thank Phil Eisenhauer for all of the hours he put in to support this work. I have had the pleasure of working with several undergraduate students over the last few years including Vedran Beganovic, Loan Dang, and Jamie Kelly. I would like to thank them for all of their hard work and recognize their significant contributions to these projects. I would also like to thank them for giving me the opportunity to guide them through their research projects. Lastly, I would like to thank Terri Messier and Barry Finette for giving me a start in science. Terri took me under her wing when I was a young student and I will not forget the impact that she has had in getting me to where I am today.

I would like to also thank my friends and family who have provided the support that has allowed me to reach this point. My parents, who imparted on me a work ethic that has driven me to achievement in many aspects of my life, but while also teaching me to stop and smell the roses once in a while. My two brothers, Matt and Jesse, who have always kept me motivated and provided support in many ways when I needed

it. My older brother Jesse has been a role model for me in more ways than he probably realizes throughout my life. And finally, I would like to thank my girlfriend and best friend Catherine for all the support and encouragement through this endeavor. It wouldn't have been nearly as great without you in my life.

TABLE OF CONTENTS

Page

LIST OF TABLES

Table **Page**

LIST OF FIGURES

Figure **Page**

CHAPTER 1: COMPREHENSIVE LITERATURE REVIEW

1.1. Introduction

Arenaviruses are a family of viruses that include several species which can cause a range of diseases in humans including severe hemorrhagic fever. Currently there are no FDA-approved drugs or vaccines available to specifically treat arenavirus infection in humans which highlights the need for an increased understanding of the basic biology of these viruses. Arenaviruses are extremely simple organisms encoding only 4 proteins. Accordingly, these 4 proteins must each be capable of engaging various machinery from their cellular host in order for the virus to replicate. One of these arenavirus proteins, Z, carries out several functions during the virus life cycle including driving the formation and release of virus particles at the plasma membrane of infected cells. The current model of Z-mediated virus release posits that Z must recruit the cellular endosomal sorting complex required for transport (ESCRT) pathway by way of its C-terminal late domain. However, a detailed understanding of Z/ESCRT-mediated arenavirus release is lacking. Additionally, little is known about the specific host proteins that the Z protein interacts with during the virus life cycle in order to accomplish release as well as its various other functions.

In this work, we sought to address deficiencies in the understanding of virus-host interactions for the arenavirus Z protein. Mass spectrometry was used to identify phosphorylation sites on the arenavirus Z protein mediated by host cell kinases as well as to uncover novel protein-protein interactions between the Z protein and its cellular host. Through subsequent functional studies, we discovered that the prototypic arenavirus,

lymphocytic meningitis virus (LCMV), uses the late domain contained within its Z protein and the cellular ESCRT pathway to specifically drive the production of defective interfering (DI) particles. A second phosphorylation site in Z was also shown to be important for both infectious virus and DI particle production. Finally we have uncovered Z-host protein-protein interactions for another arenavirus, Junín, which led to the discovery that unlike LCMV, Junín virus requires the ESCRT pathway to drive infectious virus release. These proteomics discovery studies and subsequent functional analyses have advanced the understanding of how late domains in the arenavirus Z protein and the cellular ESCRT pathway function in arenavirus release.

1.2. Arenaviruses

Arenaviruses are enveloped, negative-sense RNA viruses found in different regions of the world. Phylogeny of the *Arenaviridae* family has been recently restructured to include two genera, mammarenaviruses and reptarenaviruses (Radoshitzky et al., 2015). Both genera are zoonotic viruses which are carried in either rodents for the mammarenaviruses or snakes for the reptarenaviruses (Buchmeier et al., 2007; Hetzel et al., 2013; McCormick et al., 1986; Stenglein et al., 2012). The mammarenavirus, Tacaribe virus, is unique in the *Arenaviridae* family as it is carried in *Artibeus* bats (Downs et al., 1963). For sake of simplicity, from this point forward the mammarenaviruses will be referred to as arenaviruses and no further discussion of the reptarenaviruses will be included.

Arenaviruses typically establish a persistent, lifelong infection in their rodent hosts that is initiated through vertical transmission of the virus from infected mother to offspring (Downs et al., 1963). Horizontal transmission through exposure of naïve rodents to urine, feces, or saliva from infected rodents also occurs, but mice infected as adults are less likely to become chronically infected (Childs and Peters, 1993). The rodent carrier of each arenavirus is species-specific and thus the distribution of each arenavirus is limited to the geographic distribution of its rodent host. Thus, most arenaviruses have a relatively limited geographic range with the exception of lymphocytic choriomeningits virus (LCMV), which is carried in the common house mouse (*Mus musculus*) and has a worldwide distribution (Childs and Peters, 1993). The arenavirus family is divided into two

major groups, the Old World and New World arenaviruses, which represent viruses found primarily in Africa or the Americas, respectively (Emonet et al., 2009a).

Several of the arenaviruses cause disease in humans. Human infection with arenaviruses can occur through direct contact with infected rodents or through exposure to virus aerosolized from infected rodent excreta (Keenlyside et al., 1983). Several arenaviruses from both the Old World and New World groups cause severe hemorrhagic fever in humans with high fatality rates. The Old World arenavirus, Lassa virus (LASV), causes the greatest number of infections of all the arenaviruses with an estimated 100,000-300,000 cases per year resulting in an estimated annual toll of 5,000 deaths (McCormick et al., 1987). Additionally, ~30% of survivors of LASV infection become deaf and the mortality rate associated with infection during pregnancy is high for both the mother and fetus (Cummins et al., 1990; Price et al., 1988). Six New World arenaviruses are known to cause hemorrhagic fever in humans. Junín, Machupo, Sabiá, and Guanarito viruses are the causative agents of Argentine, Bolivian, Brazilian, and Venezuelan Hemorrhagic Fever, respectively (Charrel and Lamballerie, 2003). The North American arenavirus, White Water Arroyo virus as well as Chapere virus, found in Bolivia, also cause hemorrhagic fever in humans (Byrd et al., 2000; Delgado et al., 2008b). Finally, the first arenavirus discovered, LCMV, was identified as the causative agent in an outbreak of encephalitis in St. Louis in 1933 (Armstrong and Lillie, 1934). LCMV infections in healthy humans ranges from a sub-clinical infection to aseptic meningitis (Bonthius, 2012). LCMV is a significant concern during pregnancy, as it can result in severe birth defects or spontaneous abortion

(Barton et al., 2002; Strausbaugh et al., 2001). LCMV has also caused several deaths in cases of solid organ transplants where the donor was infected with LCMV and the immunosuppressive therapy the recipients received following organ transplantation allowed the LCMV infection to proceed virtually unchecked (Fischer et al., 2006).

There are very limited options for prevention or treatment of human infection with any of the arenaviruses. There are no U.S. Food and Drug Administration (FDA)-approved vaccines available for the prevention of any of the arenaviruses. A live, attenuated vaccine strain of the South American arenavirus, Junín virus (JUNV), called Candid 1 (C#1) has been shown to reduce cases of Argentine hemorrhagic fever in the endemic region, but it has not been approved by the U.S. FDA (Enria et al., 2008b). Off-label use of the nucleoside analog, ribavirin, has been shown to significantly reduce the case fatality rate of Lassa fever particularly when treatment was started within 6 days following fever onset (McCormick et al., 1986). A small clinical trial with ribavirin for Argentine hemorrhagic fever failed to demonstrate any efficacy in reducing mortality (Enria et al., 2008b). The use of immune plasma from convalescent survivors of arenavirus infection has been tried for Lassa fever and Argentine hemorrhagic fever, but was only effective for Argentine hemorrhagic fever (Maiztegui et al., 1979; McCormick et al., 1986).

Arenaviruses are enveloped viruses ranging in size from 50-300nM and contain protrusions on the outer surface comprised of the viral transmembrane glycoprotein (Burns and Buchmeier, 1993). Arenavirus virions have electron dense granules visible by electron microscopy that are presumed to be ribosomes from which they derive their namesake, for

the Latin word, *arenosus*, meaning sandy (Rowe et al., 1970). Arenaviruses have a segmented, negative-sense RNA genome comprised of two single-stranded segments with an ambisense coding strategy. Each genome segment encodes two proteins. The nucleoprotein (NP) and glycoprotein (GP) are encoded by the small (S) segment while the large (L) segment encodes the RNA-dependent RNA polymerase (L) and the matrix protein Z (Auperin et al., 1986; Clegg et al., 1991; Djavani et al., 1997; Lukashevich et al., 1997; Riviere et al., 1985; Salvato and Shimomaye, 1989; Singh et al., 1987). All four proteins are structural components of the virion. GP is a transmembrane protein that forms spikes on the exterior of the virion, NP and L together with the genome segments form ribonucleoprotein (RNP) complexes which are packaged into virions, and Z forms a matrix layer on the interior side of the viral membrane (Lee and de la Torre, 2002; Neuman et al., 2005; Salvato et al., 1992a; Strecker et al., 2003).

Arenaviruses enter cells through receptor-mediated endocytosis, undergo replication and assembly in the cytoplasm, and are released from the cell via budding from the plasma membrane (Urata and Yasuda, 2012). GP mediates cell entry by binding cell surface receptors including the transferrin receptor for Clade B New World arenaviruses, including JUNV, and α-dystroglycan for Old World arenaviruses (including LCMV and LASV) and clade C New World arenaviruses (Cao et al., 1998; Radoshitzky et al., 2007; Spiropoulou et al., 2002). LCMV and LASV can also use alternate cell surface receptors including DC-SIGN, LSECtin, Axl and Tyro3 (Shimojima and Kawaoka, 2012; Shimojima et al., 2012). Upon receptor binding to the cell surface receptor, the virus is endocytosed

and the bound virus enters the endocytic pathway (Borrow and Oldstone, 1994; Kunz, 2009; Martinez et al., 2007; Quirin et al., 2008). In endosomes, GP triggers fusion of the viral envelope with the endosomal membrane releasing viral ribonucleoproteins into the cytoplasm (Klewitz et al., 2007). Viral replication occurs in the cytoplasm where the genome is transcribed and replicated by the L polymerase but also requires NP (Lee et al., 2000; Lopez et al., 2001). Virus assembly occurs at the plasma membrane where the Z matrix protein coordinates the recruitment of the glycoprotein and the ribonucleoprotein (RNP) complex, which consists of the viral genome, NP and the L polymerase, into budding virions (Fehling et al., 2012). Finally, the budding and release of progeny virions is mediated by the Z protein (Perez et al., 2003; Strecker et al., 2003).

1.3. The Z Matrix Protein

The arenavirus Z matrix protein is a small protein ranging in size from 90-103 amino acids which is largely comprised of a central zinc-binding really interesting new gene (RING) domain (Salvato et al., 1992b; Salvato and Shimomaye, 1989). Z also has functionally important C-terminal tetrapeptide motifs called late domains as well as an N-terminal myristoylation site (Perez et al., 2003; Perez et al., 2004a; Strecker et al., 2003; Strecker et al., 2006). The RING domain is required for mediating certain protein-protein interactions including interaction with the viral L polymerase and certain host proteins including eIF4E, PML, PRH and the ribosomal P proteins (Borden et al., 1998a; Borden et al., 1998b; Djavani et al., 2005; Kentsis et al., 2001). The RING domain's interaction with the L polymerase and eIF4E are necessary for Z's role in the regulation of viral polymerase activity and host cell cap-dependent translation, respectively (Campbell Dwyer et al., 2000; Cornu and de la Torre, 2002; Jacamo et al., 2003a; Kentsis et al., 2001; Kranzusch and Whelan, 2011). The Z protein of every arenavirus (except Tacaribe virus) contains one or two tetrapeptide late domains, either P(S/T)AP or PPXY, within the C-terminal tail region (Fehling et al., 2012). These viral late domains are thought to be required for efficient arenavirus release and the loss of these domains has been shown to result in decreased arenavirus virus-like particle (VLP) release (Djavani et al., 1997; Fehling et al., 2012). The majority of arenavirus Z proteins, except the Old World arenaviruses LCMV, Mobala, Dandenong, Ippy, Luna and Merino Walk virus, also contain a YXXL motif within the RING domain that is involved in Z's interaction with viral NP for at least Tacaribe (TACV) and Mopeia (MOPV) virus (Fehling et al., 2012; Groseth et al., 2010; Shtanko et al., 2011;

Urata et al., 2009). Finally, the Z protein is myristoylated within its N-terminal region on the glycine residue at the second position (Perez et al., 2004a; Strecker et al., 2006). This modification mediates Z's interaction with the plasma membrane and is essential for its budding activity as well as Z's interaction with plasma membrane-localized viral GP which is necessary for proper virus assembly (Capul et al., 2007; Perez et al., 2004a; Strecker et al., 2006).

Z is responsible for a number of critical functions in the viral life cycle including regulating viral genome replication and transcription, repressing translation of viral and cellular mRNAs, antagonizing the innate immune response, coordinating virus assembly, and driving virus budding and release. The Z protein directly binds the L polymerase and results in dose-dependent inhibition of polymerase activity (Cornu and de la Torre, 2001; Jacamo et al., 2003b; Kranzusch and Whelan, 2011). Z locks the L polymerase in a promoter bound state which may serve as a mechanism to ensure recruitment of both the polymerase and the viral genome into arenavirus particles (Kranzusch and Whelan, 2011). Z can also repress the translation of capped mRNAs by directly binding to and inhibiting the translation initiation factor eIF4E through its RING domain (Campbell Dwyer et al., 2000; Kentsis et al., 2001; Kranzusch and Whelan, 2011; Volpon et al., 2010). Several host factors involved in the innate immune response depend on eIF4E for their expression, thus, Z protein inhibition of eIF4E may serve as one mechanism by which arenaviruses can suppress the host immune response (Fehling et al., 2012). Z has also been shown to antagonize the host immune response through interferon antagonism. The initial finding

indicated that Z proteins of several New World arenaviruses, but not the Old World arenaviruses LCMV or LASV, directly bind to retinoic acid-inducible gene I (RIG-I) and thus inhibit type I interferon production (Fan et al., 2010). However, a more recent study contradicted that finding in part by demonstrating that LCMV and LASV Z as well as the Z protein of other pathogenic arenaviruses, but not non-pathogenic arenaviruses, can bind to and inhibit RIG-I (Xing et al., 2015). Z from pathogenic arenaviruses can also inhibit interferon production by antagonizing melanoma differentiation-associated protein 5 (MDA5) (Xing et al., 2015). The Z protein's interaction with both RIG-I and MDA5 is mediated through Z's N-terminal domain (Xing et al., 2015).

The most prominent role of Z is to drive assembly, budding, and release of virions at the plasma membrane. The sites of virus particle assembly must contain all of the arenavirus proteins as well as the viral genome in order to produce infectious virus particles. Z functions as the central coordinator for the assembly of virus particles at sites of budding by interacting with glycoprotein (GP) and the viral ribonucleoprotein (RNP) complex (Capul et al., 2007; Schlie et al., 2010). Accordingly, Z is the only arenavirus protein to interact directly with each of the other three arenavirus proteins. The viral GP is a transmembrane protein that traffics to the cell's plasma membrane where it can be packaged into nascent virions. Z interacts with plasma membrane-localized GP by way of its N-terminal myristoylation modification (Capul et al., 2007; Perez et al., 2004a; Strecker et al., 2006). The RNP complex consists of NP, the L polymerase, and the viral genome segments. Thus, interaction of Z with any of the individual RNP components may facilitate

the recruitment of the RNP complex into nascent virions. Z's interaction with NP is well-established and appears to be conserved across the arenavirus family (Casabona et al., 2009; Eichler et al., 2004; Groseth et al., 2010; Levingston Macleod et al., 2011; Ortiz-Riano et al., 2011; Shtanko et al., 2010). Finally, Z has been shown to bind directly to the L polymerase through its RING domain (Jacamo et al., 2003b; Kranzusch and Whelan, 2011). As the Z-L interaction results in viral genome promotor-bound, inactive polymerase, the recruitment of viral genome into nascent virions may be ensured (Kranzusch and Whelan, 2011).

The release of arenavirus virions has traditionally been thought to be mediated by Z's recruitment of the cellular endosomal sorting complex required for transport (ESCRT) through its C-terminal late domains, either P(S/T)AP and/or PPXY (Perez et al., 2003; Strecker et al., 2003; Urata et al., 2006). Accordingly, Z, in the absence of other viral proteins, can induce the formation of virus-like particles (VLPs) and thus is both necessary and sufficient for driving the budding process (Eichler et al., 2004; Perez et al., 2003; Strecker et al., 2003). Mutation of the PPXY late domain, present in Old World arenavirus Z proteins, results in decreased VLP production for LCMV and LASV (Perez et al., 2003; Strecker et al., 2003). Mutation of the P(S/T)AP late domain, present in most New World and some Old World arenaviruses, similarly results in reduced VLP production for LASV and Lujo virus (LUJV), but other arenaviruses have not yet been tested (Perez et al., 2003; Strecker et al., 2003; Urata et al., 2016). Disruption of certain ESCRT proteins has also been shown to reduce arenavirus VLP production. Silencing (si)-RNA-mediated

knockdown of the ESCRT protein, TSG101, resulted in decreased LCMV and LASV Z VLP production but did not reduce LUJV VLP production (Perez et al., 2003; Urata et al., 2006; Urata et al., 2016). Supporting the role of TSG101 in VLP release, LASV Z and TSG101 have also been shown to interact in a manner that appears to require both the PPXY and P(S/T)AP late domains (Fehling et al., 2012). Knockdown or overexpression of a dominant-negative form of the ESCRT accessory protein, VPS4A/B, also decreased LASV Z, but not Lujo Z, VLP release (Urata et al., 2006; Urata et al., 2016). Finally, treatment with small molecules that inhibit the interaction between PPXY late domains and Nedd4 family ubiquitin ligases, which have been shown to be a critical link between viral matrix proteins and the ESCRT complex, reduced LASV VLP production (Han et al., 2014; Votteler and Sundquist, 2013). While these various studies have provided strong support for the role of late domains and the ESCRT pathway for the release of some arenaviruses, these experiments have relied on the use of VLP assays which do not always faithfully recapitulate all the facets of the whole virus. The only studies to date that have assessed the role of either late domains or ESCRT factors with complete, infectious virus are with Pichinde virus (PICV). In that study, recombinant PICV with mutations to its PSAP late domain was viable but the release of infectious virus particles was attenuated (Wang et al., 2012). Additionally, the New World arenavirus Tacaribe (TACV) lacks a functional late domain in its Z protein indicating that arenavirus budding and release may, at least in some cases, be independent of known late domains or require additional, unidentified factors (Urata et al., 2009).

While the PPXY and P(S/T)AP late domains found in most arenavirus Z proteins are *bona fide* late domains, the majority of arenavirus Z proteins, with the exceptions of the Old World arenaviruses LCMV, Mobala, Dandenong, Ippy, Luna and Merino Walk virus, also contain an additional motif in the central region of the protein (Fehling et al., 2012). This motif, YLCL, resembles another type of late domain found in the budding proteins of other viruses (Fehling et al., 2012). While this motif has been shown to be required for Z-NP interaction for TACV and MOPV, it has not been shown to function as a viral late domain driving arenavirus release as has been shown for the YPXL motif found in equine infectious anemia virus and other retroviruses (Groseth et al., 2010; Puffer et al., 1997; Votteler and Sundquist, 2013). LUJV represents a unique case in that it has two separate motifs that resemble the YPXL motif in equine infectious anemia virus (Urata et al., 2016). LUJV Z has a YLCL motif that does not contribute to VLP production but also has a YREL motif that does impact VLP production (Urata et al., 2016). However, knockdown of the YPXL-binding, ESCRT accessory protein, ALIX (also known as AIP1 or PDCD6IP), did not impact LUJV VLP release leaving in question whether YREL functions as a viral late domain in LUJV (Urata et al., 2016; Votteler and Sundquist, 2013). While the arenavirus Z protein is clearly the driving force of arenavirus release, substantial diversity exists among the different arenavirus Z proteins and it appears that different Z proteins may utilize host cell machinery in distinct ways to drive virus release. Substantial work is needed to understand the host cell machinery employed by the different arenavirus Z proteins to accomplish this essential function.

1.4. Defective Interfering Particles

Defective interfering (DI) particles are a class of virus particles produced by a wide range of viruses that cannot self-replicate and specifically interfere with the production of homologous infectious virus (also known as standard virus) (Huang, 1973; Huang and Baltimore, 1970). These particles were first discovered by von Magnus in the 1950's for influenza virus and in the decades that followed, many viruses were shown to produce DI particles including vesicular stomatitis virus (VSV), Sendai virus, arenaviruses, Rift Valley fever virus and others (Bellett and Cooper, 1959; Huang, 1973; Kingsbury et al., 1970; Mims, 1956; von, 1951). DI particles contain a normal viral structural protein content and at least part of the viral genome (Huang, 1973; Huang and Baltimore, 1970). For many viruses, deletions in the viral genome have been identified and associated with the defective phenotype. Large deletions in the open reading frame for the viral polymerase have been found in some DI particles for both VSV and influenza virus (Davis et al., 1980; Epstein et al., 1980; Moss and Brownlee, 1981), but there exists significant heterogeneity in the types, locations and sizes of deletions in DI genomes, as has been extensively demonstrated with VSV (Lazzarini et al., 1981). This heterogeneity fits with the model that DI genomes are produced by rare aberrant replication events in which the viral polymerase jumps to a distal site on the template strand without releasing the daughter strand yielding an incomplete genome (Lazzarini et al., 1981). DI genomes, while missing large coding regions, must have functional replication initiation and termination sites in the untranslated regions as the interfering ability of DI particles require that the DI genome can be replicated by the viral polymerase (Lazzarini et al., 1981). Accordingly, the model of DI interference

posits that the truncated genomes are replicated by the viral polymerase at higher frequencies than that of longer, intact genomes and thus replication of DI genomes will predominate (Huang, 1973; Huang and Baltimore, 1970).

DI particle-mediated interference is a distinct and highly specific mechanism that reduces the production of infectious virus. Studies with several different viruses have shown that interference occurs at an intracellular site. If DI particles are added to cultured cells well after standard virus, interference still occurs, indicating that DI particles do not simply block cell entry of standard virus by binding cell surface receptors (Cole and Baltimore, 1973; Dutko and Pfau, 1978; Huang and Wagner, 1966). DI particle interference occurs only in cells dually infected with both a DI particle and infectious virus (Kingsbury and Portner, 1970; Stampfer et al., 1971). Consequently, infections at low multiplicities result in greater standard virus production as more cells are not infected with both standard virus and DI particles (Huang and Baltimore, 1970). One of the most fascinating and not well understood aspects of DI particle interference is that DI particles will only interfere with homologous standard virus (Huang, 1973). VSV DI particles do not interfere with unrelated encephalomyocarditis virus ruling out a general cell-mediated antiviral response, such as the interferon response, induced by DI particles as the mechanism of interference (Huang and Wagner, 1966). The specificity of interference also extends to closely related viruses. For example, DI particles from the Indiana serotype of VSV were 100 times more effective at inhibiting standard virus production of the Indiana serotype than of the New Jersey serotype (Huang and Wagner, 1966). A similar observation

has been made for arenaviruses, where treatment with DI particles of the New World arenavirus, Parana, confers complete interference with Parana standard virus production but only partial interference against the related Old World arenavirus, LCMV, and vice versa (Staneck and Pfau, 1974; Welsh et al., 1972). Neither LCMV nor Parana DI particles interfere with the rhabdovirus VSV (Staneck and Pfau, 1974; Welsh et al., 1972).

Arenavirus DI particles share many of the same features as the DI particles from other virus families with a few key exceptions. They interfere with homologous but not heterologous standard virus production (Staneck and Pfau, 1974), contain a full complement of the viral structural proteins (Welsh and Buchmeier, 1979), can be neutralized by immune-specific sera (Welsh et al., 1972), and they cannot reproduce or even synthesize viral proteins without co-infection of a cell with standard helper virus (Welsh and Oldstone, 1977). DI particle-mediated interference is maintained even when arenavirus DI particles are added to cells well after infection with standard virus indicating that interference occurs intracellularly (Dutko and Pfau, 1978). However, unlike many other virus families, no large genomic deletions have been identified and associated with arenavirus DI particles. The only genomic deletions that have been identified for arenaviruses are short truncations within the untranslated regions of the genome segments (Meyer and Southern, 1997). These truncated genomes are present at both acute and persistent stages of infection but are more abundant during persistence during which DI particles predominant relative to standard virus (Lehmann-Grube et al., 1969; Meyer and Southern, 1997; Staneck et al., 1972; Welsh and Oldstone, 1977; Welsh and Pfau, 1972).

Thus, it is assumed that these terminally truncated genomes comprise the genetic material of arenavirus DI particles, but the evidence to assert this assumption is limited. This suggestion that arenavirus DI particle genomes differ by very few nucleotides from their standard virus counterpart does fit with the size and weight of arenavirus DI particles, for which little or no difference from standard virus particles exists (Gschwender and Popescu, 1976; Welsh et al., 1972; Welsh and Oldstone, 1977). In contrast, VSV DI particles, which contain larger genomic deletions, can be readily separated by gradient centrifugation as their buoyant density differs significantly from standard virus due to significant loss in total packaged nucleotides (Huang et al., 1966).

The sensitivity of arenavirus DI particles to ultra-violet (UV) light treatment is drastically reduced relative to standard virus unlike the DI particles of other well-studied viruses including VSV and Sendai virus (Huang et al., 1966; Kingsbury et al., 1970; Welsh et al., 1972). Arenavirus DI particles can sustain UV treatments that readily eliminate any standard virus activity (Damonte et al., 1983; Staneck and Pfau, 1974; Welsh et al., 1972). UV light exposure generates lesions in nucleic acids which ultimately blocks genome transcription and the amount of UV light exposure positively correlates with the frequency of damaged sites within the genome (Abraham and Banerjee, 1976; Michalke and Bremer, 1969). The decreased susceptibility to UV light of arenavirus DI particles suggests that their interfering activity may be less dependent on the genomic material than the DI particles of other viruses (Welsh et al., 1972). Intriguingly, the arenavirus Z protein can render cells refractory to infection with homotypic virus and is a strong inhibitor of the

viral polymerase (Cornu and de la Torre, 2001; Cornu et al., 2004; Jacamo et al., 2003a; Kranzusch and Whelan, 2011). As prevention of the viral polymerase from replicating the standard virus genome is thought to be the primary mechanism of DI particle-mediated interference, a role for the arenavirus Z protein in interference is logical (Lazzarini et al., 1981). Alternatively, the kinetics of UV inactivation for arenaviruses suggest that the size of the functional region for interfering activity is small. Accordingly, UV-mediated damage kinetics can be used to assess the size of the region responsible for interfering activity (Abraham and Banerjee, 1976; Bay and Reichmann, 1979). VSV DI particles are readily inactivated by UV light indicating a large functional region required for DI particle-mediated interference (Bay and Reichmann, 1979). Alternatively, certain strains of Sinbis virus DI particles retain interfering activity following much longer UV exposures, like arenaviruses, indicating that only a small region of the DI genome is required for interference (Kowal and Stollar, 1980). Finally, the relative resistance of arenavirus DI particles to UV light has been used to obtain functionally pure DI particle preparations so that they can be studied in the absence of standard virus (Welsh et al., 1972).

RNA viruses, other than retroviruses, lack the ability to establish latent infections through viral genome integration into a host cell's DNA, like retroviruses can, or to be maintained in episomes like that of DNA viruses (Boldogh et al., 1996; Perrault, 1981). Nevertheless, many RNA viruses possess the ability to maintain persistent infections. The mechanisms that permit this persistence are multifaceted, but a role for DI particles in persistent infection of some RNA viruses has been demonstrated *in vitro* (Ahmed and

Graham, 1977; Andzhaparidze et al., 1982; Carthy et al., 1981; Holland and Villarreal, 1974; Holland et al., 1976; Kawai et al., 1975; Popescu and Lehmann-Grube, 1977; Roux and Holland, 1979; Schmaljohn and Blair, 1977; Weiss et al., 1980). Cultures of persistently infected cells with viruses from different families typically have a high percentage of cells infected and express cytoplasmic viral antigen but reduced cell surface viral antigen compared to acutely infected cells (Holland et al., 1980; Roux and Waldvogel, 1983; Welsh and Oldstone, 1977). The persistently infected cultures are resistant to superinfection by homologous virus but permissive to heterologous virus and produce little standard virus (Holland et al., 1980). The reduction in cell surface antigen combined with decreased release of standard virus caused by DI particles are thought to be major factors permitting persistent infection whereby active viral replication and protein expression is permitted and balanced by the contribution of DI particles in reducing immune response to infection and protecting infected cells (Roux and Waldvogel, 1983; Welsh and Oldstone, 1977).

While the role of DI particles during persistent infections for numerous viruses *in vitro* is fairly well-established, their significance *in vivo* is less clear. DI particles have been detected in experimental persistent infections *in vivo* for some viruses including LCMV, VSV and reovirus but the lack of sensitive assays for detecting DI particles for many virus families has limited the ability to detect low levels of DI particles in animals (Barrett and Dimmock, 1986; Cave et al., 1984; Popescu and Lehmann-Grube, 1977; Spandidos and Graham, 1976). There is substantial evidence, however, demonstrating that DI particles

can protect against pathology or delay or prevent death related to viral infection *in vivo* (Barrett and Dimmock, 1986; Dimmock and Kennedy, 1978; Doyle and Holland, 1973; Help and Coto, 1980; Holland and Doyle, 1973; Spandidos and Graham, 1976; Welsh et al., 1977). This protection *in vivo* has been shown, at least in some cases, to be specific to the interfering genomes in DI particles and not to a non-specific host immune response (Barrett and Dimmock, 1986). In particular, antibody-mediated protection was ruled out by demonstrating that biologically active VSV DI particles, but not UV-inactivated DI or standard virus particles protected mice against lethal VSV challenge despite the maintenance of protein antigenicity following UV treatment (Jones and Holland, 1980). Furthermore, studies with Semliki Forest virus (SFV) have shown that the DI particle-mediated protection does not extend to heterologous viruses and that infected mice protected by DI SFV lack immune infiltrates, both providing evidence against immune involvement in protection (Crouch et al., 1982; Dimmock and Kennedy, 1978). In the case of arenaviruses, DI particles have been detected at acute and persistent stages during *in vivo* infections, and have been shown to elicit protection against standard virus challenge *in vivo* (Help and Coto, 1980; Popescu and Lehmann-Grube, 1977; Staneck and Pfau, 1974; Welsh et al., 1977). While these studies help to support the idea that DI particles are involved in the establishment and maintenance of natural persistent infections of RNA viruses, as has long been hypothesized for arenaviruses, the evidence falls substantially short of confirming this hypothesis.

1.5. The ESCRT Pathway and Late Domains

The endosomal sorting complex required for transport (ESCRT) pathway, also known as the vacuolar protein sorting (VPS) pathway in yeast, is a highly conserved system that mediates specific forms of membrane biogenesis in cells. The ESCRT pathway drives reverse topology membrane biogenesis events in which the membrane forms vesicles in a direction away from the cytoplasm where the membrane must be constricted towards the cytoplasm and is the only pathway known to mediate such events (Schoneberg et al., 2017; Votteler and Sundquist, 2013). The ESCRT pathway was originally discovered in yeast where disruption of certain VPS/ESCRT proteins resulted in an aberrant endosome-like structure, called a class E compartment, and the failure to deliver endocytosed integral plasma membrane proteins to the vacuole (Raymond et al., 1992; Rieder et al., 1996). The class E compartment results from the inability of intralumenal vesicles to bud into late endosomes and form multivesicular bodies (MVB) (Hurley, 2008; Katzmann et al., 2002). In addition to functioning in MVB formation, the ESCRT pathway is also critical for several other functions in host cells including cytokinesis (Carlton and Martin-Serrano, 2007; Morita et al., 2007), shedding of microvesicles at the plasma membrane (Nabhan et al., 2012), formation of exosomes (Hurley, 2015; Raposo and Stoorvogel, 2013), and micro- and macro-autophagy (Lee et al., 2007; Rusten et al., 2007; Sahu et al., 2011), as well as a growing list of other endogenous functions (Hurley, 2015). In 2001 it was demonstrated that the ESCRT pathway is required for HIV-1 virus release at the plasma membrane (Martin-Serrano et al., 2001). Since then, a wide range of enveloped viruses have been shown to exploit the ESCRT pathway to drive virus release at the plasma

membrane as well as for some viruses that bud into internal compartments (Tabata et al., 2016; Votteler and Sundquist, 2013). The function of the ESCRT pathway in these various processes is to cleave the thin membrane stalk formed during vesicle formation to permit separation of the newly formed vesicle from its parent membrane (Schoneberg et al., 2017). ESCRT proteins also contribute to the initial membrane curvature for MVB formation (Hanson et al., 2008). In other ESCRT-driven processes, however, adaptor proteins such as HIV-1 Gag for virus budding or non-ESCRT host proteins are thought to drive membrane curvature without help from ESCRT proteins (Campbell and Rein, 1999; Votteler and Sundquist, 2013).

The ESCRT pathway is composed of four protein complexes called ESCRT-0, -I, -II, and –III and the accessory proteins ALIX and VPS4 which are recruited in a sequential fashion to drive membrane scission. ESCRT-0, -I and –II function to assemble a stable scaffold at target membrane sites and to recruit the membrane-cleaving ESCRT-III complex (Schoneberg et al., 2017). ESCRT proteins are initially recruited to membrane sites by adaptor proteins. The ESCRT-0 proteins, Hrs and Stam, serve as adaptors for MVB formation where they bind to ubiquitinated endosomal cargos through their ubiquitin binding domains (Bache et al., 2003a; Bache et al., 2003b; Hanson and Cashikar, 2012). Other adaptor proteins include viral matrix proteins such as HIV-1 Gag or arenavirus Z protein for virus budding (Garrus et al., 2001; Perez et al., 2003), ARRDC1 for microvesicle shedding (Nabhan et al., 2012), CEP55 for cellular abscission (Carlton and Martin-Serrano, 2007), and Syntenin/Syndecan for exosome formation (Baietti et al.,

2012). These adaptor proteins can then recruit early acting ESCRT factors from the ESCRT-I complex or the accessory protein ALIX through short peptide motifs called late domains that were originally discovered in different viruses (discussed in detail below). These include the TSG101-binding P(S/T)AP found in Hrs and ARRDC1 and the ALIX-binding YPXL found in Syntenin (Bache et al., 2003a; Baietti et al., 2012; Nabhan et al., 2012). A unique ALIX-binding motif in CEP55 can also bridge the target membrane and cargo to early acting ESCRT factors (Carlton and Martin-Serrano, 2007). Each ESCRT-I complex contains a single copy of TSG101 that provides a direct link to some of the ESCRT adaptor proteins, as well as VPS28, which links ESCRT-I to the ESCRT-II protein, VPS36, through its C-terminal domain (Gill et al., 2007; Kostelansky et al., 2006). Once the ESCRT-II complex is recruited to membrane scission sites, another ESCRT-II protein, VPS25, initiates ESCRT-III complex formation through binding to CHMP6 (Carlson and Hurley, 2012; Im et al., 2009). CHMP6 can subsequently recruit another ESCRT-III protein CHMP4 which together with CHMP3 drives membrane scission (Carlson and Hurley, 2012; Im et al., 2009; Wollert et al., 2009). ESCRT adaptor proteins that recruit ALIX can bypass the ESCRT-I/II complex as ALIX interacts directly with the ESCRT-III protein CHMP4 (Kim et al., 2005; McCullough et al., 2008). Following membrane scission, the ESCRT-III protein, CHMP2, recruits the AAA ATPase VPS4, an ESCRT accessory protein, which disassembles and recycles the ESCRT complex (Obita et al., 2007; Stuchell-Brereton et al., 2007; Wollert et al., 2009).

Not all ESCRT adaptors appear to engage all ESCRT complexes starting with ESCRT-0 as with the sorting of ubiquitinated integral membrane proteins in MVB formation. ARRDC1 has a PSAP motif which directly binds Tsg101 allowing microvesicle shedding to bypass ESCRT-0 (Kuo and Freed, 2012; Nabhan et al., 2012). Syntenin and CEP55 can both directly bind ALIX, albeit through different types of motifs, permitting direct recruitment of ESCRT-III (Baietti et al., 2012; Lee et al., 2008). The ESCRT pathway has also evolved layers of redundancy to ensure recruitment of the ESCRT-III scission machinery for cellular processes. CEP55, in addition to directly binding ALIX, also directly interacts with Tsg101 thus employing a pathway that utilizes ESCRT-I (Lee et al., 2008). ALIX can also directly interact with TSG101 via the PSAP motif in ALIX raising the possibility that ALIX may provide a direct link to both ESCRT-I and ESCRT-III (Martin-Serrano et al., 2003; von Schwedler et al., 2003). Finally, ubiquitin-conjugated proteins may also play a role in recruitment of the ESCRT pathway as many ESCRT-I/II components contain ubiquitin binding domains (Shields and Piper, 2011). This could provide a means of bypassing earlier ESCRT complexes or acting as a redundant pathway for which to recruit the ESCRT-III membrane scission machinery.

Viruses hijack the ESCRT pathway by encoding motifs that mimic those found in various ESCRT pathway components. These motifs are called late domains because their disruption results in arrest of virus production at late steps in the virus life cycle, specifically virus release. The first late domain was discovered in HIV-1 where mutations to its PSAP motif in the Gag protein resulted in budded virions that were still attached to

the cell's plasma membrane by a thin membrane stalk (Göttlinger et al., 1991; Huang et al., 1995). Since that initial discovery, a diverse range of viruses have been shown to encode functional P(S/T)AP late domains including many other retroviruses, some arenaviruses, filoviruses, and the non-enveloped Bluetongue virus (Martin-Serrano et al., 2001; Perez et al., 2003; Strecker et al., 2003; Urata et al., 2007; Votteler and Sundquist, 2013; Wirblich et al., 2006). These viral motifs mimic the same motif found in the ESCRT-0 protein Hrs and allow the virus to directly recruit Tsg101 (Bache et al., 2003a). Three other types of late domains were subsequently discovered: PPXY which was first discovered in Rous sarcoma virus (RSV), FPIV in paramyxoviruses, and YPXL, first discovered in EIAV (Li et al., 2009a; Parent et al., 1995; Pei et al., 2010; Puffer et al., 1997; Schmitt et al., 2005). While the YPXL late domain was later shown to directly bind the ESCRT accessory protein ALIX, like the cellular protein Syntenin, the mechanism by which the PPXY and FPIV late domains link to the ESCRT machinery is unclear (Li et al., 2009a; Pei et al., 2010; Schmitt et al., 2005; Votteler and Sundquist, 2013).

The PPXY late domain has been found to function in the release of a diverse range of viruses including several retroviruses, filoviruses, Old World arenaviruses, hepatitis B virus and Bluetongue virus (see Table 1.1 for specific references) (reviewed in (Votteler and Sundquist, 2013)). While the mechanism by which this motif recruits the ESCRT pathway is unclear, the PPXY motif has been shown to directly interact with WW domains found in Nedd4 family E3 ubiquitin ligases (Chen and Sudol, 1995; Ingham et al., 2005; Ingham et al., 2004; Staub et al., 1996). Many PPXY-containing viruses, including

filoviruses (Han et al., 2016; Harty et al., 2000; Timmins et al., 2003; Urata and Yasuda, 2010; Yasuda et al., 2003), rhabdoviruses (Harty et al., 1999), and some retroviruses (Blot et al., 2004; Bouamr et al., 2003; Kikonyogo et al., 2001; Medina et al., 2008; Sakurai et al., 2004; Yasuda et al., 2002) have been shown to directly interact with Nedd4-like ubiquitin ligases. Furthermore, the enzymatic activity of these ligases must be intact in order to facilitate virus egress and has been demonstrated specifically for filoviruses and the retroviruses human T-cell leukemia virus (HTLV-1) and RSV (Blot et al., 2004; Han et al., 2016; Martin-Serrano et al., 2005; Sakurai et al., 2004; Segura-Morales et al., 2005; Urata and Yasuda, 2010; Vana et al., 2004; Yasuda et al., 2003). This suggests that these ligases are recruited to sites of viral budding where they ligate ubiquitin onto proteins at that site. Some viral proteins, including Marburg and Ebola virus VP40 (Han et al., 2016; Harty et al., 2000), RSV and HTLV-1 Gag (Blot et al., 2004; Strack et al., 2000; Vana et al., 2004), and VSV M (Harty et al., 2001), are ubiquitinated by these ligases. However, the target of Nedd4 family-mediated ubiquitination in other PPXY-containing viruses is unclear. Additionally, the mechanism by which Nedd4-mediated ubiquitination results in recruitment of the ESCRT-III scission machinery is unknown. Two major hypotheses exist. One posits that a ubiquitin binding domain found in some of the ESCRT-0, -I, or –II components directly binds to the ubiquitinated protein which can in turn recruit the ESCRT-III scission machinery. An alternate possibility is that the arrestin-related trafficking proteins, which also contain a PPXY motif, provide a linkage to the ESCRT-III scission machinery (Rauch and Martin-Serrano, 2011).

Table 1.1. Functional Studies on Viruses Containing PPXY Late Domain-Mutations

Virus	Matrix Protein	PPXY Late Domain	Other Late Domain(s)	Mutation to PPXY	VLP Release	Effect on Viral Release	Cell-to-Cell Spread	Cytopathic Effect	Animal Model	Reference
Rabies Virus	M	PPEY	YVPL	SPEY PAEY PPEA SAEA	nd	Infectious virus ~1% of WT Infectious virus ~10% of WT	Significantly reduced relative to WT at 72hpi (Focus size)	PAEY and PPEA exhibited increased CPE (data not shown)	Lethality eliminated in lethal mouse model	(Wirblich et al., 2008)
Vesicular Stomatitis Virus	M	PPPY	PSAP	PPAY	50% of WT	Infectious virus equal to WT	~85% of WT (Plaque Size)	No difference in CPE (data not shown)	nd	(Jayakar et al., 2000)
				APPY	23% of WT	Infectious virus ~10% of WT @ 24hpi	~50% of WT (Plaque Size)			
				AAPY	17% of WT	Infectious virus ~10% of WT @ 24hpi	~50% of WT (Plaque Size)			
				APPA	16% of WT	Infectious virus ~10% of WT @ 24hpi	nd			
				AAPA	20% of WT	Infectious virus ~10% of WT @ 24hpi	~50% of WT (Plaque Size)			
				PPPA	15% of WT	Infectious virus ~10% of WT @ 24hpi	~50% of WT (Plaque Size)			
				AAPA AAAA	Significantly reduced (not quantified)	Infectious viru reduced ~1 log @ 10hpi	~50% of WT (Plaque Size)	nd	nd	(Irie et al., 2004)
Ebola	VP40	PPEY	PTAP	PAEY AAEY	Significantly reduced (not quantified)	Infectious virus reduced greater than 2 log at 4dpi with low M.O.I.	nd	nd	nd	(Neumann et al., 2005)
				PLEY	Significantly reduced (not quantified)	nd	nd	nd	nd	(Martin-Serrano et al., 2004)
				PPEA	Significantly reduced (not quantified)	Inectious units of MLV/Ebola chimera reduced 2 fold				
Lymphocytic Choriomeningitis Virus	Z	PPPY	none	PPPF	28% of WT	Infectious virus 2.1% of WT @ 24hpi	53% of WT (Plaque Size)	325% of WT @ MOI of 0.01	nd	This Study
				PPPE	7% of WT	Infectious virus 7.2% of WT @ 24hpi	66% of WT (Plaque Size)	278% of WT @ MOI of 0.01		
				PPPA	23% of WT	Infectious virus 2.5% of WT @ 24hpi	52% of WT (Plaque Size)	335% of WT @ MOI of 0.01		

Table 1.1. Functional Studies on Viruses Containing PPXY Late Domain-Mutations

Virus	Matrix Protein	PPXY Late Domain	Other Late Domain(s)	Mutation to PPXY	VLP Release	Effect on Viral Release	Cell-to-Cell Spread	Cytopathic Effect	Animal Model	Reference
Moloney Murine Leukemia Virus	Gag (p12)	PPPY	PSAP YPAL	ΔPPPY	nd	Virus release 20% of WT (reverse transcriptase activity)	nd	nd	nd	(Yuan et al., 2000)
				AAAY	nd	Virus release 50% of WT (western blot of CA)	nd	nd	nd	(Jadwin et al., 2010)
Mason-Pfizer Monkey Virus	Gag (pp24)	PPPY	PSAP	ΔPPPY GPPY PGPY PPGY	nd	Virus release reduced to 3-5% of WT (pulse-chase analysis)	nd	nd	nd	(Yasuda and Hunter, 1998)
				PPPG		No virions detected (pulse-chase analysis)				
				PGAA	nd	Virus release ~20% of WT (western blot of CA)	nd	nd	nd	(Gottwein et al., 2003)
Human T Cell Leukemia Virus	Gag (MA)	PPPY	PTAP	LPPY PLPY PPLY PPPD	nd	No virus detected (Western blot of MA & CA)	nd	nd	nd	(Le Blanc et al., 2002)
				PPPG	nd	Virus release 17% of WT (ELISA of MA)	nd	nd	nd	(Heidecker et al., 2004)
				ΔPPPY	nd	Virus release ~10% of WT (ELISA of MA)	nd	nd	nd	(Heidecker et al., 2007)
Rous Sarcoma Virus	Gag	PPPY	YPSL	APPY	nd	Virus release ~30% of WT (western blot of CA)	Reduced (flow cytometry)	nd	nd	(Dilley et al., 2010)
				AAAA		Virus release below limit of detection (western blot of CA)	nd			
Hepatitus B Virus	Core	PPAY	None	LPAY	nd	Infectious titer of chimeric MLV 13% of WT	nd	nd	nd	(Garcia et al., 2013)
				PPAF		Infectious titer of chimeric MLV 15% of WT				
				PPAA		Infectious titer of chimeric MLV 16% of WT				

Table 1.1. Functional Studies on Viruses Containing PPXY Late Domain-Mutations

Virus	Matrix Protein	PPXY Late Domain	Other Late Domain(s)	Mutation to PPXY	VLP Release	Effect on Viral Release	Cell-to-Cell Spread	Cytopathic Effect	Animal Model	Reference
Bovine Leukemia Virus	Gag	PPPY	None	AAAA	42% of WT in COS-1 cells. 28% of WT in 293T cells	nd	nd	nd	nd	(Wang et al., 2002)
				APPY	42% of WT in COS-1 cells. 26% of WT in 293T cells.					
				PAPY	45% of WT in COS-1 cells.					
				PPAY	Reduced but not quantified.					
				PPPA	Reduced but not quantified.					
Koala retrovirus	Gag	PPPY	PSAP	nd	nd	nd	nd	nd	nd	(Shimode et al., 2013)
Bluetongue virus	NS3	PPRY	PSAP	AARY	Reduced release in HIV Gag fusion system, but not quantified.	nd	nd	nd	nd	(Wirblich et al., 2006)

1.6. Summary

Arenaviruses, like any other virus, must replicate and release progeny virions from infected cells. Knowledge of the molecular mechanisms that drive this process for arenaviruses has grown over the last 15 years, but the exact composition of the cellular components exploited by the virus to facilitate release and the modifications that regulate this process are largely unknown. Several studies have revealed that the viral late domains present in most arenavirus Z proteins are functionally important for Z-mediated release and that some of the ESCRT proteins are also required for release. However, these studies have largely relied on VLP release assays, which do not always faithfully recapitulate all the facets of the virus life cycle. Importantly, arenaviruses produce at least two classes of virus particles: standard, infectious particles and DI particles. In this work, use of a complete virus system to assess the importance of Z protein motifs and the role of the ESCRT pathway was critical for advancing our understanding of arenavirus release.

In the first study, mass spectrometry analysis identified a phosphorylation site on the LCMV Z protein at Y88. This site was of particular interest as it was part of the PPXY late domain in LCMV Z which has been shown to regulate VLP release (Perez et al., 2003). To build on this earlier finding on the late domain and assess the function of this phosphorylation site specifically, we generated recombinant viruses with mutations at Y88 that either mimicked the charge of a phosphate group or blocked phosphorylation. This work led to the discovery that the PPXY late domain and the cellular ESCRT pathway that it recruits are both required for the production of DI particles but are dispensable for standard virus. This is the first example of a virus using separate release pathways for

standard and DI particles. This also indicates that there must be other motifs in LCMV Z and additional cellular components responsible for standard virus production that are yet to be discovered. Finally, this work suggests that host cells may be able to dynamically regulate DI particle production by host kinase-mediated phosphorylation at Y88.

In the second study, a phosphorylation site at S41 in LCMV Z was discovered using mass spectrometry. This site lies outside of any motif known to function in Z protein-mediated release. Recombinant viruses harboring mutations to the S41 phosphorylation site were used to assess the overall significance of this site. While the production of standard virus and DI particles was not impacted by a non-phosphorylatable alanine substitution (S41A), a phosphomimetic substitution at this site (S41D) decreased the release of both. The impact on DI particle release was more substantial, however. This revealed that S41 is a novel regulatory motif for Z-mediated virus release and provided further evidence that host cells employ kinases to regulate this process.

In the third study, the host protein interaction network of the JUNV Z protein was mapped and the host protein content of JUNV C#1 virions was uncovered using mass spectrometry. A variety of functional host protein groups were enriched in these conditions including several ESCRT components. Functional importance of several representative proteins was assessed using siRNA screening which revealed several novel host proteins that are required for efficient arenavirus infection. Finally, this study revealed that, unlike LCMV, JUNV standard virus production requires a functional ESCRT pathway.

References

Abraham, G., and Banerjee, A.K. (1976). Sequential transcription of the genes of vesicular stomatitis virus. Proc Natl Acad Sci U S A *73*, 1504-1508.

Ahmed, R., and Graham, A.F. (1977). Persistent Infections in L Cells with Temperature-Sensitive Mutants of Reovirus. J Virol *23*, 250-262.

Andzhaparidze, O.G., Boriskin, Y.S., Bogomolova, N.N., and Drynov, I.D. (1982). Mumps Virus-persistently Infected Cell Cultures Release Defective Interfering Virus Particles. J Gen Virol *63*, 499-503.

Armstrong, C., and Lillie, R.D. (1934). Experimental Lymphocytic Choriomeningitis of Monkeys and Mice Produced by a Virus Encountered in Studies of the 1933 St. Louis Encephalitis Epidemic. Public Health Reports (1896-1970) *49*, 1019-1027.

Auperin, D.D., Sasso, D.R., and McCormick, J.B. (1986). Nucleotide sequence of the glycoprotein gene and intergenic region of the Lassa virus S genome RNA. Virology *154*, 155-167.

Bache, K.G., Brech, A., Mehlum, A., and Stenmark, H. (2003a). Hrs regulates multivesicular body formation via ESCRT recruitment to endosomes. The Journal of Cell Biology *162*, 435-442.

Bache, K.G., Raiborg, C., Mehlum, A., and Stenmark, H. (2003b). STAM and Hrs Are Subunits of a Multivalent Ubiquitin-binding Complex on Early Endosomes. J Biol Chem *278*, 12513-12521.

Baietti, M.F., Zhang, Z., Mortier, E., Melchior, A., Degeest, G., Geeraerts, A., Ivarsson, Y., Depoortere, F., Coomans, C., Vermeiren, E.*, et al.* (2012). Syndecan-syntenin-ALIX regulates the biogenesis of exosomes. Nat Cell Biol *14*, 677-685.

Barrett, A.D.T., and Dimmock, N.J. (1986). Defective Interfering Viruses and Infections of Animals. In Current Topics in Microbiology and Immunology, A. Clarke, R.W. Compans, M. Cooper, H. Eisen, W. Goebel, H. Koprowski, F. Melchers, M. Oldstone, R. Rott, P.K. Vogt*, et al.*, eds. (Berlin, Heidelberg: Springer Berlin Heidelberg), pp. 55-84.

Barton, L.L., Mets, M.B., and Beauchamp, C.L. (2002). Lymphocytic choriomeningitis virus: Emerging fetal teratogen. American Journal of Obstetrics & Gynecology *187*, 1715-1716.

Bay, P.H., and Reichmann, M.E. (1979). UV inactivation of the biological activity of defective interfering particles generated by vesicular stomatitis virus. J Virol *32*, 876-884.

Bellett, A.J., and Cooper, P.D. (1959). Some properties of the transmissible interfering component of vesicular stomatitis virus preparations. Journal of general microbiology *21*, 498-509.

Blot, V., Perugi, F., Gay, B., Prévost, M.-C., Briant, L., Tangy, F., Abriel, H., Staub, O., Dokhélar, M.-C., and Pique, C. (2004). Nedd4.1-mediated ubiquitination and subsequent recruitment of Tsg101 ensure HTLV-1 Gag trafficking towards the multivesicular body pathway prior to virus budding. J Cell Sci *117*, 2357-2367.

Boldogh, I., Albrecht, T., and Porter, D.D. (1996). Persistent Viral Infections. In Medical Microbiology, S. Baron, ed. (Galveston (TX): University of Texas Medical Branch at Galveston
The University of Texas Medical Branch at Galveston.).

Bonthius, D.J. (2012). Lymphocytic choriomeningitis virus: An under-recognized cause of neurologic disease in the fetus, child, and adult. Seminars in pediatric neurology *19*, 89-95.

Borden, K.L.B., Campbelldwyer, E.J., Carlile, G.W., Djavani, M., and Salvato, M.S. (1998a). Two RING finger proteins, the oncoprotein PML and the arenavirus Z protein, colocalize with the nuclear fraction of the ribosomal P proteins. J Virol *72*, 3819-3826.

Borden, K.L.B., Dwyer, E.J.C., and Salvato, M.S. (1998b). An arenavirus RING (zinc-binding) protein binds the oncoprotein promyelocyte leukemia protein (PML) and relocates PML nuclear bodies to the cytoplasm. J Virol *72*, 758-766.

Borrow, P., and Oldstone, M.B.A. (1994). Mechanism of Lymphocytic Choriomeningitis Virus Entry into Cells. Virology *198*, 1-9.

Bouamr, F., Melillo, J.A., Wang, M.Q., Nagashima, K., de Los Santos, M., Rein, A., and Goff, S.P. (2003). PPPYEPTAP Motif Is the Late Domain of Human T-Cell Leukemia Virus Type 1 Gag and Mediates Its Functional Interaction with Cellular Proteins Nedd4 and Tsg101. J Virol *77*, 11882-11895.

Buchmeier, M.J., de la Torre, J.C., and Peters, C.J. (2007). *Arenaviridae*: The Viruses and Their Replication. In Fields Virology, D.M. Knipe, P.M. Howley, D.E. Griffin, R.A. Lamb, M.A. Martin, B. Roizman, and S.E. Straus, eds. (Philadelphia: Wolters Kluwer Health/Lippincott Williams & Wilkins), pp. 1791-1827.

Burns, J.W., and Buchmeier, M.J. (1993). Glycoproteins of the Arenaviruses. In The Arenaviridae, M.S. Salvato, ed. (New York: Plenum Press), pp. 17-35.

Byrd, R., Cone, L., Commess, B., Williams-Herman, D., Rowland, J., Lee, B., Fitzgibbons, M., Glaser, C., Jay, M., Fritz, C.*, et al.* (2000). Fatal illnesses associated with a new world

arenavirus--California, 1999-2000. MMWR Morbidity and mortality weekly report *49*, 709-711.

Campbell Dwyer, E.J., Lai, H., MacDonald, R.C., Salvato, M.S., and Borden, K.L.B. (2000). The Lymphocytic Choriomeningitis Virus RING Protein Z Associates with Eukaryotic Initiation Factor 4E and Selectively Represses Translation in a RING-Dependent Manner. J Virol *74*, 3293-3300.

Campbell, S., and Rein, A. (1999). In Vitro Assembly Properties of Human Immunodeficiency Virus Type 1 Gag Protein Lacking the p6 Domain. J Virol *73*, 2270-2279.

Cao, W., Henry, M.D., Borrow, P., Yamada, H., Elder, J.H., Ravkov, E.V., Nichol, S.T., Compans, R.W., Campbell, K.P., and Oldstone, M.B.A. (1998). Identification of α-Dystroglycan as a Receptor for Lymphocytic Choriomeningitis Virus and Lassa Fever Virus. Science *282*, 2079-2081.

Capul, A.A., Perez, M., Burke, E., Kunz, S., Buchmeier, M.J., and de la Torre, J.C. (2007). Arenavirus Z-glycoprotein association requires Z myristoylation but not functional RING or late domains. J Virol *81*, 9451-9460.

Carlson, L.-A., and Hurley, J.H. (2012). In vitro reconstitution of the ordered assembly of the endosomal sorting complex required for transport at membrane-bound HIV-1 Gag clusters. Proceedings of the National Academy of Sciences *109*, 16928-16933.

Carlton, J.G., and Martin-Serrano, J. (2007). Parallels Between Cytokinesis and Retroviral Budding: A Role for the ESCRT Machinery. Science *316*, 1908-1912.

Carthy, M.M., Wolinsky, J.S., and Lazzarini, R.A. (1981). A persistent infection of Vero cells by egg-adapted mumps virus. Virology *114*, 343-356.

Casabona, J.C., Macleod, J.M.L., Loureiro, M.E., Gomez, G.A., and Lopez, N. (2009). The RING Domain and the L79 Residue of Z Protein Are Involved in both the Rescue of Nucleocapsids and the Incorporation of Glycoproteins into Infectious Chimeric Arenavirus-Like Particles. J Virol *83*, 7029-7039.

Cave, D.R., Hagen, F.S., Palma, E.L., and Huang, A.S. (1984). Detection of vesicular stomatitis virus RNA and its defective-interfering particles in individual mouse brains. J Virol *50*, 86-91.

Charrel, R.N., and Lamballerie, X.d. (2003). Arenaviruses other than Lassa virus. Antiviral Research *57*, 89-100.

Chen, H.I., and Sudol, M. (1995). The WW domain of Yes-associated protein binds a proline-rich ligand that differs from the consensus established for Src homology 3-binding modules. Proceedings of the National Academy of Sciences *92*, 7819-7823.

Childs, J.E., and Peters, C.J. (1993). Ecology and Epidemiology of Arenaviruses and Their Hosts. In The Arenaviridae, M.S. Salvato, ed. (New York: Plenum Press), pp. 331-384.

Clegg, J.C.S., Wilson, S.M., and Oram, J.D. (1991). Nucleotide sequence of the S RNA of Lassa virus (Nigerian strain) and comparative analysis of arenavirus gene products. Virus Research *18*, 151-164.

Cole, C.N., and Baltimore, D. (1973). Defective interfering particles of poliovirus: III. Interference and enrichment. Journal of Molecular Biology *76*, 345-361.

Cornu, T.I., and de la Torre, J.C. (2001). RING finger Z protein of lymphocytic choriomeningitis virus (LCMV) inhibits transcription and RNA replication of an LCMV S-segment minigenome. J Virol *75*, 9415-9426.

Cornu, T.I., and de la Torre, J.C. (2002). Characterization of the arenavirus RING finger Z protein regions required for Z-mediated inhibition of viral RNA synthesis. J Virol *76*, 6678-6688.

Cornu, T.I., Feldmann, H., and de la Torre, J.C. (2004). Cells expressing the RING finger Z protein are resistant to arenavirus infection. J Virol *78*, 2979-2983.

Crouch, C.F., Mackenzie, A., and Dimmock, N.J. (1982). The Effect of Defective-Interfering Semliki Forest Virus on the Histopathology of Infection with Virulent Semliki Forest Virus in Mice. The Journal of infectious diseases *146*, 411-416.

Cummins, D., McCormick, J.B., Bennett, D., and et al. (1990). Acute Sensorineural Deafness in Lassa Fever. JAMA *264*, 2093-2096.

Damonte, E.B., Mersich, S.E., and Coto, C.E. (1983). Response of cells persistently infected with arenaviruses to superinfection with homotypic and heterotypic viruses. Virology *129*.

Davis, A.R., Hiti, A.L., and Nayak, D.P. (1980). Influenza Defective Interfering Viral RNA is Formed by Internal Deletion of Genomic RNA. Proc Natl Acad Sci USA *77*, 215-219.

Delgado, S., Erickson, B.R., Agudo, R., Blair, P.J., Vallejo, E., Albariño, C.G., Vargas, J., Comer, J.A., Rollin, P.E., Ksiazek, T.G.*, et al.* (2008b). Chapare Virus, a Newly Discovered Arenavirus Isolated from a Fatal Hemorrhagic Fever Case in Bolivia. PLOS Pathogens *4*, e1000047.

Dilley, K.A., Gregory, D., Johnson, M.C., and Vogt, V.M. (2010). An LYPSL Late Domain in the Gag Protein Contributes to the Efficient Release and Replication of Rous Sarcoma Virus. J Virol *84*, 6276-6287.

Dimmock, N.J., and Kennedy, S.I.T. (1978). Prevention of Death in Semliki Forest Virus-Infected Mice by Administration of Defective-Interfering Semliki Forest Virus. J Gen Virol *39*, 231-242.

Djavani, M., Lukashevich, I.S., Sanchez, A., Nichol, S.T., and Salvato, M.S. (1997). Completion of the Lassa Fever Virus Sequence and Identification of a RING Finger Open Reading Frame at the L RNA 5′ End. Virology *235*, 414-418.

Djavani, M., Topisirovic, I., Zapata, J.C., Sadowska, M., Yang, Y., Rodas, J., Lukashevich, I.S., Bogue, C.W., Pauza, C.D., Borden, K.L.B*., et al.* (2005). The proline-rich homeodomain (PRH/HEX) protein is down-regulated in liver during infection with lymphocytic choriomeningitis virus. J Virol *79*, 2461-2473.

Downs, W.G., Anderson, C.R., Spence, L., Aitken, T.H.G., and Greenhall, A.H. (1963). Tacaribe Virus, a New Agent Isolated from Artibeus Bats and Mosquitoes in Trinidad, West Indies. The American Journal of Tropical Medicine and Hygiene *12*, 640-646.

Doyle, M., and Holland, J.J. (1973). Prophylaxis and Immunization in Mice by Use of Virus-Free Defective T Particles to Protect Against Intracerebral Infection by Vesicular Stomatitis Virus. Proc Natl Acad Sci USA *70*, 2105-2108.

Dutko, F.J., and Pfau, C.J. (1978). Arenavirus Defective Interfering Particles Mask the Cell-Killing Potential of Standard Virus. J Gen Virol *38*, 195-208.

Eichler, R., Strecker, T., Kolesnikova, L., ter Meulen, J., Weissenhorn, W., Becker, S., Klenk, H.D., Garten, W., and Lenz, O. (2004). Characterization of the Lassa virus matrix protein Z: electron microscopic study of virus-like particles and interaction with the nucleoprotein (NP). Virus Research *100*, 249-255.

Emonet, S.F., de la Torre, J.C., Domingo, E., and Sevilla, N. (2009a). Arenavirus genetic diversity and its biological implications. Infection, Genetics and Evolution *9*, 417-429.

Enria, D.A., Briggiler, A.M., and Sánchez, Z. (2008b). Treatment of Argentine hemorrhagic fever. Antiviral Research *78*, 132-139.

Epstein, D.A., Herman, R.C., Chien, I., and Lazzarini, R.A. (1980). Defective interfering particle generated by internal deletion of the vesicular stomatitis virus genome. J Virol *33*, 818-829.

Fan, L., Briese, T., and Lipkin, W.I. (2010). Z Proteins of New World Arenaviruses Bind RIG-I and Interfere with Type I Interferon Induction. J Virol *84*, 1785-1791.

Fehling, S., Lennartz, F., and Strecker, T. (2012). Multifunctional Nature of the Arenavirus RING Finger Protein Z. Viruses *4*, 2973-3011.

Fischer, S.A., Graham, M.B., Kuehnert, M.J., Kotton, C.N., Srinivasan, A., Marty, F.M., Comer, J.A., Guarner, J., Paddock, C.D., DeMeo, D.L.*, et al.* (2006). Transmission of Lymphocytic Choriomeningitis Virus by Organ Transplantation. N Engl J Med *354*, 2235-2249.

Garcia, M.L., Reynolds, T.D., Mothes, W., and Robek, M.D. (2013). Functional Characterization of the Putative Hepatitis B Virus Core Protein Late Domain Using Retrovirus Chimeras. PLoS ONE *8*, e72845.

Garrus, J.E., von Schwedler, U.K., Pornillos, O.W., Morham, S.G., Zavitz, K.H., Wang, H.E., Wettstein, D.A., Stray, K.M., Côté, M., Rich, R.L.*, et al.* (2001). Tsg101 and the Vacuolar Protein Sorting Pathway Are Essential for HIV-1 Budding. Cell *107*, 55-65.

Gill, D.J., Teo, H., Sun, J., Perisic, O., Veprintsev, D.B., Emr, S.D., and Williams, R.L. (2007). Structural insight into the ESCRT-I/-II link and its role in MVB trafficking. The EMBO Journal *26*, 600-612.

Göttlinger, H.G., Dorfman, T., Sodroski, J.G., and Haseltine, W.A. (1991). Effect of mutations affecting the p6 gag protein on human immunodeficiency virus particle release. Proceedings of the National Academy of Sciences *88*, 3195-3199.

Gottwein, E., Bodem, J., Müller, B., Schmechel, A., Zentgraf, H., and Kräusslich, H.-G. (2003). The Mason-Pfizer Monkey Virus PPPY and PSAP Motifs Both Contribute to Virus Release. J Virol *77*, 9474-9485.

Groseth, A., Wolff, S., Strecker, T., Hoenen, T., and Becker, S. (2010). Efficient Budding of the Tacaribe Virus Matrix Protein Z Requires the Nucleoprotein. J Virol *84*, 3603-3611.

Gschwender, H.H., and Popescu, M. (1976). Equilibrium Sedimentation of Virus in Density-Gradients of Iodinated Compounds. In Biological Separations in Iondinated Density-Gradient Media, D. Rickwood, ed. (London: Information Retrieval Ltd.), pp. 145-158.

Han, Z., Lu, J., Liu, Y., Davis, B., Lee, M.S., Olson, M.A., Ruthel, G., Freedman, B.D., Schnell, M.J., Wrobel, J.E.*, et al.* (2014). Small Molecule Probes Targeting the Viral PPxY-Host Nedd4 Interface Block Egress of a Broad Range of RNA Viruses. J Virol.

Han, Z., Sagum, C.A., Bedford, M.T., Sidhu, S.S., Sudol, M., and Harty, R.N. (2016). ITCH E3 Ubiquitin Ligase Interacts with Ebola Virus VP40 To Regulate Budding. J Virol *90*, 9163-9171.

Hanson, P.I., and Cashikar, A. (2012). Multivesicular body morphogenesis. Annu Rev Cell Dev Biol *28*, 337-362.

Hanson, P.I., Roth, R., Lin, Y., and Heuser, J.E. (2008). Plasma membrane deformation by circular arrays of ESCRT-III protein filaments. The Journal of Cell Biology *180*, 389-402.

Harty, R.N., Brown, M.E., McGettigan, J.P., Wang, G., Jayakar, H.R., Huibregtse, J.M., Whitt, M.A., and Schnell, M.J. (2001). Rhabdoviruses and the Cellular Ubiquitin-Proteasome System: a Budding Interaction. J Virol *75*, 10623-10629.

Harty, R.N., Brown, M.E., Wang, G., Huibregtse, J., and Hayes, F.P. (2000). A PPxY motif within the VP40 protein of Ebola virus interacts physically and functionally with a ubiquitin ligase: Implications for filovirus budding. Proceedings of the National Academy of Sciences *97*, 13871-13876.

Harty, R.N., Paragas, J., Sudol, M., and Palese, P. (1999). A Proline-Rich Motif within the Matrix Protein of Vesicular Stomatitis Virus and Rabies Virus Interacts with WW Domains of Cellular Proteins: Implications for Viral Budding. J Virol *73*, 2921-2929.

Heidecker, G., Lloyd, P.A., Fox, K., Nagashima, K., and Derse, D. (2004). Late Assembly Motifs of Human T-Cell Leukemia Virus Type 1 and Their Relative Roles in Particle Release. J Virol *78*, 6636-6648.

Heidecker, G., Lloyd, P.A., Soheilian, F., Nagashima, K., and Derse, D. (2007). The role of WWP1-Gag interaction and Gag ubiquitination in assembly and release of human T-cell leukemia virus type 1. J Virol *81*, 9769-9777.

Help, G.I., and Coto, C.E. (1980). [Genesis of interferent particles during the multiplication of Junin virus in vivo]. Medicina (B Aires) *40*, 531-536.

Hetzel, U., Sironen, T., Laurinmäki, P., Liljeroos, L., Patjas, A., Henttonen, H., Vaheri, A., Artelt, A., Kipar, A., Butcher, S.J.*, et al.* (2013). Isolation, Identification, and Characterization of Novel Arenaviruses, the Etiological Agents of Boid Inclusion Body Disease. J Virol *87*, 10918-10935.

Holland, J.J., and Doyle, M. (1973). Attempts to Detect Homologous Autointerference In vivo with Influenza Virus and Vesicular Stomatitis Virus. Infect Immun *7*, 526-531.

Holland, J.J., Kennedy, S.I.T., Semler, B.L., Jones, C.L., Roux, L., and Grabau, E.A. (1980). Defective Interfering RNA Viruses and the Host-Cell Response. In Comprehensive

Virology: Vol 16: Virus-Host Interactions: Viral Invasion, Persistence, and Disease, H. Fraenkael-Conrat, and R.R. Wagner, eds. (Boston, MA: Springer US), pp. 137-192.

Holland, J.J., and Villarreal, L.P. (1974). Persistent noncytocidal vesicular stomatitis virus infections mediated by defective T particles that suppress virion transcriptase. Proc Natl Acad Sci U S A *71*, 2956-2960.

Holland, J.J., Villarreal, L.P., Welsh, R.M., Oldstone, M.B.A., Kohne, D., Lazzarini, R., and Scolnick, E. (1976). Long-Term Persistent Vesicular Stomatitis Virus and Rabies Virus Infection of Cells In Vitro. J Gen Virol *33*, 193-211.

Huang, A.S. (1973). Defective interfering viruses. Annu Rev Microbiol *27*.

Huang, A.S., and Baltimore, D. (1970). Defective Viral Particles and Viral Disease Processes. Nature *226*, 325-327.

Huang, A.S., Greenawalt, J.W., and Wagner, R.R. (1966). Defective T particles of vesicular stomatitis virus. Virology *30*, 161-172.

Huang, A.S., and Wagner, R.R. (1966). Defective T particles of vesicular stomatitis virus. Virology *30*, 173-181.

Huang, M., Orenstein, J.M., Martin, M.A., and Freed, E.O. (1995). p6Gag is required for particle production from full-length human immunodeficiency virus type 1 molecular clones expressing protease. J Virol *69*, 6810-6818.

Hurley, J.H. (2008). ESCRT complexes and the biogenesis of multivesicular bodies. Curr Opin Cell Biol *20*, 4-11.

Hurley, J.H. (2015). ESCRTs are everywhere. The EMBO Journal *34*, 2398-2407.

Im, Y.J., Wollert, T., Boura, E., and Hurley, J.H. (2009). Structure and Function of the ESCRT-II-III Interface in Multivesicular Body Biogenesis. Developmental Cell *17*, 234-243.

Ingham, R.J., Colwill, K., Howard, C., Dettwiler, S., Lim, C.S.H., Yu, J., Hersi, K., Raaijmakers, J., Gish, G., Mbamalu, G.*, et al.* (2005). WW Domains Provide a Platform for the Assembly of Multiprotein Networks. Molecular and Cellular Biology *25*, 7092-7106.

Ingham, R.J., Gish, G., and Pawson, T. (2004). The Nedd4 family of E3 ubiquitin ligases: functional diversity within a common modular architecture. Oncogene *23*.

Irie, T., Licata, J.M., Jayakar, H.R., Whitt, M.A., Bell, P., and Harty, R.N. (2004). Functional Analysis of Late-Budding Domain Activity Associated with the PSAP Motif within the Vesicular Stomatitis Virus M Protein. J Virol *78*, 7823-7827.

Jacamo, R., Lopez, N., Wilda, M., and Franze-Fernandez, M.T. (2003a). Tacaribe Virus Z Protein Interacts with the L Polymerase Protein To Inhibit Viral RNA Synthesis. J Virol *77*, 10383-10393.

Jacamo, R., Lopez, N., Wilda, M., and Franze-Fernández, M.T. (2003b). Tacaribe virus Z protein interacts with the L polymerase protein to inhibit viral RNA synthesis. J Virol *77*.

Jadwin, J.A., Rudd, V., Sette, P., Challa, S., and Bouamr, F. (2010). Late domain-independent rescue of a release-deficient Moloney murine leukemia virus by the ubiquitin ligase itch. J Virol *84*, 704-715.

Jayakar, H.R., Murti, K.G., and Whitt, M.A. (2000). Mutations in the PPPY Motif of Vesicular Stomatitis Virus Matrix Protein Reduce Virus Budding by Inhibiting a Late Step in Virion Release. J Virol *74*, 9818-9827.

Jones, C.L., and Holland, J.J. (1980). Requirements for DI Particle Prophylaxis Against Vesicular Stomatitis Virus Infection in vivo. J Gen Virol *49*, 215-220.

Katzmann, D.J., Odorizzi, G., and Emr, S.D. (2002). Receptor downregulation and multivesicular-body sorting. Nat Rev Mol Cell Biol *3*, 893-905.

Kawai, A., Matsumoto, S., and Tanabe, K. (1975). Characterization of rabies viruses recovered from persistently infected BHK cells. Virology *67*, 520-533.

Keenlyside, R.A., McCormick, J.B., Webb, P.A., Smith, E., Elliott, L., and Johnson, K.M. (1983). Case-Control Study of Mastomys Natalensis and Humans in Lassa Virus-Infected Households in Sierra Leone. The American Journal of Tropical Medicine and Hygiene *32*, 829-837.

Kentsis, A., Dwyer, E.C., Perez, J.M., Sharma, M., Chen, A., Pan, Z.Q., and Borden, K.L.B. (2001). The RING domains of the promyelocytic leukemia protein PML and the arenaviral protein Z repress translation by directly inhibiting translation initiation factor eIF4E. Journal of Molecular Biology *312*, 609-623.

Kikonyogo, A., Bouamr, F., Vana, M.L., Xiang, Y., Aiyar, A., Carter, C., and Leis, J. (2001). Proteins related to the Nedd4 family of ubiquitin protein ligases interact with the L domain of Rous sarcoma virus and are required for gag budding from cells. Proceedings of the National Academy of Sciences *98*, 11199-11204.

Kim, J., Sitaraman, S., Hierro, A., Beach, B.M., Odorizzi, G., and Hurley, J.H. (2005). Structural Basis for Endosomal Targeting by the Bro1 Domain. Developmental Cell *8*, 937-947.

Kingsbury, D.W., and Portner, A. (1970). On the genesis of incomplete Sendai virions. Virology *42*, 872-879.

Kingsbury, D.W., Portner, A., and Darlington, R.W. (1970). Properties of incomplete Sendai virions and subgenomic viral RNAs. Virology *42*, 857-871.

Klewitz, C., Klenk, H.-D., and ter Meulen, J. (2007). Amino acids from both N-terminal hydrophobic regions of the Lassa virus envelope glycoprotein GP-2 are critical for pH-dependent membrane fusion and infectivity. J Gen Virol *88*, 2320-2328.

Kostelansky, M.S., Sun, J., Lee, S., Kim, J., Ghirlando, R., Hierro, A., Emr, S.D., and Hurley, J.H. (2006). Structural and Functional Organization of the ESCRT-I Trafficking Complex. Cell *125*, 113-126.

Kowal, K.J., and Stollar, V. (1980). Differential sensitivity of infectious and defective-interfering particles of sindbis virus to ultraviolet irradiation. Virology *103*, 149-157.

Kranzusch, P.J., and Whelan, S.P.J. (2011). Arenavirus Z protein controls viral RNA synthesis by locking a polymerase–promoter complex. Proceedings of the National Academy of Sciences *108*, 19743-19748.

Kunz, S. (2009). Receptor binding and cell entry of Old World arenaviruses reveal novel aspects of virus–host interaction. Virology *387*, 245-249.

Kuo, L., and Freed, E.O. (2012). ARRDC1 as a mediator of microvesicle budding. Proceedings of the National Academy of Sciences *109*, 4025-4026.

Lazzarini, R.A., Keene, J.D., and Schubert, M. (1981). The origins of defective interfering particles of the negative-strand RNA viruses. Cell *26*.

Le Blanc, I., Prevost, M.C., Dokhelar, M.C., and Rosenberg, A.R. (2002b). The PPPY motif of human T-cell leukemia virus type 1 Gag protein is required early in the budding process. J Virol *76*, 10024-10029.

Lee, H.H., Elia, N., Ghirlando, R., Lippincott-Schwartz, J., and Hurley, J.H. (2008). Midbody Targeting of the ESCRT Machinery by a Noncanonical Coiled Coil in CEP55. Science *322*, 576-580.

Lee, J.-A., Beigneux, A., Ahmad, S.T., Young, S.G., and Gao, F.-B. (2007). ESCRT-III Dysfunction Causes Autophagosome Accumulation and Neurodegeneration. Current Biology *17*, 1561-1567.

Lee, K.J., and de la Torre, J.C. (2002). Reverse genetics of arenaviruses. Curr Top Microbiol Immunol *262*, 175-193.

Lee, K.J., Novella, I.S., Teng, M.N., Oldstone, M.B.A., and de la Torre, J.C. (2000). NP and L Proteins of Lymphocytic Choriomeningitis Virus (LCMV) Are Sufficient for Efficient Transcription and Replication of LCMV Genomic RNA Analogs. J Virol *74*, 3470-3477.

Lehmann-Grube, F., Slenczka, W., and Tees, R. (1969). A persistent and inapparent infection of L cells with the virus of lymphocytic choriomeningitis. J Gen Virol *5*.

Levingston Macleod, J.M., D'Antuono, A., Loureiro, M.E., Casabona, J.C., Gomez, G.A., and Lopez, N. (2011). Identification of two functional domains within the arenavirus nucleoprotein. J Virol *85*.

Li, M., Schmitt, P.T., Li, Z., McCrory, T.S., He, B., and Schmitt, A.P. (2009a). Mumps Virus Matrix, Fusion, and Nucleocapsid Proteins Cooperate for Efficient Production of Virus-Like Particles. J Virol *83*, 7261-7272.

Lopez, N., Jacamo, R., and Franze-Fernandez, M.T. (2001). Transcription and RNA Replication of Tacaribe Virus Genome and Antigenome Analogs Require N and L Proteins: Z Protein Is an Inhibitor of These Processes. J Virol *75*, 12241-12251.

Lukashevich, I.S., Djavani, M., Shapiro, K., Sanchez, A., Ravkov, E., Nichol, S.T., and Salvato, M.S. (1997). The Lassa fever virus L gene: nucleotide sequence, comparison, and precipitation of a predicted 250 kDa protein with monospecific antiserum. J Gen Virol *78*, 547-551.

Maiztegui, J., Fernandez, N., and De Damilano, A. (1979). EFFICACY OF IMMUNE PLASMA IN TREATMENT OF ARGENTINE HÆMORRHAGIC FEVER AND ASSOCIATION BETWEEN TREATMENT AND A LATE NEUROLOGICAL SYNDROME. The Lancet *314*, 1216-1217.

Martin-Serrano, J., Eastman, S.W., Chung, W., and Bieniasz, P.D. (2005). HECT ubiquitin ligases link viral and cellular PPXY motifs to the vacuolar protein-sorting pathway. The Journal of Cell Biology *168*, 89-101.

Martin-Serrano, J., Perez-Caballero, D., and Bieniasz, P.D. (2004). Context-Dependent Effects of L Domains and Ubiquitination on Viral Budding. J Virol *78*, 5554-5563.

Martin-Serrano, J., Yaravoy, A., Perez-Caballero, D., and Bieniasz, P.D. (2003). Divergent retroviral late-budding domains recruit vacuolar protein sorting factors by using alternative adaptor proteins. Proceedings of the National Academy of Sciences *100*, 12414-12419.

Martin-Serrano, J., Zang, T., and Bieniasz, P.D. (2001). HIV-1 and Ebola virus encode small peptide motifs that recruit Tsg101 to sites of particle assembly to facilitate egress. Nat Med *7*, 1313-1319.

Martinez, M.G., Cordo, S.M., and Candurra, N.A. (2007). Characterization of Junín arenavirus cell entry. J Gen Virol *88*, 1776-1784.

McCormick, J.B., King, I.J., Webb, P.A., Scribner, C.L., Craven, R.B., Johnson, K.M., Elliott, L.H., and Belmont-Williams, R. (1986). Lassa Fever. N Engl J Med *314*, 20-26.

McCormick, J.B., Webb, P.A., Krebs, J.W., Johnson, K.M., and Smith, E.S. (1987). A Prospective Study of the Epidemiology and Ecology of Lassa Fever. J Infect Dis *155*, 437-444.

McCullough, J., Fisher, R.D., Whitby, F.G., Sundquist, W.I., and Hill, C.P. (2008). ALIX-CHMP4 interactions in the human ESCRT pathway. Proceedings of the National Academy of Sciences *105*, 7687-7691.

Medina, G., Pincetic, A., Ehrlich, L.S., Zhang, Y., Tang, Y., Leis, J., and Carter, C.A. (2008). Tsg101 can replace Nedd4 function in ASV Gag release but not membrane targeting. Virology *377*, 30-38.

Meyer, B.J., and Southern, P.J. (1997). A novel type of defective viral genome suggests a unique strategy to establish and maintain persistent lymphocytic choriomeningitis virus infections. J Virol *71*, 6757-6764.

Michalke, H., and Bremer, H. (1969). RNA synthesis in Escherichia coli after irradiation with ultraviolet light. Journal of Molecular Biology *41*, 1-23.

Mims, C.A. (1956). Rift Valley Fever virus in mice. IV. Incomplete virus; its production and properties. British journal of experimental pathology *37*, 129-143.

Morita, E., Sandrin, V., Chung, H.-Y., Morham, S.G., Gygi, S.P., Rodesch, C.K., and Sundquist, W.I. (2007). Human ESCRT and ALIX proteins interact with proteins of the midbody and function in cytokinesis. The EMBO Journal *26*, 4215-4227.

Moss, B.A., and Brownlee, G.G. (1981). Sequence of DNA complementry to a small RNA segment of influenza virus A/NT/60/68. Nucleic Acids Research *9*, 1941-1947.

Nabhan, J.F., Hu, R., Oh, R.S., Cohen, S.N., and Lu, Q. (2012). Formation and release of arrestin domain-containing protein 1-mediated microvesicles (ARMMs) at plasma membrane by recruitment of TSG101 protein. Proceedings of the National Academy of Sciences *109*, 4146-4151.

Neuman, B.W., Adair, B.D., Burns, J.W., Milligan, R.A., Buchmeier, M.J., and Yeager, M. (2005). Complementarity in the Supramolecular Design of Arenaviruses and Retroviruses Revealed by Electron Cryomicroscopy and Image Analysis. J Virol *79*, 3822-3830.

Neumann, G., Ebihara, H., Takada, A., Noda, T., Kobasa, D., Jasenosky, L.D., Watanabe, S., Kim, J.H., Feldmann, H., and Kawaoka, Y. (2005a). Ebola virus VP40 late domains are not essential for viral replication in cell culture. J Virol *79*.

Obita, T., Saksena, S., Ghazi-Tabatabai, S., Gill, D.J., Perisic, O., Emr, S.D., and Williams, R.L. (2007). Structural basis for selective recognition of ESCRT-III by the AAA ATPase Vps4. Nature *449*, 735-739.

Ortiz-Riano, E., Cheng, B.Y.H., de la Torre, J.C., and Martinez-Sobrido, L. (2011). The C-Terminal Region Of Lymphocytic Choriomeningitis Virus Nucleoprotein Contains Distinct And Segregable Functional Domains Involved In NP-Z Interaction And Counteraction Of The Type I IFN Response. J Virol, JVI.05834-05811.

Parent, L.J., Bennett, R.P., Craven, R.C., Nelle, T.D., Krishna, N.K., Bowzard, J.B., Wilson, C.B., Puffer, B.A., Montelaro, R.C., and Wills, J.W. (1995). Positionally independent and exchangeable late budding functions of the Rous sarcoma virus and human immunodeficiency virus Gag proteins. J Virol *69*, 5455-5460.

Pei, Z., Bai, Y., and Schmitt, A.P. (2010). PIV5 M protein interaction with host protein angiomotin-like 1. Virology *397*, 155-166.

Perez, M., Craven, R.C., and de la Torre, J.C. (2003). The small RING finger protein Z drives arenavirus budding: Implications for antiviral strategies. Proc Natl Acad Sci USA *100*, 12978-12983.

Perez, M., Greenwald, D.L., and de La Torre, J.C. (2004a). Myristoylation of the RING finger Z protein is essential for arenavirus budding. J Virol *78*, 11443-11448.

Perrault, J. (1981). Origin and replication of defective interfering particles. Curr Top Microbiol Immunol *93*, 151-207.

Popescu, M., and Lehmann-Grube, F. (1977). Defective interfering particles in mice infected with lymphocytic choriomeningitis virus. Virology *77*, 78-83.

Price, M.E., Fisher-Hoch, S.P., Craven, R.B., and McCormick, J.B. (1988). A prospective study of maternal and fetal outcome in acute Lassa fever infection during pregnancy. BMJ : British Medical Journal *297*, 584-587.

Puffer, B.A., Parent, L.J., Wills, J.W., and Montelaro, R.C. (1997). Equine infectious anemia virus utilizes a YXXL motif within the late assembly domain of the Gag p9 protein. J Virol *71*, 6541-6546.

Quirin, K., Eschli, B., Scheu, I., Poort, L., Kartenbeck, J., and Helenius, A. (2008). Lymphocytic choriomeningitis virus uses a novel endocytic pathway for infectious entry via late endosomes. Virology *378*, 21-33.

Radoshitzky, S.R., Abraham, J., Spiropoulou, C.F., Kuhn, J.H., Nguyen, D., Li, W., Nagel, J., Schmidt, P.J., Nunberg, J.H., Andrews, N.C.*, et al.* (2007). Transferrin receptor 1 is a cellular receptor for New World haemorrhagic fever arenaviruses. Nature *446*, 92-96.

Radoshitzky, S.R., Bào, Y., Buchmeier, M.J., Charrel, R.N., Clawson, A.N., Clegg, C.S., DeRisi, J.L., Emonet, S., Gonzalez, J.-P., Kuhn, J.H.*, et al.* (2015). Past, present, and future of arenavirus taxonomy. Archives of Virology *160*, 1851-1874.

Raposo, G., and Stoorvogel, W. (2013). Extracellular vesicles: Exosomes, microvesicles, and friends. The Journal of Cell Biology *200*, 373-383.

Rauch, S., and Martin-Serrano, J. (2011). Multiple Interactions between the ESCRT Machinery and Arrestin-Related Proteins: Implications for PPXY-Dependent Budding. J Virol *85*, 3546-3556.

Raymond, C.K., Howald-Stevenson, I., Vater, C.A., and Stevens, T.H. (1992). Morphological classification of the yeast vacuolar protein sorting mutants: evidence for a prevacuolar compartment in class E vps mutants. Mol Biol Cell *3*, 1389-1402.

Rieder, S.E., Banta, L.M., Köhrer, K., McCaffery, J.M., and Emr, S.D. (1996). Multilamellar endosome-like compartment accumulates in the yeast vps28 vacuolar protein sorting mutant. Mol Biol Cell *7*, 985-999.

Riviere, Y., Ahmed, R., Southern, P.J., Buchmeier, M.J., Dutko, F.J., and Oldstone, M.B. (1985). The S RNA segment of lymphocytic choriomeningitis virus codes for the nucleoprotein and glycoproteins 1 and 2. J Virol *53*, 966-968.

Roux, L., and Holland, J.J. (1979). Role of defective interfering particles of sendai virus in persistent infections. Virology *93*, 91-103.

Roux, L., and Waldvogel, F.A. (1983). Defective interfering particles of Sendai virus modulate HN expression at the surface of infected BHK cells. Virology *130*, 91-104.

Rowe, W.P., Murphy, F.A., Bergold, G.H., Casals, J., Hotchin, J., Johnson, K.M., Lehmann-Grube, F., Mims, C.A., Traub, E., and Webb, P.A. (1970). Arenoviruses: Proposed Name for a Newly Defined Virus Group. J Virol *5*, 651-652.

Rusten, T.E., Vaccari, T., Lindmo, K., Rodahl, L.M.W., Nezis, I.P., Sem-Jacobsen, C., Wendler, F., Vincent, J.-P., Brech, A., Bilder, D.*, et al.* (2007). ESCRTs and Fab1 Regulate Distinct Steps of Autophagy. Current Biology *17*, 1817-1825.

Sahu, R., Kaushik, S., Clement, C.C., Cannizzo, E.S., Scharf, B., Follenzi, A., Potolicchio, I., Nieves, E., Cuervo, A.M., and Santambrogio, L. (2011). Microautophagy of Cytosolic Proteins by Late Endosomes. Developmental Cell *20*, 131-139.

Sakurai, A., Yasuda, J., Takano, H., Tanaka, Y., Hatakeyama, M., and Shida, H. (2004). Regulation of human T-cell leukemia virus type 1 (HTLV-1) budding by ubiquitin ligase Nedd4. Microbes Infect *6*, 150-156.

Salvato, M.S., Schweighofer, K.J., Burns, J., and Shimomaye, E.M. (1992a). BIOCHEMICAL AND IMMUNOLOGICAL EVIDENCE THAT THE 11-KDA ZINC-BINDING PROTEIN OF LYMPHOCYTIC CHORIOMENINGITIS VIRUS IS A STRUCTURAL COMPONENT OF THE VIRUS. Virus Research *22*, 185-198.

Salvato, M.S., Schweighofer, K.J., Burns, J., and Shimomaye, E.M. (1992b). Biochemical and immunological evidence that the 11 kDa zinc-binding protein of lymphocytic choriomeningitis virus is a structural component of the virus. Virus Research *22*, 185-198.

Salvato, M.S., and Shimomaye, E.M. (1989). The completed sequence of lymphocytic choriomeningitis virus reveals a unique RNA structure and a gene for a zinc finger protein. Virology *173*, 1-10.

Schlie, K., Maisa, A., Freiberg, F., Groseth, A., Strecker, T., and Garten, W. (2010). Viral Protein Determinants of Lassa Virus Entry and Release from Polarized Epithelial Cells. J Virol *84*, 3178-3188.

Schmaljohn, C., and Blair, C.D. (1977). Persistent infection of cultured mammalian cells by Japanese encephalitis virus. J Virol *24*, 580-589.

Schmitt, A.P., Leser, G.P., Morita, E., Sundquist, W.I., and Lamb, R.A. (2005). Evidence for a New Viral Late-Domain Core Sequence, FPIV, Necessary for Budding of a Paramyxovirus. J Virol *79*, 2988-2997.

Schoneberg, J., Lee, I.-H., Iwasa, J.H., and Hurley, J.H. (2017). Reverse-topology membrane scission by the ESCRT proteins. Nat Rev Mol Cell Biol *18*, 5-17.

Segura-Morales, C., Pescia, C., Chatellard-Causse, C., Sadoul, R., Bertrand, E., and Basyuk, E. (2005). Tsg101 and Alix Interact with Murine Leukemia Virus Gag and Cooperate with Nedd4 Ubiquitin Ligases during Budding. J Biol Chem *280*, 27004-27012.

Shields, S.B., and Piper, R.C. (2011). How Ubiquitin Functions with ESCRTs. Traffic *12*, 1306-1317.

Shimode, S., Nakaoka, R., Hoshino, S., Abe, M., Shogen, H., Yasuda, J., and Miyazawa, T. (2013). Identification of cellular factors required for the budding of koala retrovirus. Microbiology and Immunology *57*, 543-546.

Shimojima, M., and Kawaoka, Y. (2012). Cell Surface Molecules Involved in Infection Mediated by Lymphocytic Choriomeningitis Virus Glycoprotein. Journal of Veterinary Medical Science *74*, 1363-1366.

Shimojima, M., Ströher, U., Ebihara, H., Feldmann, H., and Kawaoka, Y. (2012). Identification of Cell Surface Molecules Involved in Dystroglycan-Independent Lassa Virus Cell Entry. J Virol *86*, 2067-2078.

Shtanko, O., Imai, M., Goto, H., Lukashevich, I.S., Neumann, G., Watanabe, T., and Kawaoka, Y. (2010). A Role for the C Terminus of Mopeia Virus Nucleoprotein in Its Incorporation into Z Protein-Induced Virus-Like Particles. J Virol *84*, 5415-5422.

Shtanko, O., Watanabe, S., Jasenosky, L.D., Watanabe, T., and Kawaoka, Y. (2011). ALIX/AIP1 Is Required for NP Incorporation into Mopeia Virus Z-Induced Virus-Like Particles. J Virol *85*, 3631-3641.

Singh, M.K., Fuller-Pace, F.V., Buchmeier, M.J., and Southern, P.J. (1987). Analysis of the genomic l rna segment from lymphocytic choriomeningitis virus. Virology *161*, 448-456.

Spandidos, D.A., and Graham, A.F. (1976). Generation of defective virus after infection of newborn rats with reovirus. J Virol *20*, 234-247.

Spiropoulou, C.F., Kunz, S., Rollin, P.E., Campbell, K.P., and Oldstone, M.B.A. (2002). New World Arenavirus Clade C, but Not Clade A and B Viruses, Utilizes α-Dystroglycan as Its Major Receptor. J Virol *76*, 5140-5146.

Stampfer, M., Baltimore, D., and Huang, A.S. (1971). Absence of Interference During High-Multiplicity Infection by Clonally Purified Vesicular Stomatitis Virus. J Virol *7*, 409-411.

Staneck, L.D., and Pfau, C.J. (1974). Interfering Particles from a Culture Persistently Infected with Parana Virus. J Gen Virol *22*, 437-440.

Staneck, L.D., Trowbridge, R.S., Welsh, R.M., Wright, E.A., and Pfau, C.J. (1972). Arenaviruses: Cellular Response to Long-Term In Vitro Infection with Parana and Lymphocytic Choriomeningitis Viruses. Infect Immun *6*, 444-450.

Staub, O., Dho, S., Henry, P., Correa, J., Ishikawa, T., McGlade, J., and Rotin, D. (1996). WW domains of Nedd4 bind to the proline-rich PY motifs in the epithelial Na+ channel deleted in Liddle's syndrome. Embo j *15*, 2371-2380.

Stenglein, M.D., Sanders, C., Kistler, A.L., Ruby, J.G., Franco, J.Y., Reavill, D.R., Dunker, F., and DeRisi, J.L. (2012). Identification, Characterization, and In Vitro Culture of Highly Divergent Arenaviruses from Boa Constrictors and Annulated Tree Boas: Candidate Etiological Agents for Snake Inclusion Body Disease. mBio *3*.

Strack, B., Calistri, A., Accola, M.A., Palù, G., and Göttlinger, H.G. (2000). A role for ubiquitin ligase recruitment in retrovirus release. Proceedings of the National Academy of Sciences *97*, 13063-13068.

Strausbaugh, L.J., Barton, L.L., and Mets, M.B. (2001). Congenital Lymphocytic Choriomeningitis Virus Infection: Decade of Rediscovery. Clinical Infectious Diseases *33*, 370-374.

Strecker, T., Eichler, R., Meulen, J.t., Weissenhorn, W., Dieter Klenk, H., Garten, W., and Lenz, O. (2003). Lassa Virus Z Protein Is a Matrix Protein Sufficient for the Release of Virus-Like Particles. J Virol *77*, 10700-10705.

Strecker, T., Maisa, A., Daffis, S., Eichler, R., Lenz, O., and Garten, W. (2006). The role of myristoylation in the membrane association of the Lassa virus matrix protein Z. Virology Journal *3*, 93.

Stuchell-Brereton, M.D., Skalicky, J.J., Kieffer, C., Karren, M.A., Ghaffarian, S., and Sundquist, W.I. (2007). ESCRT-III recognition by VPS4 ATPases. Nature *449*, 740-744.

Tabata, K., Arimoto, M., Arakawa, M., Nara, A., Saito, K., Omori, H., Arai, A., Ishikawa, T., Konishi, E., Suzuki, R.*, et al.* (2016). Unique Requirement for ESCRT Factors in Flavivirus Particle Formation on the Endoplasmic Reticulum. Cell Reports *16*, 2339-2347.

Timmins, J., Schoehn, G., Ricard-Blum, S., Scianimanico, S., Vernet, T., Ruigrok, R.W.H., and Weissenhorn, W. (2003). Ebola Virus Matrix Protein VP40 Interaction with Human Cellular Factors Tsg101 and Nedd4. Journal of Molecular Biology *326*, 493-502.

Urata, S., Noda, T., Kawaoka, Y., Morikawa, S., Yokosawa, H., and Yasuda, J. (2007). Interaction of Tsg101 with Marburg Virus VP40 Depends on the PPPY Motif, but Not the PT/SAP Motif as in the Case of Ebola Virus, and Tsg101 Plays a Critical Role in the

Budding of Marburg Virus-Like Particles Induced by VP40, NP, and GP. J Virol *81*, 4895-4899.

Urata, S., Noda, T., Kawaoka, Y., Yokosawa, H., and Yasuda, J. (2006). Cellular Factors Required for Lassa Virus Budding. J Virol *80*, 4191-4195.

Urata, S., Weyer, J., Storm, N., Miyazaki, Y., van Vuren, P.J., Paweska, J.T., and Yasuda, J. (2016). Analysis of Assembly and Budding of Lujo Virus. J Virol *90*, 3257-3261.

Urata, S., and Yasuda, J. (2010). Regulation of Marburg virus (MARV) budding by Nedd4.1: a different WW domain of Nedd4.1 is critical for binding to MARV and Ebola virus VP40. Journal of General Virology *91*, 228-234.

Urata, S., and Yasuda, J. (2012). Molecular Mechanism of Arenavirus Assembly and Budding. Viruses *4*, 2049-2079.

Urata, S., Yasuda, J., and de la Torre, J.C. (2009). The Z Protein of the New World Arenavirus Tacaribe Virus Has Bona Fide Budding Activity That Does Not Depend on Known Late Domain Motifs. J Virol *83*, 12651-12655.

Vana, M.L., Tang, Y., Chen, A., Medina, G., Carter, C., and Leis, J. (2004). Role of Nedd4 and ubiquitination of Rous sarcoma virus Gag in budding of virus-like particles from cells. J Virol *78*, 13943-13953.

Volpon, L., Osborne, M.J., Capul, A.A., de la Torre, J.C., and Borden, K.L.B. (2010). Structural characterization of the Z RING-eIF4E complex reveals a distinct mode of control for eIF4E. Proc Natl Acad Sci USA *107*, 5441-5446.

von, M.P. (1951). Propagation of the PR8 strain of influenza A virus in chick embryos. II. The formation of incomplete virus following inoculation of large doses of seed virus. Acta pathologica et microbiologica Scandinavica *28*, 278-293.

von Schwedler, U.K., Stuchell, M., Müller, B., Ward, D.M., Chung, H.-Y., Morita, E., Wang, H.E., Davis, T., He, G.-P., Cimbora, D.M.*, et al.* (2003). The Protein Network of HIV Budding. Cell *114*, 701-713.

Votteler, J., and Sundquist, Wesley I. (2013). Virus Budding and the ESCRT Pathway. Cell Host & Microbe *14*, 232-241.

Wang, H., Norris, K.M., and Mansky, L.M. (2002). Analysis of Bovine Leukemia Virus Gag Membrane Targeting and Late Domain Function. J Virol *76*, 8485-8493.

Wang, J., Danzy, S., Kumar, N., Ly, H., and Liang, Y. (2012). Biological Roles and Functional Mechanisms of Arenavirus Z Protein in Viral Replication. J Virol *86*, 9794-9801.

Weiss, B., Rosenthal, R., and Schlesinger, S. (1980). Establishment and maintenance of persistent infection by Sindbis virus in BHK cells. J Virol *33*, 463-474.

Welsh, R.M., and Buchmeier, M.J. (1979). Protein analysis of defective interfering lymphocytic choriomeningitis virus and persistently infected cells. Virology *96*.

Welsh, R.M., Connell, C.M., and Pfau, C.J. (1972). Properties of Defective Lymphocytic Choriomeningitis Virus. J Gen Virol *17*, 355-359.

Welsh, R.M., Lampert, P.W., and Oldstone, M.B. (1977). Prevention of virus-induced cerebellar diseases by defective-interfering lymphocytic choriomeningitis virus. The Journal of infectious diseases *136*.

Welsh, R.M., and Oldstone, M.B. (1977). Inhibition of immunologic injury of cultured cells infected with lymphocytic choriomeningitis virus: role of defective interfering virus in regulating viral antigenic expression. J Exp Med *145*, 1449-1468.

Welsh, R.M., and Pfau, C.J. (1972). Determinants of Lymphocytic Choriomeningitis Interference. J Gen Virol *14*, 177-187.

Wirblich, C., Bhattacharya, B., and Roy, P. (2006). Nonstructural Protein 3 of Bluetongue Virus Assists Virus Release by Recruiting ESCRT-I Protein Tsg101. J Virol *80*, 460-473.

Wirblich, C., Tan, G.S., Papaneri, A., Godlewski, P.J., Orenstein, J.M., Harty, R.N., and Schnell, M.J. (2008a). PPEY motif within the rabies virus (RV) matrix protein is essential for efficient virion release and RV pathogenicity. J Virol *82*, 9730-9738.

Wollert, T., Wunder, C., Lippincott-Schwartz, J., and Hurley, J.H. (2009). Membrane scission by the ESCRT-III complex. Nature *458*, 172-177.

Xing, J., Ly, H., and Liang, Y. (2015). The Z Proteins of Pathogenic but Not Nonpathogenic Arenaviruses Inhibit RIG-i-Like Receptor-Dependent Interferon Production. J Virol *89*, 2944-2955.

Yasuda, J., and Hunter, E. (1998). A Proline-Rich Motif (PPPY) in the Gag Polyprotein of Mason-Pfizer Monkey Virus Plays a Maturation-Independent Role in Virion Release. J Virol *72*, 4095-4103.

Yasuda, J., Hunter, E., Nakao, M., and Shida, H. (2002). Functional involvement of a novel Nedd4-like ubiquitin ligase on retrovirus budding. EMBO Rep *3*, 636-640.

Yasuda, J., Nakao, M., Kawaoka, Y., and Shida, H. (2003). Nedd4 Regulates Egress of Ebola Virus-Like Particles from Host Cells. Journal of Virology *77*, 9987-9992.

Yuan, B., Campbell, S., Bacharach, E., Rein, A., and Goff, S.P. (2000a). Infectivity of Moloney murine leukemia virus defective in late assembly events is restored by late assembly domains of other retroviruses. J Virol *74*, 7250-7260.

CHAPTER 2:

THE LYMPHOCYTIC CHORIOMENINGITIS VIRUS MATRIX PROTEIN PPXY LATE DOMAIN DRIVES THE PRODUCTION OF DEFECTIVE INTERFERING PARTICLES

Christopher M. Ziegler[1,2], Philip Eisenhauer[1], Emily A. Bruce[1], Marion E. Weir[3], Benjamin R. King[1,2], Joseph P. Klaus[1,2#], Dimitry N. Krementsov[1], David J. Shirley[4], Bryan A. Ballif[3], and Jason Botten[1,4*]

[1]Department of Medicine, Division of Immunobiology, [2]Cellular, Molecular, and Biomedical Sciences Graduate Program, [3]Department of Biology, [4]Department of Microbiology and Molecular Genetics, University of Vermont, Burlington, VT 05405, USA. [#]Current address: Department of Immunology and Microbial Science, The Scripps Research Institute, La Jolla, CA 92037, USA

Short Title: PPXY Late Domain Drives the Release of LCMV DI Particles

Abstract

Arenaviruses cause severe diseases in humans but establish asymptomatic, lifelong infections in rodent reservoirs. Persistently-infected rodents harbor high levels of defective interfering (DI) particles, which are thought to be important for establishing persistence and mitigating virus-induced cytopathic effect. Little is known about what drives the production of DI particles. We show that neither the PPXY late domain encoded within the lymphocytic choriomeningitis virus (LCMV) matrix protein nor a functional endosomal sorting complex transport (ESCRT) pathway is absolutely required for the generation of standard infectious virus particles. In contrast, DI particle release critically requires the PPXY late domain and is ESCRT-dependent. Additionally, the terminal tyrosine in the PPXY motif is reversibly phosphorylated and our findings indicate that this posttranslational modification may regulate DI particle formation. Thus we have uncovered a new role for the PPXY late domain and a possible mechanism for its regulation.

Author Summary

Arenaviruses cause severe and often fatal diseases in humans yet typically establish lifelong, asymptomatic infections in their rodent reservoirs. Several families of enveloped RNA viruses, including the arenaviruses, encode short amino acid motifs, called late domains, to hijack host proteins in the endosomal sorting complex required for transport (ESCRT) to drive the release of virus particles from the host cell's outer membrane. Many late domain-containing viruses produce defective interfering (DI) particles in addition to standard, infectious virus. DI particles cannot self-replicate but interfere with the production of infectious virus and mitigate virus-induced cytopathic effect. Arenaviruses such as lymphocytic choriomeningitis virus (LCMV) generate high levels of DI particles, yet, the mechanism that drives their formation is not known. We show that LCMV's only encoded late domain, PPXY, and a functional ESCRT pathway are critical for DI particle production, but in contrast, are not absolutely required for infectious virus production. We also demonstrate that the LCMV PPXY late domain is phosphorylated and that this modification may regulate DI particle production. In summary, we have discovered a new and unexpected role for a viral late domain in selectively driving the production of DI particles independently of standard infectious virus particles.

Introduction

Arenaviruses are a family of rodent-borne viruses with a worldwide distribution. These viruses typically establish persistent, asymptomatic infections in rodent reservoir species (Salazar-Bravo et al., 2002b). In contrast, arenaviruses cause severe and often fatal diseases in humans. Several arenaviruses, including Lassa virus and Junín virus, cause hemorrhagic fever syndromes whereas infection with the prototypic arenavirus, lymphocytic choriomeningitis virus (LCMV), can lead to aseptic meningitis in immunocompetent individuals, high lethality in immunocompromised individuals, or severe birth defects in the developing fetus (Buchmeier et al., 2007; Fischer et al., 2006). U.S. Food and Drug Administration-approved vaccines do not exist for the prevention of arenavirus infection and effective antiviral therapies have been limited to the use of ribavirin for Lassa virus (McCormick et al., 1986) or immune plasma for Junín virus (Enria et al., 2008a).

Arenaviruses are enveloped viruses with a single-stranded, bi-segmented RNA genome that encodes four proteins in an ambisense manner. The small (S) segment encodes the nucleoprotein (NP) and glycoprotein (GP) while the large (L) segment encodes the RNA-dependent RNA polymerase (L) and the matrix protein (Z) (Meyer et al., 2002). Arenaviruses enter cells via receptor-mediated endocytosis (Rojek and Kunz, 2008), undergo genomic replication and transcription in the cytoplasm (Meyer et al., 2002), and assemble and bud new particles at the plasma membrane (Urata and Yasuda, 2012). The Z protein, which lines the luminal side of the viral membrane, is responsible for a number of critical functions in the virus life cycle, including driving the process of viral particle

assembly and budding (Fehling et al., 2012). Accordingly, Z can form virus-like particles (VLPs) in the absence of other viral proteins and is thought to be both necessary and sufficient for driving the budding process (Perez et al., 2003; Strecker et al., 2003).

Several VLP-based studies indicate that Z drives viral particle release by virtue of one or more encoded viral late domain(s) (P(S/T)AP, YXXL, and/or PPXY), which can recruit proteins from the cellular endosomal sorting complex required for transport (ESCRT) pathway (Perez et al., 2003; Strecker et al., 2003; Urata et al., 2006). ESCRT machinery is required for most cellular membrane scission events that result in separation away from the cytosol including multivesicular body formation and cellular abscission (Carlton and Martin-Serrano, 2007; Hurley, 2008; Morita et al., 2007). Many enveloped viruses are known to hijack cellular ESCRT machinery via their late domains to complete the final membrane scission step required for virions to bud from host membranes (for review see (Votteler and Sundquist, 2013)).

Viruses from diverse families, including arenaviruses, produce defective interfering (DI) particles in addition to standard, infectious virus during the normal course of infection (Huang and Baltimore, 1970). DI particles are largely similar to standard virus particles in their appearance and viral protein content but cannot self-replicate, and interfere with the production of homologous standard virus (Huang and Baltimore, 1970). In many cases, the primary difference between DI particles and standard virus is thought to be the presence of deletions in the viral genome (Huang, 1973). With regard to LCMV, small deletions in the terminal untranslated regions of genomic and antigenomic RNAs have been observed, but

it is not known whether these RNAs have interfering properties or are selectively incorporated in DI particles (Meyer and Southern, 1997). The interfering activity of arenavirus DI particles can be blocked by neutralizing antibodies but is maintained even after treatment with ultra-violet (UV) radiation, unlike standard particles, which are highly susceptible to both treatments (Jacobson and Pfau, 1980). Arenaviruses generate high levels of DI particles both in cell culture (Welsh and Pfau, 1972) and in host rodents (Popescu and Lehmann-Grube, 1977). It has long been postulated that arenavirus DIs are an important factor in the establishment of persistent infection (Burns and Buchmeier, 1993; Huang and Baltimore, 1970; Oldstone, 1998) but a causal link between arenavirus DI particles and persistence has yet to be firmly established.

There are several outstanding questions regarding the arenavirus matrix protein, including how its functionality is regulated and how, in the context of a fully replicating virus, encoded late domains contribute to the production of standard and DI particles. Herein we demonstrate that LCMV's sole late domain, PPXY, is not required for standard virus budding but instead is the driving force of DI particle release. Further, standard virus appears to bud independently of ESCRT machinery while DI particle release is ESCRT-dependent. Finally, we show that the LCMV PPXY motif is tyrosine phosphorylated and that this post-translational modification appears to regulate DI particle formation.

Results

The LCMV matrix protein is reversibly phosphorylated

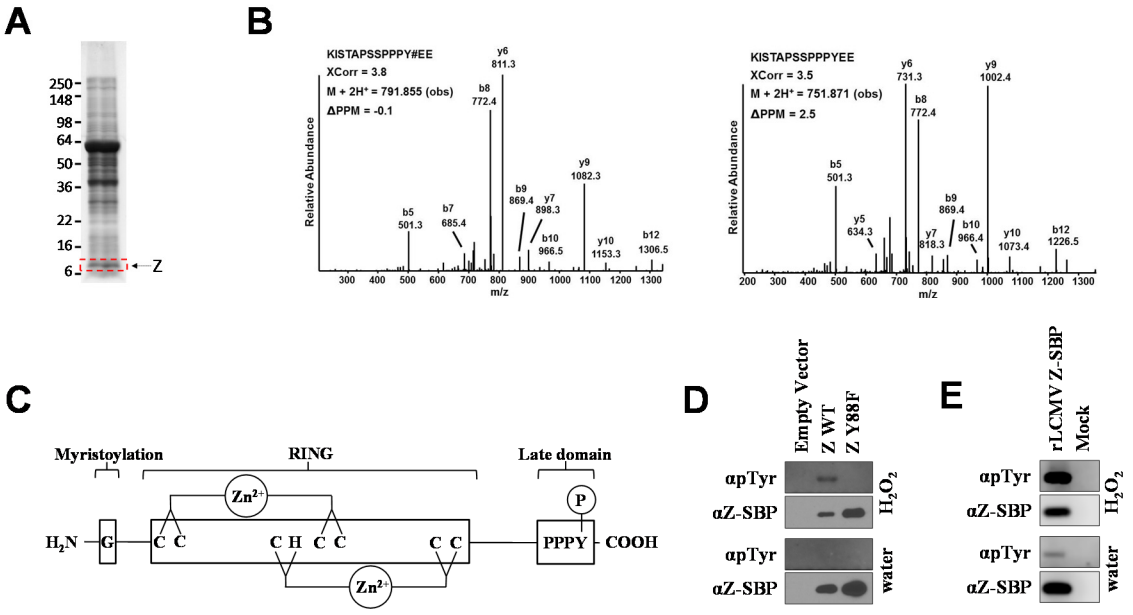

Figure 2.1. The LCMV matrix protein PPXY late domain is reversibly phosphorylated. (A) Protein lysates from sucrose-banded LCMV strain Armstrong 53b particles were separated on polyacrylamide gels and stained with Coomassie brilliant blue. A gel slice containing the Z protein (indicated by the red box) was excised, subjected to in-gel tryptic and/or chymotryptic digestion, and extracted peptides were analyzed by mass spectrometry for the presence of phosphorylated peptides as described in the Materials and Methods. (B) Representative low energy collision-induced dissociation tandem mass spectra of a chymotryptic peptide harboring the indicated phosphotyrosine residue or the same peptide unphosphorylated. Both peptides were identified from virion-derived LCMV Z protein. The tandem mass spectra were collected in an Orbitrap (MS1)-linear ion trap (MS2) mass spectrometer. Y# denotes phosphotyrosine. The SEQUEST XCorr values, the precursor observed mass and the associated PPM are indicated. Fig S1 shows the corresponding calculated and measured b- and y-type ions indicating identified fragment ion masses. (C) Depiction of the LCMV Z protein. G, glycine at position 2 that is myristoylated; RING, the central zinc-binding really interesting new gene (RING) domain; PPPY, LCMV's only known late domain that contains the Y88 site of phosphorylation. (D) Tyrosine 88 in the LCMV matrix protein is phosphorylated. HEK293T cells were transfected with an empty vector or a plasmid encoding LCMV Z (either WT or Y88F) with a C-terminal streptavidin binding peptide (SBP) tag. Following a 15 minute exposure to either water or the tyrosine phosphatase inhibitor, H2O2, Z was affinity purified from cell lysates using magnetic streptavidin beads and screened via western blot using antibodies specific for phosphotyrosine or the SBP tag. Results are representative of 3 independent experiments. (E) LCMV is phosphorylated in rodent cells. L929 cells were infected or not with a rLCMV that encodes a streptavidin binding peptide (SBP) fusion tag at the C terminus of Z. Two days later, cells were exposed to either water or the tyrosine phosphatase inhibitor, H2O2, for 15 minutes. SBP-tagged Z was then affinity purified from cell lysates using magnetic streptavidin beads and

screened via western blot using antibodies specific for phosphotyrosine or the SBP tag. Results are representative of 3 independent experiments.

The matrix protein plays a multifactorial role in the arenavirus life cycle yet little is known regarding how its various functions are regulated. Given the importance of phosphorylation for regulating the functionality of matrix proteins of other virus families (Bajorek et al., 2014; García et al., 2012; Hemonnot et al., 2004; Kolesnikova et al., 2012; Pei et al., 2011), we were interested in whether LCMV's matrix protein might also be phosphorylated. LCMV strain Armstrong 53b particles grown in Vero E6 cells were purified via sucrose-banding (Figure 2.1A) and subjected to mass spectrometry. This analysis revealed a tyrosine phosphorylation site near the C-terminus of the LCMV Z protein at position 88 (Y88) (Figures 2.1B and 2.S1), which lies within LCMV Z's PPPY late domain (Figure 2.1C). Both phosphorylated and unphosphorylated peptides containing this residue were observed at a ratio of 1 to 11, respectively, which suggests that ~10% of the total Z protein in this virion preparation is phosphorylated (Figures 2.1B and 2.S1C). Because the virion preparation contained a mixture of both standard infectious virus and DI particles, we were not able to determine whether the phosphorylated Z was derived from standard particles, DI particles, and/or both types of particles. To confirm the phosphorylation site, plasmids encoding either WT Z or a phenylalanine mutant (Y88F) that cannot be phosphorylated were transfected into HEK293T cells and 2 days later the cells were treated with either water or the tyrosine phosphatase inhibitor, hydrogen peroxide. WT Z and Y88F Z were affinity purified and probed with a phosphotyrosine-specific antibody. The phosphotyrosine signal detected from WT Z was greatly enhanced following inhibition of

tyrosine phosphatases (Figure 2.1D). Substitution of tyrosine 88 with phenylalanine, to prevent phosphorylation, resulted in a complete loss of detectable phosphotyrosine signal in both settings indicating that Y88 may be the only tyrosine of the 3 encoded in LCMV Z that is phosphorylated (Figure 2.1D) by endogenous kinases in these cells. To determine whether LCMV Z is tyrosine phosphorylated in the context of a relevant rodent cell line, we infected murine L929 cells with a rLCMV that encodes Z with a C-terminal streptavidin binding peptide (SBP) tag. Two days later, cells were either treated with hydrogen peroxide or not and Z was affinity purified from cell lysates for western blot analysis. As shown in Figure 2.1E, a phosphotyrosine signal was clearly detectable from Z and was enhanced following treatment with hydrogen peroxide.

The LCMV matrix protein PPXY late domain is dispensable for the production of standard infectious particles

A

	Sequence Alignment	
	Virus (strain)	Peptide Sequence
Old World	LCMV-Armstrong	PPPYEE
	LCMV-WE	PPPYEE
	Lassa Virus-Josiah	PPPYSP
	Dandenong virus	PPPYEE
	Mobala Virus	PPPYSP
	Mopeia Virus-Mozambique	PPPYTP
	Ippy Virus	PPPYSP
	Lujo Virus	PP-
New World	Junín Virus	PPP-
	Guanarito Virus	PPE-
	Machupo Virus	PPP-
	Sabiá Virus	PPPED-

B

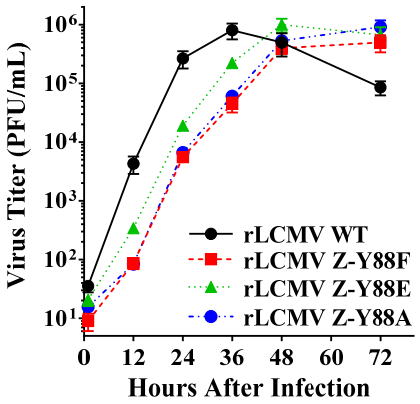

C

2-Way ANOVA Summary for Y88 Mutant Growth Curves

Hours After Infection	WT v. Y88F	WT v. Y88E	WT v. Y88A	Y88F v. Y88E	Y88F v. Y88A	Y88E v. Y88A
1	**	n.s.	n.s.	n.s.	n.s.	n.s.
12	****	****	****	***	n.s.	***
24	****	****	****	**	n.s.	**
36	****	*	****	****	n.s.	**
48	n.s.	n.s.	n.s.	n.s.	n.s.	n.s.
72	****	****	****	n.s.	n.s.	n.s.

D

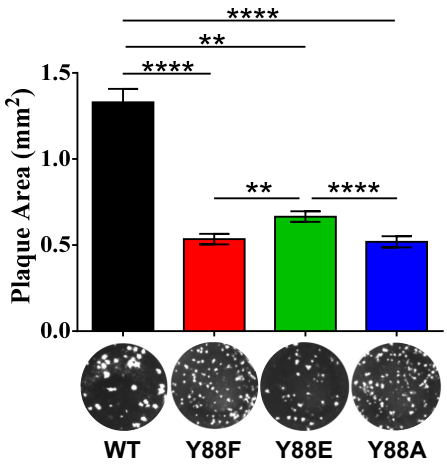

E

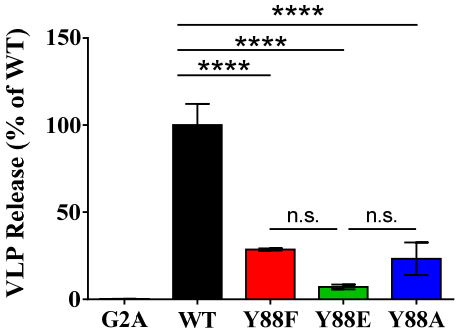

Figure 2.2. The LCMV Z PPXY late domain is dispensable for the production of infectious LCMV particles. (A) Sequence alignment of arenavirus Z proteins reveals conservation of Y88 among most Old World, but not New World, arenaviruses. (B) Recombinant (r)LCMV containing substitutions at Z Y88 that either mimic constitutive phosphorylation (Y88E) or cannot be phosphorylated (Y88F and Y88A) were generated using reverse genetics as described in the Materials and Methods. Vero E6 cells were infected at an MOI of 0.01 and the quantity of infectious virus released at each of the indicated time points was determined via plaque assay. Data are presented as mean PFU ± standard error of the mean (SEM) of 3 independent experiments. (C) Summary of two way analysis of variance (ANOVA) with Holm-Sidak's test for multiple comparisons of log-transformed data for virus growth curves in (B). (D) The area of plaques from rLCMV WT or Z Y88 mutants was measured using Image J. Data represent the mean ± SEM of plaques analyzed from 16 wells from 6-well plates. Mean values were compared using the Kruskal-Wallis non-parametric test with Dunn's multiple comparisons test. (E) Mutation of the PPXY domain reduces Z budding function in a VLP assay while phosphorylation of this domain at Y88 does not further impact budding. A plasmid encoding LCMV Z WT, Z G2A, or the indicated Z Y88 mutants was transfected into HEK293T cells and 1 day later cells and VLP-containing supernatants were collected and screened via quantitative western blot for Z. The percent VLP release was calculated as the amount of Z protein found in the cell culture media relative to the amount in cells. Data are presented as mean release ± SEM relative to WT Z from 3 independent experiments. A one way ANOVA with Holm-Sidak's test for multiple comparisons was used to compare the mean values. (C-E), n.s. (not significant), *$p < 0.05$; **$p < 0.01$; ***$p < 0.001$; ****$p < 0.0001$, as determined by the indicated statistical tests.

The finding that LCMV Z is phosphorylated at Y88 was intriguing as this residue is part of LCMV's only late domain, PPPY. This motif is well conserved among most Old World arenavirus Z proteins (Figure 2.2A) and its importance for the budding activity of LCMV and Lassa virus Z in the context of VLP-budding assays has been well described (Perez et al., 2003; Strecker et al., 2003). To investigate the role of this late domain in the context of authentic virus and to determine whether tyrosine phosphorylation may regulate its function, we generated recombinant (r)LCMV encoding either phenylalanine or alanine at position 88 to prevent phosphorylation at this site or glutamic acid to mimic constitutive phosphorylation. The alanine mutant was included as a reference to previous studies on the function of this late domain for LCMV and Lassa virus Z, which used alanine substitutions at Y88 to assess the contribution of this late domain to Z's budding efficiency in VLP assays (Perez et al., 2003; Strecker et al., 2003). Viruses containing all three mutations

were recoverable despite the well-described defect in Z's budding efficiency caused by mutation of this residue (Figure 2.2B) (Perez et al., 2003; Strecker et al., 2003). The growth kinetics of rLCMV Z-Y88F and Z-Y88A during the first 36 hours (hr) post-infection (pi) were nearly identical, but impaired ~15-fold compared to rLCMV WT ($P \leq 0.0001$; Figures 2.2B and 2.2C). The growth rate of the rLCMV Z-Y88E phosphomimetic was also attenuated compared to WT virus over this same time frame (~4-fold less PFU at 36 hr pi, $P \leq 0.05$, Figures 2.2B and 2.2C). However, the phosphomimetic virus grew to ~4–fold higher titers than the alanine or phenylalanine mutants ($P \leq 0.01$; Figures 2.2B and 2.2C). Additionally, the mean plaque size for rLCMV Z-Y88E was significantly increased compared to the Z-Y88F and Z-Y88A viruses (0.67 vs 0.53 or 0.52 mm^2; $P \leq 0.01$; Figure 2.2D), indicating that virus spread was partially restored in the phosphomimetic virus. Notably, each mutant virus eventually reached peak WT titers. Given the delayed kinetics observed in the mutant viruses, we tested for reversion mutations at 72 hr pi and confirmed that each virus retained its respective mutated residue at position 88 and its small plaque phenotype (Figure 2.2D). Collectively, these results demonstrate that the PPXY late domain is not absolutely required for the formation and release of standard infectious particles. Further, phosphorylation of Y88 may have a positive regulatory impact on viral propagation.

Phosphorylation of the PPXY late domain does not enhance Z's ability to form VLPs.

Point mutations made at Y88 suggested that dynamic phosphorylation of this residue was important for the function of the matrix protein. Given the important role of the LCMV matrix protein and its late domain motif in regulating viral budding (Perez et al., 2003; Strecker et al., 2003), we next investigated the specific effect these point mutations had on Z's budding efficiency in a VLP release assay. Because the LCMV Z protein is sufficient for the production of VLPs in the absence of any other viral proteins (Perez et al., 2003; Strecker et al., 2003), we were able to assess the budding activity of plasmid-derived WT or Y88-mutant Z proteins. As a control, we also included the LCMV Z G2A mutant, which exhibits a pronounced defect in VLP formation due to its inability to be myristoylated at this glycine residue (Perez et al., 2004b). HEK293T cells were transfected with plasmids encoding WT or Y88 mutants and 1 day later the VLP-containing supernatant and cells were collected and analyzed by quantitative western blotting. The budding activity of all three Z Y88 mutants was significantly reduced compared to WT Z, indicating that mutations in this region reduce the efficiency of VLP release (Figure 2.2E). In particular, the impaired VLP release exhibited by the Z Y88A mutant confirmed earlier findings by Perez et al. (Perez et al., 2003). We did not observe a significant difference between the budding of the Z-Y88E phosphomimetic compared to Y88F and Y88A (Figure 2.2E). This suggests that the partial gain of fitness observed with the phosphomimetic rLCMV-Z-Y88E virus in Figure 2.2B is not due to an increase in budding activity and as such Y88

phosphorylation does not appear to directly regulate the budding function of this late domain. However, because the VLP budding assay measures only the release of matrix protein, in the absence of other viral proteins, it is possible that this assay does not recapitulate all the facets of infectious virion production.

PPXY late domain mutant viruses release substantially less viral structural proteins and genomes without a corresponding loss of infectious units

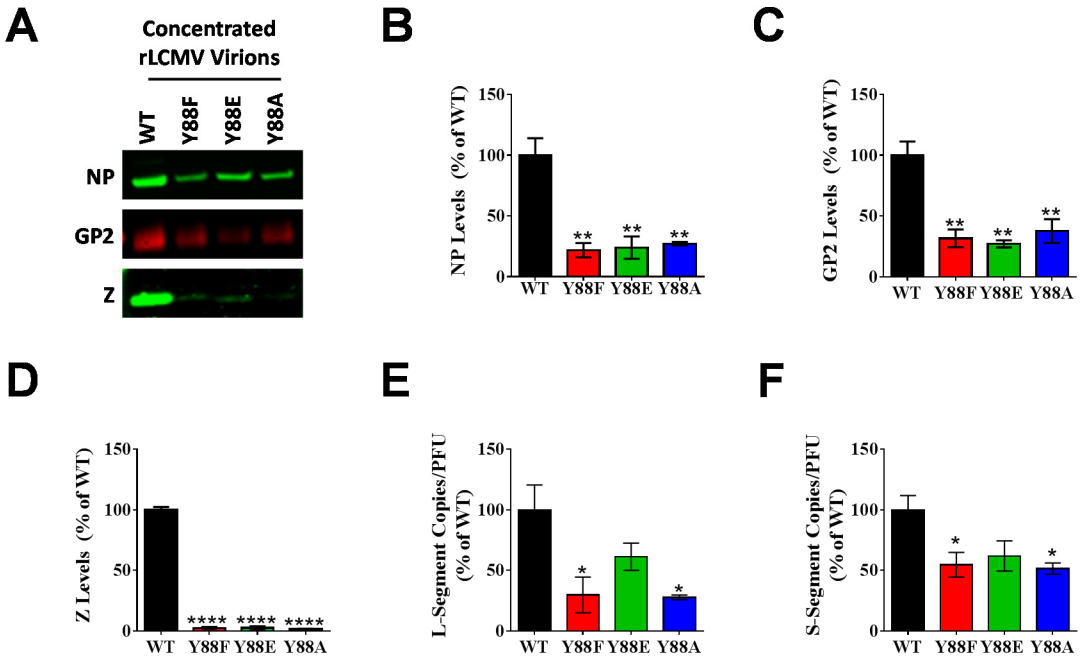

Figure 2.3. PPXY late domain mutant viruses release substantially less viral structural proteins and genomes without a corresponding loss of infectious units. (A-E) An equal quantity of PFUs of rLCMV WT, Z Y88F, Z Y88E, or Z Y88A were concentrated via ultracentrifugation through sucrose and screened for viral NP (B), GP2 (C), or Z (D) via quantitative western blot or L segment vRNA (E) or S segment vRNA (F) via qRT-PCR. Representative western blots for NP, GP2, and Z are shown in (A). Data in (B-F) are representative of the mean ± SEM relative to rLCMV WT from at least 3 independent experiments. (B-E) *p < 0.05; **p < 0.01; ****p < 0.0001, determined using the one-way ANOVA with Holm-Sidak's test for

multiple comparisons. Note that in panels B-F, the Y88 mutant viruses were not statistically different from one another.

To investigate the protein and genome composition of virions containing mutated late domains, an equivalent quantity of cell-free infectious virus particles from each rLCMV strain was concentrated for screening. Quantitative western blotting revealed substantial reductions in the total amount of NP, GP, and Z in the Y88 mutant particles relative to WT virus (Figures 2.3A-2.3D). However, no difference was observed in the levels of these proteins among the three Y88 mutant viruses (Figures 2.3A-2.3D). The quantity of Z protein detected in the Y88 mutant virus preparations was <3% of WT virus (Figure 2.3D) whereas NP and GP quantities were ~25% of WT virus (Figures 2.3B and 2.3C). Viral genome content in particles was assessed by qRT-PCR. On a per PFU basis, the quantity of either L or S segment genomic RNA in the non-phosphorylatable mutants, Y88F and Y88A, was significantly reduced versus WT ($P \leq 0.05$, Figures 2.3E and 2.3F). However, genome levels in the phosphomimetic virus, Y88E, were not significantly different than WT (Figures 2.3E and 2.3F), which may explain a component of its partially restored growth kinetics (Figure 2.2B). The observation of reduced viral proteins and/or genomes released from cells infected with the Y88 mutant viruses combined with the fact that WT LCMV is known to produce relatively large quantities of DI particles (Welsh and Pfau, 1972) led us to hypothesize that the PPXY mutants may have defects in their ability to generate DI particles, which could explain their greatly reduced levels of viral protein and genome relative to PFU.

The PPXY late domain drives the production of DI particles.

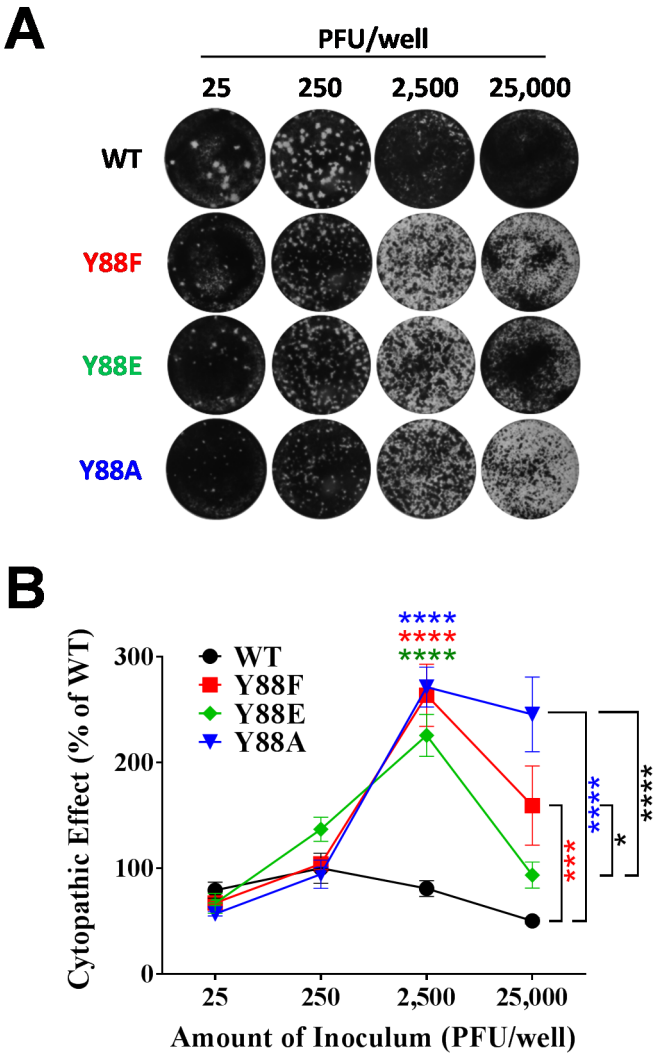

Figure 2.4. **LCMV DI particle production is impaired in the absence of a functional PPXY domain.** (A-B) Equivalent PFUs of WT, Z Y88F, Z Y88E, or Z Y88A rLCMV (range 25 to 2.5 x 104 PFUs) were inoculated onto monolayers of Vero E6 cells and a standard plaque assay was performed. Representative images of crystal violet-stained wells are shown in (A). Inhibition of standard infectious virus-induced cytopathic effect by DI particles at each dose was determined by measurement of the mean pixel intensity of each well using Image J software (B). The data in (B) are representative of the mean ± SEM relative to rLCMV WT (at 250 PFU per well) from 3 independent experiments and were tested for statistical significance with a two way ANOVA and Holm-Sidak's test for multiple comparisons. (B) *$p < 0.05$; ***$p < 0.001$; ****$p < 0.0001$, as determined by the indicated statistical tests.

A substantial fraction of virus particles produced by LCMV are DI particles (Staneck et al., 1972). Accordingly, inoculation of LCMV at low multiplicities of infection (MOI) results in efficient production of standard virus and spread, while high MOIs do not. This seemingly contradictory phenomenon is caused by DI particles, which inhibit the propagation of standard virus and its ability to cause cytopathic effect with one hit kinetics (Popescu et al., 1976; Welsh and Pfau, 1972). Monolayers inoculated with high concentrations of standard infectious LCMV exhibit no cytopathic effect due to DI particle inhibition, but as the inoculum is diluted, standard virus particles that infect cells in the absence of a co-infecting DI particle will subsequently form plaques. We exploited this phenomenon to initially evaluate the relative amounts of DI particles generated by the PPXY mutant viruses. Equal infectious doses of WT virus and each Y88 mutant, spanning a range of 25 to 25,000 PFU, were applied to Vero E6 cell monolayers in a standard plaque assay (Figures 2.4A and 2.4B). Evidence of possible DI particle interference is clearly seen in WT virus, where the most concentrated viral sample (25,000 PFU) resulted in no cell death while in successive 10-fold dilutions (2,500 and 250 PFU) the number of DI particles per cell is lowered allowing standard virus to enter cells in the absence of DI particles and form plaques (Figure 2.4A). In contrast, the PPXY-mutant viruses exhibited a considerable increase in cytopathology (Figure 2.4A, 25,000 and 2,500 PFU). Quantification of the observed cytopathology confirmed the striking phenotype and revealed significant differences between the mutant and WT viruses (Figure 2.4B). Intriguingly, the cytopathology of the rLCMV Z-Y88E phosphomimetic at 25,000 PFU was significantly

less than both Y88F or Y88A viruses and therefore more closely resembled WT virus (Figure 2.4B).

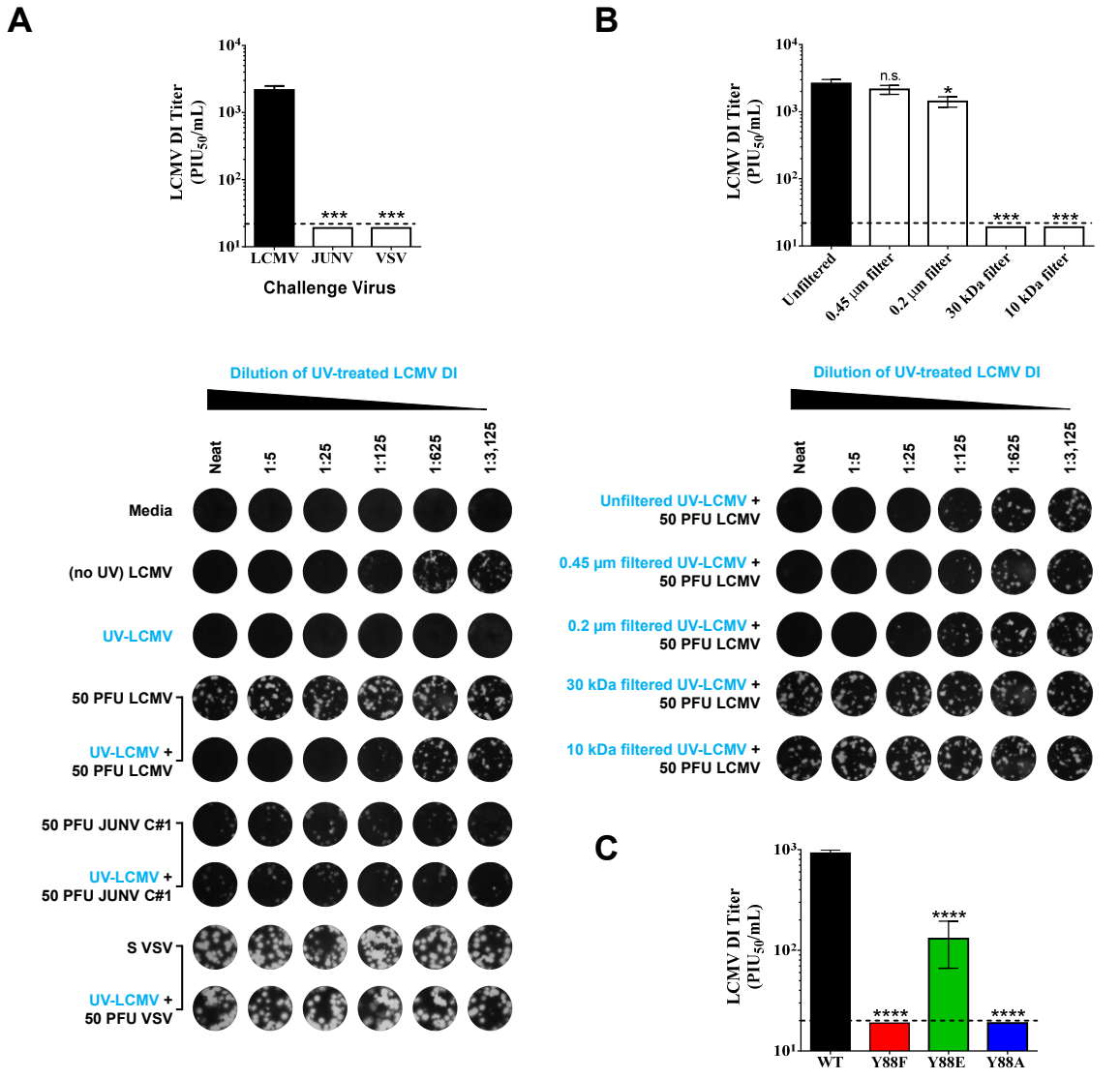

Figure 2.5. The PPXY late domain drives the production of DI particles. (A-B) Development and validation of a plaque interference assay for the measurement of LCMV DI particle activity. In (A), a stock of rLCMV WT containing both standard infectious virus particles and DI particles was subjected to UV irradiation for 2 min to inactivate standard LCMV particles but spare DI particles. Serial 5-fold dilutions of this UV-treated virus preparation (UV-LCMV) were added to Vero E6 cells followed by a fixed amount of 50 PFU of the indicated challenge virus (rLCMV WT; Junín virus Candid 1, (JUNV C#1), or vesicular stomatitis virus (VSV)). Additional controls were wells that received i) media only, ii) serial 5-fold dilutions

of the stock LCMV virus preparation before UV treatment (no UV LCMV), iii) serial 5-fold dilutions of the stock LCMV virus preparation following UV treatment (UV-LCMV), or iv) 50 PFU per well of standard LCMV, JUNV C#1, or VSV, as indicated. Following a 1 hr incubation at 37oC to permit viral particle absorption, cells were overlaid with agarose and subsequently fixed and stained with crystal violet to visualize whether the UV-LCMV preparation impacted the ability of each virus to form plaques. The LCMV DI titer is expressed as plaque interfering units50 (PIU50) per mL of a given sample and was calculated as described in the Materials and Methods. In (B), rLCMV WT containing both standard and DI particles was subjected to the indicated filtration or not and then subjected to UV irradiation as described in (A). Serial 5-fold dilutions of each UV-LCMV preparation (filtered or not) were added to Vero E6 cells followed by a fixed amount of 50 PFU of rLCMV WT. As described in (A), the ability of these UV-LCMV preparations to interfere with the ability of standard LCMV to from plaques was measured via plaque assay and LCMV DI titers are reported as PIU50/mL. In (A-B), the graphical results represent the mean LCMV DI titer ± SEM for 3 independent experiments and representative wells for each condition are shown directly below each graph. (C) LCMV DI particle production requires a functional PPXY domain. The rLCMV WT or Y88 mutants examined in Figure 4 were subjected to the assay described in (A-B) to directly measure the DI particle titer present in each virus preparation. Briefly, each indicated rLCMV preparation was subjected to UV-irradiation to inactivate standard infectious LCMV particles while preserving DI particle activity. Serial 5-fold dilutions of each UV-treated sample were inoculated onto Vero E6 cells, followed by the addition of 50 PFU of standard LCMV. Following a 1 hr incubation at 37oC to permit viral particle absorption, cells were overlaid with agarose and subsequently fixed and stained with crystal violet to visualize whether the various UV-treated rLCMV preparations impacted the ability of standard LCMV particles to form plaques. For each rLCMV, DI titer is reported as mean PIU50/mL ± SEM for 3 independent experiments. (A-C) n.s. (not significant), *$p < 0.05$; ***$p < 0.001$; ****$p < 0.0001$, determined by first substituting values of 19 PIU50/mL (just below the limit of detection value of 20 PIU50/mL) for samples that were below the limit of detection and then performing a one way ANOVA.

To confirm that the interfering activity observed in Figure 2.4 was indeed due to LCMV DI particles, we next established an assay to directly and quantitatively measure LCMV DI particle activity. At present, no consistent biochemical or genetic signature exists to distinguish LCMV DI particles from standard infectious particles (Stocker et al., 1994; Welsh and Buchmeier, 1979). In an attempt to uncover such a signature, we separated preparations of rLCMV WT or Y88 mutants via density ultracentrifugation. Similar to previous studies (Gschwender and Popescu, 1976; Pedersen, 1979; Peralta et al., 1981; Stocker et al., 1994; Welsh and Buchmeier, 1979), we were unable to isolate fractions containing pure DI particles as abundant levels of standard virus were detectable across all 15 fractions (Figure 2.S2). Therefore, it was not possible to identify a DI particle-

specific signature for screening purposes. Despite this limitation, several assays, including a yield reduction assay (Welsh and Pfau, 1972), a plaque reduction assay (Welsh et al., 1972), and a focus interfering assay (Popescu et al., 1976) have historically been used for accurate measurement of LCMV DI particle abundance and activity levels. Indeed, these assays were originally used to define LCMV DI particles. We utilized the plaque interference assay (also known as the plaque reduction assay) analogous to that used in (Welsh and Pfau, 1972) but also capitalized on the strong UV-resistance exhibited by LCMV DI particles, but not standard virus particles (Welsh et al., 1972). Briefly, cell-free virus preparations containing both standard and DI particles were treated with UV to neutralize standard virus particles while leaving the interfering properties of DI particles intact (Figure 2.5A). It should be noted that standard virus particles treated with UV do not acquire detectable interfering properties (Figure 2.5A) (Dutko and Pfau, 1978). Limiting dilutions of this UV-treated sample were applied to Vero E6 cells, followed by the addition of a fixed quantity of LCMV PFUs. As shown in Figure 2.5A, this allows for the determination of LCMV DI particle activity and is expressed as plaque interfering units$_{50}$ (PIU$_{50}$) per mL of a given sample. Importantly, we recapitulated several key controls from previous studies to demonstrate the specificity of this assay for LCMV DI particles. In particular, UV-treated LCMV DI particle preparations only interfered, in a dose-dependent manner, with the growth of homologous LCMV, but not heterologous viruses such as vesicular stomatitis virus (VSV) or the New World arenavirus Junín virus Candid 1 (JUNV C#1), which rules out a nonspecific antiviral factor as a mediator of interference (e.g.

interferon) (Figure 2.5A). Further, passing LCMV DI particle-containing supernatant through a series of filters (0.45 μm, 0.2 μm, 30 kDa, 10 kDa) showed that interference is not due to soluble factors that are smaller than 30 kDa (e.g. cytokines) or larger (>0.2 μm) membrane bound entities such as bacteria (Figure 2.5B). When this assay was applied to the rLCMV WT and Y88 mutant samples examined in Figure 2.4, it confirmed that the rLCMV WT samples exhibited substantial DI particle interfering activity (mean 926 PIU_{50}/mL ± 68 SEM), but that the mutant Y88 viruses had much less (Figure 2.5C). There was no detectable DI activity for either the Y88F or Y88A viruses while the Y88E virus contained intermediate levels of interfering activity (mean 131 PIU_{50}/mL ± 64 SEM). Collectively, the findings in Figures 2.4 and 2.5 support the hypothesis that the LCMV PPXY late domain is required for the efficient formation of DI particles and that phosphorylation of Y88 may play a regulatory role in DI particle production and the inhibition of cytopathic effect.

Efficient DI particle formation requires a functional ESCRT pathway

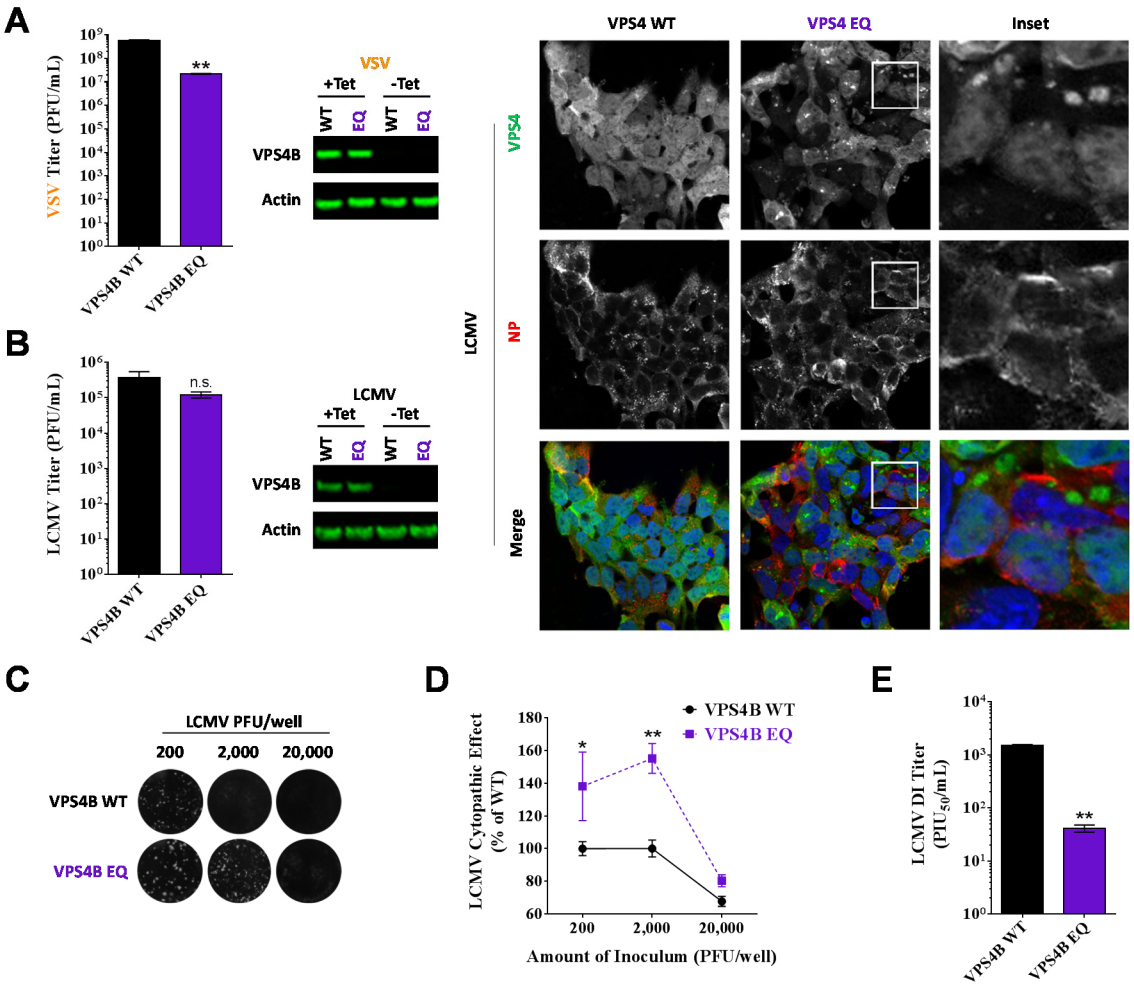

Figure 2.**6. Efficient DI particle formation requires a functional ESCRT pathway.** (A) VSV requires a functional ESCRT pathway for infectious virus release. T-Rex HEK293 cells stably transduced with vectors for tetracycline-based induction of WT vacuolar protein sorting 4B (VPS4B) or the DN VPS4B mutant, EQ, were treated with tetracycline to induce the expression of WT or DN VPS4B. Both the WT and DN VPS4B proteins have GFP fusion tags. One hr following VPS4B induction, the media was removed and cells were infected with VSV in media containing tetracycline. One hr later, the viral inoculum was removed and replaced with fresh media containing tetracycline. Six hr later (8 hr post-VPS4B induction; 7 hr post-infection), supernatants were collected to determine VSV PFU titers via plaque assay. Cell protein lysates were also generated at this time to verify the induction of VPS4B WT or EQ expression using an anti-GFP antibody. Protein lysates were also screened for actin as a loading control. Viral titers represent the mean VSV PFU ± SEM from 3 independent experiments and were tested for statistical significance with an unpaired t test with Welch's correction. (B-E) LCMV requires a functional ESCRT pathway for the release of DI particles, but not standard infectious particles. T-Rex HEK293 cells stably transduced with vectors for tetracycline-based induction of WT VPS4B or the DN VPS4B EQ were infected with rLCMV WT and 2 d

later treated with tetracycline to induce the expression of WT or DN VPS4B. Six hr after VPS4B induction (54 hr pi), the cells were washed and given fresh media containing tetracycline. Supernatants were collected 18 hr later (72 hr pi) and titered via plaque assay. Similar to (A), protein lysates were collected at 72 hr pi and screened for VPS4B WT or DN using an anti-GFP antibody or for actin as a loading control. Extra wells containing cells grown on cover slips were also fixed at 72 hr pi to examine, via immunofluorescent confocal microscopy, the expression and localization of WT or DN VPS4B (green) or LCMV NP (red). A 143 μm square is shown for each panel. The results shown in (B) represent the mean LCMV PFU ± SEM from 4 independent experiments and were tested for statistical significance with an unpaired t test with Welch's correction. (C) Equivalent PFUs of virus (range 2 x 102 to 2 x 104) produced from WT or DN VPS4B cells were inoculated onto monolayers of Vero E6 cells and a standard plaque assay was performed. Representative images of crystal violet-stained wells are shown in (C). Inhibition of standard infectious virus-induced cytopathic effect by DI particles at each dose was determined in (D) by measurement of the mean pixel intensity of each well using Image J software. The data in (D) are representative of the mean ± SEM relative to WT VSP4B (at 2,000 PFU per well) from 4 independent experiments and were tested for statistical significance with a two way ANOVA and Holm-Sidak's test for multiple comparisons. (E) The assay described in Fig 5 was used to directly measure the LCMV DI titer present in the supernatants collected from the VSP4B WT or DN cells at 72 hr pi. Briefly, each virus-containing preparation was subjected to UV-irradiation to inactivate standard infectious LCMV particles while preserving DI particle activity. Serial 5-fold dilutions of each UV-treated sample were inoculated onto Vero E6 cells, followed by the addition of 50 PFU of standard LCMV. Following a 1 hr incubation at 37oC to permit viral particle absorption, cells were overlaid with agarose and subsequently fixed and stained with crystal violet to visualize whether the various UV-treated rLCMV preparations impacted the ability of standard LCMV particles to form plaques. The LCMV DI titers are reported as mean PIU50/mL ± SEM for 4 independent experiments and were tested for statistical significance with an unpaired t test with Welch's correction. (A-B, D-E) n.s. (not significant), *$p < 0.05$, **$p < 0.01$, as determined by the indicated statistical tests.

Viral late domains can drive virus budding by recruiting components of the cellular ESCRT pathway to complete the final membrane scission step. Given the important role that the LCMV PPXY late domain played in the production of DI particles (Figures 2.4A, 2.4B, and 2.5C), we hypothesized that this late domain might be recruiting the ESCRT pathway machinery to drive DI particle formation. To test this hypothesis, we utilized cell lines that lack a functional ESCRT pathway due to inducible expression of a dominant negative (DN), E235Q point mutant, of VPS4, an ATPase involved in the final stages of ESCRT pathway function (Dalal et al., 2004; Lin et al., 2005; Taylor et al., 2007). Because the ESCRT pathway can also affect LCMV entry (Pasqual et al., 2011), we first infected cells with LCMV for 48 hr to allow the entire monolayer to become infected before

inducing expression of WT or DN VPS4. The cells were washed and fresh media containing the induction agent was added to the cells 6 hr after initial induction (54 hr pi) and the virus-containing media was collected 18 hr later (72 hr pi) to determine levels of standard infectious particles and DI particles (Figure 2.6). Western blot analysis of protein lysates at 72 hr pi confirmed the strong induction of WT and DN VPS4B expression and examination of fixed coverslips showed that all cells were expressing both the induced VSP4B as well as LCMV NP (Figure 2.6B). This infection protocol was chosen to ensure that we were examining virus that was produced in cells expressing the induced VPS4B proteins, while minimizing the effect that these proteins could exert on viral entry. Expression of DN VPS4B had no impact on the release of standard infectious LCMV ($P = 0.27$; Figure 2.6B). In contrast, expression of DN VPS4B led to a marked reduction in the release of infectious VSV particles (Figure 2.6A), which is consistent with previous studies (Taylor et al., 2007) and confirms the specificity of our findings for LCMV. Measuring LCMV DI particle activity as described in Figure 2.4 revealed that WT LCMV produced considerably fewer DI particles per standard infectious virus particle in the DN VPS4B background when compared to cells expressing WT VPS4B (Figures 2.6C and 2.6D). A similar trend for both LCMV infectious virus and DI particle activity was seen in cells expressing WT or DN VPS4A (Figure 2.S3). We next used the assay described in Figure 2.5 to directly quantitate the LCMV DI particle activity in these samples. Consistent with the findings in Figures 2.6C and 2.6D, this demonstrated that significantly fewer DI particles are made in the context of the DN VPS4B background when compared to WT

VPS4B (mean 41 ± 6 SEM vs 1,491 ± 70 PIU50/mL, respectively; P = 0.0022). Thus it appears that LCMV DI particle formation requires a functional ESCRT pathway (Figures 2.6C-2.6E) in addition to a canonical late domain (Figures 2.4 and 2.5C) while standard particles do not (Fig 6B).

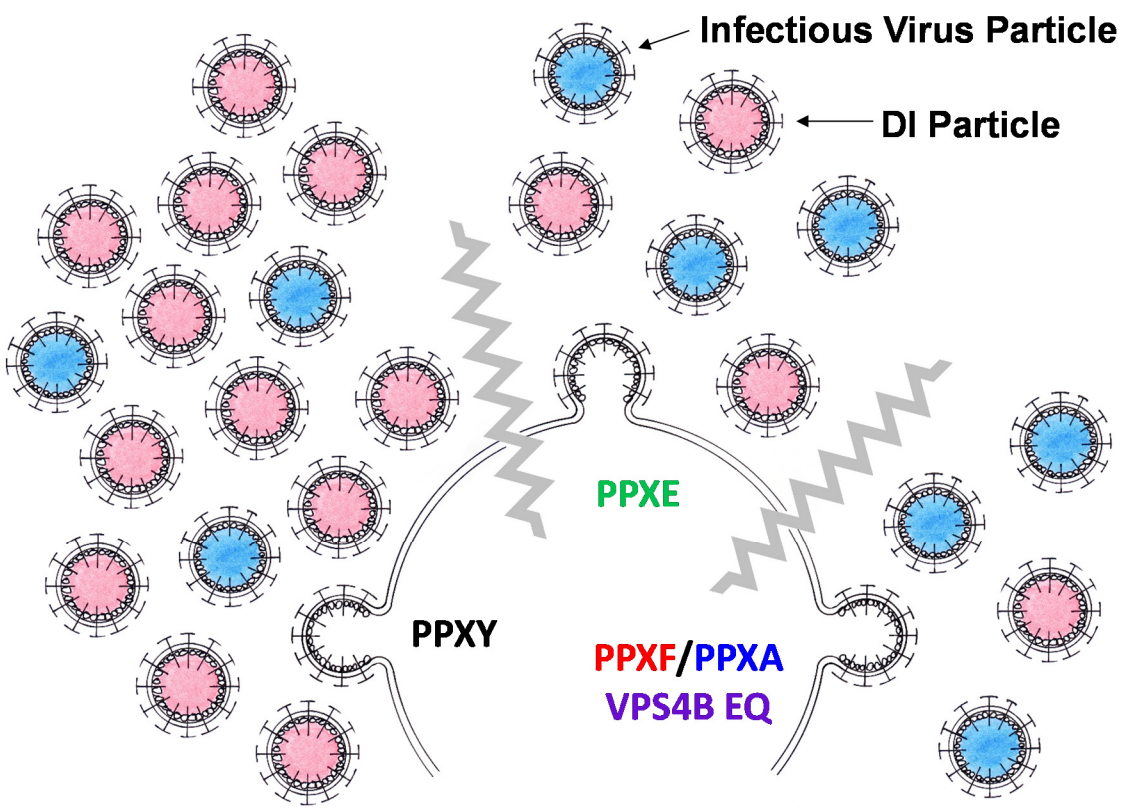

Figure 2.7**. Proposed model of PPXY-driven DI particle production.** WT virus containing an intact PPXY late domain produces high levels of infectious and DI particles. Disruption of the PPXY motif (PPXF or PPXA) or disruption of the ESCRT pathway causes decreased overall DI particle production compared to standard infectious particles. The phosphomimetic PPXE virus has an intermediate phenotype.

The ability of most arenavirus matrix proteins to drive viral budding is thought to be highly dependent upon one or more encoded late domains (Perez et al., 2003; Strecker et al., 2003). The arenavirus LCMV encodes a single late domain, PPPY. The PPXY motif is found in the matrix proteins of several families of enveloped RNA viruses and for many of these viruses is required for the release of infectious virions in an ESCRT-dependent fashion (for review see (Votteler and Sundquist, 2013)). We demonstrate here that the

PPXY late domain encoded by LCMV is not absolutely required for infectious virus release. Further, our data suggest that infectious particle release can occur in the absence of a functional ESCRT pathway. Strikingly, we show that the formation of LCMV DI particles critically requires a functional PPXY late domain and that this process is ESCRT-dependent (see Figure 2.7 for our proposed model). Last, our data demonstrate that the terminal tyrosine in the LCMV PPXY motif is phosphorylated and that this posttranslational modification may exert a regulatory effect on Z's ability to drive DI particle release. Therefore, we have uncovered an unexpected role for the PPXY late domain and a possible mechanism for its regulation of DI particle production.

Our findings raise the intriguing possibility that LCMV utilizes divergent pathways for the production of infectious and DI particles. Neither a functional PPXY motif nor ESCRT pathway were absolutely required for the release of standard infectious particles. These findings, combined with the fact that LCMV Z does not encode additional canonical late domains, strongly suggest that infectious LCMV release occurs through a novel, unknown mechanism. While the rLCMV PPXY mutants studied here initially displayed a slight lag in infectious virus release, each ultimately matched WT levels. Consistent with an earlier study by Perez et al. (Perez et al., 2003), we observed that mutation of the PPXY domain impairs the ability of LCMV Z to form VLPs (Figure 2.2E). This finding in the VLP system may accurately reflect the initial lag in infectious virus release seen for rLCMVs bearing the same PPXY mutations (Figures 2.2B and 2.2C) and/or their decreased ability to form DI particles (Figures 2.4 and 2.5). With regard to the

importance of the ESCRT pathway for infectious virus production, expression of DN VPS4B had no impact on the ability of WT rLCMV to form standard infectious virus (Figure 2.6B). Similarly, expression of DN VPS4B did not impair the ability of LCMV Z to form VLPs when compared to cells expressing WT VPS4B (see Figure 2.S5). This VLP-based result does not agree with an earlier finding by Perez et al. whereby silencing expression of the ESCRT component TSG101 impaired the release of infectious LCMV VLPs (Perez et al., 2003). This discrepancy may reflect differences in the particular VLP assays employed (VLP release versus infectious VLP release and transduction) or perhaps the format of the experiments (siRNA silencing of TSG101 versus inducible expression of WT or DN VPS4B). The different VLP systems could also recapitulate different aspects of virus particle release, with one VLP assay perhaps mimicking infectious virus production while the other more closely resembles DI formation. In similar experiments featuring rhabdoviruses (Jayakar et al., 2000; Wirblich et al., 2008b), Ebola virus (Neumann et al., 2005b), retroviruses (Dilley et al., 2010; Le Blanc et al., 2002a; Yasuda and Hunter, 1998; Yuan et al., 2000b), and Hepatitis B virus (Garcia et al., 2013), loss of the PPXY motif and/or ESCRT resulted in standard virus growth that remained attenuated compared to WT. Interestingly, the New World arenavirus Pichinde remains attenuated following disruption of its encoded late domain (PSAP) (Wang et al., 2012), while the matrix protein encoded by the New World arenavirus Tacaribe can form VLPs in the absence of its late domain (YXXL), but requires VPS4 (Urata et al., 2009). These findings suggest that arenaviruses have evolved diverse strategies to drive infectious virus release. One possible explanation

for the observed late domain-independent generation of infectious LCMV particles is that the LCMV Z protein, either by itself or in combination with other viral structural proteins, may be sufficient to drive particle release in the absence of recruited host proteins. Alternatively, LCMV may contain additional sequence motifs, either in Z or the other structural proteins, that recruit novel host protein machinery to facilitate budding.

In contrast to standard virus particles, both the PPXY late domain and the ESCRT pathway appear critical for the release of DI particles. To our knowledge, this is the first example of a virus utilizing a late domain to selectively drive the production of DI particles independently of standard virus. That LCMV has evolved such a mechanism likely reflects the presumed importance of DI particles for the successful establishment of an asymptomatic, persistent infection in reservoir rodents, which ultimately ensures the long term maintenance of LCMV in nature (Meyer and Southern, 1997; Popescu and Lehmann-Grube, 1977). While the existence of arenavirus DI particles has long been realized, surprisingly little is known about their exact composition and properties. Our data demonstrates that cells infected with the rLCMV PPXY mutants release much less NP, GP, and Z per PFU of cell-free virus when compared to WT rLCMV. This is presumably due to reduced levels of DI particles being released by the PPXY mutant viruses. Interestingly, the degree of reduction was not equivalent among the viral proteins. In particular, Z was reduced to the greatest extent (~3% of WT) when compared to NP or GP (~25% of WT), which could indicate that Z itself is enriched in DI particles and is critical for the ability of DI particles to interfere with the propagation of standard virus particles. Consistent with

this idea, Z is able to render cells refractory to superinfection with homologous virus and treatment of DI particles with RNA-damaging levels of UV does not reduce their interfering ability (Cornu et al., 2004; Welsh et al., 1972). Therefore, it is possible that particles containing high quantities of Z, or simply VLPs consisting primarily of Z, may represent a class of arenavirus DI particles.

Arenavirus matrix proteins exhibit significant diversity in the type and number of late domains they encode. The PPXY domain is found in several Old World arenavirus matrix proteins but not in New World arenaviruses (Figure 2.2A and (Fehling et al., 2012; Wolff et al., 2013)). We have observed that the New World arenavirus JUNV C#1, which encodes both a PTAP and YXXL late domain, generates considerably fewer DI particles per standard infectious particle when compared to the PPXY-containing LCMV (Figure 2.S4). While it is not known whether the PTAP and/or YXXL motifs contribute to DI particle formation in the case of JUNV C#1, this observation may indicate that the PPXY domain is particularly strong in driving DI particle assembly and release. It is possible that individual arenaviruses require different rates of DI particle formation for optimal fitness and have evolved to encode particular late domain combinations to best meet those needs.

We show that the LCMV Z protein is phosphorylated, which suggests that phosphorylation may be important for the regulation of one or more of Z's functions. The fact that this modification occurs at the terminal tyrosine of the PPXY late domain and can be detected in virion-derived Z led us to hypothesize that it may influence Z's budding function. To study the impact of this modification we generated rLCMV with mutations at

tyrosine 88 that either prevented phosphorylation (Y88F or Y88A) or mimicked it (Y88E). Relative to the mutants that cannot be phosphorylated, the Y88E phosphomimetic virus generated significantly more DI particles per infectious particle (Figures 2.4 and 2.5C). This suggests that reversible phosphorylation of the PPXY motif may act as a rheostat to regulate the rate of DI particle production independent of standard virus, possibly through the recruitment of ESCRT machinery. Interestingly, the terminal tyrosine of the PPXY late domains encoded by Ebola virus and Marburg virus VP40 is also phosphorylated. Inhibiting phosphorylation of the Ebola virus VP40 PPXY motif reduced the release of infectious virus (García et al., 2012) whereas mutation of the Marburg virus VP40 PPXY motif to prevent phosphorylation did not impact infectious VLP release, but instead impaired the recruitment and incorporation of nucleocapsids into VLPs (Kolesnikova et al., 2012). The role of the PPXY domain and/or its phosphorylation with regard to DI particle production in the filovirus model and other PPXY-containing virus families remains an open question. In the current model, it will be important to identify the host kinase responsible for phosphorylating the LCMV PPXY domain, although this may require a comprehensive tyrosine kinase screen as the flanking residues surrounding Y88 were not recognized by kinase motif prediction tools (Obenauer et al., 2003; Wong et al., 2007).

How does the PPXY late domain of LCMV promote the release of DI particles? While it is well known that the PPXY motif can drive viral budding, the exact mechanism by which it recruits ESCRT proteins to promote this process is not fully understood.

Several PPXY-dependent viruses also require NEDD4 family E3 ubiquitin ligases (e.g., NEDD4, ITCH, or WWP1), which can directly bind to the PPXY motif via their WW domains (for review see (Votteler and Sundquist, 2013)). Recruitment of ESCRT machinery could occur due to ubiquitination of Z by a NEDD4 E3 ubiquitin ligase, which in turn could recruit ESCRT components (e.g. TSG101) that can bind ubiquitinated proteins (Votteler and Sundquist, 2013). Alternatively, arrestin-related trafficking adaptors (ARTs) may provide an ESCRT linkage as these proteins interact with both NEDD4 E3 ubiquitin ligases as well as ESCRT proteins and have been shown to influence both multivesicular body formation and viral budding (Rauch and Martin-Serrano, 2011). Under this scenario, phosphorylation of the PPXY motif could regulate DI particle release by modifying the accessibility of the PPXY domain to NEDD4 E3 ubiquitin ligases.

All viruses must strike a balance between pathogenesis and persistence, with the ultimate goal of ensuring their own maintenance in nature. It has long been postulated that DI particles may be one way in which LCMV is able to tip the scales towards persistence, thus lowering its immunological profile and fitness cost to its host. By identifying the specific cellular pathway required to form these DI particles, and the apparent importance of viral phosphorylation in accessing the pathway, our findings raise the possibility that arenaviruses can dynamically adjust DI particle production in response to external environmental factors. Further, the PPXY mutant viruses we have developed represent a new tool that will allow the field to formally test the importance of DI particles for the establishment of persistent LCMV infection in reservoir rodents. The ability of the PPXY

late domain to drive the production of DI particles is a novel finding with important implications for understanding host-pathogen relationships and the design of vaccines and antivirals. In particular, PPXY-containing viruses such as Ebola virus and Lassa virus are known to persist for long periods following the resolution of acute human disease (Bausch et al., 2007; Emond et al., 1982; Varkey et al., 2015). It is possible that DI particles play a significant role in allowing these viruses to persist in humans, similar to their presumed importance for infection in reservoir species. Therefore, targeting DI particle formation could be a promising approach to clear persistent infection in humans. Finally, the possibility that the PPXY late domain and ESCRT machinery could broadly drive DI particle production in other virus families represents an exciting area of future research.

Materials and Methods

Cells and viruses

Human embryonic kidney cells (HEK-293T/17) (CRL-11268, American Type culture Collection, Manassas, VA) (referred to as HEK293T cells in the manuscript) were maintained in Dulbecco's Modified Eagle Medium (DMEM) (11965-092) supplemented with 10% fetal bovine serum (FBS) (16140-071), 1% penicillin-streptomycin (15140-122), 1% MEM Non-Essential Amino Acids Solution (11140-050), 1% HEPES Buffer Solution (15630-130), and 1% GlutaMAX (35050-061) purchased from Invitrogen (Carlsbad, CA). L929 mouse fibroblast cells (CCL-1, American Type culture Collection) were maintained in Minimum Essential Medium (MEM) (11095-080) supplemented with 10% FBS, 1% penicillin-streptomycin, 1% MEM Non-Essential Amino Acids Solution, 1% HEPES Buffer Solution, and 1% GlutaMAX. Baby hamster kidney cells (BHK-21) were kindly provided by M. J. Buchmeier (University of California, Irvine) and grown in DMEM supplemented with 10% FBS, 1% penicillin-streptomycin, and 1% GlutaMAX. African green monkey kidney cells (Vero E6) were kindly provided by J. L. Whitton (The Scripps Research Institute, La Jolla) and grown in DMEM supplemented with 10% FBS, 1% penicillin-streptomycin, and 1% HEPES Buffer Solution. T-Rex HEK293 cells stably transduced with a tetracycline-inducible plasmid encoding WT or dominant negative EQ mutant vacuolar protein sorting 4A (VPS4A) or VPS4B as described in (Dalal et al., 2004; Lin et al., 2005; Taylor et al., 2007) were generously provided by M. Kielian (Albert Einstein College of Medicine, Bronx) and were maintained in DMEM supplemented with

10% FBS, 1% penicillin-streptomycin, 1% MEM Non-Essential Amino Acids Solution, 1% HEPES Buffer Solution, 1% GlutaMAX, and 100 µg/mL Zeocin (R250-01, Invitrogen). VPS4 expression was induced by incubating cells in the above growth medium containing 1 µg/mL tetracycline as described (Taylor et al., 2007). All cell lines were grown at 37 ºC in a humidified incubator containing 5% CO_2. Lymphocytic choriomeningitis virus (LCMV) strain Armstrong 53b was kindly provided by J. L. Whitton. Wild-type vesicular stomatitis virus expressing green fluorescent protein (VSV-GFP) as described in (Stojdl et al., 2003) was kindly provided by J. Hiscott (Vaccine and Gene Therapy Institute of Florida, Port St. Lucie) and M. Shaw (Icahn School of Medicine at Mount Sinai, New York). Junín virus (JUNV) C#1, which is an attenuated vaccine strain derived from the virulent WT JUNV strain XJ as described in (Chosewood et al., 2009; Goñi et al., 2006), was kindly provided by M. Buchmeier (University of California, Irvine) and R. Tesh (The University of Texas Medical Branch at Galveston). Working stocks of these viruses were amplified and titered (via plaque assay) on Vero E6 cells. See below under "Generation of Recombinant LCMV" for a description of the recombinant (r)LCMV strain Armstrong 53b that were generated for this study.

Plasmids

The LCMV Armstrong 53b Z protein (WT, Y88A, Y88E, or Y88F) was subcloned into a modified pCAGGS expression vector (Cornillez-Ty et al., 2009) and different combinations of these plasmids were used to screen for the phosphorylation of Z (Figure 2.1D) or the budding efficiency of Z (Figure 2.2E). The WT and Y88 mutant Z genes were

fused to the streptavidin binding peptide (SBP) (MDEKTTGWRGGHVVEGLAGELEQLRARLEHHPQGQREP) through an 18 base pair linker at the C-terminus of Z to permit affinity purification and western blot detection of Z. The nucleotide sequence of the WT Z gene matches NCBI gene identifier number AY847351 while the translated amino acid sequence for the WT Z gene matches Protein Locus number AAX49343. WT Z was amplified by PCR from the pT7-L(+) plasmid generously provided by J. C. de la Torre (The Scripps Research Institute, La Jolla) (Sanchez and De la Torre, 2006) using the forward primer LCMVZf (5'-ACAAGTTTGTACAAAAAAGCAGGCTGATATCGCCACCATGGGTCAAGGCAAG TCCAGA-3'), which has a 5' overhang containing Gateway AttB1 and Kozak sequences and the reverse primer LCMVZr (5'-ACCTCCACCTCCAGCTGCCTCTTCGTAGGGA

GGTGGAGA-3'), which has an overhang containing the linker sequence. The SBP tag was amplified from the pT7-FLAG-SBP-1 plasmid (P3871, Sigma-Aldrich, St. Louis, MO) via PCR using the forward primer SBPf (5'- GCAGCTGGAGGTGGAGGTATGGACGA

AAAAACCACCGGT-3'), which has a 5' overhang containing the linker sequence, and the reverse primer SBPr (5'-ACCACTTTGTACAAGAAAGCTGGGTCTTACGGTTCA

CGCTGACCCTGCGG-3'), which contains a 3' overhang with a stop codon preceding an AttB2 sequence. The two products were fused by PCR using the Z forward primer and the SBPr primer. The cassette was subcloned into the pCAGGS vector using the Gateway cloning system (Invitrogen) following the manufacturer's instructions as has been

previously described (Cornillez-Ty et al., 2009; Klaus et al., 2013). The plasmids pC-NP and pC-GP, which express the LCMV Armstrong 53b nucleoprotein (NP) and glycoprotein (GP), respectively, and plasmids pol-I S and pol-I L, which express the LCMV L and S genome segments, respectively, were used to generate rLCMV. These reagents were generously provided by J. C. de la Torre and are described in (Flatz et al., 2006). Each of the Y88 mutant Z genes used in these studies were synthesized and subcloned into the pCAGGS or pol-I L vectors, respectively, by Biobasic, Inc. (Markham, ON, Canada). A pol-I L vector containing an SBP-tag directly fused to the C-terminus of Z was also generated by Biobasic, Inc. All plasmid sequences were verified by DNA sequencing.

Identification of phosphorylated residues by mass spectrometry

To identify phosphorylation sites on LCMV Z via mass spectrometry, Vero E6 cells were infected with LCMV strain Armstrong 53b and 48 hr later cell-free virions were purified by sucrose-banding as described previously (Burns and Buchmeier, 1991). Purified virions were then lysed in Triton buffer (0.5% NP40, 1% Triton X-100, 140mM NaCl, and 25mM Tris-HCl containing a protease inhibitor cocktail (04693159001, Roche Applied Science, Indianapolis, IN)) and mixed with Laemmli sample buffer (62.5 mM Tris-HCl, 10% glycerol, 2% sodium dodecyl sulfate and 0.01% bromophenol blue (B392, Fisher Scientific, Pittsburgh, PA)) containing 5% 2-mercaptoethanol. Virion protein lysates were separated on a 4-20% Tris-Glycine polyacrylamide gel (EC60255, Invitrogen). The gel was stained with Coomassie (40% methanol, 20% acetic acid, and 0.1% Brilliant Blue R (B7920, Sigma-Aldrich)), destained with a solution of 30% methanol and 10% acetic acid,

and then imaged using a Canon Canoscan 8800F scanner. For mass spectrometry, the protein band corresponding to the Z protein was excised and cut into 1 mm cubes and processed with chemicals from Fisher Scientific as follows. The gel pieces were rinsed with HPLC grade water and then incubated with destain solution (50 mM ammonium bicarbonate and 50% acetonitrile) for 30 minutes at 37 ºC. The destain solution was removed and the gel pieces were dehydrated by incubating twice with 100% acetonitrile for 5 minutes. The gel pieces were reduced with 25 mM dithiothreitol in 50 mM ammonium bicarbonate for 30 minutes at 55 ºC. After cooling for 10 minutes at room temperature, the gel pieces were dehydrated by incubating with 100% acetonitrile for 5 minutes and then alkylated in the dark with 10 mM iodoacetamide in 50 mM ammonium biocarbonate for 45 minutes at room temperature. The gel pieces were washed two times in destain solution for 5 minutes, dehydrated with 100% acetonitrile, then rehydrated with water for 10 minutes. The gel pieces were further dehydrated with two 5 minute incubations in 100% acetonitrile before removing all liquid and drying the gel pieces at room temperature for 10 minutes. The gel pieces were rehydrated with a solution of 12.5 ng/µL sequencing grade chymotrypsin (V1061, Promega, Madison, WI) or 12.5 ng/µL sequencing grade modified trypsin (V5111, Promega) in 50 mM ammonium bicarbonate on ice for 30 minutes, before digesting overnight at 37 ºC. Peptides were extracted with a solution of 2.5% formic acid in 50% acetonitrile while spinning in a microcentrifuge at 13,000 rpm for 10 minutes. The supernatant was removed and saved while the gel pieces were subjected to further extraction and rinsing with 100% acetonitrile. The second extraction was combined with

the initial extraction. All solvent was removed from the extracts using a vacuum centrifuge at 37 ºC. The peptides were resuspended in 2.5% formic acid, 2.5% acetonitrile prior to mass spectrometry analysis. Peptides were separated over 12 cm of Magic C18, 5 μM, 200 Å reversed phase material (PM5/66100/00, Michrom Bioresources, Auburn, CA) in a microcapillary column using a MicroAS autosampler (Thermo Scientific, Pittsburgh, PA). Following 15 minutes of isocratic loading in 2.5% acetonitrile, 0.15% formic acid, the peptides were eluted from the column with a 5-35% gradient of acetonitrile with 0.15% formic acid over 40 minutes using a Surveyor Pump Plus HPLC (Thermo Scientific). Mass spectra were acquired either in an LTQ-XL linear ion trap, or in a linear ion trap-orbitrap mass spectrometer (Thermo Scientific) as described previously (Ballif et al., 2008). Briefly, for most analyses 10 data-dependent MS/MS spectra followed each survey scan. However, in several cases after obtaining the initial spectra for phosphopeptides we followed up with targeted MS/MS spectra in order to increase fragment ion coverage. The IPI human forward and reverse concatenated database was used to search the raw data using SEQUEST software requiring tryptic peptides and either a 2 Da precursor mass tolerance (for precursor data acquired in the LTQ) or 20 PPM (for precursor data acquired in the orbitrap). In the searches the following precursor mass differences were allowed: serine, threonine, and tyrosine residues (+79.96633 Da); methionine (+15.99492 Da) and cysteines (+57.02146 Da or 71.0371).

Validation of Z phosphorylation

To confirm that Z was phosphorylated in human cells as well as cells from rodent cells, in Figures 2.1D-E, plasmid-derived Z expressed in HEK293T cells and Z from rLCMV Z-SBP-infected cells were both probed for phosphotyrosine signal via western blot. For plasmid-derived Z, 2 x 10^5 HEK293T cells were seeded in a 12-well plate and transfected the next day with 0.8 μg per well of pLCMV-Z WT, pLCMV-Z Y88F, or an empty vector using 0.8 μL of a 1 mg/mL solution of polyethylenimine (23966, Polysciences, Inc., Warrington, PA) per well. For Z derived from rLCMV Z-SBP-infected cells, 2.5 x 10^5 L929 cells were seeded in 6-well plates and infected the next day at an MOI of 0.01. Two days following the transfection or infection, H_20_2 at a final concentration of 8.8 mM or an equivalent volume of H_20 was spiked into the appropriate wells containing HEK293T or L929 growth media. After a 15 minute incubation, the cells were lysed in Triton buffer containing a protease inhibitor cocktail and PhosStop phosphatase inhibitor cocktail (04906837001, Roche Applied Science) and the SBP-tagged Z proteins were affinity purified using magnetic streptavidin beads as previous described (Klaus et al., 2013). The purified proteins were separated via SDS-PAGE and screened for Z or tyrosine phosphorylated-Z via standard chemiluminescent western blotting and detected with film (Figure 2.1D) or with a LI-COR C-Digit digital imager (LI-COR, Lincoln, NE) (Figure 2.1E).

Generation of recombinant (r)LCMV

rLCMV WT, rLCMV Z-SBP and rLCMV containing Z-Y88 mutations (Y88F, Y88E, Y88A) were generated using the previously described reverse genetics system (Flatz et al., 2006). Briefly, 10 µL of Lipofectamine 2000 (52887, Invitrogen) was mixed with 100 µL of OptiMEM (31985, Invitrogen) and then added to a plasmid mixture consisting of 1.6 µg pC-NP, 2.0 µg pC-L, 1.6 µg pol-I S, and 2.8 µg pol-I L (WT, Z-SBP or containing the described Y88 point mutations) in 100 µL OptiMEM and incubated at room temperature for 25 minutes. 200 µL of this transfection mixture and 800 µL of OptiMEM was then added to 1 well of a 6-well plate which had been seeded the previous day with 3.5×10^5 BHK-21 cells and washed prior to transfection with 1 mL of OptiMEM. The cells were incubated with the transfection mixture for 4 hr after which the media was replaced with BHK-21 growth media diluted 5-fold in DMEM. Three days later the supernatant was collected, clarified by centrifugation at 1,200 RPM for 5 minutes at 4 ^{o}C, and used to infect a fresh monolayer of 1.8×10^6 BHK-21 cells in a T-75 flask. Following a 1 hr absorption, the inoculum was removed and fresh BHK-21 growth media diluted 5-fold in DMEM was added to the cells. Three days later the supernatant of this flask was collected, clarified by centrifugation, and titered by plaque assay. To generate an expanded virus stock, Vero E6 cells were infected with this material at an MOI of 0.0001 and 48 or 72 hr later, supernatants were collected, clarified, and titered by plaque assay. A portion of the L segment (most of the Z gene, the intergenic region, and part of the L gene) of each rLCMV Y88 mutant was sequenced to ensure that these viruses had not reverted. The material used

for this sequencing was derived from the 72 hr pi time point shown in Figure 2.2B. Viral RNA from clarified supernatants was isolated using the Qiagen Viral RNA mini kit (52906, Qiagen, Valencia, CA) according to the manufacturer's protocol. Viral RNA was converted to cDNA using primer L 845- (5'- GCAGGACTTGAGGGCTATGA-3'), Superscript III (18080-044, Invitrogen), RNAse Out (10777-019, Invitrogen), and 5 μL of RNA following the manufacturer's protocol for first strand cDNA synthesis. A portion of the L-segment containing Z was amplified with 30-40 cycles of PCR using Platinum *Pfx* DNA polymerase (11708-013, Invitrogen) and primers L126+ (5'- ATAGTACAAACAGGGCCGAAATC C-3') and L764- (5'- TTTGTTGGGTTCAGAGATAAGTGT-3') following the manufacturer's protocol. The PCR product was prepared for sequencing using ExoSAP-IT (78200, Affymetrix, Santa Clara, CA) following the manufacturer's protocol and sequenced by the University of Vermont Cancer Center DNA Analysis Facility.

SDS-PAGE and western blotting

Protein lysates were diluted in Laemmli sample buffer containing 5% 2-mercaptoethanol and separated on NuPAGE 4-12% Bis-Tris gels with MES buffer. Protein was transferred to nitrocellulose membranes using iBlot gel transfer stacks (IB301001 or IB301002, Invitrogen) and the Invitrogen iBlot Device as directed by the manufacturer. Efficient protein transfer was confirmed by staining membranes with a solution containing 0.1% Ponceau S (P3504, Sigma-Aldrich) and 5% acetic acid which was subsequently removed by washing with water. Two methods were used for protein detection: quantitative LI-COR-based detection or standard chemiluminescent-based detection. For quantitative LI-

COR analysis, membranes were blocked with a solution of 5% milk in PBS for 1 hr and incubated overnight at room temperature with the indicated primary antibodies diluted in PBS containing 5% milk and 0.2% Tween 20 (BP337, Fisher Scientific). Following 5 washes in PBS with 0.5% IGEPAL CA-630 (198596, MP Biomedicals, Solon, OH), the membranes were incubated for 1 hr at room temperature with secondary antibodies diluted in PBS containing 5% milk, 0.2% Tween 20 and 0.02% sodium dodecyl sulfate, washed 5 times in PBS with 0.5% IGEPAL CA-630 and 1 time with PBS, then imaged using the LI-COR Odyssey CLx imaging system. For quantitative LI-COR analysis of VPS4B in Figures 2.6A, 2.6B, and 2.S5, membranes were probed using the iBind Flex western device (SLF2000, Thermo Scientific) with the iBind Flex fluorescent detection solution kit (SLF2019, Thermo Scientific) following the manufacturer's instructions. For chemiluminescent-based detection of phosphorylated proteins, the same general procedure was used with the following exceptions: i) membranes were blocked with either PBS containing 5% milk and 0.05% IGEPAL CA-630 or protein-free blocking buffer (37572, Thermo Scientific), ii) primary and secondary antibodies were diluted in PBS containing 5% milk, 0.05% IGEPAL CA-630 , and 3% fetal bovine serum or protein-free blocking buffer, and iii) the secondary antibodies were incubated with the membrane for 2 hr.

The following primary antibodies were used for western blotting (at the indicated concentrations): mouse anti-streptavidin binding peptide (MAB10764, Millipore, Billerica, MA) (1:10,000), rabbit anti-actin (A2066, Sigma-Aldrich) (1:10,000), mouse anti-actin (A5441, Sigma-Aldrich) (1:5,000), rabbit anti-actin (A2066, Sigma-Aldrich) (1:2,500),

mouse anti-phosphotyrosine (clone 4G10, Millipore) (0.2 μg/mL), mouse anti-green fluorescent protein (632380, Clontech, Mountain View, CA) (1:1,000), rabbit anti-LCMV Z (880) (1:500), mouse anti-LCMV GP2 (33.6) (1:2,000), and rabbit anti-LCMV nucleoprotein (2165) (1:5,000). Antibodies 880, 2165, and 33.6 were generously provided by M. J. Buchmeier (University of California, Irvine). For quantitative western blotting, the following secondary antibodies from LI-COR were used: IRDye 800CW goat anti-mouse (926-32210) for the Z release assay in Figure 2.2E at 1:20,000 and in Figure 2.6A, 6B, and S5 at 1:3,000 (for probing by iBind) and IRDye 680LT goat anti-mouse (926-68020) and IRDye 800CW Goat anti-rabbit (926-32210) were used at 1:20,000 to detect proteins in Figures 2.3A-2.3D. IRDye 680LT goat anti-mouse was used at 1:3,000 (for probing by iBind) in Figure 2.S5 to detect actin. A horseradish peroxidase-conjugated anti-mouse secondary antibody (71045, EMD Millipore, Billerica, MA) diluted 1:5,000 was used for chemiluminescent-based detection in Figures 2.1D and 2.1E.

Virus growth curve

To determine the growth kinetics of rLCMV in Figure 2.2B, 6-well plates were seeded with 1.9 x 10^5 Vero E6 cells per well. The following day the cells were infected with each respective rLCMV at an MOI of 0.01. Supernatants were collected at 12, 24, 36, 48, and 72 hr pi, clarified by centrifugation at 1,200 RPM for 5 minutes at 4 ºC, then titered by plaque assay.

Z-virus-like particle (VLP) release assay

To determine the release efficiency of the Y88 mutant Z proteins in Figures 2.2E and 2.S5, 2 x 10^5 HEK293T cells or T-Rex HEK293 cells stably transduced with a tetracycline-inducible plasmid encoding WT or dominant negative EQ mutant VPS4B were seeded in a 12-well plate. The next day cells were transfected with 0.8 μg per well of pLCMV-Z WT, Z-G2A, -Z Y88F, -Z Y88E, or -Z Y88A using 0.8 μL of a 1 mg/mL solution of polyethylenimine per well. For the experiments shown in Figure 2.S5, VPS4B expression was induced with 1 μg/mL tetracycline at the time of transfection. The following day (24 hr post-transfection) cells and VLP-containing media (which had been clarified) were collected, lysed with Triton lysis buffer, and subjected to quantitative western blotting. For detection of Z from VLPs produced in VPS4B WT or DN cell lines, SBP-tagged Z was affinity purified from lysed VLP-containing media using magnetic streptavidin beads prior to quantitative western blot analysis. To calculate the percent VLP release we first normalized each Z protein value (from supernatants or cells) by the sum of all Z protein bands on a particular gel as described in (Degasperi et al., 2014). The percent VLP release was then calculated as the quotient of the Z protein quantity in VLPs divided by the quantity of Z in cells [(Z_{mut}VLP / Z_{mut}cells) / (Z_{WT} VLP/ Z_{WT} cells)].

Plaque assay and measurement of plaque size and cytopathic effect

To measure infectious virus titers, a standard plaque assay was employed as follows. Six-well plates were seeded with 1 x 10^5 (LCMV and JUNV) or 1 x 10^6 (VSV) Vero E6 cells per well and the following day inoculated with 10-fold serial dilutions of virus in a total

volume of 0.5 mL of Vero E6 growth medium. Following a 90 minute absorption at 37 ºC, the cells were overlaid with a solution of 0.7% agarose (20-102, Apex Industrial Chemicals, Aberdeen, United Kingdom) in Vero E6 growth media. The plates were fixed 2 (VSV) or 4 (LCMV and JUNV) days later with a solution of 2.5% formaldehyde (1635-4L, Sigma) in 3x PBS. Following removal of the agarose plugs, the fixed monolayers were stained with 0.1% crystal violet (C581-100, Fisher Scientific) and 2.1% ethanol in water. To determine the plaque size of rLCMV in Figure 2.2D or the overall level of cytopathic effect induced by these viruses in Figures 2.4A, 2.4B, 2.6C, and 2.6D, the wells were imaged with an Alpha Innotech digital camera paired to a Computar H6Z0812M motorized zoom lens. The area of each plaque as well as the mean pixel intensity of each well was calculated using ImageJ software.

Plaque interference assay

To determine the titer of LCMV DI particles, samples were transferred to clear snap cap tubes (21-402-904, Thermo Scientific) and irradiated for 2 minutes with UV light in a UVP CL-1000 ultraviolet crosslinker in to kill standard infectious virus. The samples were serially diluted in 5-fold increments and added to 24-well plates which had been seeded the previous day with 20,000 (LCMV and JUNV C#1) or 100,000 (VSV) Vero E6 cells per well. Subsequently, 50 PFU per well of rLCMV WT (or 50 PFU per well of JUNV C#1 or VSV in Figure 2.5A) was added to each well containing UV-irradiated samples. UV-irradiated samples were also added to a second set of wells to which no standard virus was added to ensure that all infectious virus had been eliminated from the samples. After a 90

minute absorption period at 37 ºC, the cells were overlaid with a solution of 0.7% agarose in Vero growth media and left at 37 ºC. The plates were fixed and stained 2 (VSV) or 4 (LCMV and JUNV C#1) days later as above for the plaque assay. The plaques were counted in each well and the plaque interfering unit 50 (PIU_{50}) was calculated using the plaque reduction statistical web tool (https://exon.niaid.nih.gov/plaquereduction). Because a unique biochemical or genetic signature to differentiate standard infectious virus particles from DI particles has not been defined, the assay we employed relied on measurement of the interfering activity of DI particles as opposed to a direct physical measure of the particles themselves. For Figure 2.5B, rLCMV WT was filtered with either 0.45 μM (28145-481, VWR, Radnor, PA) or 0.2 μM (09-719C, Fisher Scientific) syringe filters or Amicon 30K (UFC903024, Millipore) or 10K (UFC901024, Millipore) centrifugal filters prior to treatment with UV light and DI titering as above.

Virus challenge in inducible VPS4A- and VPS4B-expressing cell lines

To determine the role of the ESCRT pathway in LCMV release, 2.5 x 10^5 T-Rex HEK293 cells stably transduced with a tetracycline-inducible VPS4A or VPS4B (WT or dominant negative EQ in each case) were seeded in 6-well plates that were first coated with poly D-lysine (P6407, Sigma-Aldrich) for 5 minutes then washed 3x with PBS. Cells were infected 24 hr later with rLCMV WT at an MOI of 0.001. Forty-eight hr later (when all cells were productively infected) the cells were induced with growth medium containing 1 μg/mL tetracycline or a medium only control. Six hr after induction cells were washed 3x with PBS and fresh growth medium containing 1 μg/mL tetracycline or medium alone were

added. Eighteen hr later the cells and supernatants were collected. In Figures 2.6A and 2.6B, the cell lysates were probed for VPS4B DN or WT protein (via the GFP fusion tag on these proteins) or actin expression by quantitative western blotting. Supernatants were titered by plaque assay for infectious virus and DI particle levels by measuring the cytopathic effect in a plaque assay with equal PFUs of virus in each well (as described under plaque assay) and/or by plaque interference assay. The role of VPS4B in VSV release was also tested. For the VSV challenge studies, 5 x 10^5 VPS4B WT or EQ cells were seeded in poly D-lysine treated wells and 24 hr later treated with either growth medium containing 1 μg/mL tetracycline or medium alone. One hr later, the cells were infected with VSV at an MOI of 10. One hr following infection, the cells were washed 3x with PBS and fresh growth medium containing 1 μg/mL tetracycline or medium alone was added. Six hr later the cells and supernatants were collected and assessed by quantitative western blotting and plaque assays, respectively.

In order to verify uniform VPS4B expression as well as rLCMV WT infection by microscopy, in parallel to the experiment described above, 5 x 10^4 cells were seeded on poly D-lysine-treated 12mm glass coverslips in 24-well plates. At the time of harvest (24 hr post-infection) the coverslips were rinsed with PBS, fixed with 4% paraformaldehyde (15714, Electron Microscopy Sciences, Hatfield, PA) in PBS for 20 minutes, then washed 2x with PBS for 5 minutes. The cells were permeabilized with 0.1% Triton X-100 in 1% bovine serum albumin (BSA) in PBS, blocked with 10% normal goat serum (005-000-121, Jackson, West Grove, PA) in 1% BSA in PBS, and immunostained with anti-LCMV

nucleoprotein antibody (1.3-3) (1:500) kindly provided by M. Buchmeier (University of California, Irvine) and secondary anti-mouse Alexafluor 555 (A28180, Thermo Scientific) (1:1,000) each for 1 hr in 1% BSA in PBS. DNA was detected with 4', 6-diamidino-2-phenylindole hydrochloride (DAPI) (D9542, Sigma Aldrich) in 1% BSA in PBS. Cells were washed with 1% BSA in PBS in between each step. Images were acquired on a Zeiss LSM 510 laser scanning confocal microscope using a 63X objective lens. Post-capture image processing was carried out in FIJI and Photoshop; the GFP fluorescence, NP staining, and DAPI signal are shown at equal exposures in all conditions.

Virion concentration and fractionation

To determine the NP, GP, and Z protein content of rLCMV virions in Figures 2.3A-2.3D, 2 x 10^6 Vero E6 cells were seeded in a T-150 culture flask and infected the next day at an MOI of 0.01, 0.001, or 0.0001. At 48 or 72 hr following inoculation, the supernatant was collected, clarified by centrifugation, and screened for infectious virus by plaque assay. An equal number of plaque forming units of each virus (range 1 to 3x10^7 PFU per experiment) were layered onto a solution of 20% sucrose in TNE buffer, pH 7.4 (10 mM Tris base, 1 mM EDTA, 0.2 M NaCl) and centrifuged for 2 hr at 30,000 rpm at 4 ºC in a Thermo-Scientific Sorval WX Ultra 80 ultra centrifuge equipped with a Sorval Surespin 630 rotor. The resulting virus pellet was resuspended in 2X-concentrated Laemmli buffer containing 5% 2-mercaptoethanol, then analyzed by SDS-PAGE and quantitative western blotting.

To separate rLCMV by gradient centrifugation in Figure 2.S2, 2 x 10^6 Vero E6 cells were seeded in a T-150 culture flask and infected the next day at an MOI of 0.0001. At 72

hr following inoculation, the supernatant was collected and clarified by centrifugation. The clarified supernatants were added to 50 mL tubes (430290, Corning) containing polyethylene glycol (PEG) 8000 (81268, Sigma-Aldrich) and sodium chloride such that the final concentrations were 10% and 1%, respectively. The solutions were incubated at 4 ºC on a rotating platform for 2 hr then were centrifuged for 30 minutes at 10,000 rpm at 4 ºC in a Thermo-Scientific Sorval Legend RT+ centrifuge equipped with a Sorval Fiberlite F15-8x50cy rotor. The supernatant was removed and the virus-PEG pellet was resuspended in TNE buffer and screened for infectious virus by plaque assay. Density gradients were prepared by layering solutions of 7%, 10%, 13%, 16%, and 19% optiprep (D1556, Sigma-Aldrich) diluted in PBS in 36 mL tubes (03141, Thermo Scientific) then leaving overnight at 4 ºC to allow a continuous gradient to form. An equal number of plaque forming units of each virus (range 4 x 10^7 to 1 x 10^8 PFU per experiment) was layered onto the continuous gradient and centrifuged for 12 hr at 30,000 rpm at 4 ºC in a Thermo-Scientific Sorval WX Ultra 80 ultracentrifuge equipped with a Sorval Surespin 630 rotor. The resulting separated virus was collected in 2 mL fractions using a New Era NE-9000G programmable peristaltic pump and titered via plaque assay.

Quantitative RT-PCR

To enumerate copies of LCMV S and L segment genomic RNA contained in virions for Figures 2.3E and 2.3F, viral RNA was extracted from cell-free virions using the Qiagen Viral RNA mini kit according to the manufacturer's instructions and subjected to quantitative RT-PCR as previous described (Haist et al., 2015). Briefly, cDNA was

generated in a 50 µL RT reaction containing 5 µL of viral RNA, 0.2 µM of the gene specific primer S 2865- (5'-CAGGGTGCAAGTGGTGTGGTAAGA-3') or L 5906- (5'-TGGGACTGAGTTTCGAGCATTACG-3'), which are complementary to the S or L segment genomic RNA, 5 µL of 10x PCR Buffer II (#E12874, Applied Biosystems, Carlsbad, CA), 5 µL of 10 mM dNTP mix (362275, Applied Biosystems), 1 µL RNase inhibitor (N808-0119, Applied Biosystems), and 1.25 µL of Multiscribe reverse transcriptase (4308228, Applied Biosystems). RT reaction conditions were 25 ºC for 10 minutes, 48 ºC for 30 minutes, and 95 ºC for 5 minutes. Quantitative PCR was then performed in a 25 µL reaction volume consisting of 5 µL of cDNA, 0.9 µM each of the forward primer S 2275+ (5'-CGCTGGCCTGGGTGAAT-3') or L 5517+ (5'-GGCCTTGTATGGAGTAGCACCTT-3') and reverse primer S 2338- (5'-ATGGGAAAA

CACAACAATTGATCTC-3') or L 5645- (5'-GGTCTGTGAGATATCAAGTGGTAGA

ATG-3'), 0.2 µM of the TaqMan probe S 2295+ (5'-6FAM-CTGCAGGTTTCTCGC-MGBNFQ-3') or L 5582- (5'-6FAM-CTGAAGAATACCACCTATTATACCA-MGBNFQ-3'), and 12.5 µL of the TaqMan Universal PCR Master Mix (4326614, Life Technologies, Grand Island, NY). Reaction conditions were 95 ºC for 10 minutes followed by 40 cycles of 95 ºC for 15 seconds and 60 ºC for 1 minute. Copy numbers of LCMV S or L segment genomic RNAs were calculated by comparison with a series of standard dilutions of the pT7-S or pT7-L plasmids as described (Haist et al., 2015). Data was generated on an Applied Biosystems StepOnePlus Real-Time PCR System and analyzed with the provided software.

Statistical analysis

Statistical analysis was performed using GraphPad Prism software. For the virus growth curves in Figure 2.2B, the data was first log transformed, then a two-way analysis of variance (ANOVA) was performed with a Holm-Sidak's test for multiple comparisons to compare viruses at each time point. A one-way ANOVA with Holm-Sidak's test for multiple comparisons was used to analyze the VLP release assay in Figure 2.2E, the viral protein levels in concentrated virions in Figures 2.3B-2.3D, and the S and L segment to PFU ratios in Figures 2.3E and 2.3F. To compare plaque area in Figure 2.2D, the data were first tested for normality using the D'Agostino and Pearson omnibus normality test, then the Kruskal-Wallis non-parametric test was used and multiple comparisons were made with Dunn's multiple comparisons test. To analyze the cytopathic effect induced by rLCMV WT or Z-Y88 mutants (Figure 2.4B) or by rLCMV WT generated in VPS4B WT or dominant negative cells (Figure 2.6D), a two-way ANOVA was performed with the Holm-Sidak's test for multiple comparisons. To compare VSV or LCMV virus titers, LCMV DI particle titers, or Z VLP levels produced in VPS4B WT or EQ cells (Figures 2.6A, 2.6B, 2.6E, and 2.S5) a two-tailed unpaired t test with Welch's correction was performed. To compare DI particle titers in Figures 2.5A-2.5C, a value of 19 PIU_{50}/mL (just below the limit of detection value of 20 PIU_{50}/mL) was substituted for samples that were below the limit of detection and then a one way ANOVA was performed. For all statistical analyses, the data utilized was generated from at least 3 independent experiments as indicated in each respective figure legend.

Acknowledgments

We thank the UVM Immunobiology Group for insightful discussions and Drs. Alan Howard and Cory Teuscher for statistical support and advice. We are grateful to Drs. Michael Buchmeier, Juan Carlos de la Torre, Margaret Kielian, John Hiscott, and Megan Shaw for providing critical reagents as described in the Materials and Methods.

References

Bajorek, M., Caly, L., Tran, K.C., Maertens, G.N., Tripp, R.A., Bacharach, E., Teng, M.N., Ghildyal, R., and Jans, D.A. (2014). The Thr205 Phosphorylation Site within Respiratory Syncytial Virus Matrix (M) Protein Modulates M Oligomerization and Virus Production. J Virol *88*, 6380-6393.

Ballif, B.A., Carey, G.R., Sunyaev, S.R., and Gygi, S.P. (2008). Large-Scale Identification and Evolution Indexing of Tyrosine Phosphorylation Sites from Murine Brain. J Proteome Res *7*, 311-318.

Bausch, D.G., Towner, J.S., Dowell, S.F., Kaducu, F., Lukwiya, M., Sanchez, A., Nichol, S.T., Ksiazek, T.G., and Rollin, P.E. (2007). Assessment of the Risk of Ebola Virus Transmission from Bodily Fluids and Fomites. J Infect Dis *196*, S142-S147.

Buchmeier, M.J., de la Torre, J.C., and Peters, C.J. (2007). *Arenaviridae*: The Viruses and Their Replication. In Fields Virology, D.M. Knipe, P.M. Howley, D.E. Griffin, R.A. Lamb, M.A. Martin, B. Roizman, and S.E. Straus, eds. (Philadelphia: Wolters Kluwer Health/Lippincott Williams & Wilkins), pp. 1791-1827.

Burns, J.W., and Buchmeier, M.J. (1991). Protein-protein interactions in lymphocytic choriomeningitis virus. Virology *183*, 620-629.

Burns, J.W., and Buchmeier, M.J. (1993). Glycoproteins of the Arenaviruses. In The Arenaviridae, M.S. Salvato, ed. (New York: Plenum Press), pp. 17-35.

Carlton, J.G., and Martin-Serrano, J. (2007). Parallels Between Cytokinesis and Retroviral Budding: A Role for the ESCRT Machinery. Science *316*, 1908-1912.

Chosewood, L.C., Wilson, D.E., Centers for Disease Control and Prevention (U.S.), and National Institutes of Health (U.S.) (2009). Biosafety in microbiological and biomedical laboratories, 5th edn (Washington, D.C.: U.S. Dept. of Health and Human Services, Public Health Service, Centers for Disease Control and Prevention, National Institutes of Health).

Cornillez-Ty, C.T., Liao, L., Yates, J.R., Kuhn, P., and Buchmeier, M.J. (2009). Severe Acute Respiratory Syndrome Coronavirus Nonstructural Protein 2 Interacts with a Host Protein Complex Involved in Mitochondrial Biogenesis and Intracellular Signaling. J Virol *83*, 10314-10318.

Cornu, T.I., Feldmann, H., and de la Torre, J.C. (2004). Cells expressing the RING finger Z protein are resistant to arenavirus infection. J Virol *78*, 2979-2983.

Dalal, S., Rosser, M.F.N., Cyr, D.M., and Hanson, P.I. (2004). Distinct Roles for the AAA ATPases NSF and p97 in the Secretory Pathway. Mol Biol Cell *15*, 637-648.

Degasperi, A., Birtwistle, M.R., Volinsky, N., Rauch, J., Kolch, W., and Kholodenko, B.N. (2014). Evaluating Strategies to Normalise Biological Replicates of Western Blot Data. PLoS ONE *9*, e87293.

Dilley, K.A., Gregory, D., Johnson, M.C., and Vogt, V.M. (2010). An LYPSL Late Domain in the Gag Protein Contributes to the Efficient Release and Replication of Rous Sarcoma Virus. J Virol *84*, 6276-6287.

Dutko, F.J., and Pfau, C.J. (1978). Arenavirus Defective Interfering Particles Mask the Cell-Killing Potential of Standard Virus. J Gen Virol *38*, 195-208.

Emond, R.T., Bannister, B., Lloyd, G., Southee, T.J., and Bowen, E.T. (1982). A case of Lassa fever: clinical and virological findings. Br Med J (Clin Res Ed) *285*, 1001-1002.

Enria, D.A., Briggiler, A.M., and Sanchez, Z. (2008a). Treatment of Argentine hemorrhagic fever. Antiviral Res *78*, 132-139.

Fehling, S., Lennartz, F., and Strecker, T. (2012). Multifunctional Nature of the Arenavirus RING Finger Protein Z. Viruses *4*, 2973-3011.

Fischer, S.A., Graham, M.B., Kuehnert, M.J., Kotton, C.N., Srinivasan, A., Marty, F.M., Comer, J.A., Guarner, J., Paddock, C.D., DeMeo, D.L.*, et al.* (2006). Transmission of Lymphocytic Choriomeningitis Virus by Organ Transplantation. N Engl J Med *354*, 2235-2249.

Flatz, L., Bergthaler, A., de la Torre, J.C., and Pinschewer, D.D. (2006). Recovery of an arenavirus entirely from RNA polymerase I/II-driven cDNA. Proc Natl Acad Sci USA *103*, 4663-4668.

García, M., Cooper, A., Shi, W., Bornmann, W., Carrion, R., Kalman, D., and Nabel, G.J. (2012). Productive Replication of Ebola Virus Is Regulated by the c-Abl1 Tyrosine Kinase. Sci Transl Med *4*, 123ra124.

Garcia, M.L., Reynolds, T.D., Mothes, W., and Robek, M.D. (2013). Functional Characterization of the Putative Hepatitis B Virus Core Protein Late Domain Using Retrovirus Chimeras. PLoS ONE *8*, e72845.

Goñi, S.E., Iserte, J.A., Ambrosio, A.M., Romanowski, V., Ghiringhelli, P.D., and Lozano, M.E. (2006). Genomic Features of Attenuated Junín Virus Vaccine Strain Candidate. Virus Genes *32*, 37-41.

Gschwender, H.H., and Popescu, M. (1976). Equilibrium Sedimentation of Virus in Density-Gradients of Iodinated Compounds. In Biological Separations in Iondinated

Density-Gradient Media, D. Rickwood, ed. (London: Information Retrieval Ltd.), pp. 145-158.

Haist, K., Ziegler, C., and Botten, J. (2015). Strand-Specific Quantitative Reverse Transcription-Polymerase Chain Reaction Assay for Measurement of Arenavirus Genomic and Antigenomic RNAs. PLoS ONE *10*, e0120043.

Hemonnot, B., Cartier, C., Gay, B., Rebuffat, S., Bardy, M., Devaux, C., Boyer, V., and Briant, L. (2004). The host cell MAP kinase ERK-2 regulates viral assembly and release by phosphorylating the p6(gag) protein of HIV-1. J Biol Chem *279*, 32426-32434.

Huang, A.S. (1973). Defective interfering viruses. Annu Rev Microbiol *27*.

Huang, A.S., and Baltimore, D. (1970). Defective Viral Particles and Viral Disease Processes. Nature *226*, 325-327.

Hurley, J.H. (2008). ESCRT complexes and the biogenesis of multivesicular bodies. Curr Opin Cell Biol *20*, 4-11.

Jacobson, S., and Pfau, C.J. (1980). Viral pathogenesis and resistance to defective interfering particles. Nature *283*, 311-313.

Jayakar, H.R., Murti, K.G., and Whitt, M.A. (2000). Mutations in the PPPY Motif of Vesicular Stomatitis Virus Matrix Protein Reduce Virus Budding by Inhibiting a Late Step in Virion Release. J Virol *74*, 9818-9827.

Klaus, J.P., Eisenhauer, P., Russo, J., Mason, A.B., Do, D., King, B., Taatjes, D., Cornillez-Ty, C., Boyson, J.E., Thali, M.*, et al.* (2013). The intracellular cargo receptor ERGIC-53 is required for the production of infectious arenavirus, coronavirus, and filovirus particles. Cell Host Microbe *14*, 522-534.

Kolesnikova, L., Mittler, E., Schudt, G., Shams-Eldin, H., and Becker, S. (2012). Phosphorylation of Marburg virus matrix protein VP40 triggers assembly of nucleocapsids with the viral envelope at the plasma membrane. Cell Microbiol *14*, 182-197.

Le Blanc, I., Prévost, M.-C., Dokhélar, M.-C., and Rosenberg, A.R. (2002a). The PPPY Motif of Human T-Cell Leukemia Virus Type 1 Gag Protein Is Required Early in the Budding Process. J Virol *76*, 10024-10029.

Lin, Y., Kimpler, L.A., Naismith, T.V., Lauer, J.M., and Hanson, P.I. (2005). Interaction of the Mammalian Endosomal Sorting Complex Required for Transport (ESCRT) III Protein hSnf7-1 with Itself, Membranes, and the AAA+ ATPase SKD1. J Biol Chem *280*, 12799-12809.

McCormick, J.B., King, I.J., Webb, P.A., Scribner, C.L., Craven, R.B., Johnson, K.M., Elliott, L.H., and Belmont-Williams, R. (1986). Lassa Fever. N Engl J Med *314*, 20-26.

Meyer, B.J., De La Torre, J.C., and Southern, P.J. (2002). Arenaviruses: Genomic RNAs, Transcription, and Replication. In Arenaviruses I, M.A. Oldstone, ed. (Springer Berlin Heidelberg), pp. 139-157.

Meyer, B.J., and Southern, P.J. (1997). A novel type of defective viral genome suggests a unique strategy to establish and maintain persistent lymphocytic choriomeningitis virus infections. J Virol *71*, 6757-6764.

Morita, E., Sandrin, V., Chung, H.-Y., Morham, S.G., Gygi, S.P., Rodesch, C.K., and Sundquist, W.I. (2007). Human ESCRT and ALIX proteins interact with proteins of the midbody and function in cytokinesis. The EMBO Journal *26*, 4215-4227.

Neumann, G., Ebihara, H., Takada, A., Noda, T., Kobasa, D., Jasenosky, L.D., Watanabe, S., Kim, J.H., Feldmann, H., and Kawaoka, Y. (2005b). Ebola Virus VP40 Late Domains Are Not Essential for Viral Replication in Cell Culture. J Virol *79*, 10300-10307.

Obenauer, J.C., Cantley, L.C., and Yaffe, M.B. (2003). Scansite 2.0: Proteome-wide prediction of cell signaling interactions using short sequence motifs. Nucleic Acids Res *31*, 3635-3641.

Oldstone, M.B. (1998). Viral persistence: mechanisms and consequences. Curr Opin Microbiol *1*, 436-441.

Pasqual, G., Rojek, J.M., Masin, M., Chatton, J.-Y., and Kunz, S. (2011). Old World Arenaviruses Enter the Host Cell via the Multivesicular Body and Depend on the Endosomal Sorting Complex Required for Transport. PLoS Pathog *7*, e1002232.

Pedersen, I.R. (1979). Structural Components and Replication of Arenaviruses. In Advances in virus research, M.A. Lauffer, F.B. Bang, K. Maramorosch, and K.M. Smith, eds. (Academic Press), pp. 277-330.

Pei, Z., Harrison, M.S., and Schmitt, A.P. (2011). Parainfluenza Virus 5 M Protein Interaction with Host Protein 14-3-3 Negatively Affects Virus Particle Formation. J Virol *85*, 2050-2059.

Peralta, L.M., Bruns, M., and Lehmann-Grube, F. (1981). Biochemical Composition of Lymphocytic Choriomeningitis Virus Interfering Particles. J Gen Virol *55*, 475-479.

Perez, M., Craven, R.C., and de la Torre, J.C. (2003). The small RING finger protein Z drives arenavirus budding: Implications for antiviral strategies. Proc Natl Acad Sci USA *100*, 12978-12983.

Perez, M., Greenwald, D.L., and de la Torre, J.C. (2004b). Myristoylation of the RING finger Z protein is essential for arenavirus budding. J Virol *78*, 11443-11448.

Popescu, M., and Lehmann-Grube, F. (1977). Defective interfering particles in mice infected with lymphocytic choriomeningitis virus. Virology *77*, 78-83.

Popescu, M., Schaefer, H., and Lehmann-Grube, F. (1976). Homologous interference of lymphocytic choriomeningitis virus: detection and measurement of interference focus-forming units. J Virol *20*, 1-8.

Rauch, S., and Martin-Serrano, J. (2011). Multiple Interactions between the ESCRT Machinery and Arrestin-Related Proteins: Implications for PPXY-Dependent Budding. J Virol *85*, 3546-3556.

Rojek, J.M., and Kunz, S. (2008). Cell entry by human pathogenic arenaviruses. Cell Microbiol *10*, 828-835.

Salazar-Bravo, J., Ruedas, L.A., and Yates, T.L. (2002b). Mammalian Reservoirs of Arenaviruses. In Arenaviruses I, M.A. Oldstone, ed. (Springer Berlin Heidelberg), pp. 25-63.

Sanchez, A.B., and De la Torre, J.C. (2006). Rescue of the prototypic Arenavirus LCMV entirely from plasmid. Virology *350*, 370-380.

Staneck, L.D., Trowbridge, R.S., Welsh, R.M., Wright, E.A., and Pfau, C.J. (1972). Arenaviruses: Cellular Response to Long-Term In Vitro Infection with Parana and Lymphocytic Choriomeningitis Viruses. Infect Immun *6*, 444-450.

Stocker, C., Peralta, L.M., Kratzberg, T., Lohmann, F., and Bruns, M. (1994). Characterization of a virus variant produced by L cells persistently infected with lymphocytic choriomeningitis virus. J Gen Virol *75*, 3431-3439.

Stojdl, D.F., Lichty, B.D., tenOever, B.R., Paterson, J.M., Power, A.T., Knowles, S., Marius, R., Reynard, J., Poliquin, L., Atkins, H.*, et al.* (2003). VSV strains with defects in their ability to shutdown innate immunity are potent systemic anti-cancer agents. Cancer Cell *4*, 263-275.

Strecker, T., Eichler, R., Meulen, J.t., Weissenhorn, W., Dieter Klenk, H., Garten, W., and Lenz, O. (2003). Lassa Virus Z Protein Is a Matrix Protein Sufficient for the Release of Virus-Like Particles. J Virol *77*, 10700-10705.

Taylor, G.M., Hanson, P.I., and Kielian, M. (2007). Ubiquitin Depletion and Dominant-Negative VPS4 Inhibit Rhabdovirus Budding without Affecting Alphavirus Budding. J Virol *81*, 13631-13639.

Urata, S., Noda, T., Kawaoka, Y., Yokosawa, H., and Yasuda, J. (2006). Cellular Factors Required for Lassa Virus Budding. J Virol *80*, 4191-4195.

Urata, S., and Yasuda, J. (2012). Molecular Mechanism of Arenavirus Assembly and Budding. Viruses *4*, 2049-2079.

Urata, S., Yasuda, J., and de la Torre, J.C. (2009). The Z Protein of the New World Arenavirus Tacaribe Virus Has Bona Fide Budding Activity That Does Not Depend on Known Late Domain Motifs. J Virol *83*, 12651-12655.

Varkey, J.B., Shantha, J.G., Crozier, I., Kraft, C.S., Lyon, G.M., Mehta, A.K., Kumar, G., Smith, J.R., Kainulainen, M.H., Whitmer, S.*, et al.* (2015). Persistence of Ebola Virus in Ocular Fluid during Convalescence. N Engl J Med *372*, 2423-2427.

Votteler, J., and Sundquist, Wesley I. (2013). Virus Budding and the ESCRT Pathway. Cell Host & Microbe *14*, 232-241.

Wang, J., Danzy, S., Kumar, N., Ly, H., and Liang, Y. (2012). Biological Roles and Functional Mechanisms of Arenavirus Z Protein in Viral Replication. J Virol *86*, 9794-9801.

Welsh, R.M., and Buchmeier, M.J. (1979). Protein analysis of defective interfering lymphocytic choriomeningitis virus and persistently infected cells. Virology *96*.

Welsh, R.M., Connell, C.M., and Pfau, C.J. (1972). Properties of Defective Lymphocytic Choriomeningitis Virus. J Gen Virol *17*, 355-359.

Welsh, R.M., and Pfau, C.J. (1972). Determinants of Lymphocytic Choriomeningitis Interference. J Gen Virol *14*, 177-187.

Wirblich, C., Tan, G.S., Papaneri, A., Godlewski, P.J., Orenstein, J.M., Harty, R.N., and Schnell, M.J. (2008b). PPEY Motif within the Rabies Virus (RV) Matrix Protein Is Essential for Efficient Virion Release and RV Pathogenicity. J Virol *82*, 9730-9738.

Wolff, S., Ebihara, H., and Groseth, A. (2013). Arenavirus budding: a common pathway with mechanistic differences. Viruses *5*, 528-549.

Wong, Y.H., Lee, T.Y., Liang, H.K., Huang, C.M., Wang, T.Y., Yang, Y.H., Chu, C.H., Huang, H.D., Ko, M.T., and Hwang, J.K. (2007). KinasePhos 2.0: a web server for identifying protein kinase-specific phosphorylation sites based on sequences and coupling patterns. Nucleic Acids Res *35*, W588-594.

Yasuda, J., and Hunter, E. (1998). A Proline-Rich Motif (PPPY) in the Gag Polyprotein of Mason-Pfizer Monkey Virus Plays a Maturation-Independent Role in Virion Release. J Virol *72*, 4095-4103.

Yuan, B., Campbell, S., Bacharach, E., Rein, A., and Goff, S.P. (2000b). Infectivity of Moloney Murine Leukemia Virus Defective in Late Assembly Events Is Restored by Late Assembly Domains of Other Retroviruses. J Virol *74*, 7250-7260.

Supporting Information

A

Fragment Ions z=1

Sequence

KISTAPPSPPPY#EE

Seq	#	b	y	+1
K	1	129.020	---	14
I	2	242.186	1454.609	13
S	3	329.218	1341.525	12
T	4	430.266	1254.493	11
A	5	501.303	1153.445	10
P	6	598.356	1082.408	9
S	7	685.388	985.355	8
S	8	772.420	898.323	7
P	9	869.473	811.291	6
P	10	966.525	714.238	5
P	11	1063.578	617.185	4
Y#	12	1306.608	520.133	3
E	13	1435.650	277.103	2
E	14	---	148.060	1

B

Fragment Ions z=1

Sequence

KISTAPPSPPPYEE

Seq	#	b	y	+1
K	1	129.020	---	14
I	2	242.186	1374.642	13
S	3	329.218	1261.558	12
T	4	430.266	1174.526	11
A	5	501.303	1073.479	10
P	6	598.356	1002.441	9
S	7	685.388	905.389	8
S	8	772.420	818.357	7
P	9	869.473	731.325	6
P	10	966.525	634.272	5
P	11	1063.578	537.219	4
Y	12	1226.642	440.166	3
E	13	1355.684	277.103	2
E	14	---	148.060	1

C

Number	XCorr	Peptide
1	2.503	K.ISTAPSSPPPY#EE.-
2	3.392	K.ISTAPSSPPPYEE.-
3	3.021	K.ISTAPSSPPPYEE.-
4	2.97	K.ISTAPSSPPPYEE.-
5	2.944	K.ISTAPSSPPPYEE.-
6	2.854	K.ISTAPSSPPPYEE.-
7	2.802	K.ISTAPSSPPPYEE.-
8	2.788	K.ISTAPSSPPPYEE.-
9	2.753	K.ISTAPSSPPPYEE.-
10	2.614	K.ISTAPSSPPPYEE.-
11	2.492	K.ISTAPSSPPPYEE.-
12	2.488	K.ISTAPSSPPPYEE.-

Figure 2.S1. Fragment ion tables from mass spectra and spectral counts of phosphorylated and unphosphorylated tryptic peptides. (A-B) For the indicated phosphorylated (A) and unphosphorylated (B) peptides, corresponding to the spectra shown in Fig 1B, the calculated and measured (colored numbers) m/z values of the y- and b-type ions are shown. (C) The phosphorylated and unphosphorylated peptides detected from virion-derived LCMV Z in Fig 1A are listed. Each MS/MS spectrum was manually examined and found to be correct by a comparison to spectra with the highest Xcorr values and by comparing predicted and observed fragment ions. (A and C) Y# indicates phosphorylated tyrosine.

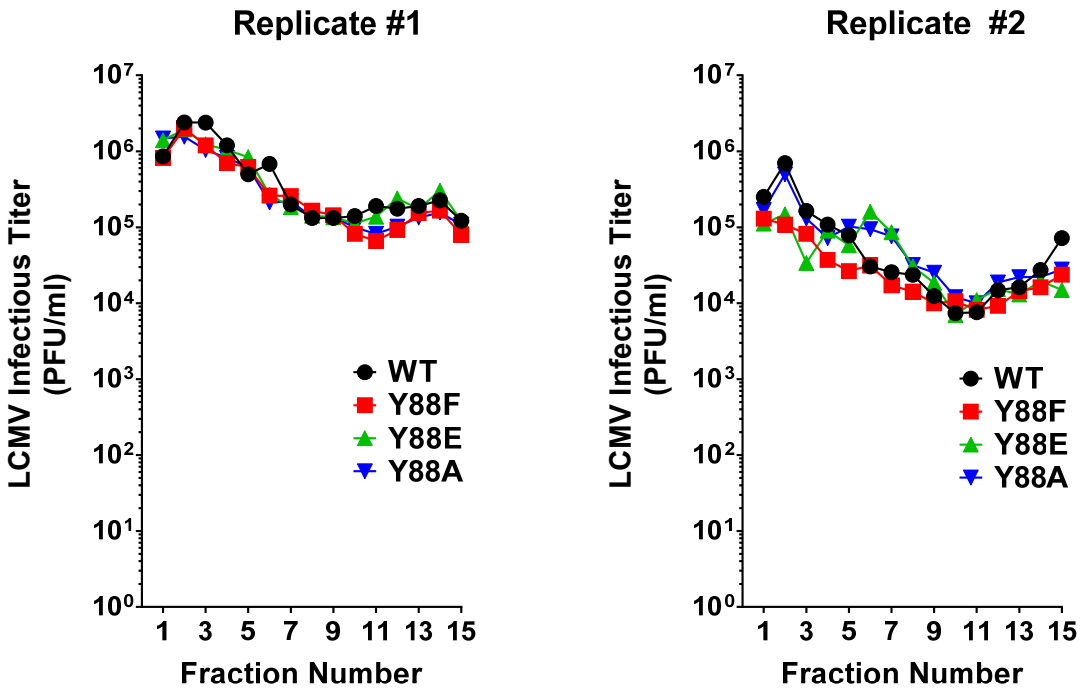

Figure 2.S2. Profile of standard infectious rLCMV WT or Y88 particles following separation via density ultracentrifugation. Vero E6 cells were infected with rLCMV WT, Y88F, Y88E, or Y88A at an MOI of 0.0001 and 72 hr later supernatants were clarified, precipitated with PEG-8000, resuspended in TNE, and titered for PFU via plaque assay. An equal number of PFU for each rLCMV was layered onto an optiprep gradient (7%, 10%, 13%, 16%, and 19%) and centrifuged for 12 hr at 30,000 RPM at 4 ºC. The entire gradient was collected in 15 fractions of 2 mL each. Each fraction was titered for PFU via plaque assay. Shown are results from 2 independent experiments.

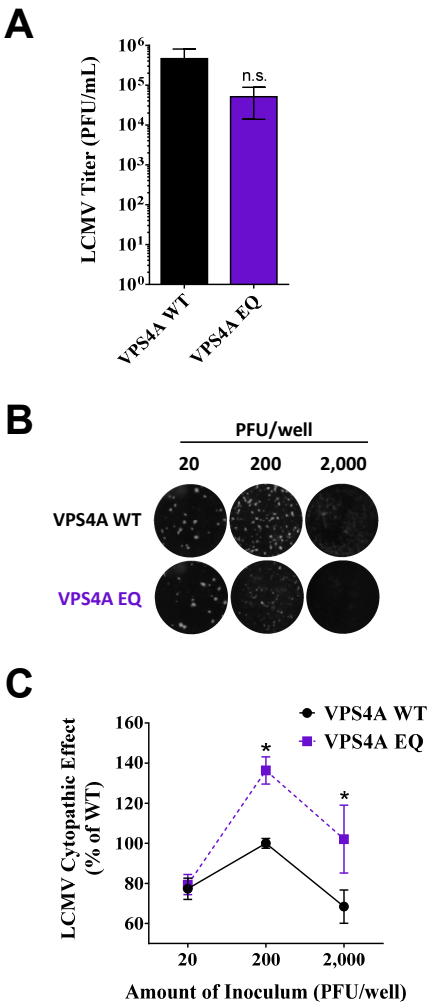

Figure 2.S3. Efficient DI particle formation requires a functional ESCRT pathway. (A-C) T-Rex HEK293 cells stably transduced with vectors for tetracycline-based induction of WT vacuolar protein sorting 4A (VPS4A) or the DN VPS4A mutant, EQ, were infected with rLCMV WT and 2 d later treated with tetracycline to induce the expression of WT or DN VPS4A. 6 hr after VPS4A induction (54 hr pi), the cells were washed and given fresh media containing tetracycline. Supernatants were collected 18 hr later (72 hr pi) and titered via plaque assay. The results shown in (A) represent the mean PFU ± SEM from 2 independent experiments that contained 3 technical replicates and were tested for statistical significance with an unpaired t test with Welch's correction. Equivalent PFUs of virus (range 2 x 101 to 2 x 103) produced from WT or DN VPS4A cells were inoculated onto monolayers of Vero E6 cells and a standard plaque assay was performed. Representative images of crystal violet-stained wells are shown in (B). Inhibition of standard infectious virus-induced cytopathic effect by DI particles at each dose was determined in (C) by measurement of the mean pixel intensity of each well using Image J software. The data in (C) are representative of the mean ± SEM relative to WT VSP4A (at 200 PFU per well) from 2 independent experiments that contained 3 technical replicates and were tested for statistical significance with a two way ANOVA and Holm-Sidak's test for multiple comparisons. (C) *$p < 0.05$, as determined by the indicated statistical tests.

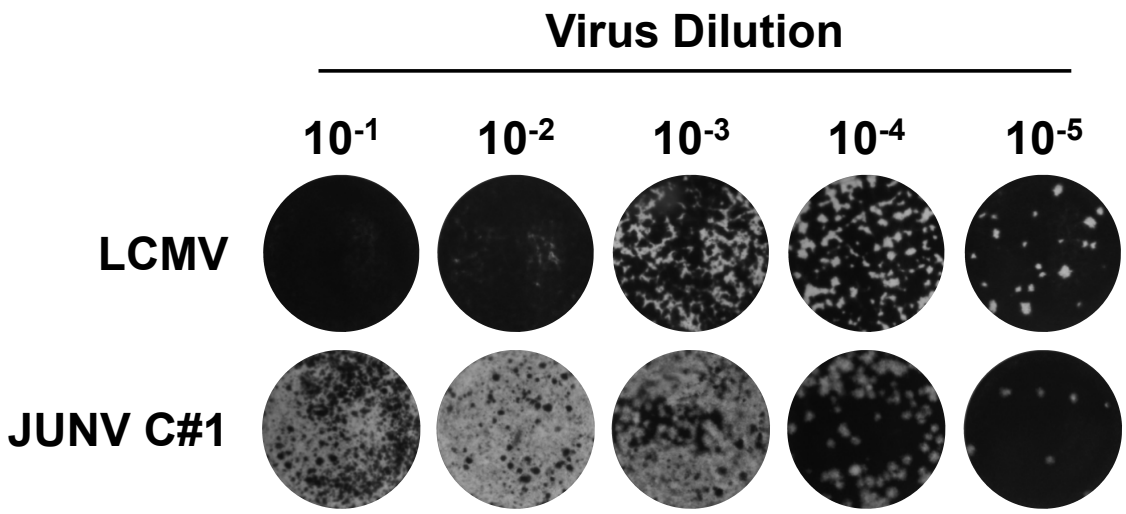

Figure 2.S4. LCMV generates more DI particles per standard infectious particle than JUNV C#1. Serial 10-fold dilutions of stock preparations of LCMV or JUNV C#1 were inoculated onto monolayers of Vero E6 cells and a standard plaque assay was performed to visualize DI-mediated interference of standard virus at low dilutions.

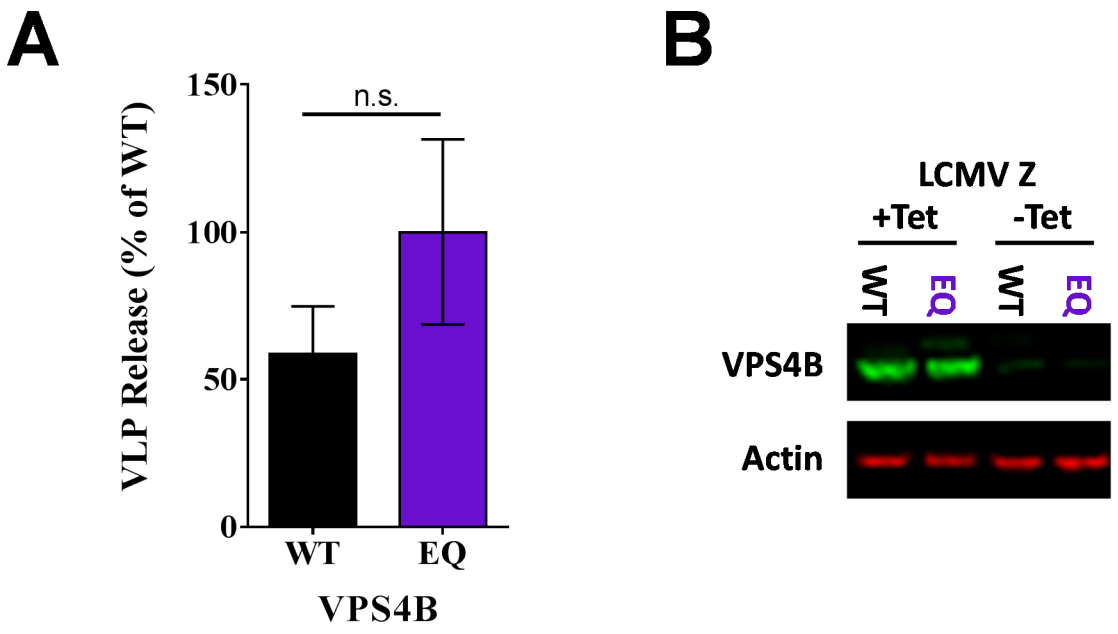

Figure 2.S5. Expression of dominant negative VPS4B does not impact the ability of LCMV Z to form VLPs. (A-B) T-Rex HEK293 cells stably transduced with a tetracycline-inducible plasmid encoding WT or dominant negative EQ mutant vacuolar protein sorting 4B (VPS4B) were simultaneously transfected with a plasmid encoding LCMV Z WT and exposed to tetracycline to drive the expression of WT or DN VPS4B. One day later both the cells and VLP-containing supernatants were collected. Z from VLP-containing supernatants was affinity purified with magnetic streptavidin beads. The quantity of Z affinity purified from VLPs or present in the corresponding whole cell lysates was determined via quantitative western blotting. The percent VLP release shown in (A) was calculated as the amount of Z protein found in the cell culture media relative to the amount in cells. Data are presented as mean release ± SEM relative to WT Z from 3 independent experiments. A one way ANOVA with Holm-Sidak's test for multiple comparisons was used to compare the mean values. n.s., not significant). In panel (B), cell lysates were also screened by western blotting to verify the induction of VPS4B WT or EQ expression using an anti-GFP antibody and for actin as a loading control.

CHAPTER 3:

A NOVEL PHOSPHOSERINE MOTIF IN THE LCMV MATRIX PROTEIN Z REGULATES THE RELEASE OF INFECTIOUS VIRUS AND DEFECTIVE INTERFERING PARTICLES

Christopher M. Ziegler[1,2], Philip Eisenhauer[1], Emily A. Bruce[1], Vedran Beganovic[1,#], Benjamin R. King[1,2], Marion E. Weir[3], Bryan A. Ballif[3], and Jason Botten[1,4*]

[1]Department of Medicine, Division of Immunobiology, [2]Cellular, Molecular, and Biomedical Sciences Graduate Program, [3]Department of Biology, [4]Department of Microbiology and Molecular Genetics, University of Vermont, Burlington, VT 05405, USA. [#]Current address: Wake Forest School of Medicine, Winston-Salem, NC 27157, USA

Running Title: Phosphoserine Motif Regulates LCMV DI Particle Release

Abstract

We report that the lymphocytic choriomeningitis virus (LCMV) matrix protein, which drives viral budding, is phosphorylated at serine 41. A recombinant (r)LCMV bearing a phosphomimetic mutation (S41D) was impaired in infectious and defective interfering (DI) particle release while a nonphosphorylatable mutant (S41A) was not. The S41D mutant was disproportionately impaired in its ability to release DI particles relative to infectious particles. Thus, DI particle production by LCMV may be dynamically regulated via phosphorylation of S41.

Main Text

Arenaviruses are enveloped RNA viruses that establish lifelong, asymptomatic infections in reservoir rodents but can cause severe disease in humans (Buchmeier et al., 2007). The prototypic arenavirus, lymphocytic choriomeningitis virus (LCMV), produces high levels of defective interfering (DI) particles during acute and persistent infection (Popescu and Lehmann-Grube, 1977; Staneck et al., 1972; Welsh and Pfau, 1972). DI particles, which are replication-deficient virus particles that can interfere with the propagation of standard infectious virus (Huang and Baltimore, 1970; Welsh et al., 1972), are thought to be critical for the establishment of LCMV persistence (Burns and Buchmeier, 1993; Huang and Baltimore, 1970; Oldstone, 1998), possibly by reducing virus-induced cytopathology in reservoir rodents. The arenavirus matrix protein Z is a multifunctional protein that drives the assembly and release of standard infectious virus (Fehling et al., 2012; Perez et al., 2003; Strecker et al., 2003) and DI particles (Ziegler et al., 2016b). For many viruses, budding is controlled by one or more late domain(s) encoded in the matrix protein that recruit the cellular endosomal sorting complex required for transport (ESCRT) pathway, which drives the final membrane scission step (Votteler and Sundquist, 2013). The LCMV matrix protein encodes a single late domain, PPXY, which has been shown to be important for the formation of infectious virus-like particles (VLPs) (Perez et al., 2003). In the context of fully infectious virus, we recently demonstrated that the LCMV matrix protein uses different cellular pathways for the production of standard versus DI particles. In particular, DI particle formation absolutely requires LCMV's PPXY late domain and the cellular ESCRT pathway while the production of standard infectious

particles does not (Ziegler et al., 2016b). Further, phosphorylation of the terminal tyrosine in the PPXY late domain may be important for regulating this late domain-driven pathway of DI particle formation. In the current study, we discovered an additional phosphorylation site in LCMV Z at serine 41 (S41). Furthermore, using site-specific mutant viruses we found that serine 41 plays an important regulatory role in the production of LCMV infectious virions and DI particles.

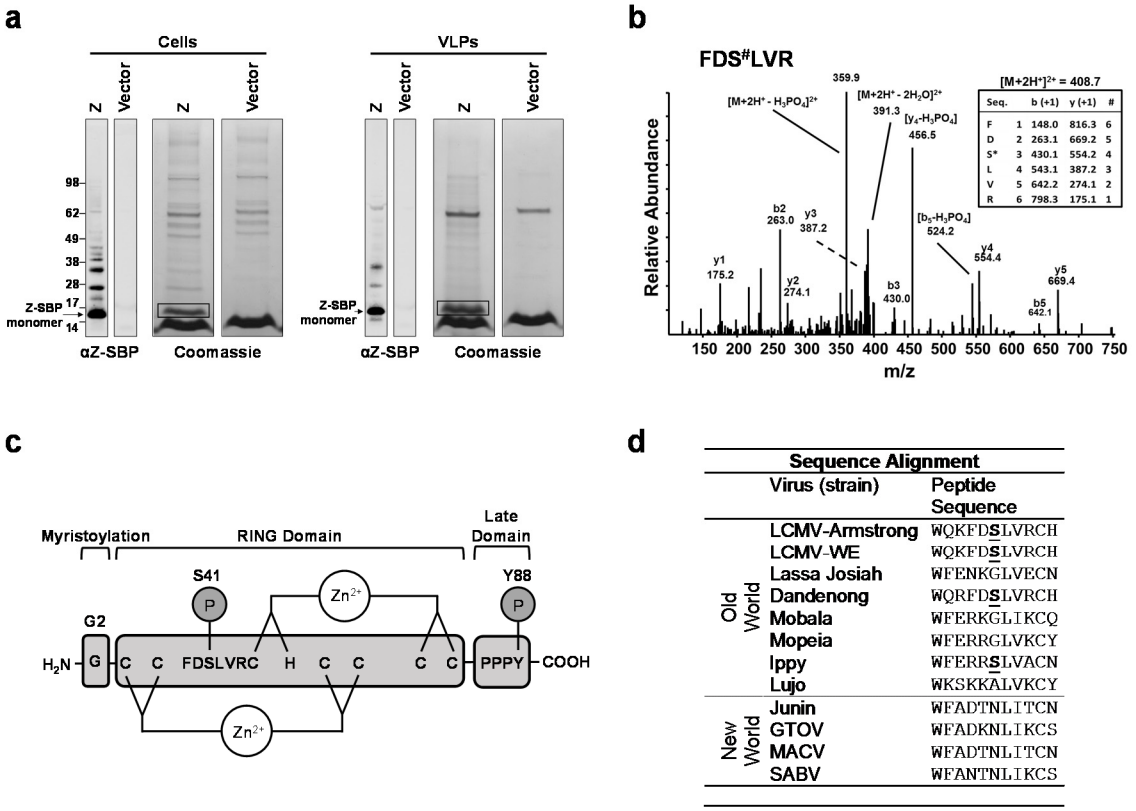

Figure 3.1. The LCMV matrix protein Z is phosphorylated at serine 41 (S41). (a) HEK-293T cells were transfected with a plasmid encoding streptavidin binding peptide (SBP)-tagged LCMV strain Armstrong Z or an empty vector. Two days later cells and virus-like particle (VLP)-containing supernatant were lysed and Z-SBP was affinity purified using streptavidin-coated magnetic beads. The purified Z-SBP was subjected to SDS-PAGE and detected by western blotting using an anti-SBP tag antibody or Coomassie stain. The presumptive monomeric Z bands from cells or VLPs were excised from the Coomassie stained gels (as indicated by the boxes) and subjected to reduction, alkylation, and in-gel tryptic digestion prior to mass spectrometry analysis of extracted peptides. (b) A representative low energy collision-induced dissociation

tandem mass spectrum with its corresponding fragment ion table from low energy collision-induced dissociation of a Z-derived tryptic peptide (FDS#LVR) containing the phosphorylated S41 where # denotes phosphorylation. The fragment ion table lists the predicted m/z values of the singly-charged b and y ions. Major measured b and y ions, as well as dominant losses of phosphoric acid are labeled. Phosphoric acid loss is a major signature in tandem mass spectra of phosphoserine/threonine-containing peptides. (c) Cartoon of the LCMV Z protein depicting the G2 myristoylation site, the central zinc-binding RING domain, and the C-terminal PPPY late domain. The S41 phosphorylation site and its flanking amino acids as well as the previously described Y88 phosphorylation site (Ziegler et al., 2016b) are indicated. (d) Alignment of Old and New World arenavirus Z protein sequences shows that S41 (bolded and underlined for LCMV strains Armstrong and WE) is conserved with the Old World arenaviruses Dandenong and Ippy virus.

To screen for phosphorylation sites in LCMV Z, we transfected HEK-293T cells with a plasmid encoding the LCMV strain Armstrong Z protein fused to a C-terminal streptavidin binding peptide (SBP) and subsequently used magnetic streptavidin beads (as described in (Ziegler et al., 2016b)) to affinity purify SBP-tagged Z from the transfected cells as well as from VLPs that had been released into the tissue culture media. Purified Z-SBP was separated by SDS-PAGE (Figure 3.1(a)), prepared for mass spectrometry analysis by in-gel tryptic digestion, and analyzed by liquid chromatography-mass spectrometry essentially as described (Ziegler et al., 2016b). This analysis revealed a novel serine phosphorylation site at S41 in Z-transfected cells (Figure 3.1(b)). S41, a site conserved in the Old Word arenaviruses Dandenong and Ippy (Figure 3.1(d)), is located in the central really interesting new gene (RING) domain of Z (Figure 3.1(c)) and is outside of any motif known to be important for arenavirus budding and release (Fehling et al., 2012).

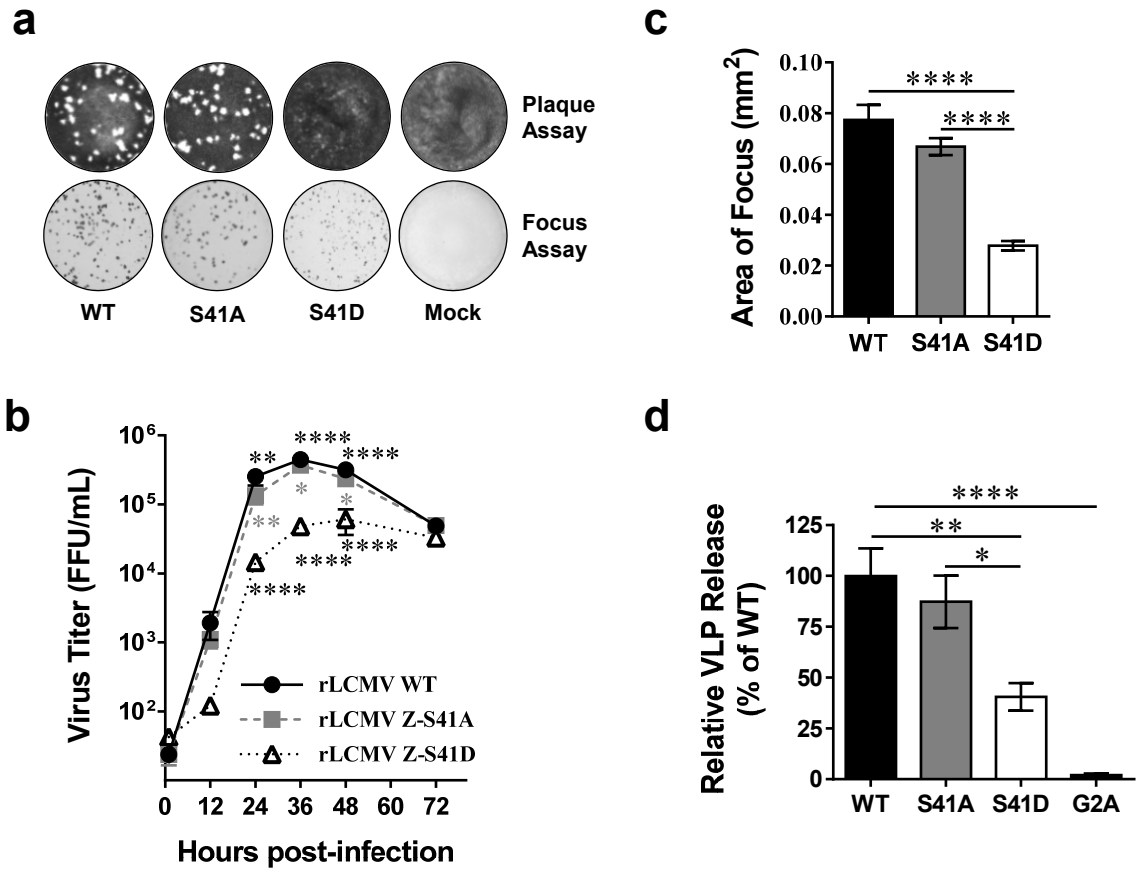

Figure 3.2. Phosphomimetic mutation of S41 significantly reduces the efficiency of infectious virus release and the ability of Z to form virus-like particles (VLPs). (a) Reverse genetics was used to generate rLCMV containing a nonphosphorylatable S41A mutation or a phosphomimetic S41D mutation. To determine whether infectious virus was recovered, both a standard plaque assay and an immunofocus assay (using an anti-nucleoprotein antibody (1.1.3)) were performed on Vero E6 cells. (b) The kinetics of infectious virus production were examined by growth curve analysis on Vero E6 cells (a multiplicity of infection (MOI) of 0.01 was used for each virus). Data represent the mean ± SEM from 3 independent experiments. For statistical analysis, the data were first log-transformed then a two-way analysis of variance (ANOVA) with Holm-Sidak's test for multiple comparisons was performed. (c) The area of foci obtained from the immunofocus assay wells shown in (A) for each rLCMV strain was measured using Image J. Data represent the mean ± SEM of foci from 8 wells for each virus. The Kruskal-Wallis non-parametric test with Dunn's multiple comparisons test was used to compare mean values. (d) The budding activity of WT or S41-mutant LCMV Z proteins was measured by a VLP release assay. The LCMV Z G2A mutant, which has a budding defect due to its inability to be myristoylated, was included as a control (Perez et al., 2004a). The results shown represent the mean ± SEM from 3 independent experiments. A one-way analysis of variance with the Holm-Sidak's test for multiple comparisons was used to compare the mean values. For the indicated statistical tests in (B-D), *, $p < 0.05$, **, $p < 0.01$; ****, and $p < 0.0001$.

To determine the importance of the S41 residue for viral fitness, recombinant (r)LCMV containing a nonphosphorylatable alanine (S41A) or a phosphomimetic aspartic acid (S41D) substitution at position 41 were recovered using reverse genetics as previously described (Emonet et al., 2009b; Flatz et al., 2006; Ziegler et al., 2016b). Initially, it appeared that the S41D phosphomimetic mutant could not be recovered as it did not produce plaques in a standard plaque assay (Figure 3.2(a)). However, staining for viral nucleoprotein (NP) (mouse anti-LCMV NP, 1.1.3, kindly provided by M. J. Buchmeier, University of California, Irvine) via immunofocus assay (Battegay et al., 1991) revealed that the S41D mutant was recoverable despite its inability to form plaques (Figure 3.2(a)). Growth curve analysis revealed that the phosphomimetic S41D virus was attenuated in its growth kinetics while the nonphosphorylatable S41A mutant grew to similar levels as wild type (Figure 3.2(b)). The attenuation of the S41D mutant was also apparent in the smaller foci it formed, which were less than 50% of WT size (Figs. 2(a) and (c)). To determine whether the reduction in infectious titer of the phosphomimetic S41D virus was due to decreased virus budding and release, we employed a Z VLP release assay as previously described (Ziegler et al., 2016b). As a control, we also included the LCMV Z G2A mutant, which exhibits a pronounced defect in VLP formation due to its inability to be myristoylated at this glycine residue (Perez et al., 2004a; Strecker et al., 2006). This experiment demonstrated that the budding efficiency of the phosphomimetic Z-S41D was reduced ~60% while the budding activity of the nonphosphorylatable S41A was not different from WT (Figure 3.2(d)). Collectively, these findings demonstrate that the S41

residue possesses a previously unappreciated capacity to drive virus budding and that this function may be regulated by phosphorylation.

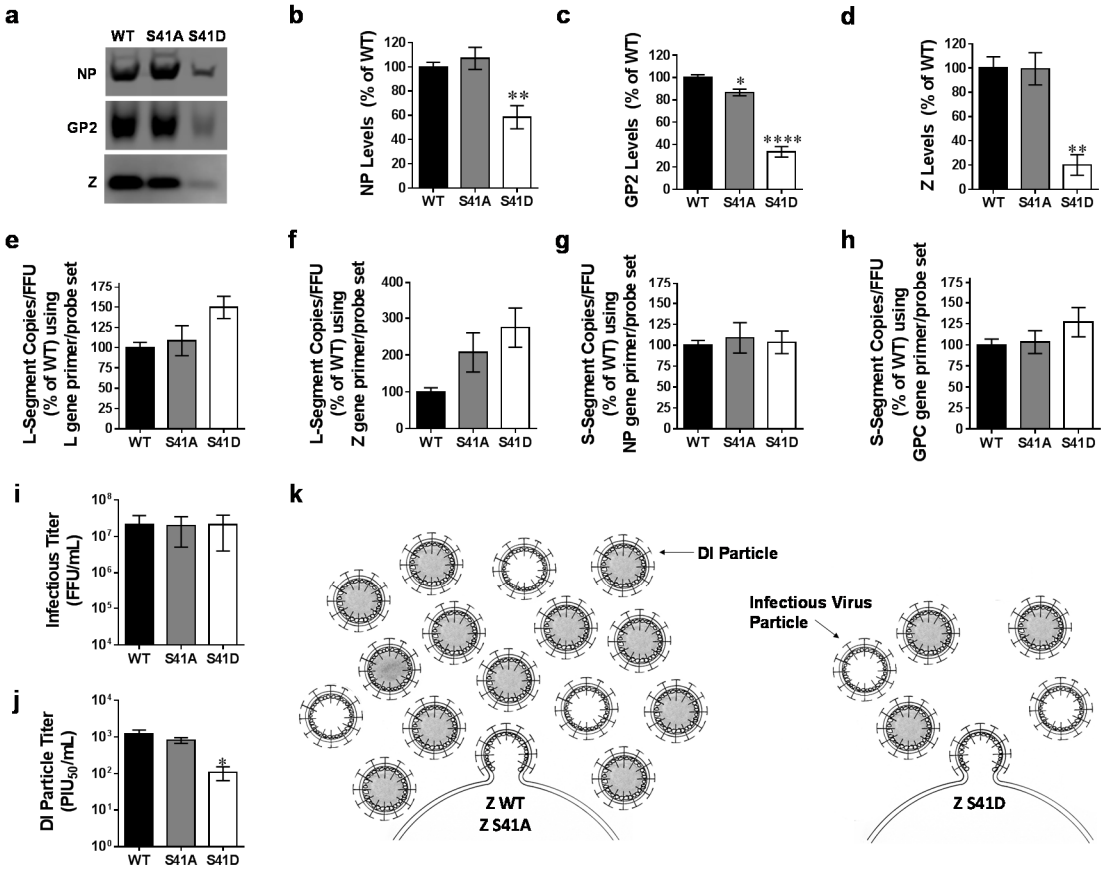

Figure 3.3. The S41 phosphomotif regulates DI particle production. (a-h) Comparison of viral structural protein and genome content in preparations of rLCMV WT, S41A, or S41D virus. Vero E6 cells were infected with WT or S41-mutant rLCMV at a multiplicity of infection (MOI) of 0.0001 and clarified supernatants were collected 72 hours later. Equivalent FFUs of each rLCMV were then concentrated through a 20% sucrose cushion by ultracentrifugation. Viral protein content in these concentrated virus preparations was analyzed by quantitative western blotting. Representative western blots (a) as well as the quantity (mean ± SEM) of NP (b), GP (c), or Z (d) contained in each rLCMV virus preparation are shown. The copies of LCMV genomic L segment (e-f) or S-segment (g-h) were determined by quantitative RT-PCR (Haist et al., 2015) and then normalized to the infectious titer (FFU). To enumerate copies of L segment vRNA, RT was performed using the RT primer 5906-, followed by QPCR using the primer probe sets located in either the L gene (primers L5517+ and L5645- and probe L5582-P) (e) or Z gene (primers L212+ and L276- and probe L251-P) (f). To determine the copies of S segment vRNA, RT was performed using the RT primer 2865-, followed by QPCR using the primer probe sets located in either the NP gene (primers S2275+ and S2338- and probe S2295+P) (g) or GPC gene (primers S929+ and S988- and probe S952+P) (h). (i-j) Measurement of standard infectious virus and DI particles produced by rLCMV WT, S41A, or S41D. The infectious titer of each of the clarified supernatants used in (a-h) was determined by focus forming assay (i) and the DI

particle titer was assessed by plaque interference assay (j). PIU50/mL, plaque interfering units50/mL. For (b-j), values represent the mean ± SEM of protein (b-d), viral genome (e-h), FFU/mL (i), or DI particle titer (j) from 4 independent experiments and statistical analyses were performed by one-way ANOVA with Holm-Sidak's test for multiple comparisons for which *, $p < 0.05$, **, $p < 0.01$; ****, and $p < 0.0001$. (k) Model of S41's impact on infectious virus and DI particle formation. WT virus containing the native S41 (Z WT) produces high levels of infectious and DI particles. Mutation of S41 to alanine (Z S41A) to prevent phosphorylation has little effect on infectious or DI particle production. Mutation of S41 to aspartic acid (Z S41D) to mimic the negative charge associated with phosphorylation of S41 results in decreased infectious virus and DI particle release. The S41D mutation disproportionately impacts DI formation over standard infectious virus.

As the reduction in VLP release by Z-S41D (Figure 3.2(d)) did not appear to fully explain the greater than 10-fold reduction in virus titer observed in Figure 3.2(b), we probed rLCMV WT or S41 mutant virion preparations (that were generated in Vero E6 cells infected at a multiplicity of infection (MOI) of 0.0001 and collected 72 hours after infection) for structural protein and/or genome deficits. To determine the composition of each virus particle preparation, an equal number of focus forming units (FFU) of cell-free rLCMV WT, S41A, or S41D viruses were concentrated through a 20% sucrose cushion by ultracentrifugation as described in (Ziegler et al., 2016b) and virion protein quantity was analyzed by quantitative western blotting (Figs. 3(a) to (d)). The S41D phosphomimetic virus preparation, despite containing equivalent infectious units as the WT and S41A preparations, had markedly reduced levels of NP, glycoprotein (GP2), and Z (Figures 3.3(a) to (d)). Interestingly, the quantities of viral genomic S and L segment RNAs, measured by quantitative polymerase chain reaction (PCR) as described in (Haist et al., 2015; Ziegler et al., 2016b), did not differ between the preparations of WT, S41A, or S41D viruses (Figs. 3(e) - (h)). The loss in viral structural protein content without a corresponding loss in infectious titer led us to hypothesize that the S41D phosphomimetic virus may be

defective in its ability to generate DI particles, which could explain the reduced levels of viral protein observed relative to infectious units. To test whether S41 can indeed act as a regulatory motif to control DI particle production, we next measured the infectious virus levels and DI particle activity of the same virus preparations used above in Figs. 3(a) to (h) using the immunofocus assay and the plaque interference assay, respectively, as described in (Welsh and Pfau, 1972; Ziegler et al., 2016b). All three viruses had approximately equivalent titers of infectious virus (Figure 3.3(i)). The DI particle titer of the S41D phosphomimetic virus, however, was reduced greater than 10-fold compared to WT virus while the DI particle titer of the S41A virus was not different from WT (Figure 3.3(j)). These results indicate that the loss of viral structural protein content observed in the phosphomimetic S41D virus preparation (Figs. 3(a)-(d)) was likely due to the reduced production of DI particles, not infectious virus particles.

The S41 phosphomotif represents a novel regulatory site within the LCMV Z protein. We recently demonstrated that the PPXY late domain in LCMV Z is not absolutely required for the production of infectious LCMV virions (Ziegler et al., 2016b). Provided that the only other motif in Z with a known role in budding activity is the myristoylation site at the glycine at position 2 (Figs. 1(c) and 2(d)) (Perez et al., 2004a; Strecker et al., 2006), our finding here expands the functional repertoire of motifs in LCMV Z that regulate the efficiency of infectious virus release. Further, we have built upon our previous findings regarding the PPXY late domain (Ziegler et al., 2016b) by showing that S41 also serves as a key regulator of DI particle formation. To our knowledge, these are the only two motifs

known to specifically regulate DI particle formation over standard particles for any virus family. While we have shown that DI particle formation requires a functional ESCRT pathway (Ziegler et al., 2016b), it will be important to determine whether the PPXY late domain and/or the S41 phosphomotif directly engage ESCRT machinery and, if so, the mechanistic basis for this interaction as it relates to DI particle production. Further, our findings support the hypothesis that phosphorylation of Z is an important mechanism by which the virus can adjust its rate of DI particle formation in response to the dynamic environment of the host cell (*e.g.* phosphorylation at Y88 appears to increase DI particle production (Ziegler et al., 2016b) whereas phosphorylation of S41 represses it (Figure 3.3(j)). In this scenario, the S41 site could function as an important rheostat for regulating the potency of the PPXY-driven DI production pathway. Other arenaviruses, if they produce fewer DI particles than LCMV (e.g. Junin virus Candid #1) (Ziegler et al., 2016b), may not require a secondary regulatory motif such as S41, which could explain why the S41 site is only found in LCMV-like viruses and the closely related Old World arenavirus Ippy (Figure 3.1d). Identifying the key kinases and phosphatases that target S41 and Y88 and determining how their activity is regulated in response to environmental stimuli will be important for understanding how DI particle formation is regulated during infection. It will also be important to determine whether phosphorylation of matrix proteins can play a similar role in the regulation of DI particle production for other relevant virus families.

Acknowledgments

We thank the UVM Immunobiology Group for insightful discussions and Drs. Alan Howard and Cory Teuscher for statistical support and advice. We are grateful to Drs. Michael Buchmeier and Juan Carlos de la Torre for providing critical reagents. The authors gratefully acknowledge NIH grants T32 AI055402 (CMZ), T32 HL076122 (BRK), R21 AI088059 (JB), AI065359 (JB) and P20RR021905 (Immunobiology and Infectious Disease COBRE) (JB). The mass spectrometry analysis was supported by the Vermont Genetics Network through NIH grant 8P20GM103449 from the INBRE program and of the NIGMS. The funders had no role in study design, data collection and analysis, decision to publish, or preparation of the manuscript.

References

Battegay, M., Cooper, S., Althage, A., Bänziger, J., Hengartner, H., and Zinkernagel, R.M. (1991). Quantification of lymphocytic choriomeningitis virus with an immunological focus assay in 24- or 96-well plates. Journal of Virological Methods *33*, 191-198.

Buchmeier, M.J., de la Torre, J.C., and Peters, C.J. (2007). *Arenaviridae*: The Viruses and Their Replication. In Fields Virology, D.M. Knipe, P.M. Howley, D.E. Griffin, R.A. Lamb, M.A. Martin, B. Roizman, and S.E. Straus, eds. (Philadelphia: Wolters Kluwer Health/Lippincott Williams & Wilkins), pp. 1791-1827.

Burns, J.W., and Buchmeier, M.J. (1993). Glycoproteins of the Arenaviruses. In The Arenaviridae, M.S. Salvato, ed. (New York: Plenum Press), pp. 17-35.

Emonet, S.F., Garidou, L., McGavern, D.B., and de la Torre, J.C. (2009b). Generation of recombinant lymphocytic choriomeningitis viruses with trisegmented genomes stably expressing two additional genes of interest. Proc Natl Acad Sci USA *106*, 3473-3478.

Fehling, S., Lennartz, F., and Strecker, T. (2012). Multifunctional Nature of the Arenavirus RING Finger Protein Z. Viruses *4*, 2973-3011.

Flatz, L., Bergthaler, A., de la Torre, J.C., and Pinschewer, D.D. (2006). Recovery of an arenavirus entirely from RNA polymerase I/II-driven cDNA. Proc Natl Acad Sci USA *103*, 4663-4668.

Haist, K., Ziegler, C., and Botten, J. (2015). Strand-Specific Quantitative Reverse Transcription-Polymerase Chain Reaction Assay for Measurement of Arenavirus Genomic and Antigenomic RNAs. PLoS ONE *10*, e0120043.

Huang, A.S., and Baltimore, D. (1970). Defective Viral Particles and Viral Disease Processes. Nature *226*, 325-327.

Oldstone, M.B. (1998). Viral persistence: mechanisms and consequences. Curr Opin Microbiol *1*, 436-441.

Perez, M., Craven, R.C., and de la Torre, J.C. (2003). The small RING finger protein Z drives arenavirus budding: Implications for antiviral strategies. Proc Natl Acad Sci USA *100*, 12978-12983.

Perez, M., Greenwald, D.L., and de La Torre, J.C. (2004a). Myristoylation of the RING finger Z protein is essential for arenavirus budding. J Virol *78*, 11443-11448.

Popescu, M., and Lehmann-Grube, F. (1977). Defective interfering particles in mice infected with lymphocytic choriomeningitis virus. Virology *77*, 78-83.

Staneck, L.D., Trowbridge, R.S., Welsh, R.M., Wright, E.A., and Pfau, C.J. (1972). Arenaviruses: Cellular Response to Long-Term In Vitro Infection with Parana and Lymphocytic Choriomeningitis Viruses. Infect Immun *6*, 444-450.

Strecker, T., Eichler, R., Meulen, J.t., Weissenhorn, W., Dieter Klenk, H., Garten, W., and Lenz, O. (2003). Lassa Virus Z Protein Is a Matrix Protein Sufficient for the Release of Virus-Like Particles. J Virol *77*, 10700-10705.

Strecker, T., Maisa, A., Daffis, S., Eichler, R., Lenz, O., and Garten, W. (2006). The role of myristoylation in the membrane association of the Lassa virus matrix protein Z. Virology Journal *3*, 93.

Votteler, J., and Sundquist, Wesley I. (2013). Virus Budding and the ESCRT Pathway. Cell Host & Microbe *14*, 232-241.

Welsh, R.M., Connell, C.M., and Pfau, C.J. (1972). Properties of Defective Lymphocytic Choriomeningitis Virus. J Gen Virol *17*, 355-359.

Welsh, R.M., and Pfau, C.J. (1972). Determinants of Lymphocytic Choriomeningitis Interference. J Gen Virol *14*, 177-187.

Ziegler, C.M., Eisenhauer, P., Bruce, E.A., Weir, M.E., King, B.R., Klaus, J.P., Krementsov, D.N., Shirley, D.J., Ballif, B.A., and Botten, J. (2016b). The Lymphocytic Choriomeningitis Virus Matrix Protein PPXY Late Domain Drives the Production of Defective Interfering Particles. PLoS Pathog *12*, e1005501.

CHAPTER 4:

MAPPING OF THE JUNÍN VIRUS MATRIX PROTEIN Z-HOST PROTEIN INTERACTOME REVEALS NOVEL REQUIRED HOST FACTORS FOR ARENAVIRUS PRODUCTION

Christopher M. Ziegler[1,2], Philip Eisenhauer[1], Jamie A. Kelly[1], Loan N. Dang[1], Vedran Beganovic[1,#], Emily A. Bruce[1], Benjamin R. King[1,2], David J. Shirley[3], Marion E. Weir[4,§], Bryan A. Ballif[4], and Jason Botten[1,3*]

[1]Department of Medicine, Division of Immunobiology; [2]Cellular, Molecular, and Biomedical Sciences Graduate Program; [3]Department of Microbiology and Molecular Genetics; [4]Department of Biology, University of Vermont, Burlington, VT 05405, USA. [#]Current address: Wake Forest School of Medicine, Winston-Salem, NC 27157, USA. [§]Current address: Cell Signaling Technology, Beverly, MA, 01915. *Corresponding author.

Running Title: Mapping the Junín Virus Z Protein-Host Interactome

Abstract

Junín virus (JUNV), the causative agent of Argentine hemorrhagic fever, belongs to the arenavirus family of rodent-borne viruses. These viruses contain a simple genome encoding only four proteins yet are capable of executing complex functions in their cellular host. The arenavirus matrix protein Z drives virus assembly and release, in addition to other functions, yet relatively little is known about which cellular proteins Z hijacks to accomplish these functions. In this study, affinity purification-mass spectrometry was used to unbiasedly determine the cellular proteins that JUNV Z interacts with in host cells and in Z-virus like particles (VLPs). Mass spectrometry was also used to determine the host protein content of *bona fide* viral particles from the Candid 1 (C#1) strain of JUNV. Several identified proteins were selected for functional screening which revealed that ARF1, ATP5B, ATP6V0D1, IMPDH2 and PRDX3 are required for JUNV infection. ATP5B, IMPDH2 and Rab5c were also required for infection of the Old World arenavirus, lymphocytic choriomeningitis virus (LCMV). Numerous endosomal sorting complex required for transport (ESCRT) proteins were identified in JUNV virions and VLPs. Inducible expression of the ESCRT accessory protein VPS4 was used to determine that efficient release of infectious JUNV virions requires a functional ESCRT pathway, in contrast to LCMV, which does not utilize ESCRT for infectious virus production. The Z-host protein-protein interaction network mapped in this study provides a framework for further identification of the critical host factors required for Z protein function and ultimately provides a basis for host-targeted antiviral therapeutic discovery.

Importance

Argentine hemorrhagic fever is a severe disease with high mortality and very limited treatment options that is caused by the arenavirus, Junín. The arenavirus matrix protein, Z, serves several roles in the virus life cycle of which most prominent is Z's required role in the assembly and release of virus particles. These various functions of Z likely require an array of host cellular proteins but little is known about which host proteins Z interacts with to accomplish these functions. This study used affinity purification and mass spectrometry to identify protein-protein interactions between Z and its cellular host. Functional assays were used to screen a subset of the host proteins which revealed that several of the identified host factors are critical for arenavirus infection. This study provides deeper insight into the cellular biology of the Z protein and identifies potential proteins for host-targeted anti-viral therapies.

Introduction

Arenaviruses are a family of viruses carried by various species of rodents found throughout the world. The family is divided into two major subclasses based on the geographic distribution of each virus, namely the Old World and New World arenaviruses which represent viruses primarily from Africa or the Americas, respectively (Charrel et al., 2008). The rodent carriers of these viruses are asymptomatic but infected lifelong and shed infectious virus which can result in human infection through exposure to infectious excreta from the infected rodents (Childs et al., 1992; Keenlyside et al., 1983; Salazar-Bravo et al., 2002a). Several arenaviruses cause severe hemorrhagic fever disease in humans with high morbidity and mortality. The causative agent of Lassa hemorrhagic fever, Lassa virus (LASV), causes ~200,000 infections per year in western Africa (McCormick et al., 1987). Similar hemorrhagic fever diseases are found in the New World caused by Guanarito, Junín, Machupo, and Sabia viruses (Charrel and Lamballerie, 2003). Junín virus (JUNV), is endemic to central Argentina and causes Argentine hemorrhagic fever in humans (Maiztegui, 1975). The live, attenuated vaccine strain of JUNV Candid 1 (C#1) has demonstrated efficacy in reducing cases of Argentine hemorrhagic fever in the endemic region but it has not been approved for use by the United States Food and Drug Administration (Enria et al., 2008b). Furthermore, the only therapy with demonstrated efficacy against JUNV infection is immune plasma and thus there is a clear need for therapeutics to treat JUNV infection (Enria et al., 2008b).

Arenaviruses have a simple, negative-sense, bi-segmented RNA genome comprised of two single-stranded segments with an ambisense coding strategy. The small

(S) segment encodes the nucleoprotein (NP) and the glycoprotein (GP) while the large (L-segment) encodes the RNA-dependent RNA polymerase (L) and the matrix protein Z (Auperin et al., 1986; Clegg et al., 1991; Djavani et al., 1997; Lukashevich et al., 1997; Riviere et al., 1985; Salvato and Shimomaye, 1989; Singh et al., 1987). All four proteins are structural components of the virion. GP forms spikes on the exterior of the virion, NP and L together with the genome form the ribonucleoprotein (RNP) complex which is packaged inside virions, and Z forms a matrix layer on the interior side of the viral membrane (Lee and de la Torre, 2002; Neuman et al., 2005; Salvato et al., 1992a; Strecker et al., 2003). Arenaviruses are enveloped and enter cells through receptor-mediated endocytosis, undergo replication and assembly in the cytoplasm, and are released from the cell via budding from the plasma membrane (Urata and Yasuda, 2012). GP mediates cell entry by binding cell surface receptors which triggers endocytosis of the bound virus into the endocytic pathway (Borrow and Oldstone, 1994; Cao et al., 1998; Kunz, 2009; Martinez et al., 2007; Quirin et al., 2008; Spiropoulou et al., 2002). In endosomes, GP triggers fusion of the viral envelope with the endosomal membrane releasing viral ribonucleoproteins into the cytoplasm (Klewitz et al., 2007). Viral replication occurs in the cytoplasm where the genome is transcribed and replicated by the L polymerase but also requires NP (Lee et al., 2000; Lopez et al., 2001).

In the present study, we focused on the multifunctional matrix protein Z. A small protein, Z is largely comprised of a central zinc-binding really interesting new gene (RING) domain and the Z protein of most arenaviruses contains one or two late domains within its

flexible C-terminal region (Djavani et al., 1997; Fehling et al., 2012). Z is responsible for a number of critical functions in the viral life cycle. Z regulates viral genome replication and transcription by antagonizing the viral L polymerase (Cornu and de la Torre, 2001; Jacamo et al., 2003b; Kranzusch and Whelan, 2011). Z can repress the translation of capped mRNAs by directly binding to and inhibiting the translation initiation factor eIF4E (Campbell Dwyer et al., 2000; Kentsis et al., 2001; Kranzusch and Whelan, 2011; Volpon et al., 2010). The Z protein of pathogenic arenaviruses can also inhibit the innate immune response by binding to and inhibiting retinoic acid-inducible gene 1-like proteins (Fan et al., 2010; Xing et al., 2015). Finally, the most prominent role of Z is to drive assembly, budding, and release of virions at the plasma membrane. Z coordinates the assembly of virus particles at sites of budding by interacting with glycoprotein and the viral ribonucleoprotein complex (Capul et al., 2007; Schlie et al., 2010). The release of arenavirus virions has traditionally been thought to be mediated by Z's recruitment of the cellular endosomal sorting complex required for transport (ESCRT) through its C-terminal late domains, either P(S/T)AP and/or PPXY (Perez et al., 2003; Strecker et al., 2003; Urata et al., 2006). Accordingly, Z, in the absence of other viral proteins, can induce the formation of virus-like particles (VLPs) and thus is both necessary and sufficient for driving the budding process (Eichler et al., 2004; Perez et al., 2003; Strecker et al., 2003). However, our lab recently reported that defective interfering particle but not infectious virus particle production for the prototypic Old World arenavirus, lymphocytic choriomeningitis virus (LCMV), requires a functional PPXY late domain and ESCRT

complex (Ziegler et al., 2016b). We also reported recently that a motif outside of any known late domain in the LCMV Z protein contributed to both infectious virus and defective interfering particle production (Ziegler et al., 2016a). The New World arenavirus Tacaribe (TACV) lacks a functional late domain in Z while a recombinant Pichinde virus (PICV) with mutations to its PSAP late domain is viable but attenuated (Urata et al., 2009; Wang et al., 2012). This highlights the level of diversity among arenaviruses and emphasizes the need to better understand the molecular machinery each of the arenaviruses employ to accomplish their various functions.

Viruses are dependent upon the cellular hosts they infect in order to carry out their life cycle. While several functions of the arenavirus Z protein are known, the specific molecular mechanisms and corresponding host machinery hijacked by Z to drive these processes is not well described. In this study, JUNV Z protein from cells or VLPs was co-purified in complex with host protein partners then subjected to mass spectrometry-based protein identification in order to map the Z-host protein interactome. The host protein content of Z VLPs was also confirmed and additional host protein content was identified by immunoprecipitation of JUNV C#1 virions and mass spectrometry. Functional characterization of six host protein partners was carried out by RNA silencing which yielded several novel pro-viral factors including a component of the mitochondrial ATP synthase complex, ATP5B, which was required for the production JUNV as well as the prototypic Old World arenavirus, LCMV. This study also revealed that ESCRT complex proteins are enriched in Z VLPs and JUNV C#1 virions. Using cells expressing *wild type*

(WT) or dominant negative (EQ) VPS4A or VPS4B, we were able to demonstrate for the first time that release of infectious JUNV C#1 virions requires a functional ESCRT pathway, in contrast to its Old World arenavirus counterpart, LCMV.

Materials and Methods

Cells, viruses and plasmids

Human embryonic kidney cells (HEK-293T/17) (CRL-11268, American Type Culture Collection, Manassas, VA) (referred to as HEK293T cells in the manuscript) were maintained in Dulbecco's Modified Eagle Medium (DMEM) (11965-092) supplemented with 10% fetal bovine serum (FBS) (16140-071), 1% penicillin-streptomycin (15140-122), 1% MEM Non-Essential Amino Acids Solution (11140-050), 1% HEPES Buffer Solution (15630-130), and 1% GlutaMAX (35050-061) purchased from Invitrogen (Carlsbad, CA). Stably transduced T-Rex HEK293 cells expressing WT or the dominant negative EQ mutant of vacuolar protein sorting 4A (VPS4A) or VPS4B under a tetracycline-inducible promoter described in (Dalal et al., 2004; Lin et al., 2005; Taylor et al., 2007) were kindly provided by M. Kielian (Albert Einstein College of Medicine, Bronx) and were maintained in the same media as HEK293T cells but were also supplemented with 100 μg/mL Zeocin (R250-01, Invitrogen). African green monkey kidney cells (Vero E6) were kindly provided by J. L. Whitton (The Scripps Research Institute, La Jolla) and grown in DMEM supplemented with 10% FBS, 1% penicillin-streptomycin, and 1% HEPES Buffer Solution. Human lung carcinoma cells (A549) (CCL-185, American Type Culture Collection) were maintained in 50:50 DMEM:F12 medium (11330-032, Invitrogen) supplemented with 10% FBS and 1% penicillin-streptomycin. All cell lines were grown at 37 ºC in a humidified incubator containing 5% CO2. Lymphocytic choriomeningitis virus (LCMV) strain Armstrong 53b was kindly provided by J. L. Whitton. Recombinant

(r)LCMV WT based on the Armstrong 53b strain used in VPS4 assays was generated as described previously (Flatz et al., 2006; Ziegler et al., 2016b). The candidate vaccine strain of Junín virus (JUNV), C#1, an attenuated strain derived from virulent JUNV strain XJ as described in (Chosewood et al., 2009; Goñi et al., 2006), was kindly provided by M. Buchmeier (University of California, Irvine) and R. Tesh (The University of Texas Medical Branch at Galveston). Working stocks of these viruses were generated and infectious titers were measured via plaque assay using Vero E6 cells.

Plasmids pLCMV-Z, pLASV-Z and pJUNV-Z contain a Z gene fused to the streptavidin binding peptide (SBP) sequence through an 18 base pair linker at the C-terminus. Z was amplified by PCR from existing constructs using the forward primer LCMVZf (5'-ACAAGTTTGTACAAAAAAGCAGGCTGATATCGCCACCATGGGTC AAGGCAAGTCCAGA-3'), LASVZf (5'-ACAAGTTTGTACAAAAAAGCAGGCTGA TATCGCCACCATGGGAAACAAGCAAGCCAAA-3') or JUNVZf (5'-ACAAGTTTG TACAAAAAAGCAGGCTGATATCGCCACCATGGGCAACTGCAACGGGGCA-3') which have a 5' overhang containing AttB1 and Kozak sequences and the reverse primer LCMVZr (5'-ACCTCCACCTCCAGCTGCCTCTTCGTAGGGAGGTGGAGA-3'), LASVZr (5'-ACCTCCACCTCCAGCTGCGGGACTGTAGGGTGGGGGTCT-3') or JUNVZr (5'-ACCTCCACCTCCAGCTGCTGGTGGTGGTGCTGTTGGCTC-3') which have an overhang containing the linker sequence. The SBP sequence was amplified by PCR from pT7-FLAG-SBP-1 (Sigma-Aldrich) using the forward primer SBPf (5'-GCAGCTGGAGGTGGAGGTATGGACGAAAAAACCACCGGT-3') which has a 5'

overhang containing the linker sequence and reverse primer SBPr (5'-ACCACTTTGTACAAGAAAGCTGGGTCTTACGGTTCACGCTGACCCTGCGG-3') containing a 3' overhang with stop codon preceding the AttB2 sequence. The two products were fused by PCR using the appropriate Z forward primer and the SBPr primer. Each cassette was subcloned using the Gateway cloning system (Invitrogen) following manufacturer's instructions into a modified pCAGGS vector containing AttB sites that was previously described (Cornillez-Ty et al., 2009; Klaus et al.).

Affinity Purification and Immunoprecipitation

For Z mass spectrometry experiments and subsequent western blot validation, 5 $x10^5$ HEK293T cells seeded in each well of two 6 well plates per condition 24 hours (hr) prior to transfection. Cells were transfected with 100µL DMEM containing 2µg of the SBP-tagged JUNV Z construct or an empty vector (p0) and 8µg of 1mg/mL polyethyleneinimine (23966, Polysciences, INC., Warrington, PA) per well. Virus-like particles (VLPs) and cells were harvested 48 hr after transfection. The VLP-containing cell culture media was clarified by centrifugation and the cells were scraped into phosphate buffered saline (PBS) and pelleted by centrifugation. VLPs and cells were lysed on ice for 20 minutes using Triton lysis buffer (final concentration of 0.5% NP40, 1% Triton X-100 (Acros), 140mM NaCl, 25mM Tris HCl) with protease inhibitor cocktail (04693159001,Roche, Indianapolis, IN) and PhosphoStop phosphatase inhibitor cocktail (4906837001, Roche). SBP-tagged Z protein in complex with host proteins was purified by incubating with Dynabeads MyOne Streptavidin T1 beads (65602, Invitrogen) for 2 hr at 4°C on a rotating

platform. The protein-bound beads were washed 4 times with Triton lysis buffer then were eluted in Laemmli sample buffer (62.5mM Tris-HCl, 10% glycerol, 2% sodium dodecyl sulfate and 0.01% bromophenol blue) containing 5% 2-mercaptoethanol by heating at 100^{o}C for 10 minutes.

For JUNV C#1 virion mass spectrometry experiments and subsequent western blot validation, 6x10^{6} HEK293T cells were seeded in 5 T-150 tissue culture flasks per condition 24 hr prior to infection. Cells were infected with JUNV C#1 at a multiplicity of infection of 0.1 plaque forming units per cell (PFU/cell). 48 hr post infection (pi) the media was aspirated and the cells were washed with warmed PBS then 8 mL of Pro293 media (12-764Q, Lonza) supplemented with 1% penicillin-streptomycin (15140-122), 1% MEM Non-Essential Amino Acids Solution (11140-050), 1% HEPES Buffer Solution (15630-130), and 1% GlutaMAX (35050-061) purchased from Invitrogen (Carlsbad, CA) was added to each flask. 72 hr pi cell culture media was pooled and clarified by centrifugation. To the virus containing media, calcium chloride was added to a final concentration of 1mM and 1 protease inhibitor cocktail tablet (04693159001,Roche) per 15 mL was added then 68 µL of magnetic, protein G-conjugated beads (10004D, Invitrogen) were added to each tube and incubated for 15 minutes on ice. The pre-cleared supernatant was then transferred to a new tube and was incubated with 34 µg of mouse monoclonal glycoprotein 1 (GP1)-specfic antibody clone QC03-BF11 (NR-2566, BEI Resources) or 34ug of mouse IgG antibody (MAB002, B&D Biosciences) for 2 hr, then 600 µL of protein G magnetic beads were added and incubated for an additional hour. The virion-bound beads were washed 4

times with PBS containing 0.1 % bovine serum albumin (BP1600-100, Fisher-Scientific) then were resuspended in 2x-concentrated Laemmli sample buffer (125mM Tris-HCl, 20% glycerol, 4% sodium dodecyl sulfate and 0.02% bromophenol blue). Virion protein content was eluted from the beads by boiling the resuspended beads at 100ºC for 10 minutes with 5% 2-mercaptoethanol or without (for western blotting with anti-GP1 antibody).

Identification of Host Proteins by Mass Spectrometry

Protein precipitates were separated using NuPAGE 4-12% Bis-Tris or 4-20% Tris-glycine gels (Invitrogen). Following electrophoresis, each gel was stained with coomassie (40% methanol, 20% acetic acid and 0.1% Brilliant Blue R (Sigma-Aldrich)) overnight then excess stain was removed with a solution of 30% methanol and 10% acetic acid and imaged using a Canon Canoscan 8800F scanner. Each sample lane was cut into 16 (Z) or 12 (virion) slices which were processed with chemicals from Fisher-Scientific as follows. Each slice was rinsed with HPLC grade water then incubated with destain solution (50mM ammonium bicarbonate and 50% acetonitrile) for 30 minutes at 37ºC. The destain solution was removed and the gel slices were dehydrated by incubating with 100% acetonitrile for 5 minutes twice. Samples were reduced with 25mM dithiothreitol in 50 mM ammonium bicarbonate for 30 minutes at 55ºC then allowed to cool for 10 minutes at room temperature. The slices were partially dehydrated by incubating with 100% acetonitrile for 5 minutes then were alkylated with 10 mM iodoacetamide in 50mM ammonium biocarbonate for 45 minutes in the dark at room temperature. The samples were washed two times by incubating with destain solution for 5 minutes, dehydrating with 100%

acetonitrile, then rehydrating with water for 10 minutes. Gel slices were then completely dehydrated by incubating two times with 100% acetonitrile for 5 minutes and dried at room temperature. The gel slices were rehydrated with a solution of 12.5 ng/μL sequencing grade modified trypsin (Promega) in 50 mM ammonium bicarbonate on ice for 30 minutes then were digested overnight at 37ºC. Peptides were extracted with a solution of 2.5% formic acid in 50% acetonitrile while spinning in a microcentrifuge at 13,000 rpm for 10 minutes. The supernatant was collected and the gel slices were dehydrated by twice incubating with 100% acetonitrile and collecting the extract. All solvent was removed from the extracts using a vacuum centrifuge at 37ºC. The peptides were resuspended in 2.5% acetonitrile and 2.5% formic acid then separated in a microcapillary column packed with 12 cm Magic C18, 200 Å, 5 μm material (PM5/66100/00, Michrom Bioresources, Auburn, CA) using a MicroAS autosampler (Thermo Scientific, Pittsburgh, PA). Peptides were eluted with a 5−35% acetonitrile (0.15% formic acid) gradient using a Surveyor Pump Plus HPLC (Thermo Scientific) over 40 minutes, after a 15 minute isocratic loading at 2.5% acetonitrile and 0.15% formic acid. Mass spectra were acquired in an LTQ-XL linear ion trap mass spectrometer (Thermo Scientific) using 10 MS/MS scans following each survey scan over the entire run. The human IPI forward and reverse concatenated databases were referenced with SEQUEST software requiring tryptic peptide matches with a 2 Da mass tolerance to analyze the raw data. For spectral analysis, the following precursor mass differences were allowed: serine, threonine, and tyrosine residues (+79.96633 Da); methionine (+15.99492 Da) and cysteines (+57.02146 Da or 71.0371). Proteins identified

in the database were further filtered by excluding peptides with XCorr scores less than 2.0 and proteins with only one unique peptide sequence identified. Proteins that were identified in both the Z protein or JUNV C#1 infected conditions were excluded if they were also identified in the empty vector or mock infected controls unless there were at least 5-fold more unique peptide sequences identified in the Z protein or JUNV C#1 infected conditions.

SDS-PAGE and Western Blotting

Protein samples diluted in Laemmli buffer with 5% 2-mercaptoethanol were subjected to polyacrylamide gel electrophoresis on NuPAGE 4-12% Bis-Tris gels with MES buffer. Western blotting was carried out using nitrocellulose iBlot gel transfer stacks (IB301001, Invitrogen) and the Invitrogen iBlot transfer apparatus. Protein transfer was confirmed by staining membranes with a solution containing 0.1% Ponceau S (P3504, Sigma-Aldrich) and 5% acetic acid which was subsequently removed by washing with water. Membranes were blocked for 1 hr using PBS containing 5% non-fat milk (fluorescent detection) or 5% non-fat milk, 0.05% IGEPAL CA-630 (198596, MP Biomedicals, Solon, OH) in PBS (chemiluminescent detection). Primary antibodies were diluted in PBS containing 5% non-fat milk and 0.2% Tween 20 (Fisher-Scientific) (fluorescent detection) or in 5% non-fat milk, 0.05% IGEPAL CA-630, and 3% fetal bovine serum (chemiluminescent detection) and were incubated overnight at room temperature. The membranes were washed 5 times for 5 minutes with western wash solution (0.05% IGEPAL CA-630 (198596, MP Biomedicals, Solon, OH) in PBS) then

incubated with secondary antibodies diluted in PBS containing 5% milk, 0.2% Tween 20 (BP337, Fisher-Scientific) and 0.02% sodium dodecyl sulfate for 1 hr at room temperature (fluorescent detection) or diluted in 5% non-fat milk, 0.05% IGEPAL CA-630, and 3% fetal bovine serum (chemiluminescent detection) and incubated for 2 hr. The membranes were then washed 5 times for 5 minutes with western wash buffer. For fluorescent detection, the membranes were washed one time for 5 minutes with PBS then imaged using a Licor Odyssey CLx imaging system. For fluorescent detection of actin, LCMV or JUNV NP, and green fluorescent protein (GFP)-tagged VPS4A and VPS4B, the iBind Flex western device (SLF2000, Thermo Scientific) and the corresponding iBind fluorescent detection solution (SLF2019, Thermo Scientific) was used. For chemiluminescent detection, membranes were developed using chemiluminescent substrate (SuperSignal West Pico (34080) or Femto (34096), Thermo Scientific) and detected with film.

The following primary antibodies (at the indicated concentrations) were used for western blotting: mouse anti-β-actin (A5441, Sigma-Aldrich) (1:2,500) rabbit anti-actin (A2066; Sigma-Aldrich) (1:2,500), mouse anti-ADP ribosylation factor 1 (ARF1) (MA4-060, Thermo Scientific) (1:1,000), mouse anti-ATP5B (sc-166443, Santa Cruz Biotechnology, Dallas, TX) (1:100), anti-ATP6V0D1 (sc-818877, Santa Cruz Biotechnology) (1:500), mouse anti-green fluorescent protein (GFP) (632380, Clontech, Mountain View, CA) (1:1,000), rabbit anti-inosine monophosphate dehydrogenase 2 (IMPDH2) (ab131158, Abcam, Cambridge, MA), rabbit anti-LCMV nucleoprotein (2165) (1:5,000), mouse anti-JUNV glycoprotein 1 (NR-2564, BEI Resources, Manassas, VA)

(1:250), mouse anti-JUNV nucleoprotein (NR-2582, BEI Resources) (1:200), rabbit anti-JUNV Z protein (1:1,000), mouse anti-peroxiredoxin 3 (PRDX3) (LF-MA0044, AbFrontier, Seoul, Korea) (1:1,000), mouse anti-Rab5c (sc-365667, Santa Cruz Biotechnology) (1:500), and anti-streptavidin binding peptide (SBP) (MAB10764; EMD Millipore, Billerica, MA) (1:10,000). LCMV nucleoprotein antibody, 2165, was generously provided by M. J. Buchmeier (University of California, Irvine). The following secondary antibodies (at the indicated concentrations) were used for western blotting: goat anti-mouse IRDye 680LT (926–68020, LI-COR) (1,20,000), goat anti-rabbit IRDye 800CW (926–32211) (1:20,000), goat anti-mouse horse radish peroxidase (HRP) (71045, EMD Millipore) (1,5,000), goat anti-mouse IgG Fcγ-specific HRP (115-035-164, Jackson Immunoresearch Laboratories, West Grove, PA) (1:50,000), goat anti-mouse light chain-specific HRP (AP200P, EMD Millipore), and goat anti-rabbit HRP (111-035-045, Jackson Immunoresearch Laboratories).

RNA Interference Virus Challenges

For RNA interference experiments, 1.2uL of RNAiMax (13778075, Life Technologies) and a 10 nM final concentration of Silencer Select silencing (si)RNA (4390824, Life Technologies) targeting ARF1 (s1551), ATP5B (s1774), ATP6V0D1 (s17395), IMPDH2 (s7416), PRDX3 (s21509), or Rab5c (s11710) or a non-targeting control siRNA (4390843) in OptiMEM (31985070, Thermo Fisher Scientific) was added to each well of a 12 well plate and then combined with 40,000 A549 cells per well in normal growth media. 48 hr after reverse transfection, the cells were infected with JUNV

C#1 at a multiplicity of infection (MOI) of 0.1 PFU/cell or with LCMV Arm at an MOI of 0.001 PFU/cell. One hour later, the virus inoculum was removed and fresh media was added. 48 hr after infection, the virus-containing supernatant and the cells were collected. Viral titers were determined by standard plaque assay and values with each independent experiment were normalized to the sum of all the values within each experiment (normalization by summation), then each value was normalized to the mean of the WT values and the mean of the WT was set to 100 % as described in (Degasperi et al., 2014). Host protein knockdown as well as viral nucleoprotein and cellular actin levels were determine by western blotting.

Virus Challenges in VPS4A- and VPS4B- Transduced Cells

VPS4A or VPS4B WT or dominant negative (EQ) T-rex HEK293 cells were used to assess the dependency of JUNV C#1 on the ESCRT pathway for infectious virus release. For these experiments, 2.5 x 10^5 cells were seeded in poly D-lysine-treated 6-well plates then were infected 24 hr later with JUNV C#1 at an MOI of 0.1 PFU/cell or with LCMV Arm at an MOI of 0.001 PFU/cell. 48 hr after infection when all cells were productively infected, expression of transduced VPS4A or VPS4B was induced with 1 µg/mL tetracycline or medium only as a control. 5 hr later, the cells were washed with PBS then fresh media containing 1 µg/mL tetracycline or medium alone was added. 15 hr later the cells and virus-containing supernatants were collected. Infectious virus titers were determined via plaque assay and expression of exogenous GFP-tagged VPS4A or VPS4B was determined by western blot.

Statistics

GraphPad Prism software was used to perform a one-way ANOVA with Holm-Sidak's test for multiple comparisons to analyze the viral titers in the siRNA challenge experiment in Figures 4.4C and D as well as the VPS4A and VPS4B challenges in Figures 4.5A and B.

Results

Affinity Purification-Mass Spectrometry Identification of Z-Host Protein-Protein Interactions and Cellular Proteins in JUNV C#1 Virions.

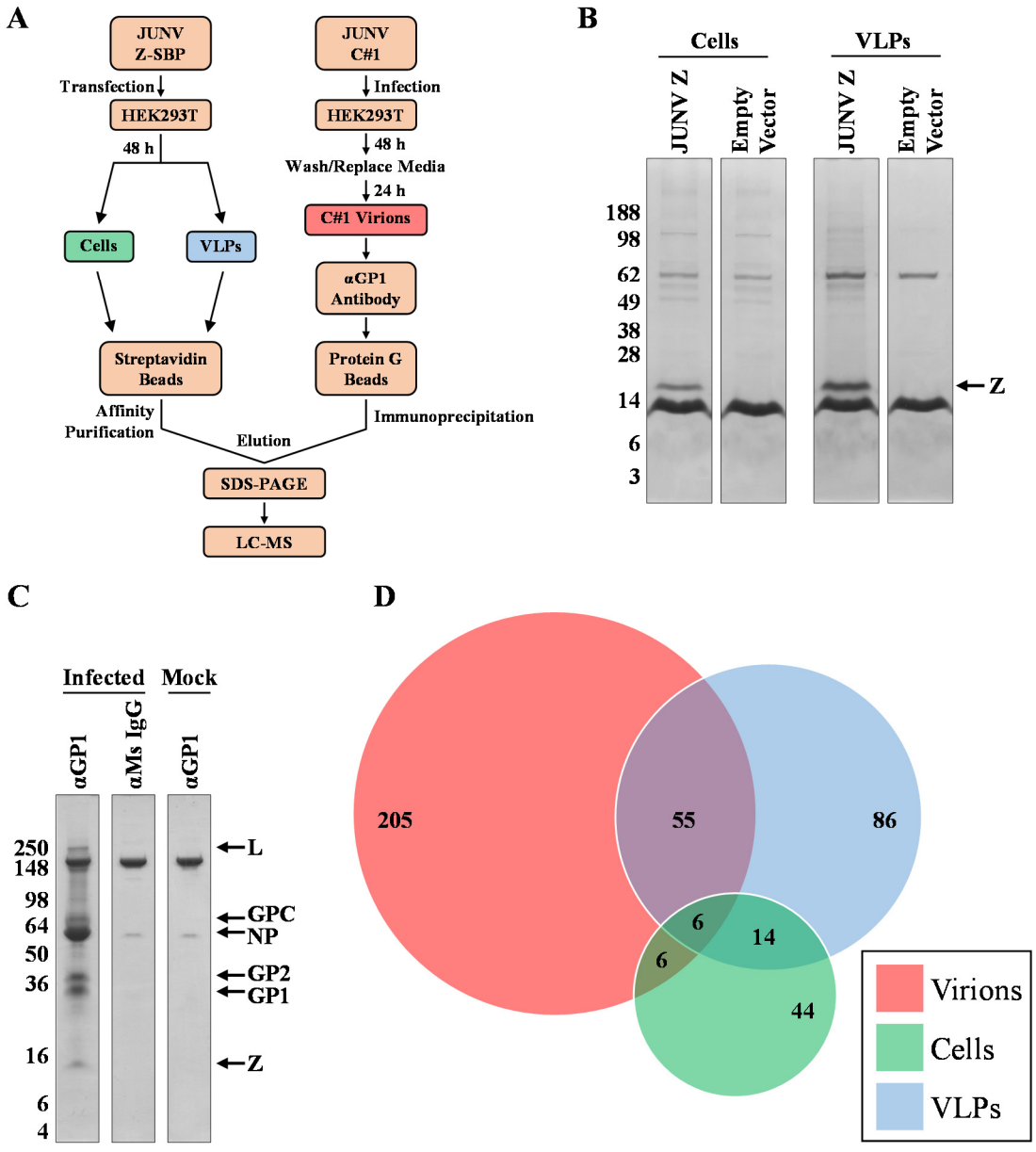

Figure 4.1. Identification of Z-host protein-protein interactions and cellular proteins in JUNV C#1 virions. (A) Flowchart of experimental strategy for mass spectrometry-based identification of host protein

partners of JUNV Z and host proteins in virions. (B and C) Coomassie stained SDS-PAGE gels of Z co-purified with its host protein partners or immunoprecipitated JUNV C#1 virions were subjected to mass spectrometry-based proteomic analysis. (B) SBP-tagged Z and co-purifying host proteins were purified from transfected HEK293T cells or virus-like particles (VLPs) produced from transfected cells. An empty vector-transfected condition was used as a control. (C) JUNV C#1 virions produced in HEK293T cells and immunoprecipitated with an antibody specific to the surface glycoprotein (GP1). Control conditions included both immunoprecipitation of virus-containing supernatants with a non-specific mouse IgG antibody and uninfected (mock) supernatants with the GP1 antibody. The molecular weight in kDa and viral proteins are indicated. Each gel is representative of two independent experiments. (D) Venn diagram indicating the number of host proteins identified in JUNV C#1 virions, interacting with Z in cells or in VLPs as well as those proteins conserved across the different conditions. The represented proteins include those that were identified in both replicate experiments and do not include proteins found in control conditions according to the criteria described in the Material and Methods.

To identify host protein binding partners of the JUNV Z protein, HEK293T cells were transfected with a streptavidin binding peptide (SBP)-tagged Z protein, which was then affinity purified with streptavidin beads from whole cell lysates and from clarified Z VLP-containing cell culture media (Figure 4.1A). The protein samples containing Z and its co-purifying host binding partners were first separated by gel electrophoresis then analyzed by liquid chromatography-mass spectrometry (Figure 4.1B). Cells transfected with empty vector were used as a control to eliminate any proteins that bound non-specifically to the streptavidin beads (Figure 4.1B). From two replicate experiments, a total of 163 host proteins were identified from cell lysates of which 70 proteins (43%) were conserved between the two replicate experiments. A total of 517 host proteins were identified in Z VLPs of which 161 (31%) were found in both replicate experiments.

To identify the host protein content in *bona fide* JUNV C#1 virions, a surface glycoprotein-specific antibody (GP1) was used to immunoprecipitate virions which were subjected to protein gel electrophoresis and in-gel tryptic digestion, followed by mass spectrometry analysis (Figure 4.1A). Two different control conditions were used to

eliminate non-specifically binding host proteins: an uninfected (mock) condition immunoprecipatated with the same GP1 antibody as well as an infected condition where a non-specific immunoglobulin control antibody was used (Figure 4.1C). A total of 179 host proteins were identified in JUNV virions and 113 (63%) were conserved across two replicate experiments. Overall, there was a relatively high degree of overlap in host protein content between Z VLPs and JUNV virions (64% of proteins found in Z VLPs were also found in virions) (Figure 4.1D). However, the host protein content of Z VLPs and JUNV C#1 virions was largely different than intracellular Z's host protein partners (Figure 4.1D).

Host Protein Partners of Z.

Virions	VLPs	Cells
Ribosomal Proteins (41.2)	Ribosomal Proteins (20.2)	Mitochondrial Membrane (9.3)
RPL10A, RPL11, RPL12, RPL13, RPL13A, RPL13P12, RPL18, RPL18A, RPL19, RPL21, RPL21P16, RPL21P19, RPL23, RPL28, RPL3, RPL30, RPL36, RPL38, RPL4, RPL5, RPL6, RPL7, RPL7A, RPL7P32, RPL8, RPL9, RPLP0, RPLP1, RPLP2, RPS10, RPS11, RPS14, RPS15A, RPS16, RPS17, RPS18, RPS19, RPS2, RPS21, RPS24, RPS27, RPS3, RPS3A, RPS4X, RPS5, RPS6, RPS8, RPS9	HEATR1, RPL10A, RPL11, RPL13A, RPL18, RPL3, RPL4, RPL6, RPL7, RPLP0, RPS2, RPS3A, RPS4X, RPS6, RPS8, RPS9, RPSAP12	CHCHD3, IMMT, MTCH2, PHB, PHB2, SLC25A6, STOML2, TIMM50, TOMM40, VDAC1, VDAC2, VDAC3
Nucleotide Binding/Chaperone/Stress Response (15.4)	Nucleotide Binding/Chaperone/Stress Response (19.3)	Nuclear Import/Export (6.4)
ABCE1, ACTBL2, CCT2, CCT3, CCT4, CCT5, CCT6A, CKB, HSP90AB1, HSPA1A, HSPA1B, HSPA1L, HSPA4, HSPA5, HSPA8, HYOU1, LARS, MYO1D, TCP1	ACTA2, ACTBL2, CCT2, CCT3, CCT4, CCT5, CCT6A, CCT7, CCT8, CKB, DDX3X, HSP90AA1, HSP90AA2, HSP90AB1, HSPA1A, HSPA1B, HSPA8, HSPA9, LARS, MARS, MCM7, RUVBL2, TCP1	CSE1L, IPO5, IPO7, KPNB1, NUP205, TNPO1, XPO1, XPO5, XPOT
ESCRT Complex (12.5)	Translation Factors (13.7)	Nucleotide Binding/Chaperone (4.5)
CHMP2A, CHMP2B, CHMP4B, CHMP5, MVB125A, MVB125B, VPS25, VPS28, VPS37B	EEF1A1, EEF1A2, EEF2, EFTUD2, TUFM	ATAD3A, CCT4, CCT5, CCT6A, CLPB, HYOU1
ATP Binding (11.3)	tRNA Synthetase (10.9)	ATPase/ATP Synthase (3.4)
ACTBL2, ASCC3, CCT3, CCT6A, DDX3X, DDX6, DYNC1H1, EIF4A1, G3BP1, MOV10, PRIC285, SNORA67	AARS, EPRS, GARS, LARS, MARS	ATP5A1, **ATP5B**, **ATP6V0D1**, ATP6V1B2
Microtubule Cytoskeleton (8.6)	Microtubule Cytoskeleton (9.2)	
TBCA, TCP1, TUBA4A, TUBB2C	TCP1, TUBA1C, TUBA4A, TUBB, TUBB1, TUBB2C	
Ras Superfamily (7.7)	Proteasomal Process (8.9)	
ARF1, ARF6, EEF2, EHD1, NRAS, RAB13, RAB1A, RAB2A, RAB35, RAB5B, **RAB5C**, RAB7A, RAB8A, RALB, RAP1B, RRAS2	CDK1, PSMC3, PSMC5, PSMC6, PSMD10, PSMD12, PSMD2, PSMD6, PSMD7, PSMD8, RPS27A, UBB, UBC	
Histone Proteins (5.5)	mRNA Processing (8.7)	
H2AFV, HIST1H1C, HIST1H4A, HIST1H4B, HIST1H4C, HIST1H4D, HIST1H4E, HIST1H4F, HIST1H4H, HIST1H4I, HIST1H4J, HIST1H4K, HIST1H4L, HIST2H2BE, HIST2H4A, HIST2H4B, HIST4H4	EFTUD2, HNRNPK, HNRNPM, HNRNPU, PCBP1, PCBP2, SFRS1	
Plasma Membrane-Associated Cytoskeletal Proteins (5.5)	Ras Superfamily (6.6)	
CTNNA1, EZR, FERMT2, MSN, RDX, TLN1	**ARF1**, RAB10, RAB1A, RAB7A	
Axonogenesis (1.9)	Nuclear Import/Export (5.5)	
CTNNA1, EZR, FERMT2, MSN, RDX, TLN1	IPO4, IPO5, IPO7, KPNA2, KPNB1, XPO1	
Transmembrane Glycoproteins (1.8)		
ALCAM, BSG, CD99, CXADR, EFNB2, IGSF3, IGSF8, MFAP3, PTGFRN		

Table 4.1. Major protein classes represented in Z protein and virion interactome. Generated using NIH DAVID Gene Functional Classification analysis using the medium stringency setting. The gene functional classification tool in DAVID version 6.7 was used to categorize all protein identified in JUNV C#1 virions or as binding partners of intracellular JUNV Z or JUNV Z in virus-like particles. A description of the gene functional class and the DAVID enrichment score are listed.

A total of 416 host proteins were identified as binding partners of Z in host cells or in VLPs, as components of virions or were found in more than one of these conditions. DAVID version 6.7 functional gene classification tool (Huang et al., 2008, 2009) was used to categorize functionally related proteins that were over-represented in each of these conditions (Table 4.1). Ribosomal proteins were the most highly represented protein class in both virions and Z VLPs. This finding was not unexpected, as arenaviruses are named for the Latin word, *arenosus*, meaning "sandy," for the electron dense granules observed in virions presumed to be ribosomes (Rowe et al., 1970). The next most highly represented protein class included nucleotide binding proteins and chaperone proteins (Table 4.1). Several of these proteins interacted with Z in cells and VLPs and were found in virions which may indicate that Z recruits these proteins into virions. Additionally, several nuclear import or export factors were over represented in VLPs as well as cells, which raises questions about whether Z executes any functions in the nucleus. Both the ESCRT complex and the Ras superfamily, both involved in intracellular vesicular trafficking, were enriched in virions as well (Table 4.1). It should be noted that the ESCRT complex proteins CHMP1A and TSG101 as well as the ESCRT accessory protein, PDCD6IP (also known as ALIX), were identified in this study (Figure 4.2 and Table 4.S1) despite not being included in the ESCRT complex protein class generated by DAVID. Additionally,

intracellular Z interacted with several ATP synthases and ATPases as well as several mitochondrial membrane proteins (Table 4.1). Finally, nearly the entire human peroxiredoxin family was represented in this study, primarily in Z VLPs (Figure 4.2 and Table 4.S1), despite not being identified using the medium stringency settings in the DAVID analysis shown in Table 4.1.

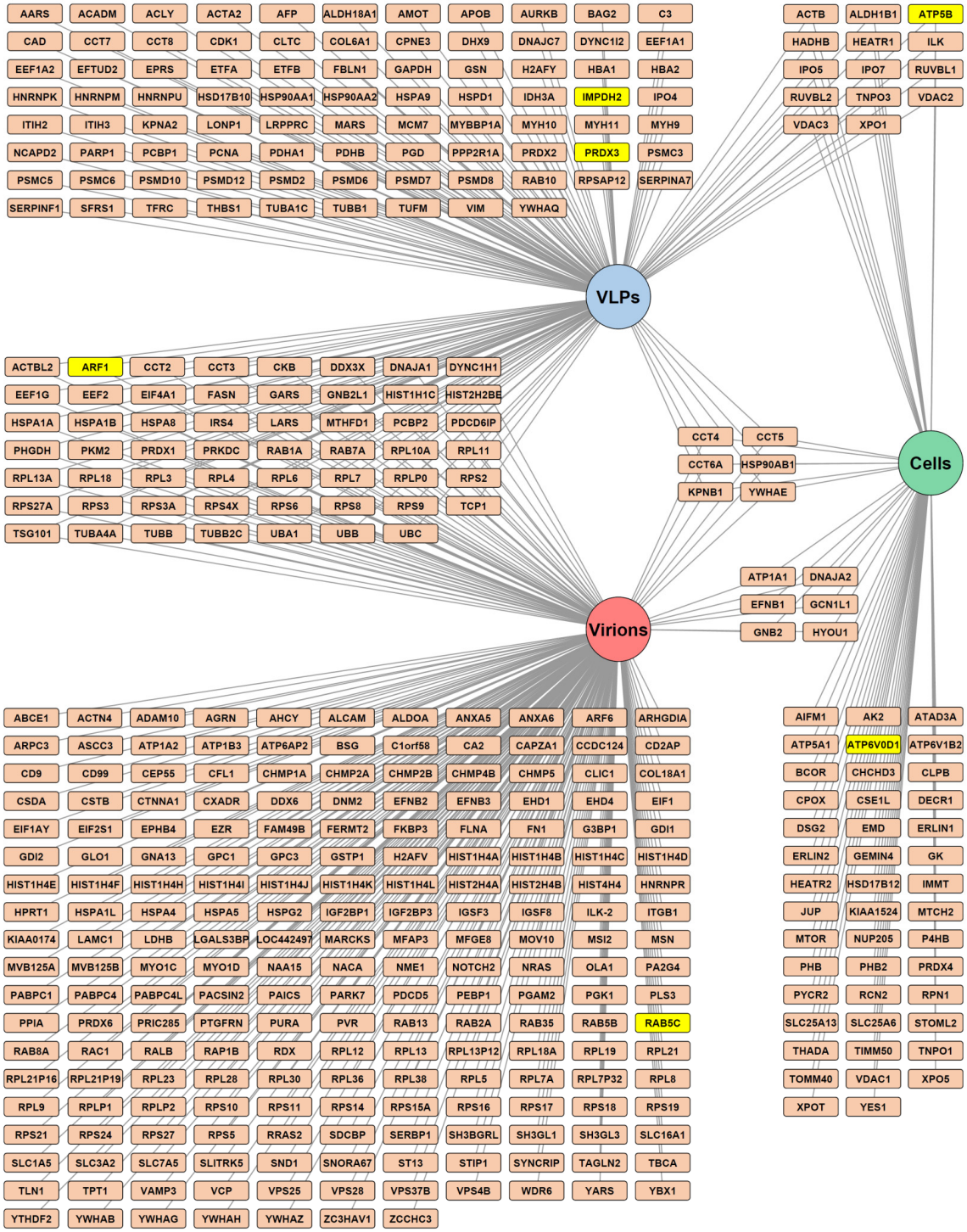

Figure 4.2. JUNV Z-host and JUNV C#1 virion host protein interactome network. Virus-host protein interaction network generated using Cytoscape 3.3.0 software. All host proteins identified in both replicate

experiments for each condition are represented by rectangles and lines indicate host protein interactions with each viral condition (circular nodes). Host proteins selected for further analysis in this study are highlighted in yellow.

Confirmation of select host protein partners.

Gene Symbol	Entrez ID	Gene Description	Cells	VLPs	Virions	Virions of Other Viruses?	Virus siRNA Studies
ARF1	375	ADP-ribosylation factor 1		x	x	Filovirus, HSV, HIV-1, VV	HIV, VSV, LCMV, CVB, PV
ATP5B	506	ATP synthase, H+ transporting, mitochondrial F1 complex, beta polypeptide	x	x		HIV-1	HIV
ATP6V0D1	9114	ATPase, H+ transporting, lysosomal 38kDa, V0 subunit d1	x			HIV-1, MMLV	DENV, IAV, VSV, LCMV, WNV, YFV
IMPDH2	3615	IMP (inosine monophosphate) dehydrogenase 2		x			
PRDX3	10935	peroxiredoxin 3		x			VACV
RAB5C	5878	RAB5C, member RAS oncogene family			x	Filovirus, HSV, HIV-1, VV	VSV, LCMV, VACV

Table 4.2. Host proteins selected for further analysis. Six host proteins identified in different representative conditions or multiple conditions were selected for western blot confirmation and functional studies. The official gene symbol, Entrez gene ID, gene description and mass spectrometry condition(s) identified in are indicated. Additionally, whether each protein was identified as a component of virions from other virus families in other proteomics studies as well as whether each host protein was a required factor for other viruses in large-scale siRNA screens is indicated.

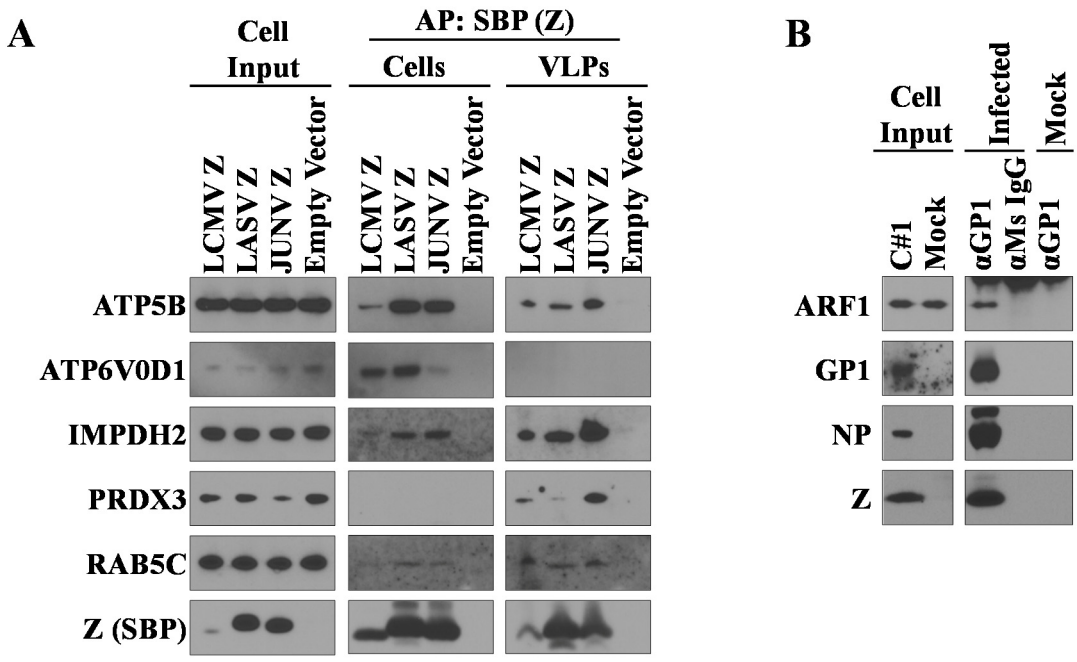

Figure 4.3. Western blot confirmation of select JUNV-host protein partners. (A) Plasmids expressing SBP-tagged Z protein of representative Old World arenaviruses, lymphocyctic choriomeningitis virus (LCMV) and Lassa virus (LASV), and JUNV were transfected into HEK293T cells and two days later cells as well as VLPs produced from transfected cells were lysed and Z and its host protein partners were co-purified with streptavidin beads. The proteins were separated by SDS-PAGE and the indicated host proteins and Z were detected by western blot using antibodies specific to each host protein or an antibody to Z's SBP affinity tag. (B) JUNV C#1 virions produced in HEK293T cells were immunoprecipitated using a GP1-specific antibody then subjected to SDS-PAGE followed by western blot detection of the host protein ARF1 as well viral GP1, nucleoprotein and Z protein using protein specific antibodies. All proteins were detected with horse radish peroxidase-conjugated secondary antibodies and chemiluminenscent-based detection with standard film. All western blots are representative of at least 2 independent experiments.

A subset of these host protein partners were selected for further characterization (Table 4.2). To confirm these interactions with the Z protein of JUNV and see if the interactions extended to the Old World arenaviruses, LCMV or LASV, western blot analysis of individually affinity purified Z proteins in complex with host proteins was performed using host protein-specific antibodies (Figure 4.3A). Western blot detection largely recapitulated the mass spectrometry based detection, but afforded greater sensitivity

for certain proteins. ATP5B and IMPDH2, which were only detected in VLPs by mass spectrometry, also interacted with intracellular Z of all three representative arenaviruses (Figure 4.3A). Mass spectrometry, despite its ability to identify proteins in a high throughput manner, may fail to consistently detect proteins in complex samples. For example, a total of 15 Rab family proteins were identified as JUNV Z protein partners or in JUNV C#1 virions in at least one replicate mass spectrometry experiment (Table 4.S1), yet only three of the Rab proteins (Rab1a, Rab7a, and Rab10) met the most stringent cutoff for Z protein partners. Additionally, Rab5c, which was only detected in JUNV C#1 virions by mass spectrometry, also interacted with LASV and JUNV intracellular Z as well as Z in VLPs for all three viruses. Thus, some of the host proteins identified in only one or two of the conditions may not actually be exclusive to that condition. However, interaction of JUNV Z (or LASV or LCMV Z) with ATP6V0D1 was not detectable in VLPs despite interacting particularly strongly with LASV and LCMV Z in cells (Figure 4.3A). An interaction of PRDX3 with intracellular Z was similarly undetectable for all three viruses despite a strong interaction with JUNV Z in VLPs (Figure 4.3A). Finally, ARF1 was confirmed as a component of JUNV C#1 virions by western blotting (Figure 4.3B). Confirmation of additional host protein content in JUNV C#1 virions from the selected panel by western blotting was obscured by signal from the heavy and light chain of the antibody used to immunoprecipitate virions. Largely, these data suggest that the Z protein of disparate arenaviruses engage a common core of host machinery to accomplish certain functions in addition to host factors engaged by specific viral Z proteins.

Screening for functional importance of select host proteins.

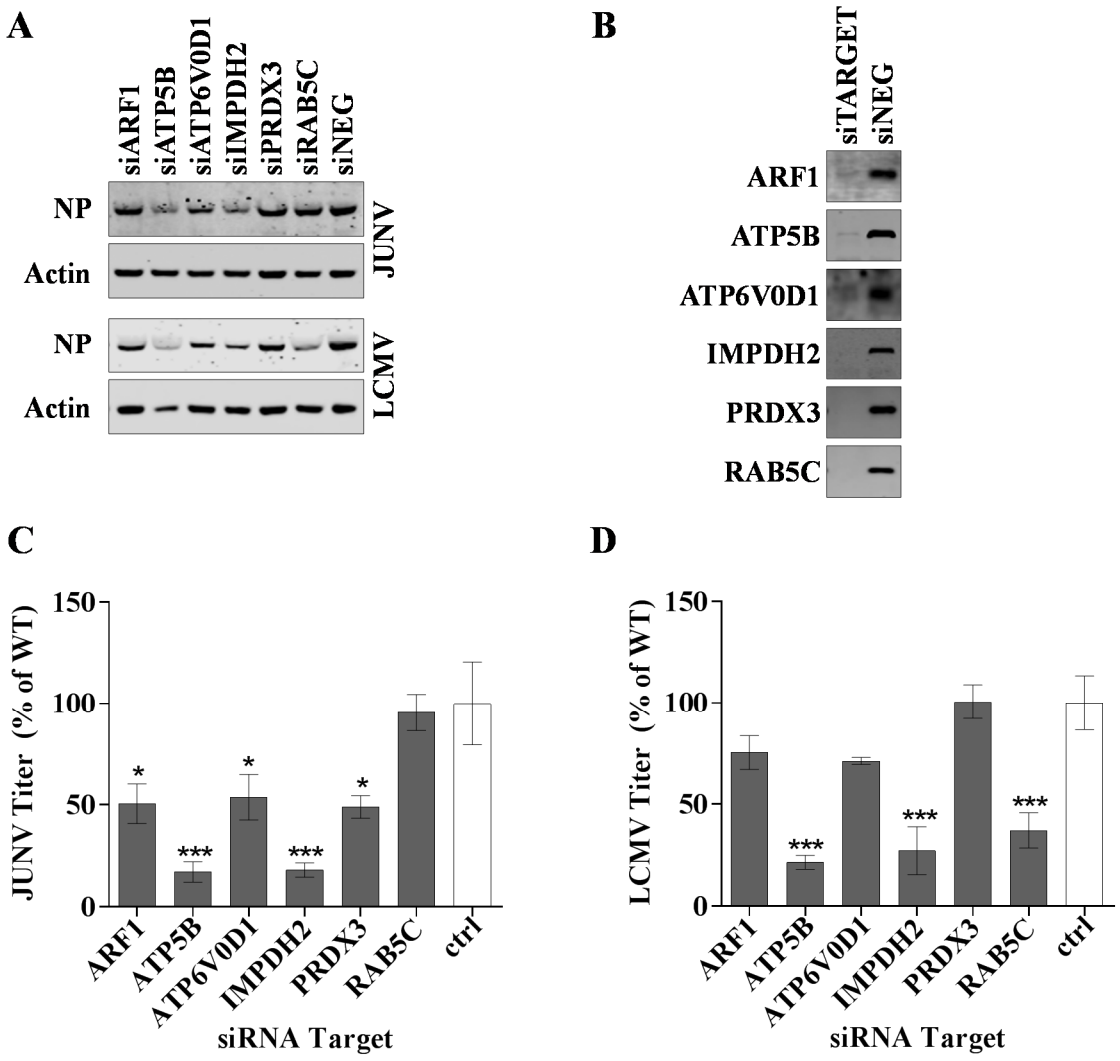

Figure 4.4. Functional siRNA screen of select JUNV-host protein partners. (A-D) A functional screen using silencing (si)RNAs was performed with JUNV C#1 virus as well as the prototypic Old World arenavirus, LCMV. Human lung carcinoma (A549) cells were reversed transfected with siRNAs then two days later infected with JUNV C#1 or LCMV Armstrong 53B (Arm) and two days later cells and the virus-containing media were collected. (A) Cell lysates were probed for JUNV C#1 or LCMV Arm nucleoprotein (NP) and cellular actin by western blotting using fluorescent detection. (B) Silencing of protein expression was confirmed by western blot using lysates from cells transfected with gene specific siRNA (siTARGET) or a non-targeting siRNA (siNEG). (C) JUNV C#1 or (D) LCMV Arm infectious titers were measured by standard plaque assay are shown as a percentage of the titer of the non-targeting control siRNA condition. Western blots are representative of 3 independent experiments and infectious titers represent the mean ±

SEM of 3 independent experiments. Mean values were compared with a one-way ANOVA with Holm-Sidak's test for multiple comparisons where *$p < 0.05$ and ***$p < 0.001$ for (C-D).

In order determine whether any of the proteins identified in the mass spectrometry study were functionally required for infectious Junín virus production, silencing (si)RNAs were used to knockdown expression of the selected host proteins. Silencing of the selected genes did not significantly decrease cellular actin levels indicating that cellular growth and overall health were not impacted (Figure 4.4A). Silencing of each gene was confirmed by western blotting (Figure 4.4B). Protein expression levels of IMPDH2, PRDX3 and Rab5c were below the limit of detection with gene-specific siRNA (siTARGET) (Fig 4B). Expression of ARF1, ATP5B and ATP6V0D1 were substantially reduced with gene-specific siRNA, but low levels of each were detected (Figure 4.4B).

Protein selection downstream of the mass spectrometry study was partly informed by a literature search for host proteins required for the propagation of other viruses. However, mapping of the Z proteome first was an effective means of prioritizing targets for functional screening. Using this approach, 5 of the 6 selected Z protein partners had a statistically significant impact on JUNV production. Infectious titers of JUNV were decreased by greater than 80% with loss of ATP5B and IMPDH2 expression ($P < 0.001$; Figure 4.4C). Viral nucleoprotein (NP) expression was also substantially decreased in infected cells transfected with ATP5B or IMPDH2 siRNAs which indicates that spread of JUNV throughout the culture was impacted, expression of the NP in infected cells was reduced or a combination of the two (Figure 4.4A). JUNV C#1 infectious titers were also

reduced ~50% with loss of ARF1, ATP6V0D1 and PRDX3 expression ($p < 0.05$; Figure 4.4C). Loss of Rab5c, however, had no impact on Junín virus production (Figure 4.4C).

This study was also extended to include the Old World arenavirus, LCMV, to allow identification of host factors utilized across the arenavirus family which could serve as potential broad spectrum antiviral targets. Levels of infectious LCMV were reduced to similar levels as observed for JUNV with loss of ATP5B and IMPDH2 (21% and 27%, respectively) ($p < 0.001$; Figure 4.4D). Infectious titers of LCMV in cells transfected with ARF1 or ATP6V0D1 siRNAs were not reduced to statistically significant levels (p value 0.13 and 0.11, respectively). Interestingly, there was specificity among the selected host proteins. Knockdown of PRDX3, which reduced JUNV titers ~50 %, had no impact on LCMV (Figures 4.4C and D) and Rab5c silencing did not impact Junín virus production, but LCMV titers were reduced 63 % ($p < 0.001$; Figure 4.4D). As several Rab family proteins were identified in JUNV Z VLPs and/or JUNV C#1 virions it will be important to understand the broader role this protein family plays in the arenavirus life cycle.

Testing for ESCRT complex dependency.

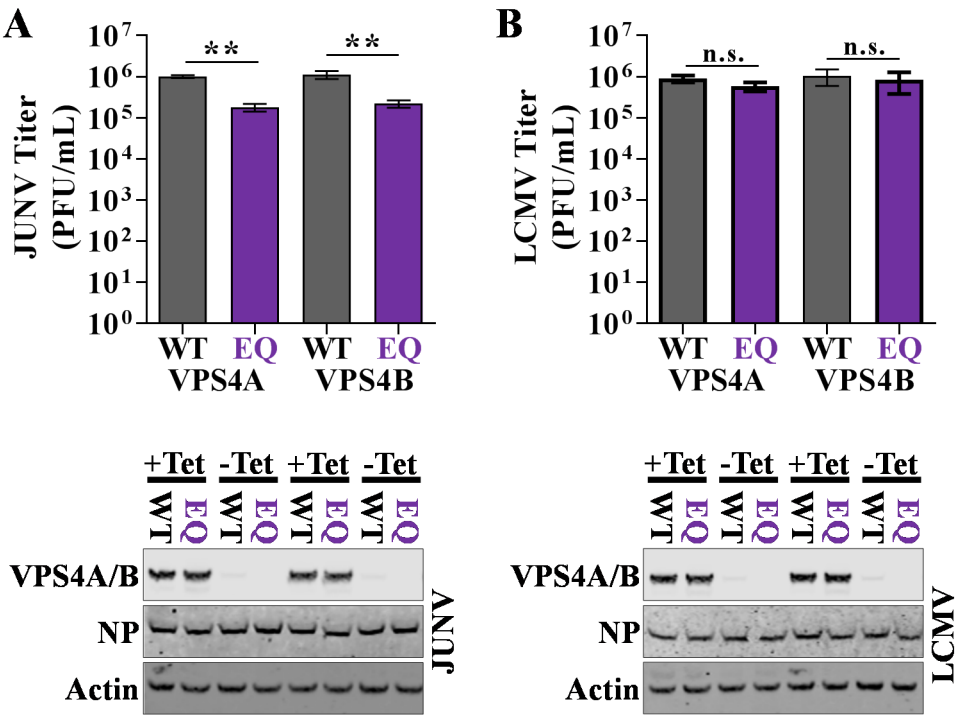

Figure 4.5. Efficient release of infectious JUNV virus particles requires the ESCRT pathway. (A-B) HEK293 T-Rex cells stably expressing tetracycline-induced, GFP-tagged WT or DN mutant (EQ) vacuolar protein sorting 4A or 4B (VPS4A or VPS4B) were infected with (A) JUNV C#1 at an multiplicity of infection (MOI) of 0.1 PFU/cell or (B) rLCMV WT at an MOI of 0.001 PFU/cell. 48 hr post-infection (pi) the cells were treated with tetracycline to induce expression of VPS4A/B WT or DN. 5 hr after induction (53 hr pi) the cells were washed and fresh tetracycline-containing media was added. The supernatants and cells were collected 68 hr pi and virus titers were determined via plaque assay and an anti-GFP antibody was used to measure GFP-tagged VPS4A/B expression, anti- (A) JUNV NP or (B) LCMV NP antibodies were used to measure global viral protein expression and actin was probed for as a loading control. Western blots are representative of 3 independent experiments and infectious titers represent the mean ± SEM of 3 independent experiments. Mean values were compared with a one-way ANOVA with Holm-Sidak's test for multiple comparisons. (A-B), n.s. (not significant), **$p < 0.01$.

In total, 14 ESCRT complex or ESCRT-associated proteins were identified in at least one experimental condition in Z VLPs or JUNV C#1 virions (Figure 4.2, Table 4.1 and Table 4.S1). The overall contribution of the ESCRT for New World arenavirus

production has not been previously assessed in the context of infection. In order to test the dependency of JUNV infectious virus production on the ESCRT pathway, cell lines stably transduced with WT or dominant negative (EQ) versions of the ESCRT accessory protein VPS4A or VPS4B were infected with JUNV or as a control, LCMV. In order to avoid measuring an impact of ESCRT inhibition on viral entry, expression of VPS4 was induced at a point when all of the cells in the culture were productively infected. This resulted in an 82 % decrease in JUNV infectious virus production in the VPS4A EQ cells (p value 0.009) and an 80 % decrease in VPS4B EQ cells (p value 0.006) (Figure 4.5A). Release of infectious LCMV virions was not affected by VPS4A EQ or VPS4B EQ expression (p value 0.98 and 0.98, respectively) in alignment with previous results (Figure 4.5B) (Ziegler et al., 2016b).

Discussion

This study has for the first time comprehensively mapped the host protein network engaged by the JUNV matrix protein Z as well as the host proteins that Z or other JUNV proteins recruit into virus particles. As relatively few virus-host protein interactions have been identified for the JUNV Z protein or other arenavirus Z proteins, identification of these interactions is a critical first step in understanding the molecular networks employed by Z to carry out its various functions. While the initial proteomics screen focused on JUNV, these findings were also extended to the Old World arenavirus Z proteins of LCMV and LASV for select proteins. The Z-host protein-protein interactions were largely conserved across the disparate arenavirus Z proteins and this conservation in protein complexes was reflected in the overall impact on virus production assessed by siRNA screening for ATP5B and IMPDH2 (Figures 4.4C and D). The finding that IMPDH2, which catalyzes the rate limiting step in guanine nucleotide biosynthesis, was required for efficient JUNV and LCMV production fits with previous studies that demonstrated that depletion of the intracellular GTP pool by mycophenolic acid (MPA) or 5-ethynyl-1-β-D-ribofuranosylimidazole-4-carboxamide (EICAR) treatment inhibits arenavirus production (Linero et al., 2012). Conversely, knockdown of PRDX3 and Rab5c had differential effects on JUNV versus LCMV production (Figures 4.4C and D) despite similar binding affinities (Figure 4.3A) which highlights the fact that these viruses utilize host machinery in both conserved and distinct ways. While the mechanism by which the PRDX3 contributes to the production of JUNV, some of the other proteins selected in this study have more obvious potential contributions to the arenavirus lifecycle.

ATP6V0D1 is a component of the vacuolar ATPase complex that is responsible for the acidification of endosomes and is an important factor in the life cycle of several RNA viruses (Table 4.2) (Forgac, 2007; Hao et al., 2008; Karlas et al., 2010; Konig et al., 2010; Krishnan et al., 2008; Le Sommer et al., 2012; Panda et al., 2011; Sessions et al., 2009). ATP6V0D1 knockdown resulted in a 46 % reduction in JUNV titer (p value 0.017) (Figure 4.4C) but only a 29 % reduction in LCMV titer (p value 0.11) (Figure 4.4D). While the reduction in LCMV titer was not statistically significant, ATP6V0D1 has been implicated in LCMV production previously (Panda et al., 2011). These data are also supported by other studies which showed that arenavirus entry is sensitive to bafilomycin treatment, which targets the vacuolar ATPase complex (Castilla et al., 2001; Cosset et al., 2009; Forgac, 2007). While it is clear that inhibiting the vacuolar ATPase complex impacts viral entry for disparate viruses, whether there is a functional role for interaction of intracellular Z with ATP6V0D1 remains unclear. Additionally, ATP6V0D1 was not detected in Z VLPs or virions which suggests that the interaction with Z could be important for a step in the life cycle prior to assembly and budding.

Several vesicular trafficking proteins including members of the Ras superfamily were enriched in Z VLPs and/or JUNV virions (Table 4.1). Representative proteins from this superfamily, ARF1 and Rab5c, were selected for functional siRNA screening (Fig 4C and D). While there was a significant reduction in JUNV titer with ARF1 depletion, LCMV titers were not reduced to the same extent (Fig 4C and D). ARF1, however, was identified as a required host factor for LCMV in a larger scale siRNA screen and thus ARF1 may be

broadly important for arenavirus infection (Panda et al., 2011). The mechanism for ARF1's impact on arenavirus production is unknown but several possibilities exist. As a regulator of intracellular traffic, ARF1 is required for human immunodeficiency virus 1 (HIV-1) Gag trafficking to the plasma membrane and ARF1 disruption results in decreased HIV-1 assembly and release (Joshi et al.). Thus, ARF1 could be important for trafficking of Z and/or other viral proteins to sites of virus assembly. ARF1 is also an important factor in the secretory pathway and regulates cargo release from the ER-Golgi intermediate compartment (ERGIC) (Donaldson and Jackson, 2011). Our lab has recently shown that a key component of the ERGIC, ERGIC-53 (LMAN1), is a component of JUNV virions and is a critical regulator of the infectivity of those virions (Klaus et al.). This raises the possibility that trafficking of ERGIC-53 into virions may be disrupted by ARF1 depletion. Additionally, trafficking of the mature viral glycoprotein into nascent virions could also be disrupted by ARF1 depletion as arenavirus glycoproteins undergo processing in the endoplasmic reticulum and Golgi apparatus (Lenz et al., 2001; Wright et al., 1990). Future work needs to investigate the mechanism by which ARF1 and the other ARF family proteins identified in this study contribute to arenavirus infection.

A preponderance of Rab family proteins were identified in Z VLPs and JUNV virions. Rab family GTPases are key mediators of intracellular vesicular trafficking and are exploited by a wide variety of viruses (Alenquer and Amorim, 2015; Bruce et al., 2012; Stenmark, 2009). In the case of arenaviruses, Rab5 has been implicated in JUNV and LASV entry, while Rab7 is required for efficient JUNV but not LASV entry (JM et al.,

2008; Martinez et al., 2009). The presence of Rab proteins in virions, however, suggests some of these Rab proteins may have a role in late steps of the virus life cycle (i.e. assembly and budding). Accordingly, Rab11 has been implicated in the assembly and budding of several viruses including influenza A virus (Bruce et al., 2010; Bruce et al., 2012). While the work here revealed that LCMV, but not JUNV infection, depended on Rab5c, the over-representation of this family of proteins suggests a functional role and that disparate arenaviruses may engage this host machinery in distinct ways. Finally, as the Z protein is a key mediator of virus assembly (Fehling et al., 2012), the interactions of Z with key Rab proteins may be critical for delivery of cargo into virions.

The Z matrix protein is required for budding and release of virus particles at the plasma membrane, a process thought to be driven largely by recruitment of ESCRT complexes (Perez et al., 2003; Strecker et al., 2003; Urata et al., 2006). In this study, we identified representative proteins in Z VLPs and JUNV C#1 virions of ESCRT-I (MVB12A/B, TSG101, VPS28 and VPS37B/C), ESCRT-II (VPS25), ESCRT-III (CHMP1A, CHMP2A/B, CHMP4, and CHMP5) and ESCRT accessory proteins (VPS4B and PDCD6IP (ALIX)) but not ESCRT-0 (Figure 4.2, Table 4.1 and Table 4.S1) (Schmidt and Teis). This fits the model whereby the PTAP-containing JUNV Z protein recruits ESCRT-I by direct binding to TSG101 which then recruits ESCRT-II, ESCRT–III, and finally VPS4A/B to drive virus release (Votteler and Sundquist, 2013). Accordingly, ESCRT proteins, including the ESCRT-I proteins TSG101 and VPS28, have been identified in virions of other viruses containing the P(T/S)AP late domain including Ebola

virus and HIV-1 presumably because these proteins are present at the final stages of virus release (Cantin et al., 2005; Spurgers et al., 2010). Finally, the ATPase VPS4, which is required for ESCRT complex disassembly, was found in JUNV virions previously in addition to in this study (Lu et al., 2014; Votteler and Sundquist, 2013).

The ESCRT complex is presumed to function in arenavirus release, yet evidence for this model is limited primarily to VLP assays. Knockdown of the ESCRT-I protein TSG101 results in decreased VLP production for LCMV and LASV (Perez et al., 2003; Strecker et al., 2003). Perturbation of the ESCRT accessory protein VPS4 reduces VLP production for Tacaribe and LASV but not Lujo virus (Urata et al., 2006; Urata et al., 2016; Urata et al., 2009). Finally, our lab has recently shown that LCMV utilizes the ESCRT complex specifically for defective interfering particle production but not release of infectious virus (Ziegler et al., 2016b). This indicates that VLP assays, while useful, may not always faithfully recapitulate all the facets of infection. Accordingly, we assessed the dependency of JUNV C#1 release on the ESCRT complex using VPS4-expressing cell lines. Importantly, expression of either WT or dominant-negative (EQ) VPS4A/B was induced once all of the cells were productively infected in order to eliminate the potential impact ESCRT inhibition could have on virus entry, as Old World arenaviruses utilize the ESCRT complex during viral entry (Pasqual et al., 2011). Efficient release of JUNV C#1 infectious virions did require a functional ESCRT pathway (Figure 4.5A) while release of infectious LCMV virions did not in concordance with our previous results (Figure 4.5B) (Ziegler et al., 2016b). The requirement of ESCRT for JUNV C#1 is also supported by

recent work which demonstrated that an inhibitor of the P(T/S)AP-TSG101 interaction reduced infectious JUNV production (Lu et al., 2014). Interestingly, the data presented here showed that depletion of ATP5B, which can function as an ATPase and can be plasma membrane localized, resulted in significantly reduced JUNV and LCMV titers (Figure 4.4C and D) (Gorai et al., 2012; Jonckheere et al., 2012). As the ATPase activity of ATP5B was recently shown to be an important factor in influenza A virus release and HIV-1 cell-to-cell transfer, our findings here raise the possibility that the energetics of arenavirus release could also involve ATP5B (Gorai et al., 2012; Yavlovich et al., 2012). The precise role and overall impact of each ESCRT protein identified in this study on arenavirus release as well as the mechanism by which ATP5B contributes to virus production remains to be determined and is the subject of future study.

In conclusion, we have provided a detailed map of the JUNV Z protein-host interactome for the first time, identified several critical host factors for JUNV infection. While the mechanism by which these host proteins function in the virus life cycle is not yet clear, this work represents a crucial step in understanding the protein networks employed by arenaviruses to drive the virus life cycle. Future studies will begin to address the mechanisms by which these host proteins contribute to Z protein functions. This study also highlights the important role the ESCRT pathway has in driving the efficient production of infectious JUNV virions. Finally, the insights provided by this work will also aid in the development of host-targeted anti-viral strategies to combat arenavirus infection.

Acknowledgments

We thank the UVM Immunobiology group for insightful discussions and are grateful to Drs. Michael Buchmeier, Margaret Kielian, Bob Tesh, Juan Carlos de la Torre, and Lindsay Whitton for providing critical reagents described in the Material and Methods.

Funding Information

The authors gratefully acknowledge NIH grants T32 AI055402 (CMZ), T32 HL076122 (BRK), R21 AI088059 (JB), AI065359 (JB) and P20RR021905 (Immunobiology and Infectious Disease COBRE) (JB). The mass spectrometry analysis was supported by the Vermont Genetics Network through NIH grant 8P20GM103449 from the INBRE program and of the NIGMS. The funders had no role in study design, data collection and analysis, decision to publish, or preparation of the manuscript.

References

Alenquer, M., and Amorim, M.J. (2015). Exosome Biogenesis, Regulation, and Function in Viral Infection. Viruses *7*, 5066-5083.

Auperin, D.D., Sasso, D.R., and McCormick, J.B. (1986). Nucleotide sequence of the glycoprotein gene and intergenic region of the Lassa virus S genome RNA. Virology *154*, 155-167.

Borrow, P., and Oldstone, M.B.A. (1994). Mechanism of Lymphocytic Choriomeningitis Virus Entry into Cells. Virology *198*, 1-9.

Bruce, E.A., Digard, P., and Stuart, A.D. (2010). The Rab11 Pathway Is Required for Influenza A Virus Budding and Filament Formation. J Virol *84*, 5848-5859.

Bruce, Emily A., Stuart, A., McCaffrey, Mary W., and Digard, P. (2012). Role of the Rab11 pathway in negative-strand virus assembly. Biochemical Society transactions *40*, 1409-1415.

Campbell Dwyer, E.J., Lai, H., MacDonald, R.C., Salvato, M.S., and Borden, K.L.B. (2000). The Lymphocytic Choriomeningitis Virus RING Protein Z Associates with Eukaryotic Initiation Factor 4E and Selectively Represses Translation in a RING-Dependent Manner. J Virol *74*, 3293-3300.

Cantin, R., Méthot, S., and Tremblay, M.J. (2005). Plunder and Stowaways: Incorporation of Cellular Proteins by Enveloped Viruses. J Virol *79*, 6577-6587.

Cao, W., Henry, M.D., Borrow, P., Yamada, H., Elder, J.H., Ravkov, E.V., Nichol, S.T., Compans, R.W., Campbell, K.P., and Oldstone, M.B.A. (1998). Identification of α-Dystroglycan as a Receptor for Lymphocytic Choriomeningitis Virus and Lassa Fever Virus. Science *282*, 2079-2081.

Capul, A.A., Perez, M., Burke, E., Kunz, S., Buchmeier, M.J., and de la Torre, J.C. (2007). Arenavirus Z-glycoprotein association requires Z myristoylation but not functional RING or late domains. J Virol *81*, 9451-9460.

Castilla, V., Palermo, M.L., and Coto, E.C. (2001). Involvement of vacuolar proton ATPase in Junin virus multiplication. Archives of Virology *146*, 251-263.

Charrel, R.N., de Lamballerie, X., and Emonet, S. (2008). Phylogeny of the genus Arenavirus. Current Opinion in Microbiology *11*, 362-368.

Charrel, R.N., and Lamballerie, X.d. (2003). Arenaviruses other than Lassa virus. Antiviral Research *57*, 89-100.

Childs, J.E., Glass, G.E., Korch, G.W., Ksiazek, T.G., and Leduc, J.W. (1992). Lymphocytic Choriomeningitis Virus Infection and House Mouse (Mus Musculus) Distribution in Urban Baltimore. The American Journal of Tropical Medicine and Hygiene *47*, 27-34.

Chosewood, L.C., Wilson, D.E., Centers for Disease Control and Prevention (U.S.), and National Institutes of Health (U.S.) (2009). Biosafety in microbiological and biomedical laboratories, 5th edn (Washington, D.C.: U.S. Dept. of Health and Human Services, Public Health Service, Centers for Disease Control and Prevention, National Institutes of Health).

Clegg, J.C.S., Wilson, S.M., and Oram, J.D. (1991). Nucleotide sequence of the S RNA of Lassa virus (Nigerian strain) and comparative analysis of arenavirus gene products. Virus Research *18*, 151-164.

Cornillez-Ty, C.T., Liao, L., Yates, J.R., Kuhn, P., and Buchmeier, M.J. (2009). Severe Acute Respiratory Syndrome Coronavirus Nonstructural Protein 2 Interacts with a Host Protein Complex Involved in Mitochondrial Biogenesis and Intracellular Signaling. J Virol *83*, 10314-10318.

Cornu, T.I., and de la Torre, J.C. (2001). RING finger Z protein of lymphocytic choriomeningitis virus (LCMV) inhibits transcription and RNA replication of an LCMV S-segment minigenome. J Virol *75*, 9415-9426.

Cosset, F.-L., Marianneau, P., Verney, G., Gallais, F., Tordo, N., Pécheur, E.-I., ter Meulen, J., Deubel, V., and Bartosch, B. (2009). Characterization of Lassa Virus Cell Entry and Neutralization with Lassa Virus Pseudoparticles. J Virol *83*, 3228-3237.

Dalal, S., Rosser, M.F.N., Cyr, D.M., and Hanson, P.I. (2004). Distinct Roles for the AAA ATPases NSF and p97 in the Secretory Pathway. Mol Biol Cell *15*, 637-648.

Degasperi, A., Birtwistle, M.R., Volinsky, N., Rauch, J., Kolch, W., and Kholodenko, B.N. (2014). Evaluating Strategies to Normalise Biological Replicates of Western Blot Data. PLoS ONE *9*, e87293.

Djavani, M., Lukashevich, I.S., Sanchez, A., Nichol, S.T., and Salvato, M.S. (1997). Completion of the Lassa Fever Virus Sequence and Identification of a RING Finger Open Reading Frame at the L RNA 5′ End. Virology *235*, 414-418.

Donaldson, J.G., and Jackson, C.L. (2011). ARF family G proteins and their regulators: roles in membrane transport, development and disease. Nat Rev Mol Cell Biol *12*, 362-375.

Eichler, R., Strecker, T., Kolesnikova, L., ter Meulen, J., Weissenhorn, W., Becker, S., Klenk, H.D., Garten, W., and Lenz, O. (2004). Characterization of the Lassa virus matrix

protein Z: electron microscopic study of virus-like particles and interaction with the nucleoprotein (NP). Virus Research *100*, 249-255.

Enria, D.A., Briggiler, A.M., and Sánchez, Z. (2008b). Treatment of Argentine hemorrhagic fever. Antiviral Research *78*, 132-139.

Fan, L., Briese, T., and Lipkin, W.I. (2010). Z Proteins of New World Arenaviruses Bind RIG-I and Interfere with Type I Interferon Induction. J Virol *84*, 1785-1791.

Fehling, S., Lennartz, F., and Strecker, T. (2012). Multifunctional Nature of the Arenavirus RING Finger Protein Z. Viruses *4*, 2973-3011.

Flatz, L., Bergthaler, A., de la Torre, J.C., and Pinschewer, D.D. (2006). Recovery of an arenavirus entirely from RNA polymerase I/II-driven cDNA. Proc Natl Acad Sci USA *103*, 4663-4668.

Forgac, M. (2007). Vacuolar ATPases: rotary proton pumps in physiology and pathophysiology. Nat Rev Mol Cell Biol *8*, 917-929.

Goñi, S.E., Iserte, J.A., Ambrosio, A.M., Romanowski, V., Ghiringhelli, P.D., and Lozano, M.E. (2006). Genomic Features of Attenuated Junín Virus Vaccine Strain Candidate. Virus Genes *32*, 37-41.

Gorai, T., Goto, H., Noda, T., Watanabe, T., Kozuka-Hata, H., Oyama, M., Takano, R., Neumann, G., Watanabe, S., and Kawaoka, Y. (2012). F1Fo-ATPase, F-type proton-translocating ATPase, at the plasma membrane is critical for efficient influenza virus budding. Proceedings of the National Academy of Sciences.

Hao, L., Sakurai, A., Watanabe, T., Sorensen, E., Nidom, C.A., Newton, M.A., Ahlquist, P., and Kawaoka, Y. (2008). Drosophila RNAi screen identifies host genes important for influenza virus replication. Nature *454*, 890-893.

Huang, D.W., Sherman, B.T., and Lempicki, R.A. (2008). Systematic and integrative analysis of large gene lists using DAVID bioinformatics resources. Nat Protocols *4*, 44-57.

Huang, D.W., Sherman, B.T., and Lempicki, R.A. (2009). Bioinformatics enrichment tools: paths toward the comprehensive functional analysis of large gene lists. Nucleic Acids Research *37*, 1-13.

Jacamo, R., Lopez, N., Wilda, M., and Franze-Fernández, M.T. (2003b). Tacaribe virus Z protein interacts with the L polymerase protein to inhibit viral RNA synthesis. J Virol *77*.

JM, R., AB, S., NT, N., JC, d.l.T., and S, K. (2008). Different mechanisms of cell entry by human-pathogenic Old World and New World arenaviruses. J Virol *82*, 7677-7687.

Jonckheere, A.I., Smeitink, J.A.M., and Rodenburg, R.J.T. (2012). Mitochondrial ATP synthase: architecture, function and pathology. Journal of Inherited Metabolic Disease *35*, 211-225.

Joshi, A., Garg, H., Nagashima, K., Bonifacino, J.S., and Freed, E.O. GGA and Arf Proteins Modulate Retrovirus Assembly and Release. Molecular cell *30*, 227-238.

Karlas, A., Machuy, N., Shin, Y., Pleissner, K.-P., Artarini, A., Heuer, D., Becker, D., Khalil, H., Ogilvie, L.A., Hess, S.*, et al.* (2010). Genome-wide RNAi screen identifies human host factors crucial for influenza virus replication. Nature *463*, 818-822.

Keenlyside, R.A., McCormick, J.B., Webb, P.A., Smith, E., Elliott, L., and Johnson, K.M. (1983). Case-Control Study of Mastomys Natalensis and Humans in Lassa Virus-Infected Households in Sierra Leone. The American Journal of Tropical Medicine and Hygiene *32*, 829-837.

Kentsis, A., Dwyer, E.C., Perez, J.M., Sharma, M., Chen, A., Pan, Z.Q., and Borden, K.L.B. (2001). The RING domains of the promyelocytic leukemia protein PML and the arenaviral protein Z repress translation by directly inhibiting translation initiation factor eIF4E. Journal of Molecular Biology *312*, 609-623.

Klaus, Joseph P., Eisenhauer, P., Russo, J., Mason, A.B., Do, D., King, B., Taatjes, D., Cornillez-Ty, C., Boyson, Jonathan E., Thali, M.*, et al.* The Intracellular Cargo Receptor ERGIC-53 Is Required for the Production of Infectious Arenavirus, Coronavirus, and Filovirus Particles. Cell Host & Microbe *14*, 522-534.

Klewitz, C., Klenk, H.-D., and ter Meulen, J. (2007). Amino acids from both N-terminal hydrophobic regions of the Lassa virus envelope glycoprotein GP-2 are critical for pH-dependent membrane fusion and infectivity. J Gen Virol *88*, 2320-2328.

Konig, R., Stertz, S., Zhou, Y., Inoue, A., Hoffmann, H.H., Bhattacharyya, S., Alamares, J.G., Tscherne, D.M., Ortigoza, M.B., Liang, Y.*, et al.* (2010). Human host factors required for influenza virus replication. Nature *463*, 813-817.

Kranzusch, P.J., and Whelan, S.P.J. (2011). Arenavirus Z protein controls viral RNA synthesis by locking a polymerase–promoter complex. Proceedings of the National Academy of Sciences *108*, 19743-19748.

Krishnan, M.N., Ng, A., Sukumaran, B., Gilfoy, F.D., Uchil, P.D., Sultana, H., Brass, A.L., Adametz, R., Tsui, M., Qian, F.*, et al.* (2008). RNA interference screen for human genes associated with West Nile virus infection. Nature *455*, 242-245.

Kunz, S. (2009). Receptor binding and cell entry of Old World arenaviruses reveal novel aspects of virus–host interaction. Virology *387*, 245-249.

Le Sommer, C., Barrows, N.J., Bradrick, S.S., Pearson, J.L., and Garcia-Blanco, M.A. (2012). G Protein-Coupled Receptor Kinase 2 Promotes <italic>Flaviviridae</italic> Entry and Replication. PLoS Negl Trop Dis *6*, e1820.

Lee, K.J., and de la Torre, J.C. (2002). Reverse genetics of arenaviruses. Curr Top Microbiol Immunol *262*, 175-193.

Lee, K.J., Novella, I.S., Teng, M.N., Oldstone, M.B.A., and de la Torre, J.C. (2000). NP and L Proteins of Lymphocytic Choriomeningitis Virus (LCMV) Are Sufficient for Efficient Transcription and Replication of LCMV Genomic RNA Analogs. J Virol *74*, 3470-3477.

Lenz, O., ter Meulen, J., Klenk, H.-D., Seidah, N.G., and Garten, W. (2001). The Lassa virus glycoprotein precursor GP-C is proteolytically processed by subtilase SKI-1/S1P. Proceedings of the National Academy of Sciences *98*, 12701-12705.

Lin, Y., Kimpler, L.A., Naismith, T.V., Lauer, J.M., and Hanson, P.I. (2005). Interaction of the Mammalian Endosomal Sorting Complex Required for Transport (ESCRT) III Protein hSnf7-1 with Itself, Membranes, and the AAA+ ATPase SKD1. J Biol Chem *280*, 12799-12809.

Linero, F.N., Sepúlveda, C.S., Giovannoni, F., Castilla, V., García, C.C., Scolaro, L.A., and Damonte, E.B. (2012). Host Cell Factors as Antiviral Targets in Arenavirus Infection. Viruses *4*, 1569.

Lopez, N., Jacamo, R., and Franze-Fernandez, M.T. (2001). Transcription and RNA Replication of Tacaribe Virus Genome and Antigenome Analogs Require N and L Proteins: Z Protein Is an Inhibitor of These Processes. J Virol *75*, 12241-12251.

Lu, J., Han, Z., Liu, Y., Liu, W., Lee, M.S., Olson, M.A., Ruthel, G., Freedman, B.D., and Harty, R.N. (2014). A Host-Oriented Inhibitor of Junin Argentine Hemorrhagic Fever Virus Egress. J Virol *88*, 4736-4743.

Lukashevich, I.S., Djavani, M., Shapiro, K., Sanchez, A., Ravkov, E., Nichol, S.T., and Salvato, M.S. (1997). The Lassa fever virus L gene: nucleotide sequence, comparison, and precipitation of a predicted 250 kDa protein with monospecific antiserum. J Gen Virol *78*, 547-551.

Maiztegui, J.I. (1975). Clinical and epidemiological patterns of Argentine haemorrhagic fever. Bulletin of the World Health Organization *52*, 567-575.

Martinez, M.G., Cordo, S.M., and Candurra, N.A. (2007). Characterization of Junín arenavirus cell entry. J Gen Virol *88*, 1776-1784.

Martinez, M.G., Forlenza, M.B., and Candurra, N.A. (2009). Involvement of cellular proteins in Junin arenavirus entry. Biotechnology journal *4*, 866-870.

McCormick, J.B., Webb, P.A., Krebs, J.W., Johnson, K.M., and Smith, E.S. (1987). A Prospective Study of the Epidemiology and Ecology of Lassa Fever. J Infect Dis *155*, 437-444.

Neuman, B.W., Adair, B.D., Burns, J.W., Milligan, R.A., Buchmeier, M.J., and Yeager, M. (2005). Complementarity in the Supramolecular Design of Arenaviruses and Retroviruses Revealed by Electron Cryomicroscopy and Image Analysis. J Virol *79*, 3822-3830.

Panda, D., Das, A., Dinh, P.X., Subramaniam, S., Nayak, D., Barrows, N.J., Pearson, J.L., Thompson, J., Kelly, D.L., Ladunga, I.*, et al.* (2011). RNAi screening reveals requirement for host cell secretory pathway in infection by diverse families of negative-strand RNA viruses. Proceedings of the National Academy of Sciences *108*, 19036-19041.

Pasqual, G., Rojek, J.M., Masin, M., Chatton, J.-Y., and Kunz, S. (2011). Old World Arenaviruses Enter the Host Cell via the Multivesicular Body and Depend on the Endosomal Sorting Complex Required for Transport. PLoS Pathog *7*, e1002232.

Perez, M., Craven, R.C., and de la Torre, J.C. (2003). The small RING finger protein Z drives arenavirus budding: Implications for antiviral strategies. Proc Natl Acad Sci USA *100*, 12978-12983.

Quirin, K., Eschli, B., Scheu, I., Poort, L., Kartenbeck, J., and Helenius, A. (2008). Lymphocytic choriomeningitis virus uses a novel endocytic pathway for infectious entry via late endosomes. Virology *378*, 21-33.

Riviere, Y., Ahmed, R., Southern, P.J., Buchmeier, M.J., Dutko, F.J., and Oldstone, M.B. (1985). The S RNA segment of lymphocytic choriomeningitis virus codes for the nucleoprotein and glycoproteins 1 and 2. J Virol *53*, 966-968.

Rowe, W.P., Murphy, F.A., Bergold, G.H., Casals, J., Hotchin, J., Johnson, K.M., Lehmann-Grube, F., Mims, C.A., Traub, E., and Webb, P.A. (1970). Arenoviruses: Proposed Name for a Newly Defined Virus Group. J Virol *5*, 651-652.

Salazar-Bravo, J., Ruedas, L.A., and Yates, T.L. (2002a). Mammalian reservoirs of arenaviruses. Curr Top Microbiol Immunol *262*, 25-63.

Salvato, M.S., Schweighofer, K.J., Burns, J., and Shimomaye, E.M. (1992a). BIOCHEMICAL AND IMMUNOLOGICAL EVIDENCE THAT THE 11-KDA ZINC-BINDING PROTEIN OF LYMPHOCYTIC CHORIOMENINGITIS VIRUS IS A STRUCTURAL COMPONENT OF THE VIRUS. Virus Research *22*, 185-198.

Salvato, M.S., and Shimomaye, E.M. (1989). The completed sequence of lymphocytic choriomeningitis virus reveals a unique RNA structure and a gene for a zinc finger protein. Virology *173*, 1-10.

Schlie, K., Maisa, A., Freiberg, F., Groseth, A., Strecker, T., and Garten, W. (2010). Viral Protein Determinants of Lassa Virus Entry and Release from Polarized Epithelial Cells. J Virol *84*, 3178-3188.

Schmidt, O., and Teis, D. The ESCRT machinery. Current Biology *22*, R116-R120.

Sessions, O.M., Barrows, N.J., Souza-Neto, J.A., Robinson, T.J., Hershey, C.L., Rodgers, M.A., Ramirez, J.L., Dimopoulos, G., Yang, P.L., Pearson, J.L.*, et al.* (2009). Discovery of insect and human dengue virus host factors. Nature *458*, 1047-1050.

Singh, M.K., Fuller-Pace, F.V., Buchmeier, M.J., and Southern, P.J. (1987). Analysis of the genomic l rna segment from lymphocytic choriomeningitis virus. Virology *161*, 448-456.

Spiropoulou, C.F., Kunz, S., Rollin, P.E., Campbell, K.P., and Oldstone, M.B.A. (2002). New World Arenavirus Clade C, but Not Clade A and B Viruses, Utilizes α-Dystroglycan as Its Major Receptor. J Virol *76*, 5140-5146.

Spurgers, K.B., Alefantis, T., Peyser, B.D., Ruthel, G.T., Bergeron, A.A., Costantino, J.A., Enterlein, S., Kota, K.P., Boltz, R.C.D., Aman, M.J.*, et al.* (2010). Identification of Essential Filovirion-associated Host Factors by Serial Proteomic Analysis and RNAi Screen. Molecular & Cellular Proteomics *9*, 2690-2703.

Stenmark, H. (2009). Rab GTPases as coordinators of vesicle traffic. Nat Rev Mol Cell Biol *10*, 513-525.

Strecker, T., Eichler, R., Meulen, J.t., Weissenhorn, W., Dieter Klenk, H., Garten, W., and Lenz, O. (2003). Lassa Virus Z Protein Is a Matrix Protein Sufficient for the Release of Virus-Like Particles. J Virol *77*, 10700-10705.

Taylor, G.M., Hanson, P.I., and Kielian, M. (2007). Ubiquitin Depletion and Dominant-Negative VPS4 Inhibit Rhabdovirus Budding without Affecting Alphavirus Budding. J Virol *81*, 13631-13639.

Urata, S., Noda, T., Kawaoka, Y., Yokosawa, H., and Yasuda, J. (2006). Cellular Factors Required for Lassa Virus Budding. J Virol *80*, 4191-4195.

Urata, S., Weyer, J., Storm, N., Miyazaki, Y., van Vuren, P.J., Paweska, J.T., and Yasuda, J. (2016). Analysis of Assembly and Budding of Lujo Virus. J Virol *90*, 3257-3261.

Urata, S., and Yasuda, J. (2012). Molecular Mechanism of Arenavirus Assembly and Budding. Viruses *4*, 2049-2079.

Urata, S., Yasuda, J., and de la Torre, J.C. (2009). The Z Protein of the New World Arenavirus Tacaribe Virus Has Bona Fide Budding Activity That Does Not Depend on Known Late Domain Motifs. J Virol *83*, 12651-12655.

Volpon, L., Osborne, M.J., Capul, A.A., de la Torre, J.C., and Borden, K.L.B. (2010). Structural characterization of the Z RING-eIF4E complex reveals a distinct mode of control for eIF4E. Proc Natl Acad Sci USA *107*, 5441-5446.

Votteler, J., and Sundquist, Wesley I. (2013). Virus Budding and the ESCRT Pathway. Cell Host & Microbe *14*, 232-241.

Wang, J., Danzy, S., Kumar, N., Ly, H., and Liang, Y. (2012). Biological Roles and Functional Mechanisms of Arenavirus Z Protein in Viral Replication. J Virol *86*, 9794-9801.

Wright, K.E., Spiro, R.C., Burns, J.W., and Buchmeier, M.J. (1990). Post-translational processing of the glycoproteins of lymphocytic choriomeningitis virus. Virology *177*, 175-183.

Xing, J., Ly, H., and Liang, Y. (2015). The Z Proteins of Pathogenic but Not Nonpathogenic Arenaviruses Inhibit RIG-i-Like Receptor-Dependent Interferon Production. J Virol *89*, 2944-2955.

Yavlovich, A., Viard, M., Zhou, M., Veenstra, T.D., Wang, J.M., Gong, W., Heldman, E., Blumenthal, R., and Raviv, Y. (2012). Ectopic ATP synthase facilitates transfer of HIV-1 from antigen-presenting cells to CD4+ target cells. Blood *120*, 1246-1253.

Ziegler, C.M., Eisenhauer, P., Bruce, E.A., Beganovic, V., King, B.R., Weir, M.E., Ballif, B.A., and Botten, J. (2016a). A novel phosphoserine motif in the LCMV matrix protein Z regulates the release of infectious virus and defective interfering particles. J Gen Virol.

Ziegler, C.M., Eisenhauer, P., Bruce, E.A., Weir, M.E., King, B.R., Klaus, J.P., Krementsov, D.N., Shirley, D.J., Ballif, B.A., and Botten, J. (2016b). The Lymphocytic Choriomeningitis Virus Matrix Protein PPXY Late Domain Drives the Production of Defective Interfering Particles. PLoS Pathog *12*, e1005501.

Supporting Information

Table 4.S1. JUNV Z & JUNV C#1 Host Protein Partners				VLPs		Cells		Virus	
Gene Symbol	Entrez ID	Gene Description	IPI ID	Run1	Run2	Run1	Run2	Run1	Run2
A2M	2	alpha-2-macroglobulin	IPI00478003	x					
AARS	16	alanyl-tRNA synthetase	IPI00027442	x	x			x	
AARS2	57505	alanyl-tRNA synthetase like	IPI00394788		x				
ABCD3	5825	ATP-binding cassette, sub-family D (ALD), member 3	IPI00002372				x		
ABCE1	6059	ATP-binding cassette, sub-family E (OABP), member 1	IPI00303207.3					x	x
ABCF1	23	ATP-binding cassette, sub-family F (GCN20), member 1	IPI00013495.1						x
ACACA	31	acetyl-Coenzyme A carboxylase alpha	IPI00011569	x					
ACAD9	28976	acyl-Coenzyme A dehydrogenase family, member 9	IPI00152981				x		
ACADM	34	acyl-Coenzyme A dehydrogenase, C-4 to C-12 straight chain	IPI00005040	x	x				
ACLY	47	ATP citrate lyase	IPI00021290	x	x		x	x	
ACTA2	59	actin, alpha 2, smooth muscle, aorta	IPI00008603	x	x			x	
ACTB	60	actin, beta	IPI00021439	x	x	x	x	x	
ACTBL2	345651	similar to RIKEN cDNA 4732495G21 gene	IPI00003269	x	x		x	x	x
ACTN1	87	actinin, alpha 1	IPI00013508.5					x	
ACTN4	81	actinin, alpha 4	IPI00013808.1					x	x
ACYP1	97	acylphosphatase 1, erythrocyte (common) type	IPI00221117.3					x	
ADAM10	102	ADAM metallopeptidase domain 10	IPI00013897.1					x	x
AFP	174	alpha-fetoprotein	IPI00022443	x	x				
AGK	55750	multiple substrate lipid kinase	IPI00019353				x		
AGPS	8540	alkylglycerone phosphate synthase	IPI00010349		x		x		
AGRN	375790	agrin	IPI00374563.3					x	x
AHCY	191	S-adenosylhomocysteine hydrolase	IPI00012007		x			x	x
AIFM1	9131	programmed cell death 8 (apoptosis-inducing factor)	IPI00000690.1			x	x		
AIMP2	7965	JTV1 gene	IPI00011916		x				
AIP	9049	aryl hydrocarbon receptor interacting protein	IPI00010460		x				
AK1	203	adenylate kinase 1	IPI00018342		x				
AK2	204	adenylate kinase 2	IPI00172460		x	x	x		
ALCAM	214	activated leukocyte cell adhesion molecule	IPI00015102.2					x	x
ALDH18A1	5832	aldehyde dehydrogenase 18 family, member A1	IPI00008982	x	x		x		
ALDH1B1	219	aldehyde dehydrogenase 1 family, member B1	IPI00103467	x	x	x	x		
ALDH2	217	aldehyde dehydrogenase 2 family (mitochondrial)	IPI00006663		x				
ALDOA	226	aldolase A, fructose-bisphosphate	IPI00465439.5					x	x
ALG1	56052	asparagine-linked glycosylation 1 homolog (yeast, beta-1,4-mannosyltransferase)	IPI00549761				x		
AMOT	154796	angiomotin	IPI00163085	x	x				

Table 4.S1. JUNV Z & JUNV C#1 Host Protein Partners				VLPs		Cells		Virus	
Gene Symbol	Entrez ID	Gene Description	IPI ID	Run1	Run2	Run1	Run2	Run1	Run2
ANXA2P2	304		IPI00334627		x				
ANXA5	308	annexin A5	IPI00329801		x			x	x
ANXA6	309	annexin A6	IPI00002459.4					x	x
AP1B1	162	adaptor-related protein complex 1, beta 1 subunit	IPI00328257		x			x	
APOB	338	apolipoprotein B (including Ag(x) antigen)	IPI00022229	x	x				
APOE	348	apolipoprotein E	IPI00021842	x					x
APRT	353	adenine phosphoribosyltransferase	IPI00218693		x			x	
ARF1	375	ADP-ribosylation factor 1	IPI00215914	x	x			x	x
ARF4	378	ADP-ribosylation factor 4	IPI00215918		x			x	
ARF6	382	ADP-ribosylation factor 6	IPI00215920.8					x	x
ARHGDIA	396	Rho GDP dissociation inhibitor (GDI) alpha	IPI00003815.3					x	x
ARPC3	10094	actin related protein 2/3 complex, subunit 3, 21kDa	IPI00005162.3					x	x
ASCC3	10973	activating signal cointegrator 1 complex subunit 3	IPI00430472		x			x	x
ATAD3A	55210	ATPase family, AAA domain containing 3A	IPI00295992		x	x	x		
ATAD3B	83858	ATPase family, AAA domain containing 3B	IPI00045921		x		x		
ATIC	471	5-aminoimidazole-4-carboxamide ribonucleotide formyltransferase/IMP cyclohydrolase	IPI00289499		x			x	
ATP1A1	476	ATPase, Na+/K+ transporting, alpha 1 polypeptide	IPI00006482.1			x	x	x	x
ATP1A2	477	ATPase, Na+/K+ transporting, alpha 2 (+) polypeptide	IPI00003021.1					x	x
ATP1B3	483	ATPase, Na+/K+ transporting, beta 3 polypeptide	IPI00008167.1					x	x
ATP2A1	487	ATPase, Ca++ transporting, cardiac muscle, fast twitch 1	IPI00024804				x		
ATP2A2	488	ATPase, Ca++ transporting, cardiac muscle, slow twitch 2	IPI00177817				x		
ATP5A1	498	ATP synthase, H+ transporting, mitochondrial F1 complex, alpha subunit 1, cardiac muscle	IPI00440493		x	x	x		
ATP5B	506	ATP synthase, H+ transporting, mitochondrial F1 complex, beta polypeptide	IPI00303476	x	x	x	x		
ATP5C1	509	ATP synthase, H+ transporting, mitochondrial F1 complex, gamma polypeptide 1	IPI00395769				x		
ATP5O	539	ATP synthase, H+ transporting, mitochondrial F1 complex, O subunit (oligomycin sensitivity conferring protein)	IPI00007611.1			x			
ATP6AP2	10159	ATPase, H+ transporting, lysosomal accessory protein 2	IPI00168884.3					x	x
ATP6V0A1	535		IPI00743576				x		
ATP6V0D1	9114	ATPase, H+ transporting, lysosomal 38kDa, V0 subunit d1	IPI00034159.1			x	x		
ATP6V1A	523	ATPase, H+ transporting, lysosomal 70kDa, V1 subunit A	IPI00007682				x		

Table 4.S1. JUNV Z & JUNV C#1 Host Protein Partners				VLPs		Cells		Virus	
Gene Symbol	Entrez ID	Gene Description	IPI ID	Run1	Run2	Run1	Run2	Run1	Run2
ATP6V1B2	526	ATPase, H+ transporting, lysosomal 56/58kDa, V1 subunit B2	IPI00007812.1			x	x		
ATP6V1C1	528	ATPase, H+ transporting, lysosomal 42kDa, V1 subunit C1	IPI00007814				x		
ATP6V1E1	529	ATPase, H+ transporting, lysosomal 31kDa, V1 subunit E1	IPI00003856				x		
ATR	545	ataxia telangiectasia and Rad3 related	IPI00412298				x		
ATXN10	25814	ataxin 10	IPI00001636		x		x		
AURKB	9212	aurora kinase B	IPI00176642	x	x		x		
BAG2	9532	BCL2-associated athanogene 2	IPI00000643	x	x	x			
BAG5	9529	BCL2-associated athanogene 5	IPI00007731.1					x	
BANF1	8815	barrier to autointegration factor 1	IPI00026087		x			x	
BAT3	7917	HLA-B associated transcript 3	IPI00465128		x		x		
BCL2L12	83596	BCL2-like 12 (proline rich)	IPI00019835		x				
BCOR	54880	BCL6 co-repressor	IPI00100291.1			x	x		
BIRC2	329	baculoviral IAP repeat-containing 2	IPI00013418				x		
BSG	682	basigin (Ok blood group)	IPI00019906.1					x	x
BTF3	689	basic transcription factor 3	IPI00221035.4					x	
BTF3L4	91408	basic transcription factor 3-like 4	IPI00412792.2					x	
BZW1	9689	basic leucine zipper and W2 domains 1	IPI00180128.4						x
C11orf59	55004	hypothetical protein FLJ20625	IPI00016670				x		
C14orf166	51637	chromosome 14 open reading frame 166	IPI00006980		x			x	
C1orf57	84284	chromosome 1 open reading frame 57	IPI00031570		x				
C1orf58	148362	chromosome 1 open reading frame 58	IPI00065500.3					x	x
C1QBP	708	complement component 1, q subcomponent binding protein	IPI00014230		x			x	
C22orf28	51493	hypothetical protein HSPC117	IPI00550689		x			x	
C3	718		IPI00783987	x	x				
C7orf20	51608	chromosome 7 open reading frame 20	IPI00419575		x				
C8orf62	137133	phosphoserine aminotransferase 1 pseudogene	IPI00001734.3						x
CA2	760	carbonic anhydrase II	IPI00218414.5					x	x
CACYBP	27101	calcyclin binding protein	IPI00395627		x			x	
CAD	790	carbamoyl-phosphate synthetase 2, aspartate transcarbamylase, and dihydroorotase	IPI00301263	x	x		x		
CALM1	801		IPI00075248				x	x	
CALM2	805	calmodulin 2 (phosphorylase kinase, delta)	IPI00075248				x	x	
CALM3	808		IPI00075248				x	x	
CAMK2D	817	calcium/calmodulin-dependent protein kinase (CaM kinase) II delta	IPI00172636		x				
CAND1	55832	cullin-associated and neddylation-dissociated 1	IPI00100160		x		x		
CAND2	23066		IPI00374208		x		x		
CANX	821	calnexin	IPI00020984				x		
CAPZA1	829	capping protein (actin filament) muscle Z-line, alpha 1	IPI00005969.3					x	x
CBR1	873	carbonyl reductase 1	IPI00295386.7						x
CBS	875	cystathionine-beta-synthase	IPI00219352.4			x			

Table 4.S1. JUNV Z & JUNV C#1 Host Protein Partners				VLPs		Cells		Virus	
Gene Symbol	Entrez ID	Gene Description	IPI ID	Run1	Run2	Run1	Run2	Run1	Run2
CCDC124	115098	coiled-coil domain containing 124	IPI00060627.2					x	x
CCDC72	51372	coiled-coil domain containing 72	IPI00006378.3					x	
CCT2	10576	chaperonin containing TCP1, subunit 2 (beta)	IPI00297779	x	x			x	x
CCT3	7203	chaperonin containing TCP1, subunit 3 (gamma)	IPI00290770	x	x		x	x	x
CCT4	10575	chaperonin containing TCP1, subunit 4 (delta)	IPI00302927	x	x	x	x	x	x
CCT5	22948	chaperonin containing TCP1, subunit 5 (epsilon)	IPI00010720	x	x	x	x	x	x
CCT6A	908	chaperonin containing TCP1, subunit 6A (zeta 1)	IPI00027626	x	x	x	x	x	x
CCT7	10574	chaperonin containing TCP1, subunit 7 (eta)	IPI00018465	x	x		x		x
CCT8	10694	chaperonin containing TCP1, subunit 8 (theta)	IPI00302925	x	x	x			x
CD2AP	23607	CD2-associated protein	IPI00412771.1					x	x
CD81	975	CD81 molecule	IPI00000190.1					x	
CD9	928	CD9 molecule	IPI00215997.5					x	x
CD99	4267	CD99 molecule	IPI00253036.5					x	x
CD99L2	83692	CD99 molecule-like 2	IPI00152488.1						x
CDC42SE2	56990	CDC42 small effector 2	IPI00024973.1					x	
CDK1	983	cell division cycle 2, G1 to S and G2 to M	IPI00026689	x	x		x		x
CDK4	1019	cyclin-dependent kinase 4	IPI00007811		x				
CECR5	27440	cat eye syndrome chromosome region, candidate 5	IPI00011511		x				
CEP55	55165	centrosomal protein 55kDa	IPI00101532		x			x	x
CFL1	1072	cofilin 1 (non-muscle)	IPI00012011		x			x	x
CHCHD3	54927	coiled-coil-helix-coiled-coil-helix domain containing 3	IPI00015833	x		x	x		
CHMP1A	5119	chromatin modifying protein 1A	IPI00382452.1					x	x
CHMP2A	27243	chromatin modifying protein 2A	IPI00004416.1					x	x
CHMP2B	25978	chromatin modifying protein 2B	IPI00550181.2					x	x
CHMP4B	128866	chromatin modifying protein 4B	IPI00025974		x		x	x	x
CHMP5	51510	chromatin modifying protein 5	IPI00100796.4					x	x
CKAP5	9793	cytoskeleton associated protein 5	IPI00028275		x		x		x
CKB	1152	creatine kinase, brain	IPI00022977	x	x			x	x
CKMT1A	548596		IPI00658109.1			x			
CKMT1B	1159	creatine kinase, mitochondrial 1B	IPI00658109.1			x			
CLIC1	1192	chloride intracellular channel 1	IPI00010896	x				x	x
CLPB	81570	ClpB caseinolytic peptidase B homolog (E. coli)	IPI00006615.3			x	x		
CLPX	10845	ClpX caseinolytic peptidase X homolog (E. coli)	IPI00008728		x				
CLTC	1213	clathrin, heavy polypeptide (Hc)	IPI00024067	x	x				
CLTCL1	8218	clathrin, heavy polypeptide-like 1	IPI00022881		x		x		
CNOT1	23019	CCR4-NOT transcription complex, subunit 1	IPI00166010		x		x	x	
CNP	1267	2',3'-cyclic nucleotide 3' phosphodiesterase	IPI00220993		x				x
COL18A1	80781	collagen, type XVIII, alpha 1	IPI00022822.5					x	x
COL6A1	1291	collagen, type VI, alpha 1	IPI00291136	x	x				
COPA	1314	coatomer protein complex, subunit alpha	IPI00295857		x				

Table 4.S1. JUNV Z & JUNV C#1 Host Protein Partners				VLPs		Cells		Virus	
Gene Symbol	Entrez ID	Gene Description	IPI ID	Run1	Run2	Run1	Run2	Run1	Run2
COPB1	1315	coatomer protein complex, subunit beta	IPI00295851		x				
CPNE1	8904	copine I	IPI00018452		x				
CPNE3	8895	copine III	IPI00024403	x	x				
CPNE8	144402	copine VIII	IPI00334276		x				
CPOX	1371	coproporphyrinogen oxidase	IPI00093057.6			x	x		
CSDA	8531	cold shock domain protein A	IPI00031801.4					x	x
CSDE1	7812	cold shock domain containing E1, RNA-binding	IPI00470891.2						x
CSE1L	1434	CSE1 chromosome segregation 1-like (yeast)	IPI00022744		x	x	x	x	
CSK	1445	c-src tyrosine kinase	IPI00013212		x				
CSNK2A1	1457	casein kinase 2, alpha 1 polypeptide	IPI00016613	x		x		x	
CSNK2A2	1459	casein kinase 2, alpha prime polypeptide	IPI00020602		x			x	
CSPG4	1464	chondroitin sulfate proteoglycan 4	IPI00019157.2					x	
CSTB	1476	cystatin B (stefin B)	IPI00021828.1					x	x
CTNNA1	1495	catenin (cadherin-associated protein), alpha 1, 102kDa	IPI00215948.4					x	x
CTNNB1	1499	catenin (cadherin-associated protein), beta 1, 88kDa	IPI00017292.1					x	
CTNND1	1500	catenin (cadherin-associated protein), delta 1	IPI00182469		x			x	
CXADR	1525	coxsackie virus and adenovirus receptor	IPI00019146.6					x	x
CYB5R3	1727	cytochrome b5 reductase 3	IPI00328415			x			
CYC1	1537	cytochrome c-1	IPI00029264				x		
DAP3	7818	death associated protein 3	IPI00018120		x				
DARS	1615	aspartyl-tRNA synthetase	IPI00216951		x				
DARS2	55157	aspartyl-tRNA synthetase 2 (mitochondrial)	IPI00100460		x				
DBT	1629	dihydrolipoamide branched chain transacylase	IPI00003944		x				
DCAF7	10238	WD repeat domain 68	IPI00006754		x				
DCTN1	1639	dynactin 1 (p150, glued homolog, Drosophila)	IPI00029485		x				
DCTN2	10540	dynactin 2 (p50)	IPI00220503		x				
DDX1	1653	DEAD (Asp-Glu-Ala-Asp) box polypeptide 1	IPI00293655.3						x
DDX20	11218	DEAD (Asp-Glu-Ala-Asp) box polypeptide 20	IPI00005904				x		
DDX3X	1654	DEAD (Asp-Glu-Ala-Asp) box polypeptide 3, X-linked	IPI00215637	x	x			x	x
DDX5	1655	DEAD (Asp-Glu-Ala-Asp) box polypeptide 5	IPI00017617		x			x	
DDX6	1656	DEAD (Asp-Glu-Ala-Asp) box polypeptide 6	IPI00030320.4					x	x
DECR1	1666	2,4-dienoyl CoA reductase 1, mitochondrial	IPI00003482.1			x	x		
DHX15	1665	DEAH (Asp-Glu-Ala-His) box polypeptide 15	IPI00396435		x				
DHX30	22907	DEAH (Asp-Glu-Ala-His) box polypeptide 30	IPI00411733		x				
DHX9	1660		IPI00844578	x	x			x	
DLAT	1737	dihydrolipoamide S-acetyltransferase (E2 component of pyruvate dehydrogenase complex)	IPI00021338		x				

Table 4.S1. JUNV Z & JUNV C#1 Host Protein Partners				VLPs		Cells		Virus	
Gene Symbol	Entrez ID	Gene Description	IPI ID	Run1	Run2	Run1	Run2	Run1	Run2
DNAJA1	3301	DnaJ (Hsp40) homolog, subfamily A, member 1	IPI00012535	x	x	x		x	x
DNAJA2	10294	DnaJ (Hsp40) homolog, subfamily A, member 2	IPI00032406		x	x	x	x	x
DNAJB1	3337	DnaJ (Hsp40) homolog, subfamily B, member 1	IPI00015947				x		
DNAJC7	7266	DnaJ (Hsp40) homolog, subfamily C, member 7	IPI00329629	x	x		x		
DNM2	1785	dynamin 2	IPI00033022		x			x	x
DOCK11	139818	dedicator of cytokinesis 11	IPI00411452.3					x	
DRG1	4733	developmentally regulated GTP binding protein 1	IPI00031836		x				
DSG2	1829	desmoglein 2	IPI00028931		x	x	x		
DSP	1832	desmoplakin	IPI00013933		x				
DTYMK	1841	deoxythymidylate kinase (thymidylate kinase)	IPI00013862		x				
DYNC1H1	1778	dynein, cytoplasmic 1, heavy chain 1	IPI00456969	x	x			x	x
DYNC1I2	1781	dynein, cytoplasmic 1, intermediate chain 2	IPI00216348	x	x				
DYNC1LI1	51143	dynein, cytoplasmic 1, light intermediate chain 1	IPI00007675		x				
ECHS1	1892	enoyl Coenzyme A hydratase, short chain, 1, mitochondrial	IPI00024993		x				
ECSIT	51295	signaling intermediate in Toll pathway, evolutionarily conserved	IPI00063188				x		
EDC3	80153	LSM16 homolog (EDC3, S. cerevisiae)	IPI00018009		x				
EDC4	23644	autoantigen	IPI00376317				x	x	
EDF1	8721	endothelial differentiation-related factor 1	IPI00006362.1					x	
EDIL3	10085	EGF-like repeats and discoidin I-like domains 3	IPI00306046.1						x
EEF1A1	1915	chemokine (C-C motif) receptor 5	IPI00025447	x	x	x			x
EEF1A2	1917	eukaryotic translation elongation factor 1 alpha 2	IPI00014424	x	x				
EEF1D	1936	eukaryotic translation elongation factor 1 delta (guanine nucleotide exchange protein)	IPI00023048		x				
EEF1G	1937	eukaryotic translation elongation factor 1 gamma	IPI00000875	x	x		x	x	x
EEF2	1938	eukaryotic translation elongation factor 2	IPI00186290	x	x			x	x
EFNB1	1947	ephrin-B1	IPI00024307.1			x	x	x	x
EFNB2	1948	ephrin-B2	IPI00005126.1					x	x
EFNB3	1949	ephrin-B3	IPI00019501.1					x	x
EFTUD2	9343	elongation factor Tu GTP binding domain containing 2	IPI00003519	x	x				
EHD1	10938	EH-domain containing 1	IPI00017184		x			x	x
EHD4	30844	EH-domain containing 4	IPI00005578		x			x	x
EIF1	10209	eukaryotic translation initiation factor 1	IPI00015077.1					x	x
EIF1AY	9086	eukaryotic translation initiation factor 1A, Y-linked	IPI00023004.7					x	x

Table 4.S1. JUNV Z & JUNV C#1 Host Protein Partners				VLPs		Cells		Virus	
Gene Symbol	Entrez ID	Gene Description	IPI ID	Run1	Run2	Run1	Run2	Run1	Run2
EIF2S1	1965	eukaryotic translation initiation factor 2, subunit 1 alpha, 35kDa	IPI00219678.3					x	x
EIF2S2	8894	eukaryotic translation initiation factor 2, subunit 2 beta, 38kDa	IPI00021728.3						x
EIF3A	8661	eukaryotic translation initiation factor 3, subunit 10 theta, 150/170kDa	IPI00029012		x			x	
EIF3B	8662	eukaryotic translation initiation factor 3, subunit B	IPI00396370.6					x	
EIF3E	3646	eukaryotic translation initiation factor 3, subunit E	IPI00013068.1						x
EIF3F	8665	eukaryotic translation initiation factor 3, subunit 5 epsilon, 47kDa	IPI00654777		x			x	
EIF3I	8668	eukaryotic translation initiation factor 3, subunit I	IPI00012795.3						x
EIF3L	51386	eukaryotic translation initiation factor 3, subunit L	IPI00465233.1					x	
EIF3M	10480	eukaryotic translation initiation factor 3, subunit M	IPI00102069.5					x	
EIF4A1	1973	eukaryotic translation initiation factor 4A, isoform 1	IPI00025491	x	x			x	x
EIF4A3	9775	DEAD (Asp-Glu-Ala-Asp) box polypeptide 48	IPI00009328		x			x	
EIF4B	1975	eukaryotic translation initiation factor 4B	IPI00012079.3					x	
EIF4G1	1981	eukaryotic translation initiation factor 4 gamma, 1	IPI00220365		x				
EIF5	1983	eukaryotic translation initiation factor 5	IPI00022648		x				
EIF5A2	56648	eukaryotic translation initiation factor 5A2	IPI00006935.3						x
EIF5B	9669	eukaryotic translation initiation factor 5B	IPI00299254		x				
EIF6	3692	integrin beta 4 binding protein	IPI00010105		x				
ELAVL1	1994	ELAV (embryonic lethal, abnormal vision, Drosophila)-like 1 (Hu antigen R)	IPI00301936		x				
EMD	2010	emerin (Emery-Dreifuss muscular dystrophy)	IPI00032003			x	x		
ENO1	2023	enolase 1, (alpha)	IPI00465248	x					x
EPHA2	1969	EPH receptor A2	IPI00021267		x				
EPHA4	2043	EPH receptor A4	IPI00008318.1					x	
EPHB4	2050	EPH receptor B4	IPI00186826		x			x	x
EPRS	2058	glutamyl-prolyl-tRNA synthetase	IPI00013452	x	x		x		
ERLIN1	10613	SPFH domain family, member 1	IPI00007940			x	x		
ERLIN2	11160	SPFH domain family, member 2	IPI00026942			x	x		
ESYT1	23344	family with sequence similarity 62 (C2 domain containing), member A	IPI00022143				x		
ETFA	2108	electron-transfer-flavoprotein, alpha polypeptide (glutaric aciduria II)	IPI00010810	x	x				
ETFB	2109	electron-transfer-flavoprotein, beta polypeptide	IPI00004902	x	x				
EXOC2	55770		IPI00783559				x		
EXOC4	60412	exocyst complex component 4	IPI00059279		x				

Table 4.S1. JUNV Z & JUNV C#1 Host Protein Partners				VLPs		Cells		Virus	
Gene Symbol	Entrez ID	Gene Description	IPI ID	Run1	Run2	Run1	Run2	Run1	Run2
EZR	7430	ezrin	IPI00746388.3					x	x
FAF2	23197	UBX domain containing 8	IPI00172656			x			
FAM125A	93343	family with sequence similarity 125, member A	IPI00744702.2					x	x
FAM125B	89853	family with sequence similarity 125, member B	IPI00022918.6					x	x
FAM49B	51571	family with sequence similarity 49, member B	IPI00303318.2					x	x
FANCA	2175	Fanconi anemia, complementation group A	IPI00006170				x		
FANCD2	2177	Fanconi anemia, complementation group D2	IPI00075081				x		
FANCI	55215	KIAA1794	IPI00019447		x		x		
FARSA	2193	phenylalanine-tRNA synthetase-like, alpha subunit	IPI00031820		x				
FARSB	10056	phenylalanyl-tRNA synthetase, beta subunit	IPI00300074.3					x	
FASN	2194	fatty acid synthase	IPI00026781	x	x			x	x
FBLN1	2192	fibulin 1	IPI00218803	x	x				
FERMT2	10979	fermitin family homolog 2 (Drosophila)	IPI00000856.7					x	x
FKBP3	2287	FK506 binding protein 3, 25kDa	IPI00024157.1					x	x
FLAD1	80308	Fad1, flavin adenine dinucleotide synthetase, homolog (yeast)	IPI00220299		x				
FLNA	2316	filamin A, alpha (actin binding protein 280)	IPI00302592		x			x	x
FLNB	2317	filamin B, beta (actin binding protein 278)	IPI00289334		x				
FLOT1	10211	flotillin 1	IPI00027438		x		x		
FLOT2	2319		IPI00789008		x		x		
FMNL2	114793	formin-like 2	IPI00044748.6						x
FN1	2335	fibronectin 1	IPI00022418.1					x	x
FTSJ1	24140	FtsJ homolog 1 (E. coli)	IPI00004308				x		
FYN	2534	FYN oncogene related to SRC, FGR, YES	IPI00166845		x				
G3BP1	10146	GTPase activating protein (SH3 domain) binding protein 1	IPI00012442.1					x	x
G3BP2	9908	GTPase activating protein (SH3 domain) binding protein 2	IPI00009057.2						x
GALK1	2584	galactokinase 1	IPI00019383		x		x		
GANAB	23193	glucosidase, alpha; neutral AB	IPI00011454			x			
GAPDH	2597	glyceraldehyde-3-phosphate dehydrogenase	IPI00219018	x	x		x		
GARS	2617		IPI00783097	x	x			x	x
GART	2618	phosphoribosylglycinamide formyltransferase, phosphoribosylglycinamide synthetase, phosphoribosylaminoimidazole synthetase	IPI00025273		x			x	
GBF1	8729	golgi-specific brefeldin A resistance factor 1	IPI00021954				x		
GCN1L1	10985	GCN1 general control of amino-acid synthesis 1-like 1 (yeast)	IPI00001159		x	x	x	x	x
GDI1	2664	GDP dissociation inhibitor 1	IPI00010154.3					x	x
GDI2	2665	GDP dissociation inhibitor 2	IPI00031461.2					x	x

Table 4.S1. JUNV Z & JUNV C#1 Host Protein Partners				VLPs		Cells		Virus	
Gene Symbol	Entrez ID	Gene Description	IPI ID	Run1	Run2	Run1	Run2	Run1	Run2
GEMIN4	50628	gem (nuclear organelle) associated protein 4	IPI00027717			x	x		
GFM1	85476	G elongation factor, mitochondrial 1	IPI00154473		x				
GFPT1	2673	glutamine-fructose-6-phosphate transaminase 1	IPI00217952		x				
GIGYF2	26058	trinucleotide repeat containing 15	IPI00647635		x				
GIPC1	10755	GIPC PDZ domain containing family, member 1	IPI00024705		x				
GK	2710	glycerol kinase	IPI00027424.3			x	x		
GLO1	2739	glyoxalase I	IPI00220766.5					x	x
GLOD4	51031	glyoxalase domain containing 4	IPI00007102.3						x
GLRX3	10539	thioredoxin-like 2	IPI00008552		x				
GNA13	10672	guanine nucleotide binding protein (G protein), alpha 13	IPI00290928		x		x	x	x
GNAI2	2771	guanine nucleotide binding protein (G protein), alpha inhibiting activity polypeptide 2	IPI00217906		x		x		
GNAI3	2773	guanine nucleotide binding protein (G protein), alpha inhibiting activity polypeptide 3	IPI00220578				x	x	
GNAS	2778	GNAS complex locus	IPI00095891		x		x		
GNB2	2783	guanine nucleotide binding protein (G protein), beta polypeptide 2	IPI00003348		x	x	x	x	x
GNB2L1	10399	guanine nucleotide binding protein (G protein), beta polypeptide 2-like 1	IPI00641950	x	x			x	x
GNL3	26354	guanine nucleotide binding protein-like 3 (nucleolar)	IPI00003886		x				
GOLGA7	51125	golgin A7	IPI00480022.1						x
GOLGB1	2804	golgi autoantigen, golgin subfamily b, macrogolgin (with transmembrane signal), 1	IPI00004671		x				
GPC1	2817	glypican 1	IPI00015688.1					x	x
GPC3	2719	glypican 3	IPI00019907.1					x	x
GPC4	2239	glypican 4	IPI00232571.1						x
GPC6	10082	glypican 6	IPI00001755.1						x
GPI	2821	glucose phosphate isomerase	IPI00027497.5					x	
GRB2	2885	growth factor receptor-bound protein 2	IPI00021327.3					x	
GRID1	2894	glutamate receptor, ionotropic, delta 1	IPI00374337.1					x	
GRSF1	2926	G-rich RNA sequence binding factor 1	IPI00478657		x				
GSN	2934	gelsolin (amyloidosis, Finnish type)	IPI00026314	x	x				
GSTM3	2947	glutathione S-transferase M3 (brain)	IPI00246975		x				
GSTP1	2950	glutathione S-transferase pi	IPI00219757		x			x	x
H2AFV	94239	H2A histone family, member V	IPI00018278		x			x	x
H2AFY	9555	H2A histone family, member Y	IPI00059366	x	x				
HADHA	3030	hydroxyacyl-Coenzyme A dehydrogenase/3-ketoacyl-Coenzyme A thiolase/enoyl-Coenzyme A hydratase (trifunctional protein), alpha subunit	IPI00031522		x				

Table 4.S1. JUNV Z & JUNV C#1 Host Protein Partners				VLPs		Cells		Virus	
Gene Symbol	Entrez ID	Gene Description	IPI ID	Run1	Run2	Run1	Run2	Run1	Run2
HADHB	3032	hydroxyacyl-Coenzyme A dehydrogenase/3-ketoacyl-Coenzyme A thiolase/enoyl-Coenzyme A hydratase (trifunctional protein), beta subunit	IPI00022793	x	x	x	x		
HAX1	10456	HCLS1 associated protein X-1	IPI00010440				x		
HBA1	3039	hemoglobin, zeta	IPI00410714	x	x				
HBA2	3040		IPI00410714	x	x				
HBS1L	10767	HBS1-like (S. cerevisiae)	IPI00009070.1					x	
HDAC2	3066	histone deacetylase 2	IPI00289601.1			x			
HDLBP	3069	high density lipoprotein binding protein (vigilin)	IPI00022228		x				
HEATR1	55127	HEAT repeat containing 1	IPI00024279	x	x	x	x		
HEATR2	54919	hypothetical protein FLJ20397	IPI00242630		x	x	x		
HEATR3	55027	hypothetical protein FLJ20718	IPI00100984				x		
HEATR6	63897	amplified in breast cancer 1	IPI00464999				x		
HERC2	8924	hect domain and RLD 2	IPI00005826.1			x			
HIST1H1C	3006	histone 1, H1c	IPI00217465	x	x			x	x
HIST1H2AA	221613	histone 1, H2aa	IPI00045109	x					
HIST1H4A	8359	histone cluster 1, H4a	IPI00453473.6					x	x
HIST1H4B	8366	histone cluster 1, H4b	IPI00453473.6					x	x
HIST1H4C	8364	histone cluster 1, H4c	IPI00453473.6					x	x
HIST1H4D	8360	histone cluster 1, H4d	IPI00453473.6					x	x
HIST1H4E	8367	histone cluster 1, H4e	IPI00453473.6					x	x
HIST1H4F	8361	histone cluster 1, H4f	IPI00453473.6					x	x
HIST1H4H	8365	histone cluster 1, H4h	IPI00453473.6					x	x
HIST1H4I	8294	histone cluster 1, H4i	IPI00453473.6					x	x
HIST1H4J	8363	histone cluster 1, H4j	IPI00453473.6					x	x
HIST1H4K	8362	histone cluster 1, H4k	IPI00453473.6					x	x
HIST1H4L	8368	histone cluster 1, H4l	IPI00453473.6					x	x
HIST2H2BE	8349	histone 2, H2be	IPI00003935	x	x			x	x
HIST2H3A	333932	histone H3/o	IPI00171611	x					
HIST2H3C	126961		IPI00171611	x					
HIST2H3D	653604		IPI00171611	x					
HIST2H4A	8370	histone cluster 2, H4a	IPI00453473.6					x	x
HIST2H4B	554313	histone cluster 2, H4b	IPI00453473.6					x	x
HIST4H4	121504	histone cluster 4, H4	IPI00453473.6					x	x
HNRNPA2B	3181	heterogeneous nuclear ribonucleoprotein A2/B1	IPI00386854		x				
HNRNPC	3183	heterogeneous nuclear ribonucleoprotein C (C1/C2)	IPI00216592		x			x	
HNRNPCL1	343069	heterogeneous nuclear ribonucleoprotein C-like 1	IPI00027569		x				
HNRNPF	3185	heterogeneous nuclear ribonucleoprotein F	IPI00003881		x				
HNRNPH3	3189	heterogeneous nuclear ribonucleoprotein H3 (2H9)	IPI00013877		x				
HNRNPK	3190	heterogeneous nuclear ribonucleoprotein K	IPI00216049	x	x				x
HNRNPM	4670	heterogeneous nuclear ribonucleoprotein M	IPI00171903	x	x				

Table 4.S1. JUNV Z & JUNV C#1 Host Protein Partners				VLPs		Cells		Virus	
Gene Symbol	Entrez ID	Gene Description	IPI ID	Run1	Run2	Run1	Run2	Run1	Run2
HNRNPR	10236	heterogeneous nuclear ribonucleoprotein R	IPI00012074.3					x	x
HNRNPU	3192	heterogeneous nuclear ribonucleoprotein U (scaffold attachment factor A)	IPI00479217	x	x			x	
HPRT1	3251	hypoxanthine phosphoribosyltransferase 1 (Lesch-Nyhan syndrome)	IPI00218493		x			x	x
HRSP12	10247	heat-responsive protein 12	IPI00005038.1					x	
HSD17B10	3028	hydroxyacyl-Coenzyme A dehydrogenase, type II	IPI00017726	x	x				
HSD17B12	51144	hydroxysteroid (17-beta) dehydrogenase 12	IPI00007676	x		x	x		
HSD17B4	3295	hydroxysteroid (17-beta) dehydrogenase 4	IPI00019912		x		x		
HSDL2	84263	hydroxysteroid dehydrogenase like 2	IPI00031107		x				
HSP90AA1	3320	heat shock protein 90kDa alpha (cytosolic), class A member 1	IPI00382470	x	x	x			
HSP90AA2	3324		IPI00031523	x	x		x		
HSP90AB1	3326	heat shock protein 90kDa alpha (cytosolic), class B member 1	IPI00414676	x	x	x	x	x	x
HSP90B1	7184	heat shock protein 90kDa beta (Grp94), member 1	IPI00027230			x			x
HSPA13	6782	stress 70 protein chaperone, microsome-associated, 60kDa	IPI00299299				x		
HSPA14	51182	heat shock 70kDa protein 14	IPI00292499		x				
HSPA1A	3303	heat shock 70kDa protein 1A	IPI00304925	x	x			x	x
HSPA1B	3304		IPI00304925	x	x			x	x
HSPA1L	3305	heat shock 70kDa protein 7 (HSP70B)	IPI00301277		x	x		x	x
HSPA4	3308	heat shock 70kDa protein 4	IPI00002966.2					x	x
HSPA5	3309	heat shock 70kDa protein 5 (glucose-regulated protein, 78kDa)	IPI00003362		x	x		x	x
HSPA8	3312	heat shock 70kDa protein 8	IPI00003865	x	x			x	x
HSPA9	3313	heat shock 70kDa protein 9B (mortalin-2)	IPI00007765	x	x	x			
HSPD1	3329		IPI00784154	x	x	x			
HSPG2	3339	heparan sulfate proteoglycan 2	IPI00024284.5					x	x
HSPH1	10808	heat shock 105kDa/110kDa protein 1	IPI00218993		x		x	x	
HYOU1	10525	hypoxia up-regulated 1	IPI00000877			x	x	x	x
HYPK	25764	-	IPI00335001.2					x	
IARS	3376	isoleucine-tRNA synthetase	IPI00514082		x		x		
IARS2	55699	isoleucine-tRNA synthetase 2, mitochondrial	IPI00017283		x				
IDE	3416	insulin-degrading enzyme	IPI00220373		x		x		
IDH2	3418	isocitrate dehydrogenase 2 (NADP+), mitochondrial	IPI00011107		x				
IDH3A	3419	isocitrate dehydrogenase 3 (NAD+) alpha	IPI00030702	x	x				
IDH3B	3420	isocitrate dehydrogenase 3 (NAD+) beta	IPI00304417		x				
IGF2BP1	10642	insulin-like growth factor 2 mRNA binding protein 1	IPI00008557		x			x	x
IGF2BP2	10644	insulin-like growth factor 2 mRNA binding protein 2	IPI00179713.6					x	
IGF2BP3	10643	insulin-like growth factor 2 mRNA binding protein 3	IPI00658000.2					x	x

Table 4.S1. JUNV Z & JUNV C#1 Host Protein Partners				VLPs		Cells		Virus	
Gene Symbol	Entrez ID	Gene Description	IPI ID	Run1	Run2	Run1	Run2	Run1	Run2
IGSF3	3321	immunoglobulin superfamily, member 3	IPI00016890.4					x	x
IGSF8	93185	immunoglobulin superfamily, member 8	IPI00056478.1					x	x
ILF2	3608	interleukin enhancer binding factor 2, 45kDa	IPI00005198		x				
ILK	3611	integrin-linked kinase	IPI00013219	x					
ILK	3611		IPI00302927	x	x	x	x		
ILK-2	55522	integrin-linked kinase-2	IPI00302927.6					x	x
IMMT	10989	inner membrane protein, mitochondrial (mitofilin)	IPI00009960		x	x	x		
IMPDH2	3615	IMP (inosine monophosphate) dehydrogenase 2	IPI00291510	x	x				
INA	9118	internexin neuronal intermediate filament protein, alpha	IPI00001453		x				
INSR	3643	insulin receptor	IPI00025803		x				
IPO13	9670	importin 13	IPI00005651				x		
IPO4	79711	importin 4	IPI00156374	x	x		x		
IPO5	3843		IPI00793443	x	x	x	x		
IPO7	10527	importin 7	IPI00007402	x	x	x	x		
IPO8	10526	importin 8	IPI00007401		x		x		
IPO9	55705	importin 9	IPI00185146		x		x		
IQGAP1	8826	IQ motif containing GTPase activating protein 1	IPI00009342		x		x	x	
IQGAP3	128239	IQ motif containing GTPase activating protein 3	IPI00328905		x				
IRS4	8471	insulin receptor substrate 4	IPI00020729	x	x		x	x	x
ITGA6	3655	integrin, alpha 6	IPI00010697.2					x	
ITGB1	3688	integrin, beta 1 (fibronectin receptor, beta polypeptide, antigen CD29 includes MDF2, MSK12)	IPI00217561.2					x	x
ITIH2	3698	inter-alpha (globulin) inhibitor H2	IPI00305461	x	x				
ITIH3	3699	inter-alpha (globulin) inhibitor H3	IPI00028413	x	x				
JUP	3728	junction plakoglobin	IPI00554711		x	x	x		
KCTD12	115207	potassium channel tetramerisation domain containing 12	IPI00060715.1						x
KIAA0174	9798	KIAA0174	IPI00024660.1					x	x
KIAA0368	23392		IPI00157790		x				
KIAA0406	9675	KIAA0406 gene product	IPI00011702				x		
KIAA0664	23277	KIAA0664	IPI00024425		x				
KIAA1524	57650	KIAA1524	IPI00154283		x	x	x		
KIF23	9493	kinesin family member 23	IPI00291579		x				
KIF5B	3799	kinesin family member 5B	IPI00012837		x				
KLHL20	27252	kelch-like 20 (Drosophila)	IPI00032338.5					x	
KPNA1	3836	karyopherin alpha 1 (importin alpha 5)	IPI00303292		x				
KPNA2	3838	karyopherin alpha 2 (RAG cohort 1, importin alpha 1)	IPI00002214	x	x	x		x	
KPNB1	3837	karyopherin (importin) beta 1	IPI00001639	x	x	x	x	x	x
LACTB	114294	lactamase, beta	IPI00294186				x		
LAMA5	3911	laminin, alpha 5	IPI00783665.4					x	

Table 4.S1. JUNV Z & JUNV C#1 Host Protein Partners				VLPs		Cells		Virus	
Gene Symbol	Entrez ID	Gene Description	IPI ID	Run1	Run2	Run1	Run2	Run1	Run2
LAMB1	3912	laminin, beta 1	IPI00013976.3					x	
LAMB2	3913	laminin, beta 2 (laminin S)	IPI00296922.4					x	
LAMC1	3915	laminin, gamma 1 (formerly LAMB2)	IPI00298281.4					x	x
LAP3	51056	leucine aminopeptidase 3	IPI00419237		x				
LARS	51520	leucyl-tRNA synthetase	IPI00103994	x	x		x	x	x
LDHA	3939	lactate dehydrogenase A	IPI00217966				x	x	
LDHB	3945	lactate dehydrogenase B	IPI00219217		x			x	x
LGALS3BP	3959	lectin, galactoside-binding, soluble, 3 binding protein	IPI00023673.1					x	x
LMNB1	4001	lamin B1	IPI00217975				x		
LOC284889	284889	hypothetical protein LOC284889	IPI00293276.1					x	
LOC389842	389842		IPI00399212	x					x
LOC442497	442497	hypothetical protein LOC442497	IPI00027493.1					x	x
LONP1	9361	protease, serine, 15	IPI00005158	x	x				
LPHN2	23266	latrophilin 2	IPI00017562		x			x	
LRBA	987	LPS-responsive vesicle trafficking, beach and anchor containing	IPI00002255				x		
LRPPRC	10128		IPI00783271	x	x				
LRRC47	57470	leucine rich repeat containing 47	IPI00170935		x				
LRRC57	255252	leucine rich repeat containing 57	IPI00470576.4					x	
LRRC59	55379	leucine rich repeat containing 59	IPI00396321.1			x			
LYN	4067	v-yes-1 Yamaguchi sarcoma viral related oncogene homolog	IPI00298625		x				
MAP2K1	5604	mitogen-activated protein kinase kinase 1	IPI00219604		x				
MAP2K2	5605	mitogen-activated protein kinase kinase 2	IPI00003783		x				
MAPK14	1432	mitogen-activated protein kinase 14	IPI00002857		x				
MAPRE2	10982	microtubule-associated protein, RP/EB family, member 2	IPI00003420		x				
MARCKS	4082	myristoylated alanine-rich protein kinase C substrate	IPI00219301.7					x	x
MARCKSL1	65108	MARCKS-like 1	IPI00641181.5						x
MARS	4141	methionine-tRNA synthetase	IPI00008240	x	x				
MATR3	9782	matrin 3	IPI00017297		x				
MCAM	4162	melanoma cell adhesion molecule	IPI00016334.2					x	
MCCC2	64087		IPI00784044		x				
MCM4	4173	MCM4 minichromosome maintenance deficient 4 (S. cerevisiae)	IPI00018349		x				
MCM7	4176	MCM7 minichromosome maintenance deficient 7 (S. cerevisiae)	IPI00219740	x	x				
MCTS1	28985	malignant T cell amplified sequence 1	IPI00179026.2					x	
MDH2	4191	malate dehydrogenase 2, NAD (mitochondrial)	IPI00291006		x			x	
MDN1	23195	MDN1, midasin homolog (yeast)	IPI00167941				x		
MFAP3	4238	microfibrillar-associated protein 3	IPI00022791.1					x	x
MFGE8	4240	milk fat globule-EGF factor 8 protein	IPI00002236.3					x	x
MIF	4282	macrophage migration inhibitory factor (glycosylation-inhibiting factor)	IPI00293276.1					x	

Table 4.S1. JUNV Z & JUNV C#1 Host Protein Partners				VLPs		Cells		Virus	
Gene Symbol	Entrez ID	Gene Description	IPI ID	Run1	Run2	Run1	Run2	Run1	Run2
MYO1D	4642	myosin ID	IPI00329719.1					x	x
NAA15	80155	N(alpha)-acetyltransferase 15, NatA auxiliary subunit	IPI00032158.3					x	x
NAA25	80018	N(alpha)-acetyltransferase 25, NatB auxiliary subunit	IPI00025890.4					x	
NAA50	80218	N(alpha)-acetyltransferase 50, NatE catalytic subunit	IPI00018627.3					x	
NACA	4666	nascent polypeptide-associated complex alpha subunit	IPI00023748.3					x	x
NAP1L1	4673	nucleosome assembly protein 1-like 1	IPI00023860		x				
NCAPD2	9918	chromosome condensation-related SMC-associated protein 1	IPI00299524	x	x				
NCAPG	64151	chromosome condensation protein G	IPI00106495		x				
NCDN	23154	neurochondrin	IPI00549543		x		x		
NCKIPSD	51517	NCK interacting protein with SH3 domain	IPI00009319		x				
NCL	4691	nucleolin	IPI00183526		x	x			
NCS1	23413	neuronal calcium sensor 1	IPI00219110.7					x	
NDUFA9	4704	NADH dehydrogenase (ubiquinone) 1 alpha subcomplex, 9, 39kDa	IPI00003968		x		x		
NDUFS1	4719	NADH dehydrogenase (ubiquinone) Fe-S protein 1, 75kDa (NADH-coenzyme Q reductase)	IPI00604664				x		
NDUFS3	4722	NADH dehydrogenase (ubiquinone) Fe-S protein 3, 30kDa (NADH-coenzyme Q reductase)	IPI00025796		x		x		
NEO1	4756	neogenin homolog 1 (chicken)	IPI00023814		x				
NME1	4830	non-metastatic cells 1, protein (NM23A) expressed in	IPI00012048.1					x	x
NME2	4831	non-metastatic cells 2, protein (NM23B) expressed in	IPI00026260.1					x	
NONO	4841	non-POU domain containing, octamer-binding	IPI00304596	x					
NOP56	10528	nucleolar protein 5A (56kDa with KKE/D repeat)	IPI00411937		x				
NOTCH2	4853	Notch homolog 2 (Drosophila)	IPI00297655		x			x	x
NPEPPS	9520	aminopeptidase puromycin sensitive	IPI00026216.4			x			x
NPM1	4869	anaplastic lymphoma kinase (Ki-1)	IPI00220740		x			x	
NRAS	4893	neuroblastoma RAS viral (v-ras) oncogene homolog	IPI00000005		x			x	x
NSF	4905	N-ethylmaleimide-sensitive factor	IPI00006451		x				
NT5DC2	64943	5'-nucleotidase domain containing 2	IPI00009662				x		
NUDC	10726	nuclear distribution gene C homolog (A. nidulans)	IPI00550746.4						x
NUP133	55746	nucleoporin 133kDa	IPI00291200		x				
NUP153	9972	nucleoporin 153kDa	IPI00292059				x		
NUP160	23279		IPI00748807		x				
NUP205	23165		IPI00783781	x		x	x		
OAT	4942	ornithine aminotransferase (gyrate atrophy)	IPI00022334		x				

Table 4.S1. JUNV Z & JUNV C#1 Host Protein Partners				VLPs		Cells		Virus	
Gene Symbol	Entrez ID	Gene Description	IPI ID	Run1	Run2	Run1	Run2	Run1	Run2
OGDH	4967	oxoglutarate (alpha-ketoglutarate) dehydrogenase (lipoamide)	IPI00098902				x		
OLA1	29789	Obg-like ATPase 1	IPI00216105.1					x	x
OPA1	4976	optic atrophy 1 (autosomal dominant)	IPI00006721				x		
OXSR1	9943	oxidative-stress responsive 1	IPI00010080		x				
P4HB	5034	procollagen-proline, 2-oxoglutarate 4-dioxygenase (proline 4-hydroxylase), beta polypeptide	IPI00010796			x	x		
PA2G4	5036	proliferation-associated 2G4, 38kDa	IPI00299000		x			x	x
PABPC1	26986	poly(A) binding protein, cytoplasmic 1	IPI00008524		x			x	x
PABPC4	8761	poly(A) binding protein, cytoplasmic 4 (inducible form)	IPI00012726.4					x	x
PABPC4L	132430	poly(A) binding protein, cytoplasmic 4-like	IPI00885166.1					x	x
PACSIN2	11252	protein kinase C and casein kinase substrate in neurons 2	IPI00027009.2					x	x
PACSIN3	29763	protein kinase C and casein kinase substrate in neurons 3	IPI00329572.4						x
PAICS	10606	phosphoribosylaminoimidazole carboxylase, phosphoribosylaminoimidazole succinocarboxamide synthetase	IPI00217223		x			x	x
PARK7	11315	Parkinson disease (autosomal recessive, early onset) 7	IPI00298547.3					x	x
PARP1	142	poly (ADP-ribose) polymerase family, member 1	IPI00449049	x	x			x	
PCBP1	5093	poly(rC) binding protein 1	IPI00016610	x	x			x	
PCBP2	5094	poly(rC) binding protein 2	IPI00012066	x	x			x	x
PCNA	5111	proliferating cell nuclear antigen	IPI00021700	x	x				
PDAP1	11333	PDGFA associated protein 1	IPI00013297.1					x	
PDCD10	11235	programmed cell death 10	IPI00298558.2					x	
PDCD5	9141	programmed cell death 5	IPI00023640.3					x	x
PDCD6	10016	programmed cell death 6	IPI00025277.5					x	
PDCD6IP	10015	programmed cell death 6 interacting protein	IPI00246058	x	x			x	x
PDHA1	5160	pyruvate dehydrogenase (lipoamide) alpha 1	IPI00306301	x	x				
PDHB	5162	pyruvate dehydrogenase (lipoamide) beta	IPI00003925	x	x				
PDIA6	10130	protein disulfide isomerase family A, member 6	IPI00299571				x		
PEBP1	5037	phosphatidylethanolamine binding protein 1	IPI00219446.5					x	x
PEF1	553115	penta-EF-hand domain containing 1	IPI00018235		x				
PELP1	27043	proline, glutamic acid and leucine rich protein 1	IPI00006702		x				
PFDN2	5202	prefoldin subunit 2	IPI00006052.3						x
PFDN6	10471	prefoldin subunit 6	IPI00005657.1					x	
PFN1	5216	profilin 1	IPI00216691		x			x	
PGAM2	5224	phosphoglycerate mutase 2 (muscle)	IPI00218570.6					x	x
PGAM5	192111	phosphoglycerate mutase family member 5	IPI00063242				x		
PGD	5226	phosphogluconate dehydrogenase	IPI00219525	x	x			x	
PGK1	5230	phosphoglycerate kinase 1	IPI00169383.3					x	x

Table 4.S1. JUNV Z & JUNV C#1 Host Protein Partners				VLPs		Cells		Virus	
Gene Symbol	Entrez ID	Gene Description	IPI ID	Run1	Run2	Run1	Run2	Run1	Run2
PHB	5245	prohibitin	IPI00017334.1			x	x	x	
PHB2	11331	prohibitin 2	IPI00027252.6			x	x		
PHGDH	26227	phosphoglycerate dehydrogenase	IPI00011200	x	x		x	x	x
PI4KA	5297	phosphatidylinositol 4-kinase, catalytic, alpha polypeptide	IPI00070943		x				
PIN4	5303	protein (peptidylprolyl cis/trans isomerase) NIMA-interacting, 4 (parvulin)	IPI00006658.4						x
PIP4K2A	5305	phosphatidylinositol-4-phosphate 5-kinase, type II, alpha	IPI00009688		x				
PIP4K2C	79837	phosphatidylinositol-4-phosphate 5-kinase, type II, gamma	IPI00152303		x				
PITRM1	10531	pitrilysin metallopeptidase 1	IPI00219613				x		
PKM2	5315	pyruvate kinase, muscle	IPI00220644	x	x		x	x	x
PLS3	5358	plastin 3	IPI00216694.3					x	x
PNP	4860	purine nucleoside phosphorylase	IPI00017672.4					x	
POLDIP2	26073	polymerase (DNA-directed), delta interacting protein 2	IPI00165506		x				
POLR1C	9533	polymerase (RNA) I polypeptide C, 30kDa	IPI00005179		x				
POLR2B	5431	polymerase (RNA) II (DNA directed) polypeptide B, 140kDa	IPI00027808		x				
POLR2C	5432	polymerase (RNA) II (DNA directed) polypeptide C, 33kDa	IPI00018288		x				
PPIA	5478	peptidylprolyl isomerase A (cyclophilin A)	IPI00419585		x			x	x
PPP1CC	5501	protein phosphatase 1, catalytic subunit, gamma isoform	IPI00005705		x				
PPP2CA	5515	protein phosphatase 2 (formerly 2A), catalytic subunit, alpha isoform	IPI00008380		x				
PPP2R1A	5518	protein phosphatase 2 (formerly 2A), regulatory subunit A (PR 65), alpha isoform	IPI00168184	x	x		x		
PPP2R1B	5519	protein phosphatase 2 (formerly 2A), regulatory subunit A (PR 65), beta isoform	IPI00294178		x				
PRDX1	5052	peroxiredoxin 1	IPI00000874	x	x			x	x
PRDX2	7001	peroxiredoxin 2	IPI00027350	x	x			x	
PRDX3	10935	peroxiredoxin 3	IPI00024919	x	x				
PRDX4	10549	peroxiredoxin 4	IPI00011937.1			x	x		
PRDX5	25824	peroxiredoxin 5	IPI00024915		x				
PRDX6	9588	peroxiredoxin 6	IPI00220301		x			x	x
PREP	5550	prolyl endopeptidase	IPI00008164		x				
PRIC285	85441	peroxisomal proliferator-activated receptor A interacting complex 285	IPI00249304.3					x	x
PRKDC	5591	protein kinase, DNA-activated, catalytic polypeptide	IPI00296337	x	x	x		x	x
PRPF8	10594	PRP8 pre-mRNA processing factor 8 homolog (yeast)	IPI00007928		x				
PSMA4	5685	proteasome (prosome, macropain) subunit, alpha type, 4	IPI00299155		x				

Table 4.S1. JUNV Z & JUNV C#1 Host Protein Partners				VLPs		Cells		Virus	
Gene Symbol	Entrez ID	Gene Description	IPI ID	Run1	Run2	Run1	Run2	Run1	Run2
PSMC1	5700	proteasome (prosome, macropain) 26S subunit, ATPase, 1	IPI00011126		x				
PSMC2	5701	proteasome (prosome, macropain) 26S subunit, ATPase, 2	IPI00021435		x		x		
PSMC3	5702	proteasome (prosome, macropain) 26S subunit, ATPase, 3	IPI00018398	x	x		x		
PSMC4	5704	proteasome (prosome, macropain) 26S subunit, ATPase, 4	IPI00020042		x				
PSMC5	5705	proteasome (prosome, macropain) 26S subunit, ATPase, 5	IPI00023919	x	x				
PSMC6	5706	proteasome (prosome, macropain) 26S subunit, ATPase, 6	IPI00021926	x	x				
PSMD1	5707	proteasome (prosome, macropain) 26S subunit, non-ATPase, 1	IPI00299608		x			x	
PSMD10	5716	proteasome (prosome, macropain) 26S subunit, non-ATPase, 10	IPI00003565	x	x				
PSMD11	5717	proteasome (prosome, macropain) 26S subunit, non-ATPase, 11	IPI00105598		x				
PSMD12	5718	proteasome (prosome, macropain) 26S subunit, non-ATPase, 12	IPI00185374	x	x	x			
PSMD13	5719	proteasome (prosome, macropain) 26S subunit, non-ATPase, 13	IPI00375380		x		x		
PSMD14	10213	proteasome (prosome, macropain) 26S subunit, non-ATPase, 14	IPI00024821		x				
PSMD2	5708	proteasome (prosome, macropain) 26S subunit, non-ATPase, 2	IPI00012268	x	x				
PSMD3	5709	proteasome (prosome, macropain) 26S subunit, non-ATPase, 3	IPI00011603		x				
PSMD4	5710	proteasome (prosome, macropain) 26S subunit, non-ATPase, 4	IPI00022694		x				
PSMD6	9861	proteasome (prosome, macropain) 26S subunit, non-ATPase, 6	IPI00014151	x	x				
PSMD7	5713	proteasome (prosome, macropain) 26S subunit, non-ATPase, 7 (Mov34 homolog)	IPI00019927	x	x		x		
PSMD8	5714	proteasome (prosome, macropain) 26S subunit, non-ATPase, 8	IPI00010201	x	x				
PSME3	10197	proteasome (prosome, macropain) activator subunit 3 (PA28 gamma; Ki)	IPI00030243		x				
PTBP1	5725	polypyrimidine tract binding protein 1	IPI00179964		x				
PTGFRN	5738	prostaglandin F2 receptor negative regulator	IPI00022048.8					x	x
PTK7	5754	PTK7 protein tyrosine kinase 7	IPI00168813		x				
PTP4A1	7803	protein tyrosine phosphatase type IVA, member 1	IPI00020164.1					x	
PTPLAD1	51495	protein tyrosine phosphatase-like A domain containing 1	IPI00008998				x		
PTPRF	5792	protein tyrosine phosphatase, receptor type, F	IPI00107831		x			x	

Table 4.S1. JUNV Z & JUNV C#1 Host Protein Partners				VLPs		Cells		Virus	
Gene Symbol	Entrez ID	Gene Description	IPI ID	Run1	Run2	Run1	Run2	Run1	Run2
PURA	5813	purine-rich element binding protein A	IPI00023591.1					x	x
PVR	5817	poliovirus receptor	IPI00219425.3					x	x
PYCR2	29920	pyrroline-5-carboxylate reductase family, member 2	IPI00335061		x	x	x		
RAB10	10890	RAB10, member RAS oncogene family	IPI00016513	x	x				x
RAB11B	9230	RAB11B, member RAS oncogene family	IPI00020436		x	x		x	
RAB13	5872	RAB13, member RAS oncogene family	IPI00016373.3					x	x
RAB14	51552	RAB14, member RAS oncogene family	IPI00291928		x			x	
RAB1A	5861	RAB1A, member RAS oncogene family	IPI00005719	x	x	x		x	x
RAB1B	81876	RAB1B, member RAS oncogene family	IPI00008964.3						x
RAB2A	5862	RAB2A, member RAS oncogene family	IPI00031169.1					x	x
RAB35	11021	RAB35, member RAS oncogene family	IPI00300096		x			x	x
RAB5A	5868	RAB5A, member RAS oncogene family	IPI00023510.1					x	
RAB5B	5869	RAB5B, member RAS oncogene family	IPI00017344.3					x	x
RAB5C	5878	RAB5C, member RAS oncogene family	IPI00016339	x				x	x
RAB7A	7879	RAB7, member RAS oncogene family	IPI00016342	x	x	x		x	x
RAB8A	4218	RAB8A, member RAS oncogene family	IPI00028481.1					x	x
RAB8B	51762	RAB8B, member RAS oncogene family	IPI00024282.1					x	
RAB9A	9367	RAB9A, member RAS oncogene family	IPI00016372		x				
RAC1	5879	ras-related C3 botulinum toxin substrate 1 (rho family, small GTP binding protein Rac1)	IPI00010271.3					x	x
RAD50	10111	RAD50 homolog (S. cerevisiae)	IPI00107531		x				
RALB	5899	v-ral simian leukemia viral oncogene homolog B (ras related; GTP binding protein)	IPI00004397.2					x	x
RAN	5901	RAN, member RAS oncogene family	IPI00643041		x			x	
RANBP6	26953	RAN binding protein 6	IPI00514622				x		
RANP1	221547	RAN, member RAS oncogene family pseudogene 1	IPI00643041.3					x	
RAP1A	5906	RAP1A, member of RAS oncogene family	IPI00019345.1					x	
RAP1B	5908	RAP1B, member of RAS oncogene family	IPI00015148		x			x	x
RAP2C	57826	RAP2C, member of RAS oncogene family	IPI00009607		x			x	
RARS	5917	arginyl-tRNA synthetase	IPI00004860		x		x		
RBBP4	5928	retinoblastoma binding protein 4	IPI00328319		x	x			
RCN2	5955	reticulocalbin 2, EF-hand calcium binding domain	IPI00029628.1			x	x		
RCTPI1	729708	TPI1 pseudogene	IPI00465028.7					x	
RDX	5962	radixin	IPI00017367.6					x	x
RFC2	5982	replication factor C (activator 1) 2, 40kDa	IPI00017412		x				
RFC3	5983	replication factor C (activator 1) 3, 38kDa	IPI00031521				x		
RFC4	5984	replication factor C (activator 1) 4, 37kDa	IPI00017381		x				
RFC5	5985	replication factor C (activator 1) 5, 36.5kDa	IPI00031514		x				
RG9MTD1	54931	RNA (guanine-9-) methyltransferase domain containing 1	IPI00099996		x				
RHEB	6009	Ras homolog enriched in brain	IPI00016669.1					x	
RHOA	387	ras homolog gene family, member A	IPI00478231.2					x	
RHOG	391	ras homolog gene family, member G (rho G)	IPI00017342.1						x
RNF160	26046		IPI00783835				x		

Table 4.S1. JUNV Z & JUNV C#1 Host Protein Partners				VLPs		Cells		Virus	
Gene Symbol	Entrez ID	Gene Description	IPI ID	Run1	Run2	Run1	Run2	Run1	Run2
RNF213	57674	ring finger protein 213	IPI00642126.3					x	
RNF214	257160		IPI00742996		x				
RNH1	6050	ribonuclease/angiogenin inhibitor 1	IPI00550069		x				
RPL10A	4736	ribosomal protein L10a	IPI00412579	x	x			x	x
RPL10L	140801	ribosomal protein L10-like	IPI00064765.3					x	
RPL10P16	284393	ribosomal protein L10 pseudogene 16	IPI00374260.4						x
RPL11	6135	ribosomal protein L11	IPI00376798	x	x			x	x
RPL12	6136	ribosomal protein L12	IPI00024933.3					x	x
RPL13	6137	ribosomal protein L13	IPI00465361.4					x	x
RPL13A	23521	ribosomal protein L13a	IPI00304612	x	x			x	x
RPL13P12	388344		IPI00397611	x				x	x
RPL15	6138	ribosomal protein L15	IPI00470528.5					x	
RPL18	6141	ribosomal protein L18	IPI00215719	x	x		x	x	x
RPL18A	6142	ribosomal protein L18a	IPI00026202.1					x	x
RPL19	6143	ribosomal protein L19	IPI00025329.1					x	x
RPL21	6144	ribosomal protein L21	IPI00247583.5					x	x
RPL21P16	729402	ribosomal protein L21 pseudogene 16	IPI00247583.5					x	x
RPL21P19	641293	ribosomal protein L21 pseudogene 19	IPI00247583.5					x	x
RPL23	9349	ribosomal protein L23	IPI00010153.5					x	x
RPL24	6152	ribosomal protein L24	IPI00306332		x				
RPL26L1	51121	ribosomal protein L26-like 1	IPI00007144	x					x
RPL27	6155	ribosomal protein L27	IPI00219155.5					x	
RPL28	6158	ribosomal protein L28	IPI00182533.5					x	x
RPL3	6122	ribosomal protein L3	IPI00550021	x	x			x	x
RPL30	6156	ribosomal protein L30	IPI00219156.7					x	x
RPL31	6160	ribosomal protein L31	IPI00026302.3						x
RPL34	6164	ribosomal protein L34	IPI00219160.3						x
RPL35	11224	ribosomal protein L35	IPI00412607		x			x	
RPL35A	6165	ribosomal protein L35a	IPI00029731.8						x
RPL36	25873	ribosomal protein L36	IPI00216237.5					x	x
RPL38	6169	ribosomal protein L38	IPI00215790		x			x	x
RPL4	6124	ribosomal protein L4	IPI00003918	x	x			x	x
RPL5	6125	ribosomal protein L5	IPI00000494		x			x	x
RPL6	6128	ribosomal protein L6	IPI00329389	x	x			x	x
RPL7	6129	ribosomal protein L7	IPI00030179	x	x		x	x	x
RPL7A	6130	ribosomal protein L7a	IPI00299573		x			x	x
RPL7P32	1E+08	ribosomal protein L7 pseudogene 32	IPI00030179.3					x	x
RPL8	6132	ribosomal protein L8	IPI00012772	x				x	x
RPL9	6133	ribosomal protein L9	IPI00031691.1					x	x
RPLP0	6175	ribosomal protein, large, P0	IPI00008530	x	x			x	x
RPLP1	6176	ribosomal protein, large, P1	IPI00008527.3					x	x
RPLP2	6181	ribosomal protein, large, P2	IPI00008529.1					x	x
RPN1	6184	ribophorin I	IPI00025874			x	x		
RPS10	6204	ribosomal protein S10	IPI00008438.1					x	x
RPS11	6205	ribosomal protein S11	IPI00025091	x				x	x
RPS12	6206	ribosomal protein S12	IPI00013917.3						x
RPS14	6208	ribosomal protein S14	IPI00026271		x			x	x
RPS15	6209	ribosomal protein S15	IPI00479058.2					x	

Table 4.S1. JUNV Z & JUNV C#1 Host Protein Partners				VLPs		Cells		Virus	
Gene Symbol	Entrez ID	Gene Description	IPI ID	Run1	Run2	Run1	Run2	Run1	Run2
RPS15A	6210	ribosomal protein S15a	IPI00221091.9					x	x
RPS16	6217	ribosomal protein S16	IPI00221092		x			x	x
RPS17	6218	ribosomal protein S17	IPI00221093.7					x	x
RPS18	6222	ribosomal protein S18	IPI00013296		x			x	x
RPS19	6223	ribosomal protein S19	IPI00215780.5					x	x
RPS2	6187	ribosomal protein S2	IPI00013485	x	x			x	x
RPS20	6224	ribosomal protein S20	IPI00012493.1					x	
RPS21	6227	ribosomal protein S21	IPI00017448.1					x	x
RPS23	6228	ribosomal protein S23	IPI00218606.7						x
RPS24	6229	ribosomal protein S24	IPI00029750		x			x	x
RPS27	6232	ribosomal protein S27	IPI00397358.4					x	x
RPS27A	6233	ribosomal protein S27a	IPI00179330	x	x	x		x	x
RPS28	6234	ribosomal protein S28	IPI00719622.1						x
RPS3	6188	ribosomal protein S3	IPI00011253	x	x			x	x
RPS3A	6189	ribosomal protein S3A	IPI00419880	x	x			x	x
RPS4X	6191	ribosomal protein S4, X-linked	IPI00217030	x	x			x	x
RPS5	6193	ribosomal protein S5	IPI00008433.4					x	x
RPS6	6194	ribosomal protein S6	IPI00021840	x	x			x	x
RPS7	6201	ribosomal protein S7	IPI00013415.1					x	
RPS7P4	149224	ribosomal protein S7 pseudogene 4	IPI00008293.4						x
RPS8	6202	ribosomal protein S8	IPI00216587	x	x			x	x
RPS9	6203	ribosomal protein S9	IPI00221088	x	x			x	x
RPSAP12	387867		IPI00398958	x	x			x	
RRAS2	22800	related RAS viral (r-ras) oncogene homolog 2	IPI00012512		x			x	x
RRM1	6240	ribonucleotide reductase M1 polypeptide	IPI00013871		x				
RSL1D1	26156	ribosomal L1 domain containing 1	IPI00008708		x				
RSU1	6251	Ras suppressor protein 1	IPI00017256		x				
RUVBL1	8607	RuvB-like 1 (E. coli)	IPI00021187	x	x	x	x	x	
RUVBL2	10856	RuvB-like 2 (E. coli)	IPI00009104	x	x	x	x		x
SAMM50	25813	sorting and assembly machinery component 50 homolog (S. cerevisiae)	IPI00412713				x		
SAPS3	55291	SAPS domain family, member 3	IPI00019540				x		
SARM1	23098	sterile alpha and TIR motif containing 1	IPI00007919				x		
SBDS	51119	Shwachman-Bodian-Diamond syndrome	IPI00427330.3					x	
SCRIB	23513	scribbled homolog (Drosophila)	IPI00410666		x			x	
SDCBP	6386	syndecan binding protein (syntenin)	IPI00299086		x			x	x
SDK2	54549	sidekick homolog 2 (chicken)	IPI00384376.3						x
SDR39U1	56948	chromosome 14 open reading frame 124	IPI00643286		x				
SEC16A	9919		IPI00031242				x		
SERBP1	26135	SERPINE1 mRNA binding protein 1	IPI00410693.3					x	x
SERPINA7	6906	serpin peptidase inhibitor, clade A (alpha-1 antiproteinase, antitrypsin), member 7	IPI00292946	x	x				
SERPINC1	462	serpin peptidase inhibitor, clade C (antithrombin), member 1	IPI00032179	x					
SERPINF1	5176	serpin peptidase inhibitor, clade F (alpha-2 antiplasmin, pigment epithelium derived factor), member 1	IPI00006114	x	x				

Table 4.S1. JUNV Z & JUNV C#1 Host Protein Partners				VLPs		Cells		Virus	
Gene Symbol	Entrez ID	Gene Description	IPI ID	Run1	Run2	Run1	Run2	Run1	Run2
SFRS1	6426	splicing factor, arginine/serine-rich 1 (splicing factor 2, alternate splicing factor)	IPI00215884	x	x				
SH3BGRL	6451	SH3 domain binding glutamic acid-rich protein like	IPI00025318.1					x	x
SH3GL1	6455	SH3-domain GRB2-like 1	IPI00019169.3					x	x
SH3GL3	6457	SH3-domain GRB2-like 3	IPI00019172.3					x	x
SH3GLB1	51100	SH3-domain GRB2-like endophilin B1	IPI00006558	x					
SH3KBP1	30011	SH3-domain kinase binding protein 1	IPI00294962.4						x
SHMT2	6472	serine hydroxymethyltransferase 2 (mitochondrial)	IPI00002520		x				
SIRT7	51547	pyrroline-5-carboxylate reductase 1	IPI00260769				x		
SLC12A2	6558	solute carrier family 12 (sodium/potassium/chloride transporters), member 2	IPI00022649		x				
SLC16A1	6566	solute carrier family 16 (monocarboxylic acid transporters), member 1	IPI00024650				x	x	x
SLC1A5	6510	solute carrier family 1 (neutral amino acid transporter), member 5	IPI00019472				x	x	x
SLC25A1	6576	solute carrier family 25 (mitochondrial carrier; citrate transporter), member 1	IPI00294159.3			x			
SLC25A10	1468	solute carrier family 25 (mitochondrial carrier; dicarboxylate transporter), member 10	IPI00015920				x		
SLC25A11	8402	solute carrier family 25 (mitochondrial carrier; oxoglutarate carrier), member 11	IPI00219729				x		
SLC25A12	8604	solute carrier family 25 (mitochondrial carrier, Aralar), member 12	IPI00386271				x		
SLC25A13	10165	solute carrier family 25, member 13 (citrin)	IPI00007084.3			x	x		
SLC25A22	79751	solute carrier family 25 (mitochondrial carrier: glutamate), member 22	IPI00003004				x		
SLC25A3	5250	solute carrier family 25 (mitochondrial carrier; phosphate carrier), member 3	IPI00022202.3			x			
SLC25A4	291	solute carrier family 25 (mitochondrial carrier; adenine nucleotide translocator), member 4	IPI00022891				x		
SLC25A40	55972	mitochondrial carrier family protein	IPI00290827				x		
SLC25A6	293	solute carrier family 25 (mitochondrial carrier; adenine nucleotide translocator), member 4	IPI00291467.7			x	x		
SLC29A1	2030	solute carrier family 29 (nucleoside transporters), member 1	IPI00550382.2						x
SLC3A2	6520	solute carrier family 3 (activators of dibasic and neutral amino acid transport), member 2	IPI00027493		x			x	x
SLC7A1	6541	solute carrier family 7 (cationic amino acid transporter, y+ system), member 1	IPI00027728.1					x	
SLC7A5	8140	solute carrier family 7 (cationic amino acid transporter, y+ system), member 5	IPI00008986.1					x	x
SLIT2	9353	slit homolog 2 (Drosophila)	IPI00006288		x				
SLITRK5	26050	SLIT and NTRK-like family, member 5	IPI00016679		x			x	x

Table 4.S1. JUNV Z & JUNV C#1 Host Protein Partners				VLPs		Cells		Virus	
Gene Symbol	Entrez ID	Gene Description	IPI ID	Run1	Run2	Run1	Run2	Run1	Run2
SMARCA5	8467	SWI/SNF related, matrix associated, actin dependent regulator of chromatin, subfamily a, member 5	IPI00297211		x				
SMC1A	8243	SMC1 structural maintenance of chromosomes 1-like 1 (yeast)	IPI00291939		x				
SMC2	10592	SMC2 structural maintenance of chromosomes 2-like 1 (yeast)	IPI00007927		x		x		
SMC3	9126	chondroitin sulfate proteoglycan 6 (bamacan)	IPI00219420		x				
SMC4	10051	SMC4 structural maintenance of chromosomes 4-like 1 (yeast)	IPI00328298		x				
SNAP29	9342	synaptosomal-associated protein, 29kDa	IPI00032831.4					x	
SND1	27044	staphylococcal nuclease domain containing 1	IPI00140420		x			x	x
SNORA67	26781	small nucleolar RNA, H/ACA box 67	IPI00025491.1					x	x
SNRNP200	23020	activating signal cointegrator 1 complex subunit 3-like 1	IPI00420014		x				
SNRPD2	6633	small nuclear ribonucleoprotein D2 polypeptide 16.5kDa	IPI00017963.1						x
SNRPE	6635	small nuclear ribonucleoprotein polypeptide E	IPI00029266.1						x
SNRPG	6637	small nuclear ribonucleoprotein polypeptide G	IPI00016572.1						x
SPC24	147841	spindle pole body component 24 homolog (S. cerevisiae)	IPI00168317		x				
SPTLC1	10558	serine palmitoyltransferase, long chain base subunit 1	IPI00005745.1			x			
SRM	6723	spermidine synthase	IPI00292020		x				
SRP68	6730	signal recognition particle 68kDa	IPI00102936.3					x	
SRSF10	10772	FUS interacting protein (serine/arginine-rich) 1	IPI00009071		x				
SSB	6741	Sjogren syndrome antigen B (autoantigen La)	IPI00009032	x					
SSR4	6748	signal sequence receptor, delta (translocon-associated protein delta)	IPI00019385.3					x	
SSRP1	6749	structure specific recognition protein 1	IPI00005154.1					x	
ST13	6767	suppression of tumorigenicity 13 (colon carcinoma) (Hsp70 interacting protein)	IPI00032826.1					x	x
STIP1	10963	stress-induced-phosphoprotein 1	IPI00013894.1					x	x
STK24	8428	serine/threonine kinase 24 (STE20 homolog, yeast)	IPI00002212		x				
STMN1	3925	stathmin 1	IPI00479997.4					x	
STOML2	30968	stomatin (EPB72)-like 2	IPI00334190		x	x	x		
STRAP	11171	serine/threonine kinase receptor associated protein	IPI00294536.2						x
STX12	23673	syntaxin 12	IPI00329332		x				
STX16	8675	syntaxin 16	IPI00023149		x				
STX4	6810	syntaxin 4	IPI00029730.1						x
STXBP3	6814	syntaxin binding protein 3	IPI00297626		x				
SUCLA2	8803	succinate-CoA ligase, ADP-forming, beta subunit	IPI00217232		x				

Table 4.S1. JUNV Z & JUNV C#1 Host Protein Partners				VLPs		Cells		Virus	
Gene Symbol	Entrez ID	Gene Description	IPI ID	Run1	Run2	Run1	Run2	Run1	Run2
SUCLG2	8801	succinate-CoA ligase, GDP-forming, beta subunit	IPI00096066		x		x		
SYNCRIP	10492	synaptotagmin binding, cytoplasmic RNA interacting protein	IPI00018140.3					x	x
TACO1	51204	coiled-coil domain containing 44	IPI00019903		x				
TAGLN2	8407	transgelin 2	IPI00550363		x			x	x
TAOK1	57551	TAO kinase 1	IPI00002232		x				
TARBP1	6894	Tar (HIV-1) RNA binding protein 1	IPI00298447			x			
TARS	6897	threonyl-tRNA synthetase	IPI00329633.5						x
TBC1D15	64786	TBC1 domain family, member 15	IPI00154645		x				
TBC1D4	9882	TBC1 domain family, member 4	IPI00220901		x				
TBCA	6902	tubulin folding cofactor A	IPI00217236.4					x	x
TBCD	6904	tubulin-specific chaperone d	IPI00030774				x		
TBCE	6905	tubulin-specific chaperone e	IPI00018402		x				
TCP1	6950	t-complex 1	IPI00290566	x	x			x	x
TELO2	9894	KIAA0683 gene product	IPI00016868		x		x		
TFAM	7019	transcription factor A, mitochondrial	IPI00020928		x				
TFRC	7037	transferrin receptor (p90, CD71)	IPI00022462	x	x	x			
THADA	63892	thyroid adenoma associated	IPI00412647			x	x		
THBS1	7057	thrombospondin 1	IPI00296099	x	x				
TIMM13	26517	translocase of inner mitochondrial membrane 13 homolog (yeast)	IPI00001589				x		
TIMM23	10431	translocase of inner mitochondrial membrane 23 homolog (yeast)	IPI00007309				x		
TIMM50	92609	translocase of inner mitochondrial membrane 50 homolog (yeast)	IPI00418497.1			x	x		
TLN1	7094	talin 1	IPI00298994		x			x	x
TLN2	83660	talin 2	IPI00219299.4						x
TMEM189-UBE2V1	387522	TMEM189-UBE2V1 readthrough	IPI00019599.1					x	
TMEM33	55161	transmembrane protein 33	IPI00299084.1			x			
TMEM43	79188	transmembrane protein 43	IPI00301280				x		
TNC	3371	tenascin C	IPI00031008.1						x
TNIP1	10318	TNFAIP3 interacting protein 1	IPI00216616		x				
TNIP2	79155	TNFAIP3 interacting protein 2	IPI00168953		x				
TNPO1	3842	transportin 1	IPI00024364		x	x	x		
TNPO3	23534	transportin 3	IPI00395694	x	x	x	x		
TOMM40	10452	translocase of outer mitochondrial membrane 40 homolog (yeast)	IPI00014053.3			x	x		
TOP2B	7155	topoisomerase (DNA) II beta 180kDa	IPI00027280		x				
TPD52L2	7165	tumor protein D52-like 2	IPI00221178.1					x	
TPI1	7167	triosephosphate isomerase 1	IPI00465028.7					x	
TPT1	7178	tumor protein, translationally-controlled 1	IPI00009943	x				x	x
TRAP1	10131	TNF receptor-associated protein 1	IPI00030275		x				
TRIM28	10155	tripartite motif-containing 28	IPI00438229		x				
TRIP13	9319	thyroid hormone receptor interactor 13	IPI00003505		x				
TSFM	10102	Ts translation elongation factor, mitochondrial	IPI00021016		x				

Table 4.S1. JUNV Z & JUNV C#1 Host Protein Partners				VLPs		Cells		Virus	
Gene Symbol	Entrez ID	Gene Description	IPI ID	Run1	Run2	Run1	Run2	Run1	Run2
TSG101	7251	tumor susceptibility gene 101	IPI00018434	x	x		x	x	x
TST	7263	thiosulfate sulfurtransferase (rhodanese)	IPI00216293		x				
TTC19	54902	tetratricopeptide repeat domain 19	IPI00170855				x		
TTLL12	23170	tubulin tyrosine ligase-like family, member 12	IPI00029048		x				
TUBA1C	84790	tubulin, alpha 6	IPI00166768	x	x				x
TUBA4A	7277	tubulin, alpha 1 (testis specific)	IPI00007750	x	x			x	x
TUBB	203068	tubulin, beta	IPI00011654	x	x			x	x
TUBB1	81027	tubulin, beta 1	IPI00006510	x	x				x
TUBB2A	7280	tubulin, beta 2A	IPI00013475		x		x		
TUBB2C	10383	tubulin, beta 2C	IPI00007752	x	x			x	x
TUBB3	10381	tubulin, beta 3	IPI00013683				x		
TUBB6	84617	tubulin, beta 6	IPI00641706				x		
TUBG1	7283	tubulin, gamma 1	IPI00295081		x				
TUFM	7284	Tu translation elongation factor, mitochondrial	IPI00027107	x	x		x		
TXN	7295	thioredoxin	IPI00216298		x		x	x	
TYMS	7298	thymidylate synthetase	IPI00103732		x				
UACA	55075	uveal autoantigen with coiled-coil domains and ankyrin repeats	IPI00173359		x				
UBA1	7317	ubiquitin-activating enzyme E1 (A1S9T and BN75 temperature sensitivity complementing)	IPI00645078	x	x			x	x
UBA6	55236	ubiquitin-activating enzyme E1-like 2	IPI00023647		x				
UBAP2L	9898	ubiquitin associated protein 2-like	IPI00029019.6					x	
UBB	7314		IPI00179330	x	x	x		x	x
UBC	7316		IPI00179330	x	x	x		x	x
UBE2L3	7332	ubiquitin-conjugating enzyme E2L 3	IPI00021347.1					x	
UBE2N	7334	ubiquitin-conjugating enzyme E2N (UBC13 homolog, yeast)	IPI00003949.1					x	
UBE2V1	7335	ubiquitin-conjugating enzyme E2 variant 1	IPI00019599.1					x	
UBP1	7342	upstream binding protein 1 (LBP-1a)	IPI00005018				x		
UCHL1	7345	ubiquitin carboxyl-terminal esterase L1 (ubiquitin thiolesterase)	IPI00018352.1					x	
UMPS	7372	uridine monophosphate synthetase (orotate phosphoribosyl transferase and orotidine-5'-decarboxylase)	IPI00003923		x				
UNC45A	55898	unc-45 homolog A (C. elegans)	IPI00072534		x				
UPF1	5976	UPF1 regulator of nonsense transcripts homolog (yeast)	IPI00034049		x				x
UQCRC2	7385	ubiquinol-cytochrome c reductase core protein II	IPI00305383				x		
USP5	8078	ubiquitin specific peptidase 5 (isopeptidase T)	IPI00024664		x				
USP9X	8239	ubiquitin specific peptidase 9, X-linked	IPI00003964		x		x		
UTRN	7402	utrophin (homologous to dystrophin)	IPI00009329		x				
VAC14	55697	Vac14 homolog (S. cerevisiae)	IPI00025160				x		
VAMP3	9341	vesicle-associated membrane protein 3 (cellubrevin)	IPI00549343.3					x	x
VARS	7407	valyl-tRNA synthetase	IPI00000873		x				

Table 4.S1. JUNV Z & JUNV C#1 Host Protein Partners				VLPs		Cells		Virus	
Gene Symbol	Entrez ID	Gene Description	IPI ID	Run1	Run2	Run1	Run2	Run1	Run2
VCP	7415	valosin-containing protein	IPI00022774				x	x	x
VDAC1	7416	voltage-dependent anion channel 1	IPI00216308.5			x	x		
VDAC2	7417	voltage-dependent anion channel 2	IPI00024145	x	x	x	x		
VDAC3	7419	voltage-dependent anion channel 3	IPI00031804	x	x	x	x		
VIM	7431	vimentin	IPI00418471	x	x	x			
VPS13C	54832	vacuolar protein sorting 13C (yeast)	IPI00412216.2			x			
VPS25	84313	vacuolar protein sorting 25 homolog (S. cerevisiae)	IPI00031655.1					x	x
VPS28	51160	vacuolar protein sorting 28 (yeast)	IPI00007155		x			x	x
VPS35	55737	vacuolar protein sorting 35 (yeast)	IPI00018931		x				x
VPS37B	79720	vacuolar protein sorting 37B (yeast)	IPI00002926		x			x	x
VPS37C	55048	vacuolar protein sorting 37C (yeast)	IPI00401773		x			x	
VPS4B	9525	vacuolar protein sorting 4 homolog B (S. cerevisiae)	IPI00182728.2					x	x
WDR43	23160		IPI00055954		x				
WDR6	11180	WD repeat domain 6	IPI00013953		x			x	x
WDR77	79084	WD repeat domain 77	IPI00012202		x				
WIBG	84305	within bgcn homolog (Drosophila)	IPI00305092.7					x	
XPO1	7514	exportin 1 (CRM1 homolog, yeast)	IPI00298961	x	x	x	x	x	
XPO4	64328	exportin 4	IPI00028357		x				
XPO5	57510	exportin 5	IPI00640703		x	x	x		
XPO6	23214	exportin 6	IPI00465296		x		x		
XPO7	23039	exportin 7	IPI00302458				x		
XPOT	11260	exportin, tRNA (nuclear export receptor for tRNAs)	IPI00306290		x	x	x		
XRCC5	7520	X-ray repair complementing defective repair in Chinese hamster cells 5 (double-strand-break rejoining)	IPI00220834.8					x	
XRCC6	2547	X-ray repair complementing defective repair in Chinese hamster cells 6	IPI00644712.4					x	
YARS	8565	tyrosyl-tRNA synthetase	IPI00007074		x			x	x
YARS2	51067	tyrosyl-tRNA synthetase 2 (mitochondrial)	IPI00165092		x				
YBX1	4904	Y box binding protein 1	IPI00031812.3					x	x
YES1	7525	v-yes-1 Yamaguchi sarcoma viral oncogene homolog 1	IPI00013981		x	x	x	x	
YKT6	10652	YKT6 v-SNARE homolog (S. cerevisiae)	IPI00008569.1					x	
YME1L1	10730	YME1-like 1 (S. cerevisiae)	IPI00045946				x		
YTHDF1	54915	YTH domain family, member 1	IPI00221345.1					x	
YTHDF2	51441	YTH domain family, member 2	IPI00306043.1					x	x
YWHAB	7529	tyrosine 3-monooxygenase/tryptophan 5-monooxygenase activation protein, beta polypeptide	IPI00216318				x	x	x
YWHAE	7531	tyrosine 3-monooxygenase/tryptophan 5-monooxygenase activation protein, epsilon polypeptide	IPI00000816	x	x	x	x	x	x

Table 4.S1. JUNV Z & JUNV C#1 Host Protein Partners				VLPs		Cells		Virus	
Gene Symbol	Entrez ID	Gene Description	IPI ID	Run1	Run2	Run1	Run2	Run1	Run2
YWHAG	7532	tyrosine 3-monooxygenase/tryptophan 5-monooxygenase activation protein, gamma polypeptide	IPI00220642.7					x	x
YWHAH	7533	tyrosine 3-monooxygenase/tryptophan 5-monooxygenase activation protein, eta polypeptide	IPI00216319.3					x	x
YWHAQ	10971	tyrosine 3-monooxygenase/tryptophan 5-monooxygenase activation protein, theta polypeptide	IPI00018146	x	x				x
YWHAZ	7534	tyrosine 3-monooxygenase/tryptophan 5-monooxygenase activation protein, zeta polypeptide	IPI00021263		x		x	x	x
ZC3HAV1	56829	zinc finger CCCH-type, antiviral 1	IPI00332936		x			x	x
ZCCHC3	85364	zinc finger, CCHC domain containing 3	IPI00011550.1					x	x
ZNF609	23060	zinc finger protein 609	IPI00307591.5			x			
ZW10	9183	ZW10, kinetochore associated, homolog (Drosophila)	IPI00011631		x		x		

CHAPTER 5: SUMMARY OF FINDINGS AND FUTURE DIRECTIONS

The work presented here has unveiled a new paradigm in arenavirus biology and rekindles an interest in defective interfering particles both in terms of therapeutic implications as well as understanding arenavirus infections in their natural rodent reservoirs. This work also demonstrates the importance of understanding the interactions of viral proteins with their cellular hosts. There are a number of key questions that these studies have raised and will be logical extensions of this work.

Defective interfering particles are generally thought to be virus particles containing genomic deletions. The deletions in DI genomes are often fairly large, which is thought to confer a replicative advantage over longer, standard genomes (Huang and Baltimore, 1970; Lazzarini et al., 1981). The replicative advantage of truncated genomes in DI particles is thought to be the basis for DI particle-mediated interference (Huang and Baltimore, 1970). In the case of arenaviruses, however, a genetic basis for DI particles has yet to be confirmed. Meyer and Southern identified short truncations in the untranslated regions of LCMV genome segments which permitted genome replication but not transcription (Meyer and Southern, 1997). The truncated genomes were identified in both acute and persistent stages of LCMV infection (Meyer and Southern, 1997). They predicted that during the establishment of persistent infection, the ratio of intact to terminally truncated genomes would decrease resulting in decreased viral protein expression due to the inability of the truncated genomes to be transcribed (Meyer and Southern, 1997). While this alternate model of DI particle interference is plausible, it is yet unclear whether these truncated

genomes are packaged into DI particles and whether they can actually interfere with standard virus. Accordingly, modern sequencing technologies need to be employed to deep sequence the population of LCMV genomes in order to identify any additional deleted genomes that could be the basis for the DI phenotype. Fortunately, the PPXY late domain-mutant viruses generated in this work represent the first strains of LCMV known to produce very low levels of DI particles and could be used to purify viral RNA from a virtually DI particle-free population.

An additional shortcoming of previous work on arenavirus DI particles was the inability to actually test the impact of any identified mutations in the viral genome using a complete virus system. However, there now exists reverse genetics systems for several arenaviruses which permit genetic manipulation of the viral genome and recovery of recombinant viruses (Albariño et al., 2009; Albariño et al., 2011; Bergeron et al., 2012; Flatz et al., 2006; Lan et al., 2009; Pinschewer et al., 2003; Sanchez and De la Torre, 2006). In order to determine whether arenavirus DI particle interference is genome mediated, it will be important to use the LCMV reverse genetics system to test impact of the deletions identified in the untranslated regions by Meyer and Southern and any additional alternate genomes identified by deep sequencing. It is possible that some of the disrupted viral genomes may prevent recovery of an infectious arenavirus (which may in itself be indicative of a defective genome). In that case, the constructs used in the reverse genetics system to express the L or S genome segments, which are expressed under control of the cellular RNA polymerase I promoter (Flatz et al., 2006), could be expressed in cells that

are also infected with wild type LCMV. A decrease in the production of infectious LCMV following transfection of the defective genomes would indicate the ability of the genomes to interfere.

While the dogmatic view maintains that DI particle interference occurs through a genetic mechanism, the work presented in Chapter 2 may suggest an alternate, protein based mechanism. In particular, this work showed that DI particles are likely enriched in Z protein (Figure 2.3) and that DI particle release is regulated by the Z protein (Figure 2.5). Early studies on the composition of arenavirus DI particles concluded that the viral protein and genome composition were virtually indistinguishable from infectious virus particles (Welsh and Buchmeier, 1979). However, the arenavirus Z protein was not discovered until almost a decade after most of the work on arenavirus DI particles had ceased (Iapalucci et al., 1989; Salvato and Shimomaye, 1989). Curiously, the arenavirus Z protein inhibits viral genome replication and transcription through direct inhibition of the viral L polymerase in a dose dependent manner (Cornu and de la Torre, 2001, 2002; Jacamo et al., 2003a; Kranzusch and Whelan, 2011; Lopez et al., 2001). This inhibition of the polymerase by Z is correlated with the genetic relatedness of the Z and L proteins; the Old World arenavirus LCMV Z protein does not inhibit the polymerase of the New World arenavirus, Machupo, but the more closely related JUNV Z does (Kranzusch and Whelan, 2011). Also, overexpression of the LCMV Z protein renders cells refractory to LCMV but not vesicular stomatitis virus infection (Cornu and de la Torre, 2001). Such homologous interference is a hallmark of DI particles, though, it has been presumed to occur through a genome

mediated mechanism. Additionally, the amount of Z protein contained in a virus particle may provide a high enough concentration to inhibit the L polymerase (Kranzusch and Whelan, 2011). Therefore, arenavirus DI particle-mediated interference may at least in part occur through a mechanism by which the high levels of Z protein in DI particles interfere with both the replication and transcription of the viral genome. In order to determine whether particle-derived Z protein is sufficient to interfere with infectious virus, the LCMV Z protein in combination with the glycoprotein could be expressed via plasmid in cells in order to produce virus like particles (VLPs) that are capable of entering cells. These VLPs could then be added to cells and subsequently infected with LCMV. The level of interference could be assessed both by measurement of viral nucleoprotein levels in the cells as well as by measuring infectious virus titers by plaque assay. It would also be interesting to determine whether these VLPs could inhibit LCMV plaque formation. While it is clear that Z is an important regulator of arenavirus infections, it is difficult to imagine, however, that the Z protein's inhibition of the viral polymerase could alone mediate the very potent interference observed with DI particles. During a normal infection, the Z protein concentration in cells must increase from the levels prior to transcription and translation of the viral genome and mRNAs in order to produce new virions. Thus if Z's repression of the polymerase was too potent, the production of progeny virions would fail to occur.

Another interesting consideration with regard to LCMV DI particles, is that our work here was done with an LCMV strain, Armstrong 53b, which was isolated from an

infected patient in the first half of the 20th, century (Armstrong and Lillie, 1934; Cesar et al., 2010). This strain has been passaged in many different ways, so it begs the question of whether the sequence of the reverse genetics system that we used here (Armstrong 53b) is representative of strains of LCMV found in the wild or of disease-causing clinical isolates. A study that looked at a variety of LCMV strains, including both clinical isolates as well as mouse-derived strains revealed up to 28% nucleotide sequence divergence across the different LCMV strains (Delgado et al., 2008a). For the Z protein, this resulted in up to 18% sequence divergence at the amino acid level (Cesar et al., 2010). However, key motifs in Z including the G2 myristoylation site, the RING domain, the PPXY late domain, and the S41 phosphorylation site identified in this study were all highly conserved (Cesar et al., 2010). In addition, a key requirement for the functionality of arenavirus reverse genetics systems is having intact 5' and 3' untranslated regions (Flatz et al., 2006). Meyer and Southern found that populations of arenavirus genomes contain significant diversity in their untranslated regions (Meyer and Southern, 1994). These deletions were found both in genomic sense viral RNA as well as the anti-genomic RNA, indicating that at least some of the terminally deleted genomes can be used as a template by the viral polymerase, but are likely not transcription-competent (Meyer and Southern, 1994, 1997). Thus, it seems likely that the Armstrong 53b reverse genetics system here is representative of a standard, infectious virus particle and does not differ significantly from other LCMV strains with regard to key identified regions of the Z protein.

Since early studies on arenavirus DI particles in the 1970's, it has been hypothesized that DI particles are critical for maintaining persistent infections in their natural rodent hosts. One major obstacle to substantiating this has been the fact that arenaviruses naturally produce DI particles during the course of infection and thus are always producing a mixture of standard and DI particles. The late domain mutant viruses used in this work represent the first strains of LCMV that produce undetectable levels of DI particles. As the titers of standard virus reach the same levels as that of WT LCMV, it also expected that they would likely grow well *in vivo*. Thus, the late domain mutant strains of LCMV could be used in an *in vivo* model of *Mus musculus* infection to assess the overall requirement of DI particles in their natural hosts and to determine whether the DI particles mediate the protective effect that they are suspected to have.

The work presented in Chapter 2 demonstrates that the PPXY late domain in LCMV Z is a key regulator of DI particle production. We also provided evidence that the New World arenavirus, JUNV, which does not contain a PPXY late domain, produces drastically less DI particles than LCMV (Figure 2.S4). It is possible, therefore, that addition of a PPXY late domain to viral matrix proteins that do not contain a PPXY motif may increase the production of DI particles for that virus. It is also possible that adding additional PPXY late domains to PPXY-containing viral matrix proteins may serve to enhance DI particle production beyond normal levels. As discussed in chapter 1.3, DI particles have been shown to elicit protection against standard virus (Barrett and Dimmock, 1986; Dimmock and Kennedy, 1978; Doyle and Holland, 1973; Help and Coto, 1980; Holland and Doyle,

1973; Spandidos and Graham, 1976; Welsh et al., 1977; Welsh and Oldstone, 1977). Consequently, enhancing the ability of a virus to produce this protective class of particles may serve as a broad spectrum attenuation strategy which could be used to generate live-attenuated vaccines. Additionally, the data in Chapter 4 suggest that host-mediated phosphorylation of LCMV Z's PPXY late domain may serve as a positive regulator of DI particle production. Therefore, we hypothesize that blocking phosphorylation of the PPXY domain through small molecule inhibition of host kinases would decrease DI particle release resulting in decreased DI particle-mediated interference and ultimately would permit infectious virus to replicate less inhibited. Such a strategy could be used to more efficiently produce virus particles for an inactivated vaccine.

The initial finding which lead to the discovery that the PPXY late domain is required for DI particle formation was that Y88 in LCMV Z was phosphorylated. In chapter 2 we were able to demonstrate that LCMV is reversible phosphorylated at Y88 and that the phosphomimetic Y88E rLCMV produced more DI particles than the Y88F or Y88A rLCMV, though this increase did not meet statistical significance. This suggests that the host cell may be able to dynamically regulate the production of DI particles through phosphorylation of Y88 in LCMV Z using host kinases. A major advance in this area would be the identification of the host kinase(s) responsible for phosphorylation of Y88. While kinase prediction algorithms fail to predict a kinase for this tyrosine, particularly due to its location near the C-terminus of the protein, there exists some evidence that may help narrow the search for the kinase. The PPXY motif in Ebola VP40 is phosphorylated by c-

Abl1 kinase (García et al., 2012) and the host proteins IFITM3 and β-dystroglycan are phosphorylated on their PPXY motifs by the Src family tyrosine kinases, Fyn and Src, respectively (Chesarino et al., 2014; Sotgia et al., 2001). As we can readily detect Y88 phosphorylation in LCMV Z by western blotting and there are several available chemical inhibitors of these kinases (Garcia et al., 2012; Golas et al., 2003), it should be relatively straightforward to identify the kinase. As some of the potential kinase inhibitors are FDA-approved drugs, it is possible that they could also be tools used for *in vivo* LCMV infection. As the data with the phosphomimetic rLCMV Y88E suggests that phosphorylation positively regulates DI particle production, we would predict that treatment with the appropriate kinase inhibitor would decrease DI particle release which would provide an additional means of studying LCMV infection in a relatively DI particle-free environment.

A key open question for PPXY late domain containing viruses is how these late domains recruit the cellular ESCRT pathway. PPXY motifs are known to bind the WW-domains found in Nedd4 family E3 ubiquitin ligases (Chen and Sudol, 1995; Ingham et al., 2005; Ingham et al., 2004; Staub et al., 1996). Accordingly, recruitment of enzymatically active Nedd4 family ubiquitin ligases has been shown to be required for ESCRT recruitment in a number of viruses including filoviruses and retroviruses (Blot et al., 2004; Han et al., 2016; Martin-Serrano et al., 2005; Sakurai et al., 2004; Segura-Morales et al., 2005; Urata and Yasuda, 2010; Vana et al., 2004; Yasuda et al., 2003). These ligases may be required for the addition of a ubiquitin group to the viral PPXY-containing protein as has been shown for filovirus VP40, VSV M and some retroviral Gag proteins (Blot et al.,

2004; Han et al., 2016; Harty et al., 2001; Harty et al., 2000; Strack et al., 2000; Vana et al., 2004). Addition of a ubiquitin molecule to the viral protein could permit direct ESCRT linkage via the ubiquitin binding domains found in many of the ESCRT-0, -I and -II proteins (Shields et al., 2009). This potential model of ESCRT complex recruitment could be analogous to multivesicular body formation where ubiquitinated integral membrane proteins are recognized by the ESCRT-0 proteins which ultimately results in the recruitment of the ESCRT-III scission machinery (Hurley, 2008). An alternative model of ESCRT recruitment by PPXY-containing viral proteins has also been proposed in which the arrestin-related trafficking (ART) proteins may serve as a direct or indirect link to the ESCRT-III scission machinery for PPXY motifs (Rauch and Martin-Serrano, 2011).

For the arenaviruses, it has been shown that LASV Z can bind Nedd4 and Nedd4 drives VLP release (Fehling et al., 2012; Han et al., 2014). It will be important to determine which Nedd4 family ligases bind to LCMV Z's PPXY late domain, whether the Nedd4 ligases directly ubiquitinate the LCMV Z protein and whether ubiquitin conjugation is ultimately required for ESCRT recruitment to sites of Z-mediated budding and for DI particle release. To facilitate these future studies, mapping the Z-host protein interactome for the Old World arenaviruses, LCMV and LASV, as we have done for JUNV Z in this work, may permit identification of proteins that interact with LCMV Z including Nedd4 family ligases, ESCRT proteins, tyrosine kinases, and SH2 domain-containing proteins. Such studies may help to provide clues to the molecular link between the PPXY late domain and the late-acting ESCRT scission machinery. Finally, determining whether

phosphorylation of the PPXY late domain regulates Nedd4 ligase binding and subsequent ESCRT pathway recruitment will help to build a more complete picture of host cell-mediated regulation of DI particle release. Such regulation of PPXY motifs has been demonstrated for the cellular proteins IFITM3 and β-dytroglycan (Chesarino et al., 2015; Sotgia et al., 2001).

The ESCRT pathway represents the only known cellular machinery capable of mediating membrane scission for membrane extrusion away from the cytoplasm (Schoneberg et al., 2017). Accordingly, many enveloped viruses depend on the ESCRT pathway for efficient virus release (Votteler and Sundquist, 2013). However, there are several examples of enveloped viruses that do not depend on ESCRT including Semliki Forest virus, influenza A virus, respiratory syncytial virus, and Andes virus (Bruce et al., 2010; Bruce et al., 2009; Rowe et al., 2008; Taylor et al., 2007; Utley et al., 2008). The data presented in Chapter 2 demonstrate that the production of infectious LCMV virions is not dependent on the Z protein's PPXY late domain or the cellular ESCRT pathway which raises the question of how infectious virus particles are released from cells. The PPXY late domain represents the only canonical late domain in LCMV Z. The only other site within LCMV Z that is known to impact virus release is the glycine residue at position 2, which is myristoylated and regulates membrane association of Z (Perez et al., 2004a; Strecker et al., 2006). In Chapter 3, we present data suggesting that a novel motif in LCMV Z, S41, that does not appear to resemble motifs found in other viruses required for release, is important for both infectious and DI particle release. A phosphomimetic substitution at S41

decreased both infectious and DI particle release, indicating that the host cell may be regulating the ability of this motif to mediate virus release. However, it remains to be determined whether S41 requires interaction with specific host machinery in order to drive virion release and what the identity of that machinery is. Semliki Forest virus appears to be capable of driving membrane budding and fission through the action of its external glycoprotein and thus it is possible that release of infectious virus particles could happen without any cellular machinery (Votteler and Sundquist, 2013).

Various host machinery may be recruited by the Z protein in order to facilitate infectious virus release. In chapter 4, we identified several host proteins that may impact arenavirus release. The ATPase, ATP5B, was required for infection of both JUNV and LCMV. This protein co-purified with JUNV, LCMV and LASV Z from both transfected cells and in VLP-derived Z. This protein, ATP5B, has been shown to be required for the release of influenza A virus VLPs at the plasma membrane (Gorai et al., 2012). Accordingly, ATP5B is found in Z VLPs which suggests that it may be required at late steps in the virus life cycle. Additional studies are needed to determine the precise step in the virus life cycle in which ATP5B functions, but the evidence points to a possible role in virus release. An abundance of Rab family proteins were also identified in JUNV C#1 virions which may similarly suggest a role in late steps of arenavirus release. One of these proteins, Rab5c was shown to be required during LCMV infection in Chapter 4, but it is unclear the specific viral function Rab5c depletion impacts. (Bruce et al., 2010; Bruce et al., 2012). Rab family proteins are important regulators of intracellular vesicular trafficking

and Rab11 in particular has been shown to impact the budding and release of ESCRT-independent viruses including the bunyavirus, Andes virus (Bruce et al., 2012; Vale-Costa and Amorim, 2016). Whether Rab proteins contribute to arenavirus assembly and release beyond trafficking of viral components to sites of assembly remains to be determined. In summary, this study has provided the groundwork for the identification of factors potentially involved in the ESCRT-independent budding of LCMV.

Finally, in Chapter 4, a long list of JUNV Z host protein partners were identified. We were able to demonstrate the functional importance of several of the proteins in JUNV and LCMV infection. The siRNA studies did not, however, reveal the mechanism by which the various proteins contribute to the arenavirus life cycle. One of the identified proteins, ARF1, is particularly interesting as this protein regulates cargo release from the ER-Golgi intermediate compartment (ERGIC) and the Botten lab has recently shown that ERGIC-53 is a key regulator of infectivity of JUNV virus particles (Donaldson and Jackson, 2011; Klaus et al., 2013). It would be enlightening to determine whether ARF1 depletion results in a failure of ERGIC-53 or the JUNV glycoprotein to traffic through the secretory pathway resulting in a loss of infectivity of released virions. There are also many other proteins which were identified as Z protein partners for which the functional relevance has not been determined. A comprehensive functional screen of the identified Z protein partners would be a valuable next step that may allow identification of essential host proteins which could be therapeutically targeted in order to treat arenavirus infections.

A large scale silencing (si)RNA screen targeting Z protein partners would be one effective approach for identifying functionally important targets. Such screening has been done on a genome-wide level for several viruses including HIV (Brass et al., 2008; König et al., 2008; Zhou et al., 2008), influenza virus (Brass et al., 2009; Karlas et al., 2010; Konig et al., 2010; Shapira et al., 2009), dengue virus (Sessions et al., 2009), hepatitis C virus (Li et al., 2009b; Tai et al., 2009), West Nile virus (Krishnan et al., 2008), and vesicular stomatitis virus (Lee et al., 2014; Panda et al., 2011). The 2011 study on VSV (Panda et al., 2011), also conducted a functional siRNA screen targeting 72 of the host proteins required for VSV. Several of the targeted proteins that were required for LCMV infection in that study including ARF1, COPA, COPB1, EIF3A, HNRNPK, HSPA9, NOP56, and RAB5C were also identified as JUNV Z protein partners in this work (see Table 4.S1). Building on this data with a broader scope RNAi screen for arenaviruses including all of the identified Z protein partners or potentially a genome-wide screen would provide a powerful combination of functional data and the virus-host protein interaction network. Such a study would aid future work focusing on the functional roles of the Z protein's host partners and would help in the rational design of therapeutics that impinge on the molecular networks of host proteins that contribute to the arenavirus life cycle .

References

Albariño, C.G., Bergeron, É., Erickson, B.R., Khristova, M.L., Rollin, P.E., and Nichol, S.T. (2009). Efficient Reverse Genetics Generation of Infectious Junin Viruses Differing in Glycoprotein Processing. J Virol *83*, 5606-5614.

Albariño, C.G., Bird, B.H., Chakrabarti, A.K., Dodd, K.A., Flint, M., Bergeron, É., White, D.M., and Nichol, S.T. (2011). The Major Determinant of Attenuation in Mice of the Candid1 Vaccine for Argentine Hemorrhagic Fever Is Located in the G2 Glycoprotein Transmembrane Domain. J Virol *85*, 10404-10408.

Armstrong, C., and Lillie, R.D. (1934). Experimental Lymphocytic Choriomeningitis of Monkeys and Mice Produced by a Virus Encountered in Studies of the 1933 St. Louis Encephalitis Epidemic. Public Health Reports (1896-1970) *49*, 1019-1027.

Barrett, A.D.T., and Dimmock, N.J. (1986). Defective Interfering Viruses and Infections of Animals. In Current Topics in Microbiology and Immunology, A. Clarke, R.W. Compans, M. Cooper, H. Eisen, W. Goebel, H. Koprowski, F. Melchers, M. Oldstone, R. Rott, P.K. Vogt*, et al.*, eds. (Berlin, Heidelberg: Springer Berlin Heidelberg), pp. 55-84.

Bergeron, É., Chakrabarti, A.K., Bird, B.H., Dodd, K.A., McMullan, L.K., Spiropoulou, C.F., Nichol, S.T., and Albariño, C.G. (2012). Reverse Genetics Recovery of Lujo Virus and Role of Virus RNA Secondary Structures in Efficient Virus Growth. J Virol *86*, 10759-10765.

Blot, V., Perugi, F., Gay, B., Prévost, M.-C., Briant, L., Tangy, F., Abriel, H., Staub, O., Dokhélar, M.-C., and Pique, C. (2004). Nedd4.1-mediated ubiquitination and subsequent recruitment of Tsg101 ensure HTLV-1 Gag trafficking towards the multivesicular body pathway prior to virus budding. J Cell Sci *117*, 2357-2367.

Brass, A.L., Dykxhoorn, D.M., Benita, Y., Yan, N., Engelman, A., Xavier, R.J., Lieberman, J., and Elledge, S.J. (2008). Identification of Host Proteins Required for HIV Infection Through a Functional Genomic Screen. Science *319*, 921-926.

Brass, A.L., Huang, I.C., Benita, Y., John, S.P., Krishnan, M.N., Feeley, E.M., Ryan, B.J., Weyer, J.L., van der Weyden, L., Fikrig, E.*, et al.* (2009). The IFITM Proteins Mediate Cellular Resistance to Influenza A H1N1 Virus, West Nile Virus, and Dengue Virus. Cell *139*, 1243-1254.

Bruce, E.A., Digard, P., and Stuart, A.D. (2010). The Rab11 Pathway Is Required for Influenza A Virus Budding and Filament Formation. J Virol *84*, 5848-5859.

Bruce, E.A., Medcalf, L., Crump, C.M., Noton, S.L., Stuart, A.D., Wise, H.M., Elton, D., Bowers, K., and Digard, P. (2009). Budding of filamentous and non-filamentous influenza A virus occurs via a VPS4 and VPS28-independent pathway. Virology *390*, 268-278.

Bruce, Emily A., Stuart, A., McCaffrey, Mary W., and Digard, P. (2012). Role of the Rab11 pathway in negative-strand virus assembly. Biochemical Society transactions *40*, 1409-1415.

Cesar, G.A., Gustavo, P., Marina, L.K., Bobbie, R.E., Serena, A.C., James, A.C., Jeffrey, H., Thomas, B., Kirsten St, G., Thomas, G.K.*, et al.* (2010). High Diversity and Ancient Common Ancestry of Lymphocytic Choriomeningitis Virus. Emerging Infectious Disease journal *16*, 1093.

Chen, H.I., and Sudol, M. (1995). The WW domain of Yes-associated protein binds a proline-rich ligand that differs from the consensus established for Src homology 3-binding modules. Proceedings of the National Academy of Sciences *92*, 7819-7823.

Chesarino, N.M., McMichael, T.M., Hach, J.C., and Yount, J.S. (2014). Phosphorylation of the Antiviral Protein Interferon-inducible Transmembrane Protein 3 (IFITM3) Dually Regulates Its Endocytosis and Ubiquitination. J Biol Chem *289*, 11986-11992.

Chesarino, N.M., McMichael, T.M., and Yount, J.S. (2015). E3 Ubiquitin Ligase NEDD4 Promotes Influenza Virus Infection by Decreasing Levels of the Antiviral Protein IFITM3. PLOS Pathogens *11*, e1005095.

Cornu, T.I., and de la Torre, J.C. (2001). RING finger Z protein of lymphocytic choriomeningitis virus (LCMV) inhibits transcription and RNA replication of an LCMV S-segment minigenome. J Virol *75*, 9415-9426.

Cornu, T.I., and de la Torre, J.C. (2002). Characterization of the arenavirus RING finger Z protein regions required for Z-mediated inhibition of viral RNA synthesis. J Virol *76*, 6678-6688.

Delgado, S., Erickson, B.R., Agudo, R., Blair, P.J., Vallejo, E., Albarino, C.G., Vargas, J., Comer, J.A., Rollin, P.E., Ksiazek, T.G.*, et al.* (2008a). Chapare virus, a newly discovered arenavirus isolated from a fatal hemorrhagic fever case in Bolivia. Plos Pathogens *4*.

Dimmock, N.J., and Kennedy, S.I.T. (1978). Prevention of Death in Semliki Forest Virus-Infected Mice by Administration of Defective-Interfering Semliki Forest Virus. J Gen Virol *39*, 231-242.

Donaldson, J.G., and Jackson, C.L. (2011). ARF family G proteins and their regulators: roles in membrane transport, development and disease. Nat Rev Mol Cell Biol *12*, 362-375.

Doyle, M., and Holland, J.J. (1973). Prophylaxis and Immunization in Mice by Use of Virus-Free Defective T Particles to Protect Against Intracerebral Infection by Vesicular Stomatitis Virus. Proc Natl Acad Sci USA *70*, 2105-2108.

Fehling, S., Lennartz, F., and Strecker, T. (2012). Multifunctional Nature of the Arenavirus RING Finger Protein Z. Viruses *4*, 2973-3011.

Flatz, L., Bergthaler, A., de la Torre, J.C., and Pinschewer, D.D. (2006). Recovery of an arenavirus entirely from RNA polymerase I/II-driven cDNA. Proc Natl Acad Sci USA *103*, 4663-4668.

Garcia, M., Cooper, A., Shi, W., Bornmann, W., Carrion, R., Kalman, D., and Nabel, G.J. (2012). Productive replication of Ebola virus is regulated by the c-Abl1 tyrosine kinase. Sci Transl Med *4*.

García, M., Cooper, A., Shi, W., Bornmann, W., Carrion, R., Kalman, D., and Nabel, G.J. (2012). Productive Replication of Ebola Virus Is Regulated by the c-Abl1 Tyrosine Kinase. Sci Transl Med *4*, 123ra124.

Golas, J.M., Arndt, K., Etienne, C., Lucas, J., Nardin, D., Gibbons, J., Frost, P., Ye, F., Boschelli, D.H., and Boschelli, F. (2003). SKI-606, a 4-Anilino-3-quinolinecarbonitrile Dual Inhibitor of Src and Abl Kinases, Is a Potent Antiproliferative Agent against Chronic Myelogenous Leukemia Cells in Culture and Causes Regression of K562 Xenografts in Nude Mice. Cancer Research *63*, 375-381.

Gorai, T., Goto, H., Noda, T., Watanabe, T., Kozuka-Hata, H., Oyama, M., Takano, R., Neumann, G., Watanabe, S., and Kawaoka, Y. (2012). F1Fo-ATPase, F-type proton-translocating ATPase, at the plasma membrane is critical for efficient influenza virus budding. Proceedings of the National Academy of Sciences.

Han, Z., Lu, J., Liu, Y., Davis, B., Lee, M.S., Olson, M.A., Ruthel, G., Freedman, B.D., Schnell, M.J., Wrobel, J.E*., et al.* (2014). Small Molecule Probes Targeting the Viral PPxY-Host Nedd4 Interface Block Egress of a Broad Range of RNA Viruses. J Virol.

Han, Z., Sagum, C.A., Bedford, M.T., Sidhu, S.S., Sudol, M., and Harty, R.N. (2016). ITCH E3 Ubiquitin Ligase Interacts with Ebola Virus VP40 To Regulate Budding. J Virol *90*, 9163-9171.

Harty, R.N., Brown, M.E., McGettigan, J.P., Wang, G., Jayakar, H.R., Huibregtse, J.M., Whitt, M.A., and Schnell, M.J. (2001). Rhabdoviruses and the Cellular Ubiquitin-Proteasome System: a Budding Interaction. J Virol *75*, 10623-10629.

Harty, R.N., Brown, M.E., Wang, G., Huibregtse, J., and Hayes, F.P. (2000). A PPxY motif within the VP40 protein of Ebola virus interacts physically and functionally with a

ubiquitin ligase: Implications for filovirus budding. Proceedings of the National Academy of Sciences *97*, 13871-13876.

Help, G.I., and Coto, C.E. (1980). [Genesis of interferent particles during the multiplication of Junin virus in vivo]. Medicina (B Aires) *40*, 531-536.

Holland, J.J., and Doyle, M. (1973). Attempts to Detect Homologous Autointerference In vivo with Influenza Virus and Vesicular Stomatitis Virus. Infect Immun *7*, 526-531.

Huang, A.S., and Baltimore, D. (1970). Defective Viral Particles and Viral Disease Processes. Nature *226*, 325-327.

Hurley, J.H. (2008). ESCRT complexes and the biogenesis of multivesicular bodies. Curr Opin Cell Biol *20*, 4-11.

Iapalucci, S., López, N., Rey, O., Zakin, M.M., Cohen, G.N., and Franze-Fernández, M.T. (1989). The 5′ region of Tacaribe virus L RNA encodes a protein with a potential metal binding domain. Virology *173*, 357-361.

Ingham, R.J., Colwill, K., Howard, C., Dettwiler, S., Lim, C.S.H., Yu, J., Hersi, K., Raaijmakers, J., Gish, G., Mbamalu, G.*, et al.* (2005). WW Domains Provide a Platform for the Assembly of Multiprotein Networks. Molecular and Cellular Biology *25*, 7092-7106.

Ingham, R.J., Gish, G., and Pawson, T. (2004). The Nedd4 family of E3 ubiquitin ligases: functional diversity within a common modular architecture. Oncogene *23*.

Jacamo, R., Lopez, N., Wilda, M., and Franze-Fernandez, M.T. (2003a). Tacaribe Virus Z Protein Interacts with the L Polymerase Protein To Inhibit Viral RNA Synthesis. J Virol *77*, 10383-10393.

Karlas, A., Machuy, N., Shin, Y., Pleissner, K.-P., Artarini, A., Heuer, D., Becker, D., Khalil, H., Ogilvie, L.A., Hess, S.*, et al.* (2010). Genome-wide RNAi screen identifies human host factors crucial for influenza virus replication. Nature *463*, 818-822.

Klaus, J.P., Eisenhauer, P., Russo, J., Mason, A.B., Do, D., King, B., Taatjes, D., Cornillez-Ty, C., Boyson, J.E., Thali, M.*, et al.* (2013). The intracellular cargo receptor ERGIC-53 is required for the production of infectious arenavirus, coronavirus, and filovirus particles. Cell Host Microbe *14*, 522-534.

Konig, R., Stertz, S., Zhou, Y., Inoue, A., Hoffmann, H.H., Bhattacharyya, S., Alamares, J.G., Tscherne, D.M., Ortigoza, M.B., Liang, Y.*, et al.* (2010). Human host factors required for influenza virus replication. Nature *463*, 813-817.

König, R., Zhou, Y., Elleder, D., Diamond, T.L., Bonamy, G.M.C., Irelan, J.T., Chiang, C.-y., Tu, B.P., De Jesus, P.D., Lilley, C.E.*, et al.* (2008). Global Analysis of Host-Pathogen Interactions that Regulate Early-Stage HIV-1 Replication. Cell *135*, 49-60.

Kranzusch, P.J., and Whelan, S.P.J. (2011). Arenavirus Z protein controls viral RNA synthesis by locking a polymerase–promoter complex. Proceedings of the National Academy of Sciences *108*, 19743-19748.

Krishnan, M.N., Ng, A., Sukumaran, B., Gilfoy, F.D., Uchil, P.D., Sultana, H., Brass, A.L., Adametz, R., Tsui, M., Qian, F.*, et al.* (2008). RNA interference screen for human genes associated with West Nile virus infection. Nature *455*, 242-245.

Lan, S., McLay Schelde, L., Wang, J., Kumar, N., Ly, H., and Liang, Y. (2009). Development of Infectious Clones for Virulent and Avirulent Pichinde Viruses: a Model Virus To Study Arenavirus-Induced Hemorrhagic Fevers. J Virol *83*, 6357-6362.

Lazzarini, R.A., Keene, J.D., and Schubert, M. (1981). The origins of defective interfering particles of the negative-strand RNA viruses. Cell *26*.

Lee, A.S.-Y., Burdeinick-Kerr, R., and Whelan, S.P.J. (2014). A genome-wide siRNA screen identifies host factors required for vesicular stomatitis virus infection. J Virol.

Li, Q., Brass, A.L., Ng, A., Hu, Z., Xavier, R.J., Liang, T.J., and Elledge, S.J. (2009b). A genome-wide genetic screen for host factors required for hepatitis C virus propagation. Proceedings of the National Academy of Sciences.

Lopez, N., Jacamo, R., and Franze-Fernandez, M.T. (2001). Transcription and RNA Replication of Tacaribe Virus Genome and Antigenome Analogs Require N and L Proteins: Z Protein Is an Inhibitor of These Processes. J Virol *75*, 12241-12251.

Martin-Serrano, J., Eastman, S.W., Chung, W., and Bieniasz, P.D. (2005). HECT ubiquitin ligases link viral and cellular PPXY motifs to the vacuolar protein-sorting pathway. The Journal of Cell Biology *168*, 89-101.

Meyer, B.J., and Southern, P.J. (1994). Sequence heterogeneity in the termini of lymphocytic choriomeningitis virus genomic and antigenomic RNAs. J Virol *68*, 7659-7664.

Meyer, B.J., and Southern, P.J. (1997). A novel type of defective viral genome suggests a unique strategy to establish and maintain persistent lymphocytic choriomeningitis virus infections. J Virol *71*, 6757-6764.

Panda, D., Das, A., Dinh, P.X., Subramaniam, S., Nayak, D., Barrows, N.J., Pearson, J.L., Thompson, J., Kelly, D.L., Ladunga, I.*, et al.* (2011). RNAi screening reveals requirement

for host cell secretory pathway in infection by diverse families of negative-strand RNA viruses. Proceedings of the National Academy of Sciences *108*, 19036-19041.

Perez, M., Greenwald, D.L., and de La Torre, J.C. (2004a). Myristoylation of the RING finger Z protein is essential for arenavirus budding. J Virol *78*, 11443-11448.

Pinschewer, D.D., Perez, M., Sanchez, A.B., and de la Torre, J.C. (2003). Recombinant lymphocytic choriomeningitis virus expressing vesicular stomatitis virus glycoprotein. Proceedings of the National Academy of Sciences *100*, 7895-7900.

Rauch, S., and Martin-Serrano, J. (2011). Multiple Interactions between the ESCRT Machinery and Arrestin-Related Proteins: Implications for PPXY-Dependent Budding. J Virol *85*, 3546-3556.

Rowe, R.K., Suszko, J.W., and Pekosz, A. (2008). Roles for the recycling endosome, Rab8, and Rab11 in hantavirus release from epithelial cells. Virology *382*, 239-249.

Sakurai, A., Yasuda, J., Takano, H., Tanaka, Y., Hatakeyama, M., and Shida, H. (2004). Regulation of human T-cell leukemia virus type 1 (HTLV-1) budding by ubiquitin ligase Nedd4. Microbes Infect *6*, 150-156.

Salvato, M.S., and Shimomaye, E.M. (1989). The completed sequence of lymphocytic choriomeningitis virus reveals a unique RNA structure and a gene for a zinc finger protein. Virology *173*, 1-10.

Sanchez, A.B., and De la Torre, J.C. (2006). Rescue of the prototypic Arenavirus LCMV entirely from plasmid. Virology *350*, 370-380.

Schoneberg, J., Lee, I.-H., Iwasa, J.H., and Hurley, J.H. (2017). Reverse-topology membrane scission by the ESCRT proteins. Nat Rev Mol Cell Biol *18*, 5-17.

Segura-Morales, C., Pescia, C., Chatellard-Causse, C., Sadoul, R., Bertrand, E., and Basyuk, E. (2005). Tsg101 and Alix Interact with Murine Leukemia Virus Gag and Cooperate with Nedd4 Ubiquitin Ligases during Budding. J Biol Chem *280*, 27004-27012.

Sessions, O.M., Barrows, N.J., Souza-Neto, J.A., Robinson, T.J., Hershey, C.L., Rodgers, M.A., Ramirez, J.L., Dimopoulos, G., Yang, P.L., Pearson, J.L.*, et al.* (2009). Discovery of insect and human dengue virus host factors. Nature *458*, 1047-1050.

Shapira, S.D., Gat-Viks, I., Shum, B.O.V., Dricot, A., de Grace, M.M., Wu, L., Gupta, P.B., Hao, T., Silver, S.J., Root, D.E.*, et al.* (2009). A Physical and Regulatory Map of Host-Influenza Interactions Reveals Pathways in H1N1 Infection. Cell *139*, 1255-1267.

Shields, S.B., Oestreich, A.J., Winistorfer, S., Nguyen, D., Payne, J.A., Katzmann, D.J., and Piper, R. (2009). ESCRT ubiquitin-binding domains function cooperatively during MVB cargo sorting. The Journal of Cell Biology *185*, 213-224.

Sotgia, F., Lee, H., Bedford, M.T., Petrucci, T., Sudol, M., and Lisanti, M.P. (2001). Tyrosine Phosphorylation of β-Dystroglycan at Its WW Domain Binding Motif, PPxY, Recruits SH2 Domain Containing Proteins†. Biochemistry *40*, 14585-14592.

Spandidos, D.A., and Graham, A.F. (1976). Generation of defective virus after infection of newborn rats with reovirus. J Virol *20*, 234-247.

Staub, O., Dho, S., Henry, P., Correa, J., Ishikawa, T., McGlade, J., and Rotin, D. (1996). WW domains of Nedd4 bind to the proline-rich PY motifs in the epithelial Na+ channel deleted in Liddle's syndrome. Embo j *15*, 2371-2380.

Strack, B., Calistri, A., Accola, M.A., Palù, G., and Göttlinger, H.G. (2000). A role for ubiquitin ligase recruitment in retrovirus release. Proceedings of the National Academy of Sciences *97*, 13063-13068.

Strecker, T., Maisa, A., Daffis, S., Eichler, R., Lenz, O., and Garten, W. (2006). The role of myristoylation in the membrane association of the Lassa virus matrix protein Z. Virology Journal *3*, 93.

Tai, A.W., Benita, Y., Peng, L.F., Kim, S.-S., Sakamoto, N., Xavier, R.J., and Chung, R.T. (2009). A Functional Genomic Screen Identifies Cellular Cofactors of Hepatitis C Virus Replication. Cell Host & Microbe *5*, 298-307.

Taylor, G.M., Hanson, P.I., and Kielian, M. (2007). Ubiquitin Depletion and Dominant-Negative VPS4 Inhibit Rhabdovirus Budding without Affecting Alphavirus Budding. J Virol *81*, 13631-13639.

Urata, S., and Yasuda, J. (2010). Regulation of Marburg virus (MARV) budding by Nedd4.1: a different WW domain of Nedd4.1 is critical for binding to MARV and Ebola virus VP40. Journal of General Virology *91*, 228-234.

Utley, T.J., Ducharme, N.A., Varthakavi, V., Shepherd, B.E., Santangelo, P.J., Lindquist, M.E., Goldenring, J.R., and Crowe, J.E. (2008). Respiratory syncytial virus uses a Vps4-independent budding mechanism controlled by Rab11-FIP2. Proceedings of the National Academy of Sciences *105*, 10209-10214.

Vale-Costa, S., and Amorim, M. (2016). Recycling Endosomes and Viral Infection. Viruses *8*, 64.

Vana, M.L., Tang, Y., Chen, A., Medina, G., Carter, C., and Leis, J. (2004). Role of Nedd4 and ubiquitination of Rous sarcoma virus Gag in budding of virus-like particles from cells. J Virol *78*, 13943-13953.

Votteler, J., and Sundquist, Wesley I. (2013). Virus Budding and the ESCRT Pathway. Cell Host & Microbe *14*, 232-241.

Welsh, R.M., and Buchmeier, M.J. (1979). Protein analysis of defective interfering lymphocytic choriomeningitis virus and persistently infected cells. Virology *96*.

Welsh, R.M., Lampert, P.W., and Oldstone, M.B. (1977). Prevention of virus-induced cerebellar diseases by defective-interfering lymphocytic choriomeningitis virus. The Journal of infectious diseases *136*.

Welsh, R.M., and Oldstone, M.B. (1977). Inhibition of immunologic injury of cultured cells infected with lymphocytic choriomeningitis virus: role of defective interfering virus in regulating viral antigenic expression. J Exp Med *145*, 1449-1468.

Yasuda, J., Nakao, M., Kawaoka, Y., and Shida, H. (2003). Nedd4 Regulates Egress of Ebola Virus-Like Particles from Host Cells. Journal of Virology *77*, 9987-9992.

Zhou, H., Xu, M., Huang, Q., Gates, A.T., Zhang, X.D., Castle, J.C., Stec, E., Ferrer, M., Strulovici, B., Hazuda, D.J.*, et al.* (2008). Genome-Scale RNAi Screen for Host Factors Required for HIV Replication. Cell Host & Microbe *4*, 495-504.

COMPREHENSIVE BIBLIOGRAPHY

Abraham, G., and Banerjee, A.K. (1976). Sequential transcription of the genes of vesicular stomatitis virus. Proc Natl Acad Sci U S A *73*, 1504-1508.

Ahmed, R., and Graham, A.F. (1977). Persistent Infections in L Cells with Temperature-Sensitive Mutants of Reovirus. J Virol *23*, 250-262.

Albariño, C.G., Bergeron, É., Erickson, B.R., Khristova, M.L., Rollin, P.E., and Nichol, S.T. (2009). Efficient Reverse Genetics Generation of Infectious Junin Viruses Differing in Glycoprotein Processing. J Virol *83*, 5606-5614.

Albariño, C.G., Bird, B.H., Chakrabarti, A.K., Dodd, K.A., Flint, M., Bergeron, É., White, D.M., and Nichol, S.T. (2011). The Major Determinant of Attenuation in Mice of the Candid1 Vaccine for Argentine Hemorrhagic Fever Is Located in the G2 Glycoprotein Transmembrane Domain. J Virol *85*, 10404-10408.

Alenquer, M., and Amorim, M.J. (2015). Exosome Biogenesis, Regulation, and Function in Viral Infection. Viruses *7*, 5066-5083.

Andzhaparidze, O.G., Boriskin, Y.S., Bogomolova, N.N., and Drynov, I.D. (1982). Mumps Virus-persistently Infected Cell Cultures Release Defective Interfering Virus Particles. J Gen Virol *63*, 499-503.

Armstrong, C., and Lillie, R.D. (1934). Experimental Lymphocytic Choriomeningitis of Monkeys and Mice Produced by a Virus Encountered in Studies of the 1933 St. Louis Encephalitis Epidemic. Public Health Reports (1896-1970) *49*, 1019-1027.

Auperin, D.D., Sasso, D.R., and McCormick, J.B. (1986). Nucleotide sequence of the glycoprotein gene and intergenic region of the Lassa virus S genome RNA. Virology *154*, 155-167.

Bache, K.G., Brech, A., Mehlum, A., and Stenmark, H. (2003a). Hrs regulates multivesicular body formation via ESCRT recruitment to endosomes. The Journal of Cell Biology *162*, 435-442.

Bache, K.G., Raiborg, C., Mehlum, A., and Stenmark, H. (2003b). STAM and Hrs Are Subunits of a Multivalent Ubiquitin-binding Complex on Early Endosomes. J Biol Chem *278*, 12513-12521.

Baietti, M.F., Zhang, Z., Mortier, E., Melchior, A., Degeest, G., Geeraerts, A., Ivarsson, Y., Depoortere, F., Coomans, C., Vermeiren, E.*, et al.* (2012). Syndecan-syntenin-ALIX regulates the biogenesis of exosomes. Nat Cell Biol *14*, 677-685.

Bajorek, M., Caly, L., Tran, K.C., Maertens, G.N., Tripp, R.A., Bacharach, E., Teng, M.N., Ghildyal, R., and Jans, D.A. (2014). The Thr205 Phosphorylation Site within Respiratory Syncytial Virus Matrix (M) Protein Modulates M Oligomerization and Virus Production. J Virol *88*, 6380-6393.

Ballif, B.A., Carey, G.R., Sunyaev, S.R., and Gygi, S.P. (2008). Large-Scale Identification and Evolution Indexing of Tyrosine Phosphorylation Sites from Murine Brain. J Proteome Res *7*, 311-318.

Barrett, A.D.T., and Dimmock, N.J. (1986). Defective Interfering Viruses and Infections of Animals. In Current Topics in Microbiology and Immunology, A. Clarke, R.W. Compans, M. Cooper, H. Eisen, W. Goebel, H. Koprowski, F. Melchers, M. Oldstone, R. Rott, P.K. Vogt*, et al.*, eds. (Berlin, Heidelberg: Springer Berlin Heidelberg), pp. 55-84.

Barton, L.L., Mets, M.B., and Beauchamp, C.L. (2002). Lymphocytic choriomeningitis virus: Emerging fetal teratogen. American Journal of Obstetrics & Gynecology *187*, 1715-1716.

Battegay, M., Cooper, S., Althage, A., Bänziger, J., Hengartner, H., and Zinkernagel, R.M. (1991). Quantification of lymphocytic choriomeningitis virus with an immunological focus assay in 24- or 96-well plates. Journal of Virological Methods *33*, 191-198.

Bausch, D.G., Towner, J.S., Dowell, S.F., Kaducu, F., Lukwiya, M., Sanchez, A., Nichol, S.T., Ksiazek, T.G., and Rollin, P.E. (2007). Assessment of the Risk of Ebola Virus Transmission from Bodily Fluids and Fomites. J Infect Dis *196*, S142-S147.

Bay, P.H., and Reichmann, M.E. (1979). UV inactivation of the biological activity of defective interfering particles generated by vesicular stomatitis virus. J Virol *32*, 876-884.

Bellett, A.J., and Cooper, P.D. (1959). Some properties of the transmissible interfering component of vesicular stomatitis virus preparations. Journal of general microbiology *21*, 498-509.

Bergeron, É., Chakrabarti, A.K., Bird, B.H., Dodd, K.A., McMullan, L.K., Spiropoulou, C.F., Nichol, S.T., and Albariño, C.G. (2012). Reverse Genetics Recovery of Lujo Virus and Role of Virus RNA Secondary Structures in Efficient Virus Growth. J Virol *86*, 10759-10765.

Blot, V., Perugi, F., Gay, B., Prévost, M.-C., Briant, L., Tangy, F., Abriel, H., Staub, O., Dokhélar, M.-C., and Pique, C. (2004). Nedd4.1-mediated ubiquitination and subsequent recruitment of Tsg101 ensure HTLV-1 Gag trafficking towards the multivesicular body pathway prior to virus budding. J Cell Sci *117*, 2357-2367.

Boldogh, I., Albrecht, T., and Porter, D.D. (1996). Persistent Viral Infections. In Medical Microbiology, S. Baron, ed. (Galveston (TX): University of Texas Medical Branch at Galveston
The University of Texas Medical Branch at Galveston.).

Bonthius, D.J. (2012). Lymphocytic choriomeningitis virus: An under-recognized cause of neurologic disease in the fetus, child, and adult. Seminars in pediatric neurology *19*, 89-95.

Borden, K.L.B., Campbelldwyer, E.J., Carlile, G.W., Djavani, M., and Salvato, M.S. (1998a). Two RING finger proteins, the oncoprotein PML and the arenavirus Z protein, colocalize with the nuclear fraction of the ribosomal P proteins. J Virol *72*, 3819-3826.

Borden, K.L.B., Dwyer, E.J.C., and Salvato, M.S. (1998b). An arenavirus RING (zinc-binding) protein binds the oncoprotein promyelocyte leukemia protein (PML) and relocates PML nuclear bodies to the cytoplasm. J Virol *72*, 758-766.

Borrow, P., and Oldstone, M.B.A. (1994). Mechanism of Lymphocytic Choriomeningitis Virus Entry into Cells. Virology *198*, 1-9.

Bouamr, F., Melillo, J.A., Wang, M.Q., Nagashima, K., de Los Santos, M., Rein, A., and Goff, S.P. (2003). PPPYEPTAP Motif Is the Late Domain of Human T-Cell Leukemia Virus Type 1 Gag and Mediates Its Functional Interaction with Cellular Proteins Nedd4 and Tsg101. J Virol *77*, 11882-11895.

Brass, A.L., Dykxhoorn, D.M., Benita, Y., Yan, N., Engelman, A., Xavier, R.J., Lieberman, J., and Elledge, S.J. (2008). Identification of Host Proteins Required for HIV Infection Through a Functional Genomic Screen. Science *319*, 921-926.

Brass, A.L., Huang, I.C., Benita, Y., John, S.P., Krishnan, M.N., Feeley, E.M., Ryan, B.J., Weyer, J.L., van der Weyden, L., Fikrig, E.*, et al.* (2009). The IFITM Proteins Mediate Cellular Resistance to Influenza A H1N1 Virus, West Nile Virus, and Dengue Virus. Cell *139*, 1243-1254.

Bruce, E.A., Digard, P., and Stuart, A.D. (2010). The Rab11 Pathway Is Required for Influenza A Virus Budding and Filament Formation. J Virol *84*, 5848-5859.

Bruce, E.A., Medcalf, L., Crump, C.M., Noton, S.L., Stuart, A.D., Wise, H.M., Elton, D., Bowers, K., and Digard, P. (2009). Budding of filamentous and non-filamentous influenza A virus occurs via a VPS4 and VPS28-independent pathway. Virology *390*, 268-278.

Bruce, Emily A., Stuart, A., McCaffrey, Mary W., and Digard, P. (2012). Role of the Rab11 pathway in negative-strand virus assembly. Biochemical Society transactions *40*, 1409-1415.

Buchmeier, M.J., de la Torre, J.C., and Peters, C.J. (2007). *Arenaviridae*: The Viruses and Their Replication. In Fields Virology, D.M. Knipe, P.M. Howley, D.E. Griffin, R.A. Lamb, M.A. Martin, B. Roizman, and S.E. Straus, eds. (Philadelphia: Wolters Kluwer Health/Lippincott Williams & Wilkins), pp. 1791-1827.

Burns, J.W., and Buchmeier, M.J. (1991). Protein-protein interactions in lymphocytic choriomeningitis virus. Virology *183*, 620-629.

Burns, J.W., and Buchmeier, M.J. (1993). Glycoproteins of the Arenaviruses. In The Arenaviridae, M.S. Salvato, ed. (New York: Plenum Press), pp. 17-35.

Byrd, R., Cone, L., Commess, B., Williams-Herman, D., Rowland, J., Lee, B., Fitzgibbons, M., Glaser, C., Jay, M., Fritz, C.*, et al.* (2000). Fatal illnesses associated with a new world arenavirus--California, 1999-2000. MMWR Morbidity and mortality weekly report *49*, 709-711.

Campbell Dwyer, E.J., Lai, H., MacDonald, R.C., Salvato, M.S., and Borden, K.L.B. (2000). The Lymphocytic Choriomeningitis Virus RING Protein Z Associates with Eukaryotic Initiation Factor 4E and Selectively Represses Translation in a RING-Dependent Manner. J Virol *74*, 3293-3300.

Campbell, S., and Rein, A. (1999). In Vitro Assembly Properties of Human Immunodeficiency Virus Type 1 Gag Protein Lacking the p6 Domain. J Virol *73*, 2270-2279.

Cantin, R., Méthot, S., and Tremblay, M.J. (2005). Plunder and Stowaways: Incorporation of Cellular Proteins by Enveloped Viruses. J Virol *79*, 6577-6587.

Cao, W., Henry, M.D., Borrow, P., Yamada, H., Elder, J.H., Ravkov, E.V., Nichol, S.T., Compans, R.W., Campbell, K.P., and Oldstone, M.B.A. (1998). Identification of α-Dystroglycan as a Receptor for Lymphocytic Choriomeningitis Virus and Lassa Fever Virus. Science *282*, 2079-2081.

Capul, A.A., Perez, M., Burke, E., Kunz, S., Buchmeier, M.J., and de la Torre, J.C. (2007). Arenavirus Z-glycoprotein association requires Z myristoylation but not functional RING or late domains. J Virol *81*, 9451-9460.

Carlson, L.-A., and Hurley, J.H. (2012). In vitro reconstitution of the ordered assembly of the endosomal sorting complex required for transport at membrane-bound HIV-1 Gag clusters. Proceedings of the National Academy of Sciences *109*, 16928-16933.

Carlton, J.G., and Martin-Serrano, J. (2007). Parallels Between Cytokinesis and Retroviral Budding: A Role for the ESCRT Machinery. Science *316*, 1908-1912.

Carthy, M.M., Wolinsky, J.S., and Lazzarini, R.A. (1981). A persistent infection of Vero cells by egg-adapted mumps virus. Virology *114*, 343-356.

Casabona, J.C., Macleod, J.M.L., Loureiro, M.E., Gomez, G.A., and Lopez, N. (2009). The RING Domain and the L79 Residue of Z Protein Are Involved in both the Rescue of Nucleocapsids and the Incorporation of Glycoproteins into Infectious Chimeric Arenavirus-Like Particles. J Virol *83*, 7029-7039.

Castilla, V., Palermo, M.L., and Coto, E.C. (2001). Involvement of vacuolar proton ATPase in Junin virus multiplication. Archives of Virology *146*, 251-263.

Cave, D.R., Hagen, F.S., Palma, E.L., and Huang, A.S. (1984). Detection of vesicular stomatitis virus RNA and its defective-interfering particles in individual mouse brains. J Virol *50*, 86-91.

Cesar, G.A., Gustavo, P., Marina, L.K., Bobbie, R.E., Serena, A.C., James, A.C., Jeffrey, H., Thomas, B., Kirsten St, G., Thomas, G.K.*, et al.* (2010). High Diversity and Ancient Common Ancestry of Lymphocytic Choriomeningitis Virus. Emerging Infectious Disease journal *16*, 1093.

Charrel, R.N., de Lamballerie, X., and Emonet, S. (2008). Phylogeny of the genus Arenavirus. Current Opinion in Microbiology *11*, 362-368.

Charrel, R.N., and Lamballerie, X.d. (2003). Arenaviruses other than Lassa virus. Antiviral Research *57*, 89-100.

Chen, H.I., and Sudol, M. (1995). The WW domain of Yes-associated protein binds a proline-rich ligand that differs from the consensus established for Src homology 3-binding modules. Proceedings of the National Academy of Sciences *92*, 7819-7823.

Chesarino, N.M., McMichael, T.M., Hach, J.C., and Yount, J.S. (2014). Phosphorylation of the Antiviral Protein Interferon-inducible Transmembrane Protein 3 (IFITM3) Dually Regulates Its Endocytosis and Ubiquitination. J Biol Chem *289*, 11986-11992.

Chesarino, N.M., McMichael, T.M., and Yount, J.S. (2015). E3 Ubiquitin Ligase NEDD4 Promotes Influenza Virus Infection by Decreasing Levels of the Antiviral Protein IFITM3. PLOS Pathogens *11*, e1005095.

Childs, J.E., Glass, G.E., Korch, G.W., Ksiazek, T.G., and Leduc, J.W. (1992). Lymphocytic Choriomeningitis Virus Infection and House Mouse (Mus Musculus) Distribution in Urban Baltimore. The American Journal of Tropical Medicine and Hygiene *47*, 27-34.

Childs, J.E., and Peters, C.J. (1993). Ecology and Epidemiology of Arenaviruses and Their Hosts. In The Arenaviridae, M.S. Salvato, ed. (New York: Plenum Press), pp. 331-384.

Chosewood, L.C., Wilson, D.E., Centers for Disease Control and Prevention (U.S.), and National Institutes of Health (U.S.) (2009). Biosafety in microbiological and biomedical laboratories, 5th edn (Washington, D.C.: U.S. Dept. of Health and Human Services, Public Health Service, Centers for Disease Control and Prevention, National Institutes of Health).

Clegg, J.C.S., Wilson, S.M., and Oram, J.D. (1991). Nucleotide sequence of the S RNA of Lassa virus (Nigerian strain) and comparative analysis of arenavirus gene products. Virus Research *18*, 151-164.

Cole, C.N., and Baltimore, D. (1973). Defective interfering particles of poliovirus: III. Interference and enrichment. Journal of Molecular Biology *76*, 345-361.

Cornillez-Ty, C.T., Liao, L., Yates, J.R., Kuhn, P., and Buchmeier, M.J. (2009). Severe Acute Respiratory Syndrome Coronavirus Nonstructural Protein 2 Interacts with a Host Protein Complex Involved in Mitochondrial Biogenesis and Intracellular Signaling. J Virol *83*, 10314-10318.

Cornu, T.I., and de la Torre, J.C. (2001). RING finger Z protein of lymphocytic choriomeningitis virus (LCMV) inhibits transcription and RNA replication of an LCMV S-segment minigenome. J Virol *75*, 9415-9426.

Cornu, T.I., and de la Torre, J.C. (2002). Characterization of the arenavirus RING finger Z protein regions required for Z-mediated inhibition of viral RNA synthesis. J Virol *76*, 6678-6688.

Cornu, T.I., Feldmann, H., and de la Torre, J.C. (2004). Cells expressing the RING finger Z protein are resistant to arenavirus infection. J Virol *78*, 2979-2983.

Cosset, F.-L., Marianneau, P., Verney, G., Gallais, F., Tordo, N., Pécheur, E.-I., ter Meulen, J., Deubel, V., and Bartosch, B. (2009). Characterization of Lassa Virus Cell Entry and Neutralization with Lassa Virus Pseudoparticles. J Virol *83*, 3228-3237.

Crouch, C.F., Mackenzie, A., and Dimmock, N.J. (1982). The Effect of Defective-Interfering Semliki Forest Virus on the Histopathology of Infection with Virulent Semliki Forest Virus in Mice. The Journal of infectious diseases *146*, 411-416.

Cummins, D., McCormick, J.B., Bennett, D., and et al. (1990). Acute Sensorineural Deafness in Lassa Fever. JAMA *264*, 2093-2096.

Dalal, S., Rosser, M.F.N., Cyr, D.M., and Hanson, P.I. (2004). Distinct Roles for the AAA ATPases NSF and p97 in the Secretory Pathway. Mol Biol Cell *15*, 637-648.

Damonte, E.B., Mersich, S.E., and Coto, C.E. (1983). Response of cells persistently infected with arenaviruses to superinfection with homotypic and heterotypic viruses. Virology *129*.

Davis, A.R., Hiti, A.L., and Nayak, D.P. (1980). Influenza Defective Interfering Viral RNA is Formed by Internal Deletion of Genomic RNA. Proc Natl Acad Sci USA *77*, 215-219.

Degasperi, A., Birtwistle, M.R., Volinsky, N., Rauch, J., Kolch, W., and Kholodenko, B.N. (2014). Evaluating Strategies to Normalise Biological Replicates of Western Blot Data. PLoS ONE *9*, e87293.

Delgado, S., Erickson, B.R., Agudo, R., Blair, P.J., Vallejo, E., Albarino, C.G., Vargas, J., Comer, J.A., Rollin, P.E., Ksiazek, T.G.*, et al.* (2008a). Chapare virus, a newly discovered arenavirus isolated from a fatal hemorrhagic fever case in Bolivia. Plos Pathogens *4*.

Delgado, S., Erickson, B.R., Agudo, R., Blair, P.J., Vallejo, E., Albariño, C.G., Vargas, J., Comer, J.A., Rollin, P.E., Ksiazek, T.G.*, et al.* (2008b). Chapare Virus, a Newly Discovered Arenavirus Isolated from a Fatal Hemorrhagic Fever Case in Bolivia. PLOS Pathogens *4*, e1000047.

Dilley, K.A., Gregory, D., Johnson, M.C., and Vogt, V.M. (2010). An LYPSL Late Domain in the Gag Protein Contributes to the Efficient Release and Replication of Rous Sarcoma Virus. J Virol *84*, 6276-6287.

Dimmock, N.J., and Kennedy, S.I.T. (1978). Prevention of Death in Semliki Forest Virus-Infected Mice by Administration of Defective-Interfering Semliki Forest Virus. J Gen Virol *39*, 231-242.

Djavani, M., Lukashevich, I.S., Sanchez, A., Nichol, S.T., and Salvato, M.S. (1997). Completion of the Lassa Fever Virus Sequence and Identification of a RING Finger Open Reading Frame at the L RNA 5′ End. Virology *235*, 414-418.

Djavani, M., Topisirovic, I., Zapata, J.C., Sadowska, M., Yang, Y., Rodas, J., Lukashevich, I.S., Bogue, C.W., Pauza, C.D., Borden, K.L.B.*, et al.* (2005). The proline-rich homeodomain (PRH/HEX) protein is down-regulated in liver during infection with lymphocytic choriomeningitis virus. J Virol *79*, 2461-2473.

Donaldson, J.G., and Jackson, C.L. (2011). ARF family G proteins and their regulators: roles in membrane transport, development and disease. Nat Rev Mol Cell Biol *12*, 362-375.

Downs, W.G., Anderson, C.R., Spence, L., Aitken, T.H.G., and Greenhall, A.H. (1963). Tacaribe Virus, a New Agent Isolated from Artibeus Bats and Mosquitoes in Trinidad, West Indies. The American Journal of Tropical Medicine and Hygiene *12*, 640-646.

Doyle, M., and Holland, J.J. (1973). Prophylaxis and Immunization in Mice by Use of Virus-Free Defective T Particles to Protect Against Intracerebral Infection by Vesicular Stomatitis Virus. Proc Natl Acad Sci USA *70*, 2105-2108.

Dutko, F.J., and Pfau, C.J. (1978). Arenavirus Defective Interfering Particles Mask the Cell-Killing Potential of Standard Virus. J Gen Virol *38*, 195-208.

Eichler, R., Strecker, T., Kolesnikova, L., ter Meulen, J., Weissenhorn, W., Becker, S., Klenk, H.D., Garten, W., and Lenz, O. (2004). Characterization of the Lassa virus matrix protein Z: electron microscopic study of virus-like particles and interaction with the nucleoprotein (NP). Virus Research *100*, 249-255.

Emond, R.T., Bannister, B., Lloyd, G., Southee, T.J., and Bowen, E.T. (1982). A case of Lassa fever: clinical and virological findings. Br Med J (Clin Res Ed) *285*, 1001-1002.

Emonet, S.F., de la Torre, J.C., Domingo, E., and Sevilla, N. (2009a). Arenavirus genetic diversity and its biological implications. Infection, Genetics and Evolution *9*, 417-429.

Emonet, S.F., Garidou, L., McGavern, D.B., and de la Torre, J.C. (2009b). Generation of recombinant lymphocytic choriomeningitis viruses with trisegmented genomes stably expressing two additional genes of interest. Proc Natl Acad Sci USA *106*, 3473-3478.

Enria, D.A., Briggiler, A.M., and Sanchez, Z. (2008a). Treatment of Argentine hemorrhagic fever. Antiviral Res *78*, 132-139.

Enria, D.A., Briggiler, A.M., and Sánchez, Z. (2008b). Treatment of Argentine hemorrhagic fever. Antiviral Research *78*, 132-139.

Epstein, D.A., Herman, R.C., Chien, I., and Lazzarini, R.A. (1980). Defective interfering particle generated by internal deletion of the vesicular stomatitis virus genome. J Virol *33*, 818-829.

Fan, L., Briese, T., and Lipkin, W.I. (2010). Z Proteins of New World Arenaviruses Bind RIG-I and Interfere with Type I Interferon Induction. J Virol *84*, 1785-1791.

Fehling, S., Lennartz, F., and Strecker, T. (2012). Multifunctional Nature of the Arenavirus RING Finger Protein Z. Viruses *4*, 2973-3011.

Fischer, S.A., Graham, M.B., Kuehnert, M.J., Kotton, C.N., Srinivasan, A., Marty, F.M., Comer, J.A., Guarner, J., Paddock, C.D., DeMeo, D.L.*, et al.* (2006). Transmission of Lymphocytic Choriomeningitis Virus by Organ Transplantation. N Engl J Med *354*, 2235-2249.

Flatz, L., Bergthaler, A., de la Torre, J.C., and Pinschewer, D.D. (2006). Recovery of an arenavirus entirely from RNA polymerase I/II-driven cDNA. Proc Natl Acad Sci USA *103*, 4663-4668.

Forgac, M. (2007). Vacuolar ATPases: rotary proton pumps in physiology and pathophysiology. Nat Rev Mol Cell Biol *8*, 917-929.

Garcia, M., Cooper, A., Shi, W., Bornmann, W., Carrion, R., Kalman, D., and Nabel, G.J. (2012). Productive replication of Ebola virus is regulated by the c-Abl1 tyrosine kinase. Sci Transl Med *4*.

García, M., Cooper, A., Shi, W., Bornmann, W., Carrion, R., Kalman, D., and Nabel, G.J. (2012). Productive Replication of Ebola Virus Is Regulated by the c-Abl1 Tyrosine Kinase. Sci Transl Med *4*, 123ra124.

Garcia, M.L., Reynolds, T.D., Mothes, W., and Robek, M.D. (2013). Functional Characterization of the Putative Hepatitis B Virus Core Protein Late Domain Using Retrovirus Chimeras. PLoS ONE *8*, e72845.

Garrus, J.E., von Schwedler, U.K., Pornillos, O.W., Morham, S.G., Zavitz, K.H., Wang, H.E., Wettstein, D.A., Stray, K.M., Côté, M., Rich, R.L.*, et al.* (2001). Tsg101 and the Vacuolar Protein Sorting Pathway Are Essential for HIV-1 Budding. Cell *107*, 55-65.

Gill, D.J., Teo, H., Sun, J., Perisic, O., Veprintsev, D.B., Emr, S.D., and Williams, R.L. (2007). Structural insight into the ESCRT-I/-II link and its role in MVB trafficking. The EMBO Journal *26*, 600-612.

Golas, J.M., Arndt, K., Etienne, C., Lucas, J., Nardin, D., Gibbons, J., Frost, P., Ye, F., Boschelli, D.H., and Boschelli, F. (2003). SKI-606, a 4-Anilino-3-quinolinecarbonitrile Dual Inhibitor of Src and Abl Kinases, Is a Potent Antiproliferative Agent against Chronic Myelogenous Leukemia Cells in Culture and Causes Regression of K562 Xenografts in Nude Mice. Cancer Research *63*, 375-381.

Goñi, S.E., Iserte, J.A., Ambrosio, A.M., Romanowski, V., Ghiringhelli, P.D., and Lozano, M.E. (2006). Genomic Features of Attenuated Junín Virus Vaccine Strain Candidate. Virus Genes *32*, 37-41.

Gorai, T., Goto, H., Noda, T., Watanabe, T., Kozuka-Hata, H., Oyama, M., Takano, R., Neumann, G., Watanabe, S., and Kawaoka, Y. (2012). F1Fo-ATPase, F-type proton-translocating ATPase, at the plasma membrane is critical for efficient influenza virus budding. Proceedings of the National Academy of Sciences.

Göttlinger, H.G., Dorfman, T., Sodroski, J.G., and Haseltine, W.A. (1991). Effect of mutations affecting the p6 gag protein on human immunodeficiency virus particle release. Proceedings of the National Academy of Sciences *88*, 3195-3199.

Gottwein, E., Bodem, J., Müller, B., Schmechel, A., Zentgraf, H., and Kräusslich, H.-G. (2003). The Mason-Pfizer Monkey Virus PPPY and PSAP Motifs Both Contribute to Virus Release. J Virol *77*, 9474-9485.

Groseth, A., Wolff, S., Strecker, T., Hoenen, T., and Becker, S. (2010). Efficient Budding of the Tacaribe Virus Matrix Protein Z Requires the Nucleoprotein. J Virol *84*, 3603-3611.

Gschwender, H.H., and Popescu, M. (1976). Equilibrium Sedimentation of Virus in Density-Gradients of Iodinated Compounds. In Biological Separations in Iondinated Density-Gradient Media, D. Rickwood, ed. (London: Information Retrieval Ltd.), pp. 145-158.

Haist, K., Ziegler, C., and Botten, J. (2015). Strand-Specific Quantitative Reverse Transcription-Polymerase Chain Reaction Assay for Measurement of Arenavirus Genomic and Antigenomic RNAs. PLoS ONE *10*, e0120043.

Han, Z., Lu, J., Liu, Y., Davis, B., Lee, M.S., Olson, M.A., Ruthel, G., Freedman, B.D., Schnell, M.J., Wrobel, J.E.*, et al.* (2014). Small Molecule Probes Targeting the Viral PPxY-Host Nedd4 Interface Block Egress of a Broad Range of RNA Viruses. J Virol.

Han, Z., Sagum, C.A., Bedford, M.T., Sidhu, S.S., Sudol, M., and Harty, R.N. (2016). ITCH E3 Ubiquitin Ligase Interacts with Ebola Virus VP40 To Regulate Budding. J Virol *90*, 9163-9171.

Hanson, P.I., and Cashikar, A. (2012). Multivesicular body morphogenesis. Annu Rev Cell Dev Biol *28*, 337-362.

Hanson, P.I., Roth, R., Lin, Y., and Heuser, J.E. (2008). Plasma membrane deformation by circular arrays of ESCRT-III protein filaments. The Journal of Cell Biology *180*, 389-402.

Hao, L., Sakurai, A., Watanabe, T., Sorensen, E., Nidom, C.A., Newton, M.A., Ahlquist, P., and Kawaoka, Y. (2008). Drosophila RNAi screen identifies host genes important for influenza virus replication. Nature *454*, 890-893.

Harty, R.N., Brown, M.E., McGettigan, J.P., Wang, G., Jayakar, H.R., Huibregtse, J.M., Whitt, M.A., and Schnell, M.J. (2001). Rhabdoviruses and the Cellular Ubiquitin-Proteasome System: a Budding Interaction. J Virol *75*, 10623-10629.

Harty, R.N., Brown, M.E., Wang, G., Huibregtse, J., and Hayes, F.P. (2000). A PPxY motif within the VP40 protein of Ebola virus interacts physically and functionally with a

ubiquitin ligase: Implications for filovirus budding. Proceedings of the National Academy of Sciences *97*, 13871-13876.

Harty, R.N., Paragas, J., Sudol, M., and Palese, P. (1999). A Proline-Rich Motif within the Matrix Protein of Vesicular Stomatitis Virus and Rabies Virus Interacts with WW Domains of Cellular Proteins: Implications for Viral Budding. J Virol *73*, 2921-2929.

Heidecker, G., Lloyd, P.A., Fox, K., Nagashima, K., and Derse, D. (2004). Late Assembly Motifs of Human T-Cell Leukemia Virus Type 1 and Their Relative Roles in Particle Release. J Virol *78*, 6636-6648.

Heidecker, G., Lloyd, P.A., Soheilian, F., Nagashima, K., and Derse, D. (2007). The role of WWP1-Gag interaction and Gag ubiquitination in assembly and release of human T-cell leukemia virus type 1. J Virol *81*, 9769-9777.

Help, G.I., and Coto, C.E. (1980). [Genesis of interferent particles during the multiplication of Junin virus in vivo]. Medicina (B Aires) *40*, 531-536.

Hemonnot, B., Cartier, C., Gay, B., Rebuffat, S., Bardy, M., Devaux, C., Boyer, V., and Briant, L. (2004). The host cell MAP kinase ERK-2 regulates viral assembly and release by phosphorylating the p6(gag) protein of HIV-1. J Biol Chem *279*, 32426-32434.

Hetzel, U., Sironen, T., Laurinmäki, P., Liljeroos, L., Patjas, A., Henttonen, H., Vaheri, A., Artelt, A., Kipar, A., Butcher, S.J.*, et al.* (2013). Isolation, Identification, and Characterization of Novel Arenaviruses, the Etiological Agents of Boid Inclusion Body Disease. J Virol *87*, 10918-10935.

Holland, J.J., and Doyle, M. (1973). Attempts to Detect Homologous Autointerference In vivo with Influenza Virus and Vesicular Stomatitis Virus. Infect Immun *7*, 526-531.

Holland, J.J., Kennedy, S.I.T., Semler, B.L., Jones, C.L., Roux, L., and Grabau, E.A. (1980). Defective Interfering RNA Viruses and the Host-Cell Response. In Comprehensive Virology: Vol 16: Virus-Host Interactions: Viral Invasion, Persistence, and Disease, H. Fraenkael-Conrat, and R.R. Wagner, eds. (Boston, MA: Springer US), pp. 137-192.

Holland, J.J., and Villarreal, L.P. (1974). Persistent noncytocidal vesicular stomatitis virus infections mediated by defective T particles that suppress virion transcriptase. Proc Natl Acad Sci U S A *71*, 2956-2960.

Holland, J.J., Villarreal, L.P., Welsh, R.M., Oldstone, M.B.A., Kohne, D., Lazzarini, R., and Scolnick, E. (1976). Long-Term Persistent Vesicular Stomatitis Virus and Rabies Virus Infection of Cells In Vitro. J Gen Virol *33*, 193-211.

Huang, A.S. (1973). Defective interfering viruses. Annu Rev Microbiol *27*.

Huang, A.S., and Baltimore, D. (1970). Defective Viral Particles and Viral Disease Processes. Nature *226*, 325-327.

Huang, A.S., Greenawalt, J.W., and Wagner, R.R. (1966). Defective T particles of vesicular stomatitis virus. Virology *30*, 161-172.

Huang, A.S., and Wagner, R.R. (1966). Defective T particles of vesicular stomatitis virus. Virology *30*, 173-181.

Huang, D.W., Sherman, B.T., and Lempicki, R.A. (2008). Systematic and integrative analysis of large gene lists using DAVID bioinformatics resources. Nat Protocols *4*, 44-57.

Huang, D.W., Sherman, B.T., and Lempicki, R.A. (2009). Bioinformatics enrichment tools: paths toward the comprehensive functional analysis of large gene lists. Nucleic Acids Research *37*, 1-13.

Huang, M., Orenstein, J.M., Martin, M.A., and Freed, E.O. (1995). p6Gag is required for particle production from full-length human immunodeficiency virus type 1 molecular clones expressing protease. J Virol *69*, 6810-6818.

Hurley, J.H. (2008). ESCRT complexes and the biogenesis of multivesicular bodies. Curr Opin Cell Biol *20*, 4-11.

Hurley, J.H. (2015). ESCRTs are everywhere. The EMBO Journal *34*, 2398-2407.

Iapalucci, S., López, N., Rey, O., Zakin, M.M., Cohen, G.N., and Franze-Fernández, M.T. (1989). The 5′ region of Tacaribe virus L RNA encodes a protein with a potential metal binding domain. Virology *173*, 357-361.

Im, Y.J., Wollert, T., Boura, E., and Hurley, J.H. (2009). Structure and Function of the ESCRT-II-III Interface in Multivesicular Body Biogenesis. Developmental Cell *17*, 234-243.

Ingham, R.J., Colwill, K., Howard, C., Dettwiler, S., Lim, C.S.H., Yu, J., Hersi, K., Raaijmakers, J., Gish, G., Mbamalu, G.*, et al.* (2005). WW Domains Provide a Platform for the Assembly of Multiprotein Networks. Molecular and Cellular Biology *25*, 7092-7106.

Ingham, R.J., Gish, G., and Pawson, T. (2004). The Nedd4 family of E3 ubiquitin ligases: functional diversity within a common modular architecture. Oncogene *23*.

Irie, T., Licata, J.M., Jayakar, H.R., Whitt, M.A., Bell, P., and Harty, R.N. (2004). Functional Analysis of Late-Budding Domain Activity Associated with the PSAP Motif within the Vesicular Stomatitis Virus M Protein. J Virol *78*, 7823-7827.

Jacamo, R., Lopez, N., Wilda, M., and Franze-Fernandez, M.T. (2003a). Tacaribe Virus Z Protein Interacts with the L Polymerase Protein To Inhibit Viral RNA Synthesis. J Virol *77*, 10383-10393.

Jacamo, R., Lopez, N., Wilda, M., and Franze-Fernández, M.T. (2003b). Tacaribe virus Z protein interacts with the L polymerase protein to inhibit viral RNA synthesis. J Virol *77*.

Jacobson, S., and Pfau, C.J. (1980). Viral pathogenesis and resistance to defective interfering particles. Nature *283*, 311-313.

Jadwin, J.A., Rudd, V., Sette, P., Challa, S., and Bouamr, F. (2010). Late domain-independent rescue of a release-deficient Moloney murine leukemia virus by the ubiquitin ligase itch. J Virol *84*, 704-715.

Jayakar, H.R., Murti, K.G., and Whitt, M.A. (2000). Mutations in the PPPY Motif of Vesicular Stomatitis Virus Matrix Protein Reduce Virus Budding by Inhibiting a Late Step in Virion Release. J Virol *74*, 9818-9827.

JM, R., AB, S., NT, N., JC, d.l.T., and S, K. (2008). Different mechanisms of cell entry by human-pathogenic Old World and New World arenaviruses. J Virol *82*, 7677-7687.

Jonckheere, A.I., Smeitink, J.A.M., and Rodenburg, R.J.T. (2012). Mitochondrial ATP synthase: architecture, function and pathology. Journal of Inherited Metabolic Disease *35*, 211-225.

Jones, C.L., and Holland, J.J. (1980). Requirements for DI Particle Prophylaxis Against Vesicular Stomatitis Virus Infection in vivo. J Gen Virol *49*, 215-220.

Joshi, A., Garg, H., Nagashima, K., Bonifacino, J.S., and Freed, E.O. GGA and Arf Proteins Modulate Retrovirus Assembly and Release. Molecular cell *30*, 227-238.

Karlas, A., Machuy, N., Shin, Y., Pleissner, K.-P., Artarini, A., Heuer, D., Becker, D., Khalil, H., Ogilvie, L.A., Hess, S.*, et al.* (2010). Genome-wide RNAi screen identifies human host factors crucial for influenza virus replication. Nature *463*, 818-822.

Katzmann, D.J., Odorizzi, G., and Emr, S.D. (2002). Receptor downregulation and multivesicular-body sorting. Nat Rev Mol Cell Biol *3*, 893-905.

Kawai, A., Matsumoto, S., and Tanabe, K. (1975). Characterization of rabies viruses recovered from persistently infected BHK cells. Virology *67*, 520-533.

Keenlyside, R.A., McCormick, J.B., Webb, P.A., Smith, E., Elliott, L., and Johnson, K.M. (1983). Case-Control Study of Mastomys Natalensis and Humans in Lassa Virus-Infected

Households in Sierra Leone. The American Journal of Tropical Medicine and Hygiene *32*, 829-837.

Kentsis, A., Dwyer, E.C., Perez, J.M., Sharma, M., Chen, A., Pan, Z.Q., and Borden, K.L.B. (2001). The RING domains of the promyelocytic leukemia protein PML and the arenaviral protein Z repress translation by directly inhibiting translation initiation factor eIF4E. Journal of Molecular Biology *312*, 609-623.

Kikonyogo, A., Bouamr, F., Vana, M.L., Xiang, Y., Aiyar, A., Carter, C., and Leis, J. (2001). Proteins related to the Nedd4 family of ubiquitin protein ligases interact with the L domain of Rous sarcoma virus and are required for gag budding from cells. Proceedings of the National Academy of Sciences *98*, 11199-11204.

Kim, J., Sitaraman, S., Hierro, A., Beach, B.M., Odorizzi, G., and Hurley, J.H. (2005). Structural Basis for Endosomal Targeting by the Bro1 Domain. Developmental Cell *8*, 937-947.

Kingsbury, D.W., and Portner, A. (1970). On the genesis of incomplete Sendai virions. Virology *42*, 872-879.

Kingsbury, D.W., Portner, A., and Darlington, R.W. (1970). Properties of incomplete Sendai virions and subgenomic viral RNAs. Virology *42*, 857-871.

Klaus, J.P., Eisenhauer, P., Russo, J., Mason, A.B., Do, D., King, B., Taatjes, D., Cornillez-Ty, C., Boyson, J.E., Thali, M.*, et al.* (2013). The intracellular cargo receptor ERGIC-53 is required for the production of infectious arenavirus, coronavirus, and filovirus particles. Cell Host Microbe *14*, 522-534.

Klaus, Joseph P., Eisenhauer, P., Russo, J., Mason, A.B., Do, D., King, B., Taatjes, D., Cornillez-Ty, C., Boyson, Jonathan E., Thali, M.*, et al.* The Intracellular Cargo Receptor ERGIC-53 Is Required for the Production of Infectious Arenavirus, Coronavirus, and Filovirus Particles. Cell Host & Microbe *14*, 522-534.

Klewitz, C., Klenk, H.-D., and ter Meulen, J. (2007). Amino acids from both N-terminal hydrophobic regions of the Lassa virus envelope glycoprotein GP-2 are critical for pH-dependent membrane fusion and infectivity. J Gen Virol *88*, 2320-2328.

Kolesnikova, L., Mittler, E., Schudt, G., Shams-Eldin, H., and Becker, S. (2012). Phosphorylation of Marburg virus matrix protein VP40 triggers assembly of nucleocapsids with the viral envelope at the plasma membrane. Cell Microbiol *14*, 182-197.

Konig, R., Stertz, S., Zhou, Y., Inoue, A., Hoffmann, H.H., Bhattacharyya, S., Alamares, J.G., Tscherne, D.M., Ortigoza, M.B., Liang, Y.*, et al.* (2010). Human host factors required for influenza virus replication. Nature *463*, 813-817.

König, R., Zhou, Y., Elleder, D., Diamond, T.L., Bonamy, G.M.C., Irelan, J.T., Chiang, C.-y., Tu, B.P., De Jesus, P.D., Lilley, C.E.*, et al.* (2008). Global Analysis of Host-Pathogen Interactions that Regulate Early-Stage HIV-1 Replication. Cell *135*, 49-60.

Kostelansky, M.S., Sun, J., Lee, S., Kim, J., Ghirlando, R., Hierro, A., Emr, S.D., and Hurley, J.H. (2006). Structural and Functional Organization of the ESCRT-I Trafficking Complex. Cell *125*, 113-126.

Kowal, K.J., and Stollar, V. (1980). Differential sensitivity of infectious and defective-interfering particles of sindbis virus to ultraviolet irradiation. Virology *103*, 149-157.

Kranzusch, P.J., and Whelan, S.P.J. (2011). Arenavirus Z protein controls viral RNA synthesis by locking a polymerase–promoter complex. Proceedings of the National Academy of Sciences *108*, 19743-19748.

Krishnan, M.N., Ng, A., Sukumaran, B., Gilfoy, F.D., Uchil, P.D., Sultana, H., Brass, A.L., Adametz, R., Tsui, M., Qian, F.*, et al.* (2008). RNA interference screen for human genes associated with West Nile virus infection. Nature *455*, 242-245.

Kunz, S. (2009). Receptor binding and cell entry of Old World arenaviruses reveal novel aspects of virus–host interaction. Virology *387*, 245-249.

Kuo, L., and Freed, E.O. (2012). ARRDC1 as a mediator of microvesicle budding. Proceedings of the National Academy of Sciences *109*, 4025-4026.

Lan, S., McLay Schelde, L., Wang, J., Kumar, N., Ly, H., and Liang, Y. (2009). Development of Infectious Clones for Virulent and Avirulent Pichinde Viruses: a Model Virus To Study Arenavirus-Induced Hemorrhagic Fevers. J Virol *83*, 6357-6362.

Lazzarini, R.A., Keene, J.D., and Schubert, M. (1981). The origins of defective interfering particles of the negative-strand RNA viruses. Cell *26*.

Le Blanc, I., Prévost, M.-C., Dokhélar, M.-C., and Rosenberg, A.R. (2002a). The PPPY Motif of Human T-Cell Leukemia Virus Type 1 Gag Protein Is Required Early in the Budding Process. J Virol *76*, 10024-10029.

Le Blanc, I., Prevost, M.C., Dokhelar, M.C., and Rosenberg, A.R. (2002b). The PPPY motif of human T-cell leukemia virus type 1 Gag protein is required early in the budding process. J Virol *76*, 10024-10029.

Le Sommer, C., Barrows, N.J., Bradrick, S.S., Pearson, J.L., and Garcia-Blanco, M.A. (2012). G Protein-Coupled Receptor Kinase 2 Promotes <italic>Flaviviridae</italic> Entry and Replication. PLoS Negl Trop Dis *6*, e1820.

Lee, A.S.-Y., Burdeinick-Kerr, R., and Whelan, S.P.J. (2014). A genome-wide siRNA screen identifies host factors required for vesicular stomatitis virus infection. J Virol.

Lee, H.H., Elia, N., Ghirlando, R., Lippincott-Schwartz, J., and Hurley, J.H. (2008). Midbody Targeting of the ESCRT Machinery by a Noncanonical Coiled Coil in CEP55. Science *322*, 576-580.

Lee, J.-A., Beigneux, A., Ahmad, S.T., Young, S.G., and Gao, F.-B. (2007). ESCRT-III Dysfunction Causes Autophagosome Accumulation and Neurodegeneration. Current Biology *17*, 1561-1567.

Lee, K.J., and de la Torre, J.C. (2002). Reverse genetics of arenaviruses. Curr Top Microbiol Immunol *262*, 175-193.

Lee, K.J., Novella, I.S., Teng, M.N., Oldstone, M.B.A., and de la Torre, J.C. (2000). NP and L Proteins of Lymphocytic Choriomeningitis Virus (LCMV) Are Sufficient for Efficient Transcription and Replication of LCMV Genomic RNA Analogs. J Virol *74*, 3470-3477.

Lehmann-Grube, F., Slenczka, W., and Tees, R. (1969). A persistent and inapparent infection of L cells with the virus of lymphocytic choriomeningitis. J Gen Virol *5*.

Lenz, O., ter Meulen, J., Klenk, H.-D., Seidah, N.G., and Garten, W. (2001). The Lassa virus glycoprotein precursor GP-C is proteolytically processed by subtilase SKI-1/S1P. Proceedings of the National Academy of Sciences *98*, 12701-12705.

Levingston Macleod, J.M., D'Antuono, A., Loureiro, M.E., Casabona, J.C., Gomez, G.A., and Lopez, N. (2011). Identification of two functional domains within the arenavirus nucleoprotein. J Virol *85*.

Li, M., Schmitt, P.T., Li, Z., McCrory, T.S., He, B., and Schmitt, A.P. (2009a). Mumps Virus Matrix, Fusion, and Nucleocapsid Proteins Cooperate for Efficient Production of Virus-Like Particles. J Virol *83*, 7261-7272.

Li, Q., Brass, A.L., Ng, A., Hu, Z., Xavier, R.J., Liang, T.J., and Elledge, S.J. (2009b). A genome-wide genetic screen for host factors required for hepatitis C virus propagation. Proceedings of the National Academy of Sciences.

Lin, Y., Kimpler, L.A., Naismith, T.V., Lauer, J.M., and Hanson, P.I. (2005). Interaction of the Mammalian Endosomal Sorting Complex Required for Transport (ESCRT) III Protein hSnf7-1 with Itself, Membranes, and the AAA+ ATPase SKD1. J Biol Chem *280*, 12799-12809.

Linero, F.N., Sepúlveda, C.S., Giovannoni, F., Castilla, V., García, C.C., Scolaro, L.A., and Damonte, E.B. (2012). Host Cell Factors as Antiviral Targets in Arenavirus Infection. Viruses *4*, 1569.

Lopez, N., Jacamo, R., and Franze-Fernandez, M.T. (2001). Transcription and RNA Replication of Tacaribe Virus Genome and Antigenome Analogs Require N and L Proteins: Z Protein Is an Inhibitor of These Processes. J Virol *75*, 12241-12251.

Lu, J., Han, Z., Liu, Y., Liu, W., Lee, M.S., Olson, M.A., Ruthel, G., Freedman, B.D., and Harty, R.N. (2014). A Host-Oriented Inhibitor of Junin Argentine Hemorrhagic Fever Virus Egress. J Virol *88*, 4736-4743.

Lukashevich, I.S., Djavani, M., Shapiro, K., Sanchez, A., Ravkov, E., Nichol, S.T., and Salvato, M.S. (1997). The Lassa fever virus L gene: nucleotide sequence, comparison, and precipitation of a predicted 250 kDa protein with monospecific antiserum. J Gen Virol *78*, 547-551.

Maiztegui, J., Fernandez, N., and De Damilano, A. (1979). EFFICACY OF IMMUNE PLASMA IN TREATMENT OF ARGENTINE HÆMORRHAGIC FEVER AND ASSOCIATION BETWEEN TREATMENT AND A LATE NEUROLOGICAL SYNDROME. The Lancet *314*, 1216-1217.

Maiztegui, J.I. (1975). Clinical and epidemiological patterns of Argentine haemorrhagic fever. Bulletin of the World Health Organization *52*, 567-575.

Martin-Serrano, J., Eastman, S.W., Chung, W., and Bieniasz, P.D. (2005). HECT ubiquitin ligases link viral and cellular PPXY motifs to the vacuolar protein-sorting pathway. The Journal of Cell Biology *168*, 89-101.

Martin-Serrano, J., Perez-Caballero, D., and Bieniasz, P.D. (2004). Context-Dependent Effects of L Domains and Ubiquitination on Viral Budding. J Virol *78*, 5554-5563.

Martin-Serrano, J., Yaravoy, A., Perez-Caballero, D., and Bieniasz, P.D. (2003). Divergent retroviral late-budding domains recruit vacuolar protein sorting factors by using alternative adaptor proteins. Proceedings of the National Academy of Sciences *100*, 12414-12419.

Martin-Serrano, J., Zang, T., and Bieniasz, P.D. (2001). HIV-1 and Ebola virus encode small peptide motifs that recruit Tsg101 to sites of particle assembly to facilitate egress. Nat Med *7*, 1313-1319.

Martinez, M.G., Cordo, S.M., and Candurra, N.A. (2007). Characterization of Junín arenavirus cell entry. J Gen Virol *88*, 1776-1784.

Martinez, M.G., Forlenza, M.B., and Candurra, N.A. (2009). Involvement of cellular proteins in Junin arenavirus entry. Biotechnology journal *4*, 866-870.

McCormick, J.B., King, I.J., Webb, P.A., Scribner, C.L., Craven, R.B., Johnson, K.M., Elliott, L.H., and Belmont-Williams, R. (1986). Lassa Fever. N Engl J Med *314*, 20-26.

McCormick, J.B., Webb, P.A., Krebs, J.W., Johnson, K.M., and Smith, E.S. (1987). A Prospective Study of the Epidemiology and Ecology of Lassa Fever. J Infect Dis *155*, 437-444.

McCullough, J., Fisher, R.D., Whitby, F.G., Sundquist, W.I., and Hill, C.P. (2008). ALIX-CHMP4 interactions in the human ESCRT pathway. Proceedings of the National Academy of Sciences *105*, 7687-7691.

Medina, G., Pincetic, A., Ehrlich, L.S., Zhang, Y., Tang, Y., Leis, J., and Carter, C.A. (2008). Tsg101 can replace Nedd4 function in ASV Gag release but not membrane targeting. Virology *377*, 30-38.

Meyer, B.J., De La Torre, J.C., and Southern, P.J. (2002). Arenaviruses: Genomic RNAs, Transcription, and Replication. In Arenaviruses I, M.A. Oldstone, ed. (Springer Berlin Heidelberg), pp. 139-157.

Meyer, B.J., and Southern, P.J. (1994). Sequence heterogeneity in the termini of lymphocytic choriomeningitis virus genomic and antigenomic RNAs. J Virol *68*, 7659-7664.

Meyer, B.J., and Southern, P.J. (1997). A novel type of defective viral genome suggests a unique strategy to establish and maintain persistent lymphocytic choriomeningitis virus infections. J Virol *71*, 6757-6764.

Michalke, H., and Bremer, H. (1969). RNA synthesis in Escherichia coli after irradiation with ultraviolet light. Journal of Molecular Biology *41*, 1-23.

Mims, C.A. (1956). Rift Valley Fever virus in mice. IV. Incomplete virus; its production and properties. British journal of experimental pathology *37*, 129-143.

Morita, E., Sandrin, V., Chung, H.-Y., Morham, S.G., Gygi, S.P., Rodesch, C.K., and Sundquist, W.I. (2007). Human ESCRT and ALIX proteins interact with proteins of the midbody and function in cytokinesis. The EMBO Journal *26*, 4215-4227.

Moss, B.A., and Brownlee, G.G. (1981). Sequence of DNA complementry to a small RNA segment of influenza virus A/NT/60/68. Nucleic Acids Research *9*, 1941-1947.

Nabhan, J.F., Hu, R., Oh, R.S., Cohen, S.N., and Lu, Q. (2012). Formation and release of arrestin domain-containing protein 1-mediated microvesicles (ARMMs) at plasma membrane by recruitment of TSG101 protein. Proceedings of the National Academy of Sciences *109*, 4146-4151.

Neuman, B.W., Adair, B.D., Burns, J.W., Milligan, R.A., Buchmeier, M.J., and Yeager, M. (2005). Complementarity in the Supramolecular Design of Arenaviruses and Retroviruses Revealed by Electron Cryomicroscopy and Image Analysis. J Virol *79*, 3822-3830.

Neumann, G., Ebihara, H., Takada, A., Noda, T., Kobasa, D., Jasenosky, L.D., Watanabe, S., Kim, J.H., Feldmann, H., and Kawaoka, Y. (2005a). Ebola virus VP40 late domains are not essential for viral replication in cell culture. J Virol *79*.

Neumann, G., Ebihara, H., Takada, A., Noda, T., Kobasa, D., Jasenosky, L.D., Watanabe, S., Kim, J.H., Feldmann, H., and Kawaoka, Y. (2005b). Ebola Virus VP40 Late Domains Are Not Essential for Viral Replication in Cell Culture. J Virol *79*, 10300-10307.

Obenauer, J.C., Cantley, L.C., and Yaffe, M.B. (2003). Scansite 2.0: Proteome-wide prediction of cell signaling interactions using short sequence motifs. Nucleic Acids Res *31*, 3635-3641.

Obita, T., Saksena, S., Ghazi-Tabatabai, S., Gill, D.J., Perisic, O., Emr, S.D., and Williams, R.L. (2007). Structural basis for selective recognition of ESCRT-III by the AAA ATPase Vps4. Nature *449*, 735-739.

Oldstone, M.B. (1998). Viral persistence: mechanisms and consequences. Curr Opin Microbiol *1*, 436-441.

Ortiz-Riano, E., Cheng, B.Y.H., de la Torre, J.C., and Martinez-Sobrido, L. (2011). The C-Terminal Region Of Lymphocytic Choriomeningitis Virus Nucleoprotein Contains Distinct And Segregable Functional Domains Involved In NP-Z Interaction And Counteraction Of The Type I IFN Response. J Virol, JVI.05834-05811.

Panda, D., Das, A., Dinh, P.X., Subramaniam, S., Nayak, D., Barrows, N.J., Pearson, J.L., Thompson, J., Kelly, D.L., Ladunga, I.*, et al.* (2011). RNAi screening reveals requirement for host cell secretory pathway in infection by diverse families of negative-strand RNA viruses. Proceedings of the National Academy of Sciences *108*, 19036-19041.

Parent, L.J., Bennett, R.P., Craven, R.C., Nelle, T.D., Krishna, N.K., Bowzard, J.B., Wilson, C.B., Puffer, B.A., Montelaro, R.C., and Wills, J.W. (1995). Positionally independent and exchangeable late budding functions of the Rous sarcoma virus and human immunodeficiency virus Gag proteins. J Virol *69*, 5455-5460.

Pasqual, G., Rojek, J.M., Masin, M., Chatton, J.-Y., and Kunz, S. (2011). Old World Arenaviruses Enter the Host Cell via the Multivesicular Body and Depend on the Endosomal Sorting Complex Required for Transport. PLoS Pathog *7*, e1002232.

Pedersen, I.R. (1979). Structural Components and Replication of Arenaviruses. In Advances in virus research, M.A. Lauffer, F.B. Bang, K. Maramorosch, and K.M. Smith, eds. (Academic Press), pp. 277-330.

Pei, Z., Bai, Y., and Schmitt, A.P. (2010). PIV5 M protein interaction with host protein angiomotin-like 1. Virology *397*, 155-166.

Pei, Z., Harrison, M.S., and Schmitt, A.P. (2011). Parainfluenza Virus 5 M Protein Interaction with Host Protein 14-3-3 Negatively Affects Virus Particle Formation. J Virol *85*, 2050-2059.

Peralta, L.M., Bruns, M., and Lehmann-Grube, F. (1981). Biochemical Composition of Lymphocytic Choriomeningitis Virus Interfering Particles. J Gen Virol *55*, 475-479.

Perez, M., Craven, R.C., and de la Torre, J.C. (2003). The small RING finger protein Z drives arenavirus budding: Implications for antiviral strategies. Proc Natl Acad Sci USA *100*, 12978-12983.

Perez, M., Greenwald, D.L., and de La Torre, J.C. (2004a). Myristoylation of the RING finger Z protein is essential for arenavirus budding. J Virol *78*, 11443-11448.

Perez, M., Greenwald, D.L., and de la Torre, J.C. (2004b). Myristoylation of the RING finger Z protein is essential for arenavirus budding. J Virol *78*, 11443-11448.

Perrault, J. (1981). Origin and replication of defective interfering particles. Curr Top Microbiol Immunol *93*, 151-207.

Pinschewer, D.D., Perez, M., Sanchez, A.B., and de la Torre, J.C. (2003). Recombinant lymphocytic choriomeningitis virus expressing vesicular stomatitis virus glycoprotein. Proceedings of the National Academy of Sciences *100*, 7895-7900.

Popescu, M., and Lehmann-Grube, F. (1977). Defective interfering particles in mice infected with lymphocytic choriomeningitis virus. Virology *77*, 78-83.

Popescu, M., Schaefer, H., and Lehmann-Grube, F. (1976). Homologous interference of lymphocytic choriomeningitis virus: detection and measurement of interference focus-forming units. J Virol *20*, 1-8.

Price, M.E., Fisher-Hoch, S.P., Craven, R.B., and McCormick, J.B. (1988). A prospective study of maternal and fetal outcome in acute Lassa fever infection during pregnancy. BMJ : British Medical Journal *297*, 584-587.

Puffer, B.A., Parent, L.J., Wills, J.W., and Montelaro, R.C. (1997). Equine infectious anemia virus utilizes a YXXL motif within the late assembly domain of the Gag p9 protein. J Virol *71*, 6541-6546.

Quirin, K., Eschli, B., Scheu, I., Poort, L., Kartenbeck, J., and Helenius, A. (2008). Lymphocytic choriomeningitis virus uses a novel endocytic pathway for infectious entry via late endosomes. Virology *378*, 21-33.

Radoshitzky, S.R., Abraham, J., Spiropoulou, C.F., Kuhn, J.H., Nguyen, D., Li, W., Nagel, J., Schmidt, P.J., Nunberg, J.H., Andrews, N.C.*, et al.* (2007). Transferrin receptor 1 is a cellular receptor for New World haemorrhagic fever arenaviruses. Nature *446*, 92-96.

Radoshitzky, S.R., Bào, Y., Buchmeier, M.J., Charrel, R.N., Clawson, A.N., Clegg, C.S., DeRisi, J.L., Emonet, S., Gonzalez, J.-P., Kuhn, J.H.*, et al.* (2015). Past, present, and future of arenavirus taxonomy. Archives of Virology *160*, 1851-1874.

Raposo, G., and Stoorvogel, W. (2013). Extracellular vesicles: Exosomes, microvesicles, and friends. The Journal of Cell Biology *200*, 373-383.

Rauch, S., and Martin-Serrano, J. (2011). Multiple Interactions between the ESCRT Machinery and Arrestin-Related Proteins: Implications for PPXY-Dependent Budding. J Virol *85*, 3546-3556.

Raymond, C.K., Howald-Stevenson, I., Vater, C.A., and Stevens, T.H. (1992). Morphological classification of the yeast vacuolar protein sorting mutants: evidence for a prevacuolar compartment in class E vps mutants. Mol Biol Cell *3*, 1389-1402.

Rieder, S.E., Banta, L.M., Köhrer, K., McCaffery, J.M., and Emr, S.D. (1996). Multilamellar endosome-like compartment accumulates in the yeast vps28 vacuolar protein sorting mutant. Mol Biol Cell *7*, 985-999.

Riviere, Y., Ahmed, R., Southern, P.J., Buchmeier, M.J., Dutko, F.J., and Oldstone, M.B. (1985). The S RNA segment of lymphocytic choriomeningitis virus codes for the nucleoprotein and glycoproteins 1 and 2. J Virol *53*, 966-968.

Rojek, J.M., and Kunz, S. (2008). Cell entry by human pathogenic arenaviruses. Cell Microbiol *10*, 828-835.

Roux, L., and Holland, J.J. (1979). Role of defective interfering particles of sendai virus in persistent infections. Virology *93*, 91-103.

Roux, L., and Waldvogel, F.A. (1983). Defective interfering particles of Sendai virus modulate HN expression at the surface of infected BHK cells. Virology *130*, 91-104.

Rowe, R.K., Suszko, J.W., and Pekosz, A. (2008). Roles for the recycling endosome, Rab8, and Rab11 in hantavirus release from epithelial cells. Virology *382*, 239-249.

Rowe, W.P., Murphy, F.A., Bergold, G.H., Casals, J., Hotchin, J., Johnson, K.M., Lehmann-Grube, F., Mims, C.A., Traub, E., and Webb, P.A. (1970). Arenoviruses: Proposed Name for a Newly Defined Virus Group. J Virol *5*, 651-652.

Rusten, T.E., Vaccari, T., Lindmo, K., Rodahl, L.M.W., Nezis, I.P., Sem-Jacobsen, C., Wendler, F., Vincent, J.-P., Brech, A., Bilder, D.*, et al.* (2007). ESCRTs and Fab1 Regulate Distinct Steps of Autophagy. Current Biology *17*, 1817-1825.

Sahu, R., Kaushik, S., Clement, C.C., Cannizzo, E.S., Scharf, B., Follenzi, A., Potolicchio, I., Nieves, E., Cuervo, A.M., and Santambrogio, L. (2011). Microautophagy of Cytosolic Proteins by Late Endosomes. Developmental Cell *20*, 131-139.

Sakurai, A., Yasuda, J., Takano, H., Tanaka, Y., Hatakeyama, M., and Shida, H. (2004). Regulation of human T-cell leukemia virus type 1 (HTLV-1) budding by ubiquitin ligase Nedd4. Microbes Infect *6*, 150-156.

Salazar-Bravo, J., Ruedas, L.A., and Yates, T.L. (2002a). Mammalian reservoirs of arenaviruses. Curr Top Microbiol Immunol *262*, 25-63.

Salazar-Bravo, J., Ruedas, L.A., and Yates, T.L. (2002b). Mammalian Reservoirs of Arenaviruses. In Arenaviruses I, M.A. Oldstone, ed. (Springer Berlin Heidelberg), pp. 25-63.

Salvato, M.S., Schweighofer, K.J., Burns, J., and Shimomaye, E.M. (1992a). BIOCHEMICAL AND IMMUNOLOGICAL EVIDENCE THAT THE 11-KDA ZINC-BINDING PROTEIN OF LYMPHOCYTIC CHORIOMENINGITIS VIRUS IS A STRUCTURAL COMPONENT OF THE VIRUS. Virus Research *22*, 185-198.

Salvato, M.S., Schweighofer, K.J., Burns, J., and Shimomaye, E.M. (1992b). Biochemical and immunological evidence that the 11 kDa zinc-binding protein of lymphocytic choriomeningitis virus is a structural component of the virus. Virus Research *22*, 185-198.

Salvato, M.S., and Shimomaye, E.M. (1989). The completed sequence of lymphocytic choriomeningitis virus reveals a unique RNA structure and a gene for a zinc finger protein. Virology *173*, 1-10.

Sanchez, A.B., and De la Torre, J.C. (2006). Rescue of the prototypic Arenavirus LCMV entirely from plasmid. Virology *350*, 370-380.

Schlie, K., Maisa, A., Freiberg, F., Groseth, A., Strecker, T., and Garten, W. (2010). Viral Protein Determinants of Lassa Virus Entry and Release from Polarized Epithelial Cells. J Virol *84*, 3178-3188.

Schmaljohn, C., and Blair, C.D. (1977). Persistent infection of cultured mammalian cells by Japanese encephalitis virus. J Virol *24*, 580-589.

Schmidt, O., and Teis, D. The ESCRT machinery. Current Biology *22*, R116-R120.

Schmitt, A.P., Leser, G.P., Morita, E., Sundquist, W.I., and Lamb, R.A. (2005). Evidence for a New Viral Late-Domain Core Sequence, FPIV, Necessary for Budding of a Paramyxovirus. J Virol *79*, 2988-2997.

Schoneberg, J., Lee, I.-H., Iwasa, J.H., and Hurley, J.H. (2017). Reverse-topology membrane scission by the ESCRT proteins. Nat Rev Mol Cell Biol *18*, 5-17.

Segura-Morales, C., Pescia, C., Chatellard-Causse, C., Sadoul, R., Bertrand, E., and Basyuk, E. (2005). Tsg101 and Alix Interact with Murine Leukemia Virus Gag and Cooperate with Nedd4 Ubiquitin Ligases during Budding. J Biol Chem *280*, 27004-27012.

Sessions, O.M., Barrows, N.J., Souza-Neto, J.A., Robinson, T.J., Hershey, C.L., Rodgers, M.A., Ramirez, J.L., Dimopoulos, G., Yang, P.L., Pearson, J.L.*, et al.* (2009). Discovery of insect and human dengue virus host factors. Nature *458*, 1047-1050.

Shapira, S.D., Gat-Viks, I., Shum, B.O.V., Dricot, A., de Grace, M.M., Wu, L., Gupta, P.B., Hao, T., Silver, S.J., Root, D.E.*, et al.* (2009). A Physical and Regulatory Map of Host-Influenza Interactions Reveals Pathways in H1N1 Infection. Cell *139*, 1255-1267.

Shields, S.B., Oestreich, A.J., Winistorfer, S., Nguyen, D., Payne, J.A., Katzmann, D.J., and Piper, R. (2009). ESCRT ubiquitin-binding domains function cooperatively during MVB cargo sorting. The Journal of Cell Biology *185*, 213-224.

Shields, S.B., and Piper, R.C. (2011). How Ubiquitin Functions with ESCRTs. Traffic *12*, 1306-1317.

Shimode, S., Nakaoka, R., Hoshino, S., Abe, M., Shogen, H., Yasuda, J., and Miyazawa, T. (2013). Identification of cellular factors required for the budding of koala retrovirus. Microbiology and Immunology *57*, 543-546.

Shimojima, M., and Kawaoka, Y. (2012). Cell Surface Molecules Involved in Infection Mediated by Lymphocytic Choriomeningitis Virus Glycoprotein. Journal of Veterinary Medical Science *74*, 1363-1366.

Shimojima, M., Ströher, U., Ebihara, H., Feldmann, H., and Kawaoka, Y. (2012). Identification of Cell Surface Molecules Involved in Dystroglycan-Independent Lassa Virus Cell Entry. J Virol *86*, 2067-2078.

Shtanko, O., Imai, M., Goto, H., Lukashevich, I.S., Neumann, G., Watanabe, T., and Kawaoka, Y. (2010). A Role for the C Terminus of Mopeia Virus Nucleoprotein in Its Incorporation into Z Protein-Induced Virus-Like Particles. J Virol *84*, 5415-5422.

Shtanko, O., Watanabe, S., Jasenosky, L.D., Watanabe, T., and Kawaoka, Y. (2011). ALIX/AIP1 Is Required for NP Incorporation into Mopeia Virus Z-Induced Virus-Like Particles. J Virol *85*, 3631-3641.

Singh, M.K., Fuller-Pace, F.V., Buchmeier, M.J., and Southern, P.J. (1987). Analysis of the genomic l rna segment from lymphocytic choriomeningitis virus. Virology *161*, 448-456.

Sotgia, F., Lee, H., Bedford, M.T., Petrucci, T., Sudol, M., and Lisanti, M.P. (2001). Tyrosine Phosphorylation of β-Dystroglycan at Its WW Domain Binding Motif, PPxY, Recruits SH2 Domain Containing Proteins†. Biochemistry *40*, 14585-14592.

Spandidos, D.A., and Graham, A.F. (1976). Generation of defective virus after infection of newborn rats with reovirus. J Virol *20*, 234-247.

Spiropoulou, C.F., Kunz, S., Rollin, P.E., Campbell, K.P., and Oldstone, M.B.A. (2002). New World Arenavirus Clade C, but Not Clade A and B Viruses, Utilizes α-Dystroglycan as Its Major Receptor. J Virol *76*, 5140-5146.

Spurgers, K.B., Alefantis, T., Peyser, B.D., Ruthel, G.T., Bergeron, A.A., Costantino, J.A., Enterlein, S., Kota, K.P., Boltz, R.C.D., Aman, M.J.*, et al.* (2010). Identification of Essential Filovirion-associated Host Factors by Serial Proteomic Analysis and RNAi Screen. Molecular & Cellular Proteomics *9*, 2690-2703.

Stampfer, M., Baltimore, D., and Huang, A.S. (1971). Absence of Interference During High-Multiplicity Infection by Clonally Purified Vesicular Stomatitis Virus. J Virol *7*, 409-411.

Staneck, L.D., and Pfau, C.J. (1974). Interfering Particles from a Culture Persistently Infected with Parana Virus. J Gen Virol *22*, 437-440.

Staneck, L.D., Trowbridge, R.S., Welsh, R.M., Wright, E.A., and Pfau, C.J. (1972). Arenaviruses: Cellular Response to Long-Term In Vitro Infection with Parana and Lymphocytic Choriomeningitis Viruses. Infect Immun *6*, 444-450.

Staub, O., Dho, S., Henry, P., Correa, J., Ishikawa, T., McGlade, J., and Rotin, D. (1996). WW domains of Nedd4 bind to the proline-rich PY motifs in the epithelial Na+ channel deleted in Liddle's syndrome. Embo j *15*, 2371-2380.

Stenglein, M.D., Sanders, C., Kistler, A.L., Ruby, J.G., Franco, J.Y., Reavill, D.R., Dunker, F., and DeRisi, J.L. (2012). Identification, Characterization, and In Vitro Culture of Highly Divergent Arenaviruses from Boa Constrictors and Annulated Tree Boas: Candidate Etiological Agents for Snake Inclusion Body Disease. mBio *3*.

Stenmark, H. (2009). Rab GTPases as coordinators of vesicle traffic. Nat Rev Mol Cell Biol *10*, 513-525.

Stocker, C., Peralta, L.M., Kratzberg, T., Lohmann, F., and Bruns, M. (1994). Characterization of a virus variant produced by L cells persistently infected with lymphocytic choriomeningitis virus. J Gen Virol *75*, 3431-3439.

Stojdl, D.F., Lichty, B.D., tenOever, B.R., Paterson, J.M., Power, A.T., Knowles, S., Marius, R., Reynard, J., Poliquin, L., Atkins, H.*, et al.* (2003). VSV strains with defects in their ability to shutdown innate immunity are potent systemic anti-cancer agents. Cancer Cell *4*, 263-275.

Strack, B., Calistri, A., Accola, M.A., Palù, G., and Göttlinger, H.G. (2000). A role for ubiquitin ligase recruitment in retrovirus release. Proceedings of the National Academy of Sciences *97*, 13063-13068.

Strausbaugh, L.J., Barton, L.L., and Mets, M.B. (2001). Congenital Lymphocytic Choriomeningitis Virus Infection: Decade of Rediscovery. Clinical Infectious Diseases *33*, 370-374.

Strecker, T., Eichler, R., Meulen, J.t., Weissenhorn, W., Dieter Klenk, H., Garten, W., and Lenz, O. (2003). Lassa Virus Z Protein Is a Matrix Protein Sufficient for the Release of Virus-Like Particles. J Virol *77*, 10700-10705.

Strecker, T., Maisa, A., Daffis, S., Eichler, R., Lenz, O., and Garten, W. (2006). The role of myristoylation in the membrane association of the Lassa virus matrix protein Z. Virology Journal *3*, 93.

Stuchell-Brereton, M.D., Skalicky, J.J., Kieffer, C., Karren, M.A., Ghaffarian, S., and Sundquist, W.I. (2007). ESCRT-III recognition by VPS4 ATPases. Nature *449*, 740-744.

Tabata, K., Arimoto, M., Arakawa, M., Nara, A., Saito, K., Omori, H., Arai, A., Ishikawa, T., Konishi, E., Suzuki, R.*, et al.* (2016). Unique Requirement for ESCRT Factors in Flavivirus Particle Formation on the Endoplasmic Reticulum. Cell Reports *16*, 2339-2347.

Tai, A.W., Benita, Y., Peng, L.F., Kim, S.-S., Sakamoto, N., Xavier, R.J., and Chung, R.T. (2009). A Functional Genomic Screen Identifies Cellular Cofactors of Hepatitis C Virus Replication. Cell Host & Microbe *5*, 298-307.

Taylor, G.M., Hanson, P.I., and Kielian, M. (2007). Ubiquitin Depletion and Dominant-Negative VPS4 Inhibit Rhabdovirus Budding without Affecting Alphavirus Budding. J Virol *81*, 13631-13639.

Timmins, J., Schoehn, G., Ricard-Blum, S., Scianimanico, S., Vernet, T., Ruigrok, R.W.H., and Weissenhorn, W. (2003). Ebola Virus Matrix Protein VP40 Interaction with Human Cellular Factors Tsg101 and Nedd4. Journal of Molecular Biology *326*, 493-502.

Urata, S., Noda, T., Kawaoka, Y., Morikawa, S., Yokosawa, H., and Yasuda, J. (2007). Interaction of Tsg101 with Marburg Virus VP40 Depends on the PPPY Motif, but Not the PT/SAP Motif as in the Case of Ebola Virus, and Tsg101 Plays a Critical Role in the Budding of Marburg Virus-Like Particles Induced by VP40, NP, and GP. J Virol *81*, 4895-4899.

Urata, S., Noda, T., Kawaoka, Y., Yokosawa, H., and Yasuda, J. (2006). Cellular Factors Required for Lassa Virus Budding. J Virol *80*, 4191-4195.

Urata, S., Weyer, J., Storm, N., Miyazaki, Y., van Vuren, P.J., Paweska, J.T., and Yasuda, J. (2016). Analysis of Assembly and Budding of Lujo Virus. J Virol *90*, 3257-3261.

Urata, S., and Yasuda, J. (2010). Regulation of Marburg virus (MARV) budding by Nedd4.1: a different WW domain of Nedd4.1 is critical for binding to MARV and Ebola virus VP40. Journal of General Virology *91*, 228-234.

Urata, S., and Yasuda, J. (2012). Molecular Mechanism of Arenavirus Assembly and Budding. Viruses *4*, 2049-2079.

Urata, S., Yasuda, J., and de la Torre, J.C. (2009). The Z Protein of the New World Arenavirus Tacaribe Virus Has Bona Fide Budding Activity That Does Not Depend on Known Late Domain Motifs. J Virol *83*, 12651-12655.

Utley, T.J., Ducharme, N.A., Varthakavi, V., Shepherd, B.E., Santangelo, P.J., Lindquist, M.E., Goldenring, J.R., and Crowe, J.E. (2008). Respiratory syncytial virus uses a Vps4-independent budding mechanism controlled by Rab11-FIP2. Proceedings of the National Academy of Sciences *105*, 10209-10214.

Vale-Costa, S., and Amorim, M. (2016). Recycling Endosomes and Viral Infection. Viruses *8*, 64.

Vana, M.L., Tang, Y., Chen, A., Medina, G., Carter, C., and Leis, J. (2004). Role of Nedd4 and ubiquitination of Rous sarcoma virus Gag in budding of virus-like particles from cells. J Virol *78*, 13943-13953.

Varkey, J.B., Shantha, J.G., Crozier, I., Kraft, C.S., Lyon, G.M., Mehta, A.K., Kumar, G., Smith, J.R., Kainulainen, M.H., Whitmer, S.*, et al.* (2015). Persistence of Ebola Virus in Ocular Fluid during Convalescence. N Engl J Med *372*, 2423-2427.

Volpon, L., Osborne, M.J., Capul, A.A., de la Torre, J.C., and Borden, K.L.B. (2010). Structural characterization of the Z RING-eIF4E complex reveals a distinct mode of control for eIF4E. Proc Natl Acad Sci USA *107*, 5441-5446.

von, M.P. (1951). Propagation of the PR8 strain of influenza A virus in chick embryos. II. The formation of incomplete virus following inoculation of large doses of seed virus. Acta pathologica et microbiologica Scandinavica *28*, 278-293.

von Schwedler, U.K., Stuchell, M., Müller, B., Ward, D.M., Chung, H.-Y., Morita, E., Wang, H.E., Davis, T., He, G.-P., Cimbora, D.M.*, et al.* (2003). The Protein Network of HIV Budding. Cell *114*, 701-713.

Votteler, J., and Sundquist, Wesley I. (2013). Virus Budding and the ESCRT Pathway. Cell Host & Microbe *14*, 232-241.

Wang, H., Norris, K.M., and Mansky, L.M. (2002). Analysis of Bovine Leukemia Virus Gag Membrane Targeting and Late Domain Function. J Virol *76*, 8485-8493.

Wang, J., Danzy, S., Kumar, N., Ly, H., and Liang, Y. (2012). Biological Roles and Functional Mechanisms of Arenavirus Z Protein in Viral Replication. J Virol *86*, 9794-9801.

Weiss, B., Rosenthal, R., and Schlesinger, S. (1980). Establishment and maintenance of persistent infection by Sindbis virus in BHK cells. J Virol *33*, 463-474.

Welsh, R.M., and Buchmeier, M.J. (1979). Protein analysis of defective interfering lymphocytic choriomeningitis virus and persistently infected cells. Virology *96*.

Welsh, R.M., Connell, C.M., and Pfau, C.J. (1972). Properties of Defective Lymphocytic Choriomeningitis Virus. J Gen Virol *17*, 355-359.

Welsh, R.M., Lampert, P.W., and Oldstone, M.B. (1977). Prevention of virus-induced cerebellar diseases by defective-interfering lymphocytic choriomeningitis virus. The Journal of infectious diseases *136*.

Welsh, R.M., and Oldstone, M.B. (1977). Inhibition of immunologic injury of cultured cells infected with lymphocytic choriomeningitis virus: role of defective interfering virus in regulating viral antigenic expression. J Exp Med *145*, 1449-1468.

Welsh, R.M., and Pfau, C.J. (1972). Determinants of Lymphocytic Choriomeningitis Interference. J Gen Virol *14*, 177-187.

Wirblich, C., Bhattacharya, B., and Roy, P. (2006). Nonstructural Protein 3 of Bluetongue Virus Assists Virus Release by Recruiting ESCRT-I Protein Tsg101. J Virol *80*, 460-473.

Wirblich, C., Tan, G.S., Papaneri, A., Godlewski, P.J., Orenstein, J.M., Harty, R.N., and Schnell, M.J. (2008a). PPEY motif within the rabies virus (RV) matrix protein is essential for efficient virion release and RV pathogenicity. J Virol *82*, 9730-9738.

Wirblich, C., Tan, G.S., Papaneri, A., Godlewski, P.J., Orenstein, J.M., Harty, R.N., and Schnell, M.J. (2008b). PPEY Motif within the Rabies Virus (RV) Matrix Protein Is Essential for Efficient Virion Release and RV Pathogenicity. J Virol *82*, 9730-9738.

Wolff, S., Ebihara, H., and Groseth, A. (2013). Arenavirus budding: a common pathway with mechanistic differences. Viruses *5*, 528-549.

Wollert, T., Wunder, C., Lippincott-Schwartz, J., and Hurley, J.H. (2009). Membrane scission by the ESCRT-III complex. Nature *458*, 172-177.

Wong, Y.H., Lee, T.Y., Liang, H.K., Huang, C.M., Wang, T.Y., Yang, Y.H., Chu, C.H., Huang, H.D., Ko, M.T., and Hwang, J.K. (2007). KinasePhos 2.0: a web server for identifying protein kinase-specific phosphorylation sites based on sequences and coupling patterns. Nucleic Acids Res *35*, W588-594.

Wright, K.E., Spiro, R.C., Burns, J.W., and Buchmeier, M.J. (1990). Post-translational processing of the glycoproteins of lymphocytic choriomeningitis virus. Virology *177*, 175-183.

Xing, J., Ly, H., and Liang, Y. (2015). The Z Proteins of Pathogenic but Not Nonpathogenic Arenaviruses Inhibit RIG-i-Like Receptor-Dependent Interferon Production. J Virol *89*, 2944-2955.

Yasuda, J., and Hunter, E. (1998). A Proline-Rich Motif (PPPY) in the Gag Polyprotein of Mason-Pfizer Monkey Virus Plays a Maturation-Independent Role in Virion Release. J Virol *72*, 4095-4103.

Yasuda, J., Hunter, E., Nakao, M., and Shida, H. (2002). Functional involvement of a novel Nedd4-like ubiquitin ligase on retrovirus budding. EMBO Rep *3*, 636-640.

Yasuda, J., Nakao, M., Kawaoka, Y., and Shida, H. (2003). Nedd4 Regulates Egress of Ebola Virus-Like Particles from Host Cells. Journal of Virology *77*, 9987-9992.

Yavlovich, A., Viard, M., Zhou, M., Veenstra, T.D., Wang, J.M., Gong, W., Heldman, E., Blumenthal, R., and Raviv, Y. (2012). Ectopic ATP synthase facilitates transfer of HIV-1 from antigen-presenting cells to CD4+ target cells. Blood *120*, 1246-1253.

Yuan, B., Campbell, S., Bacharach, E., Rein, A., and Goff, S.P. (2000a). Infectivity of Moloney murine leukemia virus defective in late assembly events is restored by late assembly domains of other retroviruses. J Virol *74*, 7250-7260.

Yuan, B., Campbell, S., Bacharach, E., Rein, A., and Goff, S.P. (2000b). Infectivity of Moloney Murine Leukemia Virus Defective in Late Assembly Events Is Restored by Late Assembly Domains of Other Retroviruses. J Virol *74*, 7250-7260.

Zhou, H., Xu, M., Huang, Q., Gates, A.T., Zhang, X.D., Castle, J.C., Stec, E., Ferrer, M., Strulovici, B., Hazuda, D.J.*, et al.* (2008). Genome-Scale RNAi Screen for Host Factors Required for HIV Replication. Cell Host & Microbe *4*, 495-504.

Ziegler, C.M., Eisenhauer, P., Bruce, E.A., Beganovic, V., King, B.R., Weir, M.E., Ballif, B.A., and Botten, J. (2016a). A novel phosphoserine motif in the LCMV matrix protein Z regulates the release of infectious virus and defective interfering particles. J Gen Virol.

Ziegler, C.M., Eisenhauer, P., Bruce, E.A., Weir, M.E., King, B.R., Klaus, J.P., Krementsov, D.N., Shirley, D.J., Ballif, B.A., and Botten, J. (2016b). The Lymphocytic Choriomeningitis Virus Matrix Protein PPXY Late Domain Drives the Production of Defective Interfering Particles. PLoS Pathog *12*, e1005501.